Performance of Dynamic Vibration Absorbers on Buildings with Coupled Modes

PERFORMANCE OF DYNAMIC VIBRATION ABSORBERS ON BUILDINGS WITH COUPLED MODES

BY

YAT FUNG HO, B.Eng.

A Thesis

Submitted to the School of Graduate Studies

in Partial Fulfilment of the Requirements

for the Degree of

Master of Applied Science

McMaster University

Master of Applied Science (2009) McMaster University

(Civil Engineering) Hamilton, Ontario, Canada

TITLE:	Performance of Dynamic Vibration Absorbers on Buildings with Coupled Modes
AUTHOR:	Yat Fung Ho B.Eng. (Civil Engineering) McMaster University, Hamilton, Canada
SUPERVISORS:	Dr. K.S. Sivakumaran and Dr. Michael J. Tait
NUMBER OF PAGES:	xxxviii, 519

Abstract

Dynamic absorbers, including the tuned mass damper (TMD) and the tuned liquid damper (TLD), have been widely used in buildings to attenuate dynamic response. As the complexity of buildings increases, their response may become susceptible to torsional motion. The induced torsional motion can be suppressed by utilizing TMDs or TLDs. As such, the performance of different absorber arrangements are important for torsionally coupled structures. Also, a rapid design tool to reduce the computational effort for the design of the absorbers optimal parameters in torsionally coupled system is essential.

In this study, the performance of different TMD/TLD configurations under both random and harmonic excitation are studied and evaluated. The effectiveness of the absorber configurations considered is accessed by the response reduction factor, which is defined as the ratio of the response of structure equipped with absorber(s) to the response of structure without absorber(s). Also, a preliminary design tool to determine optimal TMD parameters is developed by introducing the concept of a generalized structure-TMD system.

Acknowledgements

I would like to thank my parents and my sister. Their generous patients made this journey possible.

I would like to extend my gratitude to my supervisors, Dr. K. S. Sivakumaran and Dr. Michael J. Tait. They gave me this chance for progressing my academic career, so that I can achieve even more in the future. Also, I am truly grateful for Dr. Tait's extra effort on helping me in this thesis.

My special thanks to my friend, Henry Ko, for his constant support and advice throughout this journey. I would also like to thank Melissa Mak for listening to my complaints and the encouragements that she gave.

I would like to thank my colleagues, Ahmed Mostafa, Amr Nassr, Eric Tiedje and Badr Abou Zeid, for having valuable opinions and relaxing coffee time with me. I would also like to thank the graduate students, faculty, administrative and technical members in Department of Civil Engineering at McMaster University for their assistance during my study and research.

Last but not least, I would like to thank all my friends for their support, especially to Nicole Ye. The encouragements and love from this very important person during the hardest time in the final stage of my journey gave me the extra motivation to be successful until the end.

Notation and Abbreviations

B	length of the idealized structure
b	tank width
C_c	contraction coefficient
C_d	drag coefficient
C_l	loss coefficient
c_{eq}	equivalent damping
c_s	total translational damping of structure
c_θ	total torsional damping of structure
CM	centre of mass of the structure
CR	centre of resistance
D	width of the idealized structure
DE	energy dissipation
DMF	dynamic magnification factor
DVA	dynamic vibration absorber
e_s	eccentricity
f_o	amplitude of applied force
$f(t)$	external forcing function
f_d	drag force
g	gravitational constant
h	quiescent fluid height
I	moment of inertia
k_{eq}	equivalent stiffness
k_s	total translational stiffness of structure
k_θ	total torsional stiffness of structure
L	tank length
m_{eq}	equivalent mass
m_i	mass of the i^{th} number of absorber
m_o	non-participating fluid mass

m_s	mass of structure
q	generalized coordinate
R	dynamic magnification factor
R_o	response reduction factor
RMS	root mean square
r	radius of gyration of the structure
S	screen solidity
S_o	constant spectral density
T	kinetic energy
TMD	tuned mass damper
TLD	tuned liquid damper
t	time
V	potential energy
W_{nc}	work done by non-conservative drag force
$X(\omega)$	mechanical admittance of the system's maximum corner's displacements
x	spatial coordinate (horizontal)
x_c	corner displacement of structure
x_j	screen location
x_r	relative translational motion between the structure and absorber
x_s	translational motion
y_i	distance between the CM and the location of the i^{th} TMD/TLD
z	spatial coordinate (vertical)
α	forcing frequency ratio, ω/ω_n
β	forcing frequency ratio, ω/ω_s
η	free surface response
Γ	modal participation factor
γ	excitation factor
μ	total mass ratio
μ_i	mass ratio of the i^{th} number of absorber
ν	tuning ratio (ω_i/ω_s)
ω	excitation frequency (rad/s)
ω_i	absorber natural frequency (rad/s)
ω_n	structural natural frequency (rad/s)
ω_s	uncoupled translational frequency (rad/s)
ω_θ	uncoupled torsional frequency (rad/s)
ω_θ/ω_s	uncoupled frequency ratio
Ω	tuning ratio (ω_i/ω_n)
θ_s	torsional motion
ϕ	mode shape

ρ	fluid density
σ_q	root mean square motion of the fluid response
σ_{x_c}	corner root mean square displacements
ζ	damping ratio
ζ_{eff}	effective damping

Common Subscripts

a	dynamic absorber property
eq	equivalent mechanical parameter
opt	optimized parameter
w	water

Common Superscripts

$*$	generalized parameter
$'$	modified parameter
$\dot{}$	velocity
$\ddot{}$	acceleration

Contents

List of Tables

List of Figures

Chapter 1

Introduction and Literature Review

1.1 Introduction

Advanced analysis tools, modern construction techniques and materials development have led to economical structures that are light weight and flexible. These slender lightly damped structures, however, are susceptible to dynamic excitation (Kareem, 1983). Consequently, serviceability requirements, which include limits on deflections and accelerations, can govern the design. In order to satisfy serviceability requirements, passive energy dissipation devices, including dynamic vibration absorbers, are increasingly being used to reduce the overall structural response (Kareem *et al.*, 1999). The two most common types of dynamic vibration absorbers (DVAs), are tuned mass dampers (TMDs) and tuned liquid dampers (TLDs) (Soong and Dargush, 1997). They are passive devices since they are only activated once excited by the response of the structure subjected to the excitation force. The main purpose of

adding these devices is to dissipate part of the energy input by the excitation force such that the dynamic response is reduced to an acceptable level.

1.1.1 TMD Applications

One of the earliest buildings to be equipped with a tuned mass damper is the 278 m tall Citicorp building (Figure 1.1), in New York, United States in 1978. The TMD system was installed due to the building's aspect ratio (i.e. building's height to width ratio) and dynamic features. The TMD system consists of a 410 ton concrete block with two spring damping mechanisms, one in the north-south direction and one in the east-west direction. The system, located on 63rd floor, has dimension of 9.14 x 9.14 x 3.05 m. The system is activated at a critical acceleration threshold of 3 milli-g's and is able to attenuate the response by 40% in both north-south and east-west directions. (Kareem *et al.*, 1999)

More recent applications of TMD systems include the 508 m tall structure in Taiwan, Taipei 101. The building process started in 1998 and entered into service in 2004. The TMD, located between the 87th and 91st floors, has a gross weight of 660 metric tons. The TMD consists of 41 layers of 12.5 cm steel plates welded together with a maximum centre diameter of 5.5 metres. The large mass is suspended by a total of eight 9 cm thick steel cables hanging from the 92nd floor. Also, eight hydraulic viscous dampers are installed beneath the mass to absorb and dissipate energy. The building's vibration can be reduced by 40%. A schematic of the TMD is shown in Figure 1.2. (Taipei Financial Center Corp., 2005)

Other notable buildings equipped with TMDs include Toronto's CN Tower (1975), Nagasaki's Huis Ten Bosch Domtoren (1992), Washington D.C.'s Washington

National Airport Tower (1997) and Sendai's Sendai AERU (1998) (Kareem *et al.*, 1999).

1.1.2 TLD Applications

The installation of TLDs in structures began in the early 1980s. For instance, a TLD system was installed in Japan's Nagasaki Airport Tower in 1987. The steel-frame tower was constructed in 1974 on an artificial island on a low-rise reinforced concrete building. The TLD system consisted of 25 cylindrical multilayered vessels containing water. Twelve units were installed on the air-traffic control room floor and remaining thirteen units were placed on the stair landing. Study results have shown the wind induced response was reduced by 35% in 20m/s wind. (Tamura *et al.*, 1995; Kareem *et al.*, 1999). Since 1980, other TLD installations include the Nagasaki Airport Tower, Yokohama Marine Tower and Shin-Yokohama Prince Hotel (Tamura *et al.*, 1995).

Recently, a TLD system was installed in the 51 storey residential building, One King West, located in Toronto. The tallest residential building in Canada, it was completed in 2005 and is one of the most slender buildings in the world (see Figure 1.3). The building's height to width ratio (aspect ratio) is approximately 11:1 as compared to the more usual values of 4:1 to 6:1. Owing to its slender nature, the building is very susceptible to wind induced excitation. A TLD system, located on the top of the building, was installed to reduce wind induced accelerations. The TLD is capable of reducing the building top floor acceleration to an acceptable level. (OCCDC, 2005; Halcrow Yolles, 2007)

1.2 Literature Review

1.2.1 Dynamic Vibration Absorbers

According to Den Hartog (1956), the idea of a DVA was first introduced by Frahm in 1902. The first DVA was developed to reduce the rolling action of ships in rough seas when waves strike periodically. Different types of DVAs have evolved over the years. The most common type of DVA is the tuned mass dampers (TMD) (Kareem *et al.*, 1999). For instance, two TMDs were installed in the Hancock Tower back in 1977 to suppress torsional motion, which is one of the earliest applications of TMDs (Kareem *et al.*, 1999). Recently, TLDs have become an increasingly popular damping device since they can utilize the existing water tanks in a building without adverscly affecting its functional use.

1.2.2 Tuned Mass Damper

A tuned mass damper is essentially a large mass m_a, attached to the structure through a spring k_a and a dashpot c_a as shown in Figure 1.4. The main structure can be represented by single-degree-of-freedom (SDOF) system with the generalized mass $M_s{}^*$, stiffness $K_s{}^*$, and damping $C_s{}^*$ corresponding to the mode being targeted. The natural frequency of the TMD, ω_a, is usually tuned to target the natural frequency of the structure, ω_n, such that the TMDs vibrates out of phase when the structure is at resonance. Thus, the TMD exerts an inertial force back onto the structure such that the structural response is reduced. Following Den Hartog (1956), the natural

frequency of the structure and the TMD are defined as

$$\omega_n = \sqrt{\frac{K_s^*}{M_s^*}} \tag{1.1}$$

$$\omega_a = \sqrt{\frac{k_a}{m_a}} \tag{1.2}$$

According to Asami *et al.* (2002), expressions for the optimal parameters for a damped DVA attached to a undamped structure under sinusoidal excitation were derived by Hahnkamm (1932) and Brock (1946) and later introduced by Den Hartog (1956). It was shown that the performance of the damper is dictated by the two optimal parameters known as the tuning ratio, Ω, and the absorber damping ratio, ζ_a. The tuning ratio is defined as ratio of the natural frequency of the damper to the natural frequency of the structure

$$\Omega = \frac{\omega_a}{\omega_n} \tag{1.3}$$

and the absorber damping ratio is given by

$$\zeta_a = \frac{c_a}{2m_a\omega_a} \tag{1.4}$$

The optimal parameters for sinusoidal excitation for an undamped primary structure are related to the mass ratio μ,

$$\Omega_{opt} = \frac{1}{1+\mu} \tag{1.5}$$

$$\zeta_{opt} = \sqrt{\frac{3\mu}{8(1+\mu)}} \tag{1.6}$$

where μ is defined as the ratio of the mass of the damper to the mass of the structure. The dynamic magnification factor, defined as the dynamic response divided by the static response, is given by

$$R = \sqrt{\frac{(\Omega^2-\alpha^2)^2+(2\zeta_a\Omega\alpha)^2}{((\Omega^2-\alpha^2)-\Omega^2\alpha^2\mu)^2+(2\zeta_a\Omega\alpha)^2(1-\alpha^2-\alpha^2\mu)^2}} \tag{1.7}$$

where α is the forcing frequency ratio, defined as the excitation frequency divided by the natural frequency of the undamped structure. To illustrate Den Hartog's work, the frequency response graph is plotted for a mass ratio value of 5% along with the optimal tuning ratio, Ω_{opt}, as shown in Figure 1.5. As shown in the figure, for $\zeta_a = 0$ or $\zeta_a = \infty$, the peak response is infinite. When $\zeta_a = 0$, the two masses behave independently with the two peaks appearing on the frequency response graphs tending to infinity. When $\zeta_a = \infty$, the damper is fused with the structure and the system behaves as a single-degree-of-freedom system. When the damping ratio is not at its optimal value such as $\zeta_a = 0.5\zeta_{opt}$, two peaks of different height appear. When both the tuning ratio and damping ratio are at their optimal values, two peaks of equal height occur with the lowest peak response. As demonstrated in Figure 1.5, it is important to properly design the tuned mass damper to achieve its maximum performance. The performance of a TMD is often evaluated in terms of the effective damping added to the structure by the TMD. The effective damping, ζ_{eff}, is defined as a single damping parameter in a single-degree-of-freedom structure that will give the same performance as if the structure is attached with a TMD (McNamara, 1977).

The mechanical representation of the effective damping parameter is shown in Figure 1.6.

Warburton and Ayorinde (1980) studied the effect on the tuning ratio and damping ratio of a lightly damped structure equipped with a TMD. It was found that the effect on the optimal parameters values are negligible if the damping in the main system is small. Subsequently, Warburton (1982) provided simple optimal parameter expressions for an undamped structure under both sinusoidal and random white noise excitation with force and base acceleration as the excitation input. The tuning ratio and the damping ratio were optimized for different response parameters. Warburton (1982) determined the exact optimal parameters for an undamped structure under random excitation

$$\Omega_{opt} = \frac{1}{1+\mu}\sqrt{1+\frac{\mu}{2}} \tag{1.8}$$

$$\zeta_{opt} = \sqrt{\frac{\mu(4+3\mu)}{8(1+\mu)(2+\mu)}} \tag{1.9}$$

Asami *et al.* (1991) determined a numerical solution for a damped structure subjected to unit input acceleration from ideal white noise with optimization criterion aiming at minimizing the performance measure, defined by the mean square acceleration response. Asami *et al.* (2002) published series solutions for a damped structure under sinusoidal excitation using H_∞ optimization technique. He also provided the exact solution for a damped structure under stationary random white noise excitation using H_2 optimization technique. According to Asami *et al.* (2002), H_∞ is a optimization criterion proposed by Den Hartog and Ormondroyd in 1928. The H_∞ optimization

technique minimizes the peak response such that the lowest possible response is obtained. As for H_2 optimization technique, which was first proposed by Crandall and Mark (1963), it minimizes the overall vibration energy over all excitation frequencies. Mathematically, the area bounded by the frequency response function is minimized to achieve the lowest possible vibration energy for all frequencies. Ozer and Royston (2005) extended Den Hartong's optimization technique to a multi-degree-of-freedom undamped main system by deriving an expression that would yield the invariants points of an undamped multi-degree-of-freedom system using the Sherman-Morrison matrix inversion theorem. The absorber optimal stiffness and damping were obtained based on the derived expression. The study showed that the absorber location can influence the response of the neighboring modes such that the response of an active mode, which the absorber is attached to, was attenuated even though the absorber was not tuned to that particular mode. Petit *et al.* (2009) further studied on the placement of the DVAs. It was found that, for a DVA with large mass, the efficiency of the DVA can be improved by maximizing the spectral gap between the resonant mode and the eigenfrequencies close to that mode. A procedure was given to determine the DVA location by maximizing this spectral gap.

1.2.2.1 Torsionally Coupled Structure-TMD Systems

Research has been conducted on buildings with unsymmetrical shapes equipped with multiple-tuned mass dampers (MTMDs). The main concern with an unsymmetrical building is its torsional motion. Hence, most of the research has focused on the effect of multiple TMDs on the torsional motion. Jangid and Datta (1997) studied the effectiveness of multiple-tuned mass dampers on reducing the response of torsionally

coupled system, which consists of a two-degree-of-freedom structure with rotational and translational motion under stationary random excitation. The frequencies of the MTMDs is uniformly distributed and they are located at fixed locations. It was found that the optimal frequency bandwidth depends on parameters of the torsionally coupled system such as the eccentricity of the structure, the damping of the MTMDs and the ratio of the uncoupled torsional frequency to the uncoupled translational frequency. Lin *et al.* (1999) studied the response of a multi-storey torsionally coupled shear wall building under earthquake excitation with one and two TMDs. They first identified the dominant mode (i.e. provides the greatest contribution to the total response) and obtained the optimal parameters for the dampers by minimizing the root mean square response of displacement of the dominant mode. The study indicated that tuned mass dampers should be located as far from the centre of mass as possible and the vibration direction of the TMD should be along the moving direction of the dominant mode. Wu *et al.* (1997) studied the optimal placement of DVA for three-dimensional structures by taking into account the translation-torsion coupling effect in the structure or the unsymmetrically placement of the DVAs. The interstorey drifts of the 3D structures were taken as the performance index to evaluate the safety of the structures. The study showed that the structural performance cannot be improved significantly by adding more than a certain number of devices to the structure. Also, the placement of a limited number devices can have a significant influence on the level of response reduction. Singh *et al.* (2002) presented an approach for optimizing the design of multiple tuned mass dampers for a torsional multi-storey building subjected to bi-directional seismic excitation. Optimal parameters were obtained using a genetic

algorithm (Holland, 1975) to maximize the performance function, such as floor accelerations and storey drifts, that quantify a reduction in response. The study showed that it is beneficial in the design of TMDs to have greater flexibility in the selection of parameters. For instance, during the optimization process, imposing a fixed mass ratio value to all TMDs does not minimize the response as significantly as that when the mass ratio value for each TMD is permitted to vary. Pansare and Jangid (2003) studied the influence of tuned mass dampers on torsional systems with two-degree-of-freedom, rotation and translation, under harmonic excitation. Different ratios of uncoupled torsional frequency to uncoupled translational frequency (0.5, 1.0 and 1.5) and different arrangements of TMDs were considered such as (i) single TMD, (ii) two identical TMDs, (iii) two independent TMDs, and (iv) four TMDs. The TMDs were optimally tuned by using a numerical searching technique that minimizes the peak corner displacement response. Comparisons were drawn for different arrangements of TMDs corresponding to different uncoupled torsional frequency to uncoupled translational frequency ratios. Zhang *et al.* (2009) established a mathematical model of a multi-storey building structure including a bi-directional TMD system subjected to 2-dimensional earthquake ground motions. The TMD was optimized by using a genetic algorithm method to control the translational and rotational response. The study indicated that the mass centre displacement in both x and y directions of each floor were reduced. Petti and De Iuliis (2009) studied the robustness of a single TMD to control the torsional response of asymmetric-plan systems subjected to earthquake excitation. The performance index was defined by the H_∞ norm. A detail parametric study was carried out to obtain the design formulae for a single TMD. The design of

a single TMD position and stiffness were optimized by optimizing these design formulae. The robustness of a single TMD was confirmed by different recorded seismic events.

1.2.3 Tuned Liquid Damper

The tuned liquid damper was first employed to reduce the rolling motion of large ships by Frahm in 1902 (Den Hartog, 1956) and has also been used to reduce the oscillations of space satellites (Carrier and Miles, 1960). Research on TLDs applied to civil engineering structures was initiated in the 1980s by several different researchers including Bauer (1984), Kareem and Sun (1987), Fujino *et al.* (1988) and Weld and Modi (1989). A TLD consists of a rigid tank partially filled with fluid, typically water. The shape of the rigid tank can be of many forms, the most common shapes include rectangular, cylindrical, annular and conical. A TLD utilizes the sloshing motion of the fluid to reduce structural response by absorbing excitation energy as kinetic energy through liquid motion and dissipating the absorbed energy through friction between the liquid and the container wall (Tamura, 1998). A structure-TLD system is shown in Figure 1.7(a) and a mechanical representation of a structure equipped with a TLD is shown in Figure 1.7(b).

TLDs can be broadly categorized as either shallow water dampers or deep water dampers. The classification is based on the water depth to tank length ratio. In shallow water dampers, energy is dissipated through the action of internal viscous forces and wave breaking. For the case of deep water dampers, energy can be dissipated by viscous forces and the presence of damping devices such as screens or baffles which increase the inherent damping of the TLDs. (Kareem, 1990)

The basics of applying TLDs to reduce the dynamic response of a structure are quite similar to that of TMDs. However, in contrast to a TMD, the response of a TLD is non-linear due to the nature of the fluid motion. Since the damping mechanism and natural frequency depend on the liquid motion, the response of TLD is amplitude dependent. In addition, not all the fluid participates in the sloshing motion. Thus, TMDs models can not be directly applied to TLDs. An equivalent TMD analogy of a TLD system is represented in Figure 1.7(b) in which the non-participating fluid mass, m_o, is added to the structure. The viscous damping and the gravity force on the fluid are represented by an amplitude dependent dashpot and spring, respectively.

A significant amount of research has focused on the modelling of the sloshing fluid motion. In early TLD applications, shallow water TLDs were utilized in order to take advantage of the inherent damping achieved through wave breaking. Shimizu and Hayama (1987) modelled the fluid response in a rectangular tank, which was subjected to horizontal excitation, using shallow water wave theory. A finite difference approach was used to restore dispersion characteristics in the fluid motion. Good agreement between simulations and physical experimental results were obtained. Sun *et al.* (1989) proposed a nonlinear model by extending the model adopted by Shimizu and Hayama (1987) by introducing a rational damping term to model the vicious damping in fluid motion. Good correlation between experimental work and simulations at low excitations was obtained. At higher excitation levels, simulation results began to deviate from the experimental results at the onset of wave breaking. Since the proposed model did not include the effect of wave breaking, simulations tended to over predict the results. Later, Fujino *et al.* (1992) utilized this model to study the response of a structure-TLD system. Sun *et al.* (1992) subsequently extended the

original model to account for the effect of wave breaking by proposing two empirical coefficients obtained from shake table tests. These two coefficients were introduced to account for the liquid response behavior once wave breaking occurs, which includes a change in wave phase velocity and increased energy dissipation.

The inherent damping in a tuned liquid damper is often significantly less than the required optimal value. Thus, energy dissipating devices, such as screen or baffles, are placed in the TLD to increase the inherent damping. Fediw *et al.* (1995) proposed a linear model for a rectangular tank with damping screens under small excitation amplitudes by solving the linear wave equation with proper boundary conditions incorporated. Kaneko and Ishikawa (1999) developed a nonlinear model for a TLD equipped with damping screen using shallow water theory. This model was validated for a 0.0025 excitation amplitude to tank length ratio (A/L). Kaneko and Yoshida (1999) also proposed an analytical model for utilizing deep water in a rectangular TLD with submerged nets by employing finite amplitude wave theory and subsequently confirmed this model with experimental work. Tait *et al.* (2004) performed extensive experimental work to study the effect of damping screen on the free surface motion, base shear forces, and the amount of energy dissipated. An equivalent TMD model was also developed using an energy equivalence approach. Tait *et al.* (2005) utilized the linear model from Fediw *et al.* (1995) and the nonlinear model from Kaneko and Ishikawa (1999) to study the effect of damping screens on a TLD. In this work, the numerical models were validated over a larger excitations amplitudes, A, larger fluid depth, h, to tank length, L, ratio, and for the use of multiple screens in the nonlinear model. In this study, the nonlinear model was validated for $0.0026 < A/L < 0.0414$, and for h/L values that are approximately 1.5 times larger than those from pervious

studies. The nonlinear model was also able to model a TLD with multiple screens at various locations. Tait *et al.* (2007) performed experimental work and numerical simulations to study the behavior of a 2D structure-TLD system. The TLD was equipped with damping screens in both principal directions. The results indicated that a 1D nonlinear numerical model could be used to predict the response of a 2D structure-TLD system. This greatly reduces the design effort of a 2D structure-TLD system as the system can be design as two uncoupled 1D structure-TLD systems. Recently, Cassolato (2007) studied the influence of inclined and oscillating damping screens on a rectangular TLD while Hamelin (2007) investigated the effect of screen geometry on a rectangular TLD.

1.2.3.1 Equivalent TMD Models

As previously stated, a TLD can be modelled as an equivalent TMD with the mechanical properties, m_a, c_a and k_a, being amplitude dependent. The reason for developing such an equivalent TMD model is to provide a quick way for preliminary design and to investigate its performance. Several researchers have modelled a TLD as an equivalent TMD. Sun *et al.* (1995) utilized the concept of virtual mass and virtual damping to express the nonlinear TLD properties using a TMD analogy. The properties considered include the effective mass, frequency and damping. A series of shake table test were carried out on different tank geometries including rectangular, annular and circular. Results from TMD analogy were found to be in agreement with experimental results, which showed the basic properties could be expressed qualitatively by TMD analogy. However, as stated by the authors, the conclusions could not be considered as general in nature since limited experimental cases were presented.

Yu *et al.* (1999) developed a nonlinear numerical model for a rectangular TLD based on energy dissipation equivalence. The nonlinear damping and nonlinear stiffness model was derived empirically with the assumption that the entire water mass participated in the sloshing motion under large amplitude of excitation. Warnitchai and Pinkaew (1998) developed an analytical model for a rectangular tank by employing the concept of a velocity potential and generalized coordinates. The influence of a damping screen, located at the centre of the tank, was also taken into consideration. The proposed model was validated by a series of shake table test under sinusoidal excitation. Tait (2008) extended the analytical model proposed by Warnitchai and Pinkaew (1998) with multiple screens to evaluate the equivalent mass, stiffness and damping under both sinusoidal and random excitation. The model was subsequently verified experimentally. It was found that for both sinusoidal and random excitation, the equivalent damping of a TLD can be expressed in terms of the relative motion between the damper and the structure. A preliminary design procedure was also outlined for a targeted structural response level.

1.3 Research Scope and Objectives

Owing to the increased popularity in utilizing multiple dynamic vibration absorbers to suppress torsional motion, the objective of this thesis is to study the dynamic response behavior of torsionally coupled systems equipped with different types of dynamic vibration absorbers (tuned mass damper and tuned liquid damper). The idealized structure is subjected to harmonic and stationary random excitation with different DVA configurations. The overall structural response is minimized using MATLAB (R2007b) optimization toolboxes (fminimax and fmincon), such that the

optimal parameters of the dynamic vibration absorber(s) are obtained numerically. A method which permits a torsionally coupled structure equipped with multiple DVAs to be expressed as an equivalent generalized structure-DVA system is introduced. The closed-form solution for a two-degree-of-freedom system, available in the literature, is subsequently utilized to target the response of a particular mode. Comparisons are drawn between targeting the entire system and a particular mode such that an efficient way to estimate the structural response and optimal parameters for the DVAs can be provided to the designer.

1.4 Organization of Thesis

Chapter 2 presents the idealized structural model with multiple TMDs along with the derivation of the equations of motion. Important structural parameters are introduced. The equivalent mechanical model for a TLD, developed by Tait (2008), is presented and then the necessary modification of the TMD model is presented.

Chapter 3 presents the numerical simulation results for torsionally coupled structures equipped with TMDs under harmonic excitation. The efficiency of the TMDs is studied for different torsionally coupled systems.

Chapter 4 reports on the dynamic response of torsionally coupled structures equipped with multiple DVAs under random excitation. The efficiency of TMDs and TLDs is subsequently discussed.

Chapter 5 discusses the use of a closed-form method to target the response of a particular mode. This solution was developed for a structure with three-degree-of-freedom. The response behavior obtained from targeting a particular mode to that obtained from targeting the entire system is compared.

Chapter 6 summarizes the major conclusions of this research and provides recommendations for future extensions to this research.

1.5 Chapter Figures

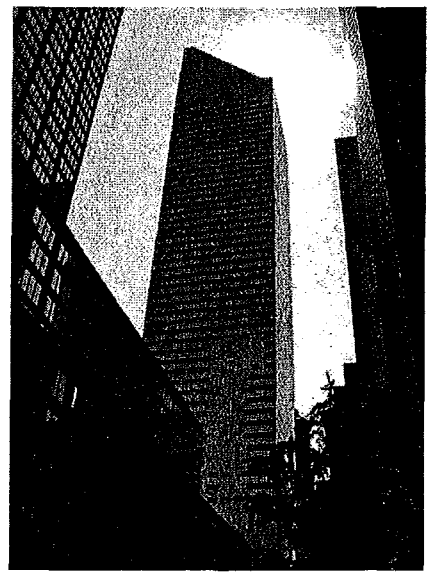

Figure 1.1: Citicorp Building, New York
(taken from <www.nyc-architecture.com/UES/UES001.htm>)

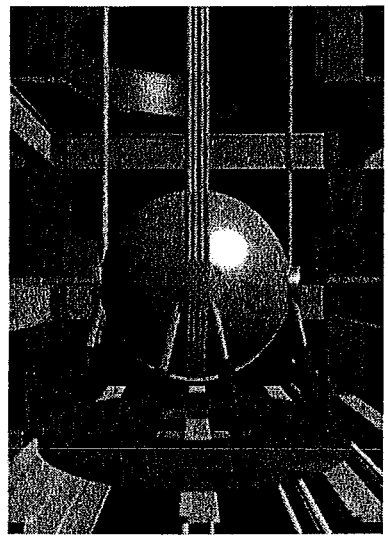

Figure 1.2: A Schematic of the Taipei 101 TMD
(taken from Taipei Financial Center Corp.
<www.taipei-101.com.tw/en/OB/about/damper.asp>)

Figure 1.3: One King West, Toronto
(taken from OCCDC (2005)
<http://occdc.org/pdf/1%20King%20West.pdf>)

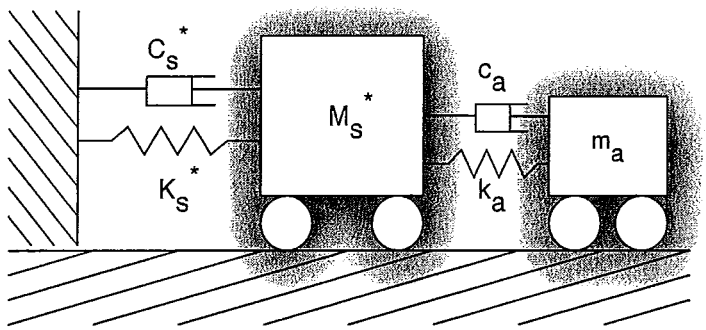

Figure 1.4: Mechanical Representation of a TMD System

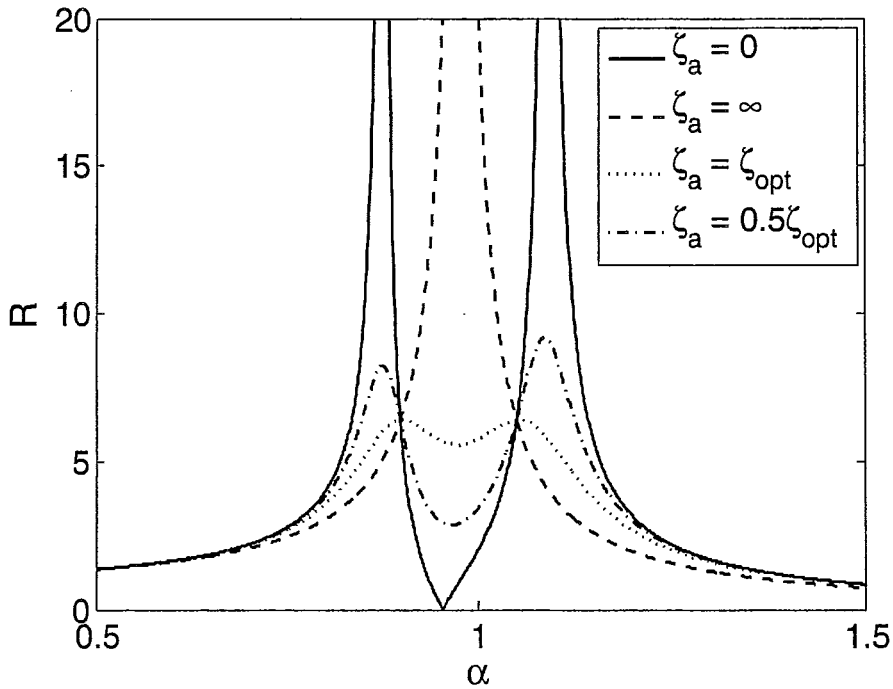

Figure 1.5: Frequency Response Function Plot of Structure-TMD System with $\mu = 0.05$ and Ω_{opt}

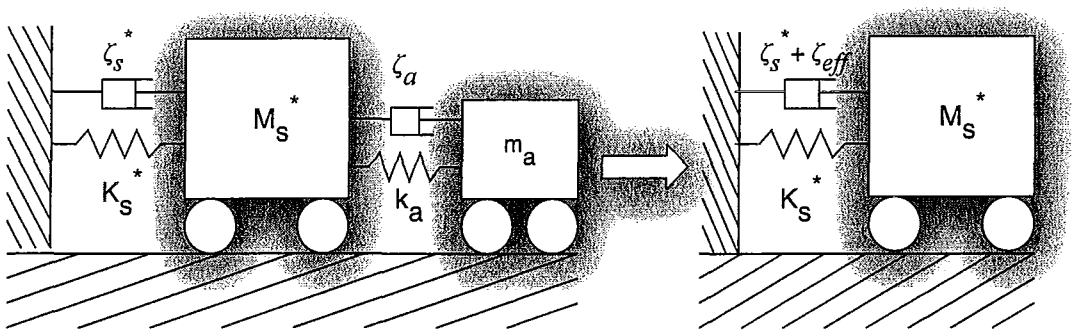

Figure 1.6: Mechanical Representation of Effective Damping

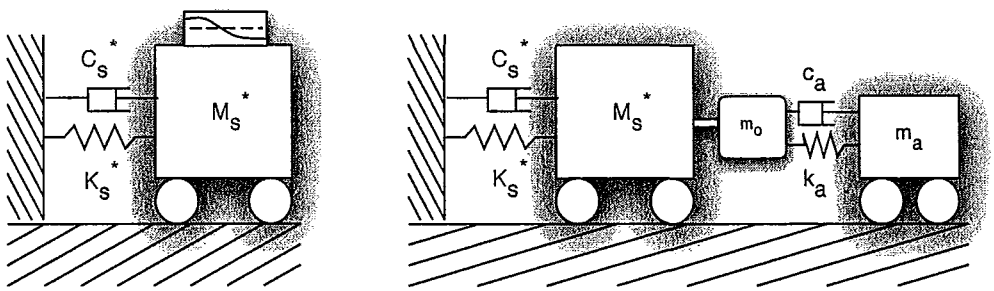

(a) Structure-TLD System

(b) Mechanical Representation of a Structure-TLD System

Figure 1.7: TLD Modelling (a), (b)

Chapter 2

Structural Modelling

2.1 Introduction

This chapter focuses on the details of the structural model with n number of TMDs used as well as the derivation of the equations of motion. Important parameters related to the structural model are introduced. An equivalent mechanical model for a TLD with rectangular tank is presented, followed by the necessary modifications to the original TMD model.

2.2 Structural Model Descriptions

The structural model is shown in Figure 2.1 with n number of TMDs attached. The structure is idealized as a rectangular block with two-degree-of-freedom, translation, x_s, and rotation, θ_s. Hence, the entire system has a total of $n+2$ degree-of-freedom. The idealized structure has a length of B and a width of D supported by two springs located at a distance of y_{s1} and y_{s2} from the centre of mass, CM, of the

structure. A total of three aspect ratio values, $B/D = 1$, 2 and 3, are considered. The two springs have independent stiffness values, k_{s1} and k_{s2}, such that the total lateral stiffness provided k_s is equal to $k_{s1} + k_{s2}$. The damping of the idealized structure is represented by the two dashpots with damping values of c_{s1} and c_{s2}. The structure is designed in such a way that the centre of mass (CM) does not coincide with the centre of resistance (CR). The centre of resistance is defined as the location where the resultant stiffness (k_s) acts on the structure. Thus, the structure will experience both lateral motion and torsional motion even when the structure is only excited in the lateral direction. The total torsional stiffness provided by the springs, k_θ, is equal to $k_{s1}{y_{s1}}^2 + k_{s2}{y_{s2}}^2$. The eccentricity ($e_s$), which is the distance between the centre of mass and the centre of resistance, of the structure can be related through the following relationship,

$$e_s = \frac{k_{s1}y_{s1} - k_{s2}y_{s2}}{k_s} \tag{2.1}$$

and it is selected to be 5% of B, which indicates torsional motion arises only due to accidental eccentricity in the structure (Uniform Building Code, 1997). Two important parameters that define the torsionally coupled system are the uncoupled lateral frequency, ω_s, and the uncoupled torsional frequency, ω_θ. The two uncoupled frequencies are defined as

$$w_s = \sqrt{\frac{k_s}{m_s}} \tag{2.2}$$

$$w_\theta = \sqrt{\frac{k_\theta}{m_s r^2}} \tag{2.3}$$

where m_s and r are the total mass and the radius of gyration of the structure, respectively. The ratio ω_θ/ω_s is defined as the uncoupled frequency ratio. A total of eight uncoupled frequency ratios, 0.5, 0.7, 0.8, 0.9, 1.0, 1.1, 1.2 and 1.3, for the numerical studies are investigated. The ratio is obtained by adjusting the structural parameters $(k_{s1}, k_{s2}, y_{s1}, y_{s2})$. For $\omega_\theta/\omega_s > 1.0$, the structure is defined as torsionally stiff while it is considered torsionally flexible when $\omega_\theta/\omega_s < 1.0$. For $\omega_\theta/\omega_s = 1.0$, the structure is strongly torsionally coupled. The modal damping ratio is assumed to be 2% in both the torsional and lateral modes of vibration, except for studies investigating the response behavior corresponding to structures with equal modal peak amplitude values. TMDs are placed at distances of $y_1, y_2, y_3...y_n$ from the CM of the main system. The properties of the i^{th} TMD are characterized by the stiffness and the damping, and are given by

$$k_i = m_i\omega_i^2 \tag{2.4}$$

$$c_i = 2\zeta_i m_i \omega_i \tag{2.5}$$

where m_i, c_i, k_i, ω_i and ζ_i are the mass, damping, stiffness, natural frequency and damping ratio of the i^{th} TMD, respectively. The tuning ratio, ν_i, which is defined as ratio of the natural frequency of the TMD to the structure's uncoupled translational frequency, and the mass ratio, μ_i, for the i^{th} TMD are defined as

$$\nu_i = \frac{\omega_i}{\omega_s} \tag{2.6}$$

$$\mu_i = \frac{m_i}{m_s} \tag{2.7}$$

The total mass ratio of the TMDs is given by

$$\mu = \sum_{i=1}^{n} \mu_i \tag{2.8}$$

Note that the tuning ratio, ν_i, is different from the definition in Chapter 1. The tuning ratio, previously defined as Ω (in Equation 1.3), is the ratio of the natural frequency of the TMD to the natural frequency of the mode being targeted. The tuning ratio parameter is defined as to the ratio of the natural frequency of the TMD to the structure's uncoupled translational frequency (see Equation 2.6) in the remaining chapters of the thesis.

2.3 Equations of Motion

The equations of motion are derived by applying the well-known Lagrange's equation (Beards, 1995)

$$\frac{\partial}{\partial t}(\frac{\partial T}{\partial \dot{q}_i}) - \frac{\partial T}{\partial q_i} + \frac{\partial V}{\partial q_i} + \frac{\partial (W_{nc})}{\partial \dot{q}_i} = Q_i \tag{2.9}$$

where q_i is the generalized coordinate, T is the total kinetic energy, V is the total potential energy, W_{nc} is the total energy dissipated and Q_i is the external forcing function. The total kinetic energy, potential energy and energy dissipation can be expressed as

$$T = \frac{1}{2} m_s \dot{x_s}^2 + \frac{1}{2} m_s r^2 \dot{\theta_s}^2 + \frac{1}{2} m_1 \dot{x_1}^2 + \cdots + \frac{1}{2} m_n \dot{x_n}^2 \tag{2.10}$$

$$V = \frac{1}{2}k_{s1}v_1{}^2 + \frac{1}{2}k_{s2}v_2^2 + \frac{1}{2}k_1(x_1 - u_1)^2 + \cdots + \frac{1}{2}k_i(x_i - u_i)^2 \quad (2.11)$$

$$W_{nc} = \frac{1}{2}c_{s1}\dot{v_1}{}^2 + \frac{1}{2}c_{s2}\dot{v_2^2} + \frac{1}{2}c_1(\dot{x_1} - \dot{u_1})^2 + \cdots + \frac{1}{2}c_i(\dot{x_i} - \dot{u_i})^2 \quad (2.12)$$

where v_1, v_2 and u_i (see Figure 2.2) are expressed as

$$v_1 = y_{s1}\theta_s + x_s \quad (2.13)$$

$$v_2 = x_s - y_{s2}\theta_s \quad (2.14)$$

$$u_i = y_i\theta_s + x_s \quad (2.15)$$

Substituting Equations 2.13, 2.14 and 2.15 into Equations 2.11 and 2.12, the total potential energy and the total energy dissipation are expressed as

$$V = \frac{1}{2}k_{s1}(x_s + y_{s1}\theta_s)^2 + \frac{1}{2}k_{s2}(x_s - y_{s2}\theta_s)^2 + \frac{1}{2}k_1(x_1 - (y_1\theta_s + x_s))^2 + \cdots + \frac{1}{2}k_i(x_i - (y_i\theta_s + x_s))^2 \quad (2.16)$$

$$W_{nc} = \frac{1}{2}c_{s1}(y_{s1}\dot{\theta_s} + \dot{x_s})^2 + \frac{1}{2}c_{s2}(\dot{x_s} - y_{s2}\dot{\theta_s})^2 + \frac{1}{2}c_1(\dot{x_1} - (y_1\dot{\theta_s} + \dot{x_s}))^2 + \cdots + \frac{1}{2}c_i(\dot{x_i} - (y_i\dot{\theta_s} + \dot{x_s}))^2 \quad (2.17)$$

Applying Lagrange's equation to Equations 2.10, 2.16 and 2.17, the equations of motion are obtained as shown in Equation 2.18

$$[M]\{\ddot{X}\} + [C]\{\dot{X}\} + [K]\{X\} = \{1\}f(t) \tag{2.18}$$

where $\{X\} = \{x_s, \theta_s, x_1, \ldots, x_n\}$ is the displacement vector. The mass, damping and stiffness matrices of size $(n+2)$ by $(n+2)$ are given as,

$$[M] = \begin{bmatrix} m_s & 0 & 0 & 0 & \cdots & 0 \\ & m_s r^2 & 0 & 0 & \cdots & 0 \\ & & m_1 & 0 & \cdots & 0 \\ & & & m_2 & \cdots & 0 \\ & & & & \ddots & \vdots \\ sym & & & & & m_n \end{bmatrix} \tag{2.19}$$

$$[C] = \begin{bmatrix} c_s + \sum c_i & c_{s\theta} + \sum c_i y_i & -c_1 & -c_2 & \cdots & -c_n \\ & c_\theta + \sum c_i {y_i}^2 & -c_1 y_1 & -c_2 y_2 & \cdots & -c_n y_n \\ & & c_1 & 0 & \cdots & 0 \\ & & & c_2 & \cdots & 0 \\ & & & & \ddots & \vdots \\ sym & & & & & c_n \end{bmatrix} \tag{2.20}$$

$$[K] = \begin{bmatrix} k_s + \sum k_i & k_{s\theta} + \sum k_i y_i & -k_1 & -k_2 & \cdots & -k_n \\ & k_\theta + \sum k_i {y_i}^2 & -k_1 y_1 & -k_2 y_2 & \cdots & -k_n y_n \\ & & k_1 & 0 & \cdots & 0 \\ & & & k_2 & \cdots & 0 \\ & & & & \ddots & \vdots \\ sym & & & & & k_n \end{bmatrix} \quad (2.21)$$

The above equations of motion are found to be in agreement with those obtained by Jangid and Datta (1997). The element c_s, $c_{s\theta}$ and c_θ are the modal damping matrix elements of the main system and can be expressed as $c_{s1} + c_{s2}$, $c_{s1}y_{s1} - c_{s2}y_{s2}$ and $c_{s1}y_{s1}^2 + c_{s2}y_{s2}^2$, respectively. The element $k_{s\theta}$ can be expressed as $k_s e_s$. The external forcing function, $f(t)$, applied at the centre of mass can be expressed as $\{1, 0, 0 \ldots, 0\}^T$.

2.4 Equivalent Mechanical Model for TLD

An analytical model was developed by Warnitchai and Pinkaew (1998) to determine the generalized properties for a rectangular TLD using Lagrange's equations and Morison's formula. The rectangular TLD is equipped with damping device located at the centre of tank and it is subjected to sinusoidal excitation. Tait (2008) expanded the model with multiple damping screens under random excitation using the concept of virtual work. The details of the analytical model are presented here and will be employed in the numerical studies.

2.4.1 Fluid Response

A rectangular TLD with damping screens is shown in Figure 2.3. The rectangular tank has a length of L, a quiescent fluid depth of h and a tank width of b. The screens are located at position x_j. The assumption of a rigid tank, inviscid, incompressible, irrotational flow and negligible surface tension are made. The sloshing motion in the damper with damping screens is formulated using potential flow theory. It is further assumed that the screens do not significantly alter the flow of sloshing fluid, and the response amplitude, η, is small as compared to the quiescent fluid depth, such that $h \gg \eta$. Employing the above assumptions, the velocity of a liquid particle relative to the tank can be expressed as the gradient of the velocity potential, $\phi(x, z, t)$. The kinematic continuity requires

$$\frac{\partial^2 \phi}{\partial x^2} + \frac{\partial^2 \phi}{\partial z^2} = 0 \tag{2.22}$$

The kinematic boundary conditions require the component of the velocity perpendicular to the ends walls and the bottom of the tank to be zero and can be expressed as

$$\frac{\partial \phi}{\partial x}|_{x=0,x=L} = 0 \tag{2.23}$$

$$\frac{\partial \phi}{\partial z}|_{z=-h} = 0 \tag{2.24}$$

At the free surface, the linearized kinematic boundary condition requires

$$\frac{\partial \phi}{\partial z}|_{z=0} = \frac{\partial \eta}{\partial t} \tag{2.25}$$

The solution that satisfies all boundary conditions is given in a general form as a sum of infinite sloshing modes, n, as (Warnitchai and Pinkaew, 1998)

$$\phi(x,z,t) = \sum_{n=1}^{\infty} \dot{q}_n(t) \frac{\cosh(\frac{n\pi(z+h)}{L}) \cos(\frac{n\pi x}{L})}{\frac{n\pi}{L} \sinh(\frac{n\pi h}{L})} \tag{2.26}$$

Substituting Equation 2.26 into Equation 2.25, the free surface response can be expressed as

$$\eta(x,t) = \sum_{n=1}^{\infty} q_n(t) \cos(\frac{n\pi x}{L}) \tag{2.27}$$

Therefore, the liquid sloshing motions can be described by a set of generalized coordinates, $q_n(t)$ where $n = 1, 2, 3 \ldots$. The gravitational potential, V, and the kinematic potential energy, T, for a system of standing waves of simple harmonic type can be expressed as (Lamb, 1932)

$$V = \frac{1}{2}\rho b g \int_0^L \eta^2(x,t)\, dx \tag{2.28}$$

$$T = \frac{1}{2}\rho b \int_{-h}^{o} \int_0^h [(\dot{X} + \frac{\partial \phi}{\partial x})^2 + (\frac{\partial \phi}{\partial z})^2]\, dx\, dz \tag{2.29}$$

where ρ is the density of the fluid and $\dot{X}$ is the horizontal velocity of the tank.

2.4.2 Additional Damping Due to Screens

The addition of damping to the TLD due to the installation of damping screens is attributed to the drag force, $f_d(x,z,t)$, which is a flow-induced force in the horizontal direction of flow (Morison *et al.*, 1950). The drag force is proportional to the square of the fluid velocity and can be expressed as (Tait, 2008)

$$f_{d_n}(x_j,z,t) = \frac{1}{2}\rho b C_l[\sin(\frac{n\pi x_j}{L})]^2[\frac{\cosh[\frac{n\pi(z+h)}{L}]}{\sinh(\frac{n\pi h}{L})}]^2|\dot{q}_n(t)|\dot{q}_n(t) \tag{2.30}$$

where C_l is the loss coefficient and ρ is the density of the fluid. A set of virtual horizontal displacements is given as

$$\delta q_n(x_j,z,t) = \frac{\cosh(\frac{n\pi(z+h)}{L})}{\sinh(\frac{n\pi L}{L})}\sin(\frac{n\pi x_j}{L})\partial q_n(t) \tag{2.31}$$

The virtual work done caused by the non-conservative drag forces can be expressed as

$$\delta W_{nc} = -\sum_{j=1}^{ns}\int_{-h}^{0} f_{d_n}\partial q_n\, dz \tag{2.32}$$

Substituting Equations 2.30 and 2.31 into Equation 2.32, the work done can be expressed as

$$\delta W_{nc} = -\frac{1}{2}\rho b C_l \sum_{j=1}^{ns}[\sin(\frac{n\pi x_j}{L})]^2|\sin(\frac{n\pi x_j}{L})| * \int_{-h}^{0}[\frac{\cosh(\frac{n\pi(z+h)}{L})}{\sinh(\frac{n\pi h}{L})}]^3 dz|\dot{q}_n|\dot{q}_n\partial q_n \tag{2.33}$$

Alternatively, the work done can be expressed in terms of the non-conservative non-linear damping forces in the direction of q_n as

$$\delta W_{nc} = -\sum_{j=1}^{ns} Q_n \partial q_n \tag{2.34}$$

and Q_n can be expressed in a compact form

$$Q_n = -\frac{\rho b L C_l}{2n\pi}\Delta_n \Xi_n |\dot{q}_n|\dot{q}_n \tag{2.35}$$

in which

$$\Delta = \frac{1}{3} + \frac{1}{[\sinh\frac{n\pi h}{L}]^2} \tag{2.36}$$

$$\Xi = \sum_{j=1}^{ns}[\sin(\frac{n\pi x_j}{L})]^2|\sin(\frac{n\pi x_j}{L})| \tag{2.37}$$

The solidity value, S, is defined as A/bh where A is the area of the screen normal to the flow. The drag coefficient, C_d, and the loss coefficient, C_l, are related through the

solidity as (Baines and Peterson, 1951; Fediw *et al.*, 1995; Tait *et al.*, 2005)

$$C_l = SC_d \tag{2.38}$$

For steady state flow, Baines and Peterson (1951) suggested the loss coefficient can be estimated as

$$C_l = [\frac{1}{C_c(1-S)} - 1]^2 \tag{2.39}$$

where C_c is a contraction coefficient and can be estimated as (Tait *et al.*, 2005)

$$C_c = 0.405e^{(-\pi S)} + 0.595 \tag{2.40}$$

for solidity values greater than 0.30. For solidity values less than 0.30, the relationship between C_l, C_d and S can be obtained from the modified curves presented by Baines and Peterson (1951), shown in Figure 2.4.

2.4.3 Generalized TLD Properties

By applying Lagrange's equations

$$\frac{\partial}{\partial t}(\frac{\partial T}{\partial \dot{q}_i}) - \frac{\partial T}{\partial q_i} + \frac{\partial V}{\partial q_i} = Q_i \tag{2.41}$$

the resulting equation of motion can be obtained and can be expressed as

$$m_n{}^*\ddot{q}_n(t) + c_n{}^*\dot{q}_n(t) + m_n{}^*\omega_n{}^2 q_n(t) = \gamma_n{}^*\ddot{X}(t) \tag{2.42}$$

where $n = 1, 2, 3 \ldots \infty$. Hence, the generalized mass, ${m_n}^*$, generalized stiffness, ${k_n}^*$, the natural frequency of the nth sloshing mode and the excitation factor, ${\gamma_n}^*$ can be expressed as follow

$$ {m_n}^* = \frac{1}{2} \frac{\rho b L^2}{n\pi \tanh(\frac{n\pi h}{L})} \tag{2.43} $$

$$ {k_n}^* = \frac{\rho b L g}{2} \tag{2.44} $$

$$ {\omega_n}^2 = \frac{n\pi g}{L} \tanh(\frac{n\pi h}{L}) \tag{2.45} $$

$$ {\gamma_n}^* = \rho b L^2 \frac{(1 - \cos(n\pi))}{(n\pi)^2} \tag{2.46} $$

The modal participation factor, Γ_n, is defined as

$$ \Gamma_n = \frac{{\gamma_n}^*}{{m_n}^*} \tag{2.47} $$

which can be expressed as

$$ \Gamma_n = \frac{2}{n\pi}(1 - \cos(n\pi)) \tanh(\frac{n\pi h}{L}) \tag{2.48} $$

2.4.4 Linearization of Damping Term

Since a TLD is usually designed to operate in its fundamental sloshing mode, the linearization of the damping term is applied to this mode exclusively. Consider

the nonlinear damping force as shown in Equation 2.35, the generalized damping force can be obtained by minimizing the error, ϵ, between the actual damping force and the linearized damping force (Caughey, 1963). The error can be expressed as follow

$$\epsilon = c^*\dot{q} - {c_{eq}}^*\dot{q} \tag{2.49}$$

$$\epsilon = C_l\frac{\rho bL}{2\pi}\Delta\Xi|\dot{q}|\dot{q} - c^*_{eq}\dot{q} \tag{2.50}$$

To minimize the error between the nonlinear and linearized terms, the following condition is required

$$\frac{\partial E(\epsilon^2)}{\partial c^*_{eq}} = 0 \tag{2.51}$$

where $E()$ is the expected value. The linearized damping term for the case subjected to random excitation was solved by Tait (2008) and is given as

$$c^*_{eq} = C_l\sqrt{\frac{2}{\pi}}\frac{\rho bL}{\pi}\Xi\Delta\sigma_q\omega \tag{2.52}$$

where σ_q is the root mean square (RMS) motion of the fluid response in the fundamental sloshing mode.

2.4.5 Equivalent Mechanical Properties

The equivalent mechanical properties can be obtained by modifying the equation of motion for a structure equipped with a continuous vibration absorber similar to Figure 1.7(a). Langrange's equation can be applied and results in the following

equations (Jacquot and Foster, 1977)

$$\begin{bmatrix} (M_s + \rho bhL) & \gamma^* \\ \gamma^* & m^* \end{bmatrix} \begin{Bmatrix} \ddot{X}_s \\ \ddot{q} \end{Bmatrix} + \begin{bmatrix} C_s & 0 \\ 0 & c^*_{eq} \end{bmatrix} \begin{Bmatrix} \dot{X}_s \\ \dot{q} \end{Bmatrix} + \begin{bmatrix} K_s & 0 \\ 0 & k^*_{eq} \end{bmatrix} \begin{Bmatrix} X_s \\ q \end{Bmatrix} = \begin{Bmatrix} F(t) \\ 0 \end{Bmatrix} \tag{2.53}$$

where q, M_s, K_s and C_s are the generalized coordinate related to the free surface motion, mass, stiffness and damping of the structure. In order to allow the direct use of linear TMD design procedures, the TLD properties has to be expressed in terms of an equivalent or effective TMD properties. This can be done by introducing a displacement variable, x_r, and can be expressed as

$$q = \Gamma x_r \tag{2.54}$$

where x_r is the relative motion between the motion of the structure and an equivalent TMD as shown in Figure 2.5. Substituting Equation 2.54 into Equation 2.53, multiplying the second row in Equation 2.53 by Γ and modifying the mass of the structure to account for the non-participating fluid's mass associated with the fundamental sloshing mode. The equation of motion of an equivalent structure-TMD system can

be expressed as

$$\begin{bmatrix} (M_s{}' + m_{eq}) & m_{eq} \\ m_{eq} & m_{eq} \end{bmatrix} \begin{Bmatrix} \ddot{X}_s \\ \ddot{x}_r \end{Bmatrix} + \begin{bmatrix} C_s & 0 \\ 0 & c_{eq} \end{bmatrix} \begin{Bmatrix} \dot{X}_s \\ \dot{x}_r \end{Bmatrix} + \begin{bmatrix} K_s & 0 \\ 0 & k_{eq} \end{bmatrix} \begin{Bmatrix} X_s \\ x_r \end{Bmatrix} = \begin{Bmatrix} F(t) \\ 0 \end{Bmatrix} \tag{2.55}$$

where $M_s{}'$ can be expressed as (Vandiver and Mitome, 1979)

$$M_s{}' = M_s + (\rho bhL - m_{eq}) \tag{2.56}$$

Thus, the equivalent mechanical properties for a TLD with multiple damping screens subjected to random excitation can be expressed as

$$m_{eq} = \frac{8\rho bL^2}{\pi^3} \tanh(\frac{\pi h}{L}) \tag{2.57}$$

$$k_{eq} = \frac{8\rho bLg}{\pi^2} \tanh^2(\frac{\pi h}{L}) \tag{2.58}$$

$$c_{eq} = C_l \frac{16\rho bL}{\pi^3} \sqrt{\frac{32}{\pi^3}} \tanh^3(\frac{\pi h}{L}) \Delta \Xi \omega \sigma_r \tag{2.59}$$

2.5 Modifications of TMD Model

To utilize the equivalent mechanical model developed by Tait (2008), the mass, stiffness and damping matrices shown in Equations 2.19 to 2.21 must be manipulated. Since not all of the fluid participates in the fluid sloshing motion, the non-participating fluid's mass, m_{o_i}, must be added to the structure, as shown in Figure 2.6. Introducing the relative motion, $x_{r_n} = x_n - x_s$, between the equivalent TMD and the structure, and substituting $x_n = x_{r_n} + x_s$ into Equations 2.10, 2.16 and 2.17. Lagrange's equation is applied to modify the equations of motion (Equation 2.18). The modified mass, damping, stiffness matrices and displacement vector can be expressed as

$$[M] = \begin{bmatrix} m_s{}' + \sum m_{eq_i} & 0 & m_{eq_1} & \cdots & \cdots & m_{eq_n} \\ 0 & I' & 0 & 0 & \cdots & 0 \\ m_{eq_1} & 0 & m_{eq_1} & \ddots & \ddots & 0 \\ \vdots & \vdots & 0 & m_{eq_2} & \ddots & 0 \\ \vdots & \vdots & \vdots & \ddots & \ddots & \cdots \\ m_{eq_n} & 0 & \cdots & \cdots & \cdots & m_{eq_n} \end{bmatrix} \tag{2.60}$$

$$[C] = \begin{bmatrix} c_s & c_{s\theta} & 0 & \cdots & \cdots & 0 \\ c_{s\theta} & c_\theta + \sum c_{eq_i} y_i{}^2 & -c_{eq_1} y_1 & -c_{eq_2} y_2 & \cdots & -c_{eq_n} y_n \\ 0 & -c_{eq_1} y_1 & c_{eq_1} & 0 & \cdots & 0 \\ \vdots & -c_{eq_2} y_2 & 0 & c_{eq_2} & \ddots & 0 \\ \vdots & \vdots & \vdots & \ddots & \ddots & \vdots \\ 0 & -c_{eq_n} y_n & 0 & \cdots & \cdots & c_{eq_n} \end{bmatrix} \tag{2.61}$$

$$[K] = \begin{bmatrix} k_s & k_{s\theta} & 0 & \cdots & \cdots & 0 \\ k_{s\theta} & k_\theta + \sum k_{eq_i} {y_i}^2 & -k_{eq_1} y_1 & -k_{eq_2} y_2 & \cdots & -k_{eq_n} y_n \\ 0 & -k_{eq_1} y_1 & k_{eq_1} & 0 & \cdots & 0 \\ \vdots & -k_{eq_2} y_2 & 0 & k_{eq_2} & \ddots & 0 \\ \vdots & \vdots & \vdots & \ddots & \ddots & \vdots \\ 0 & -k_{eq_n} y_n & 0 & \cdots & \cdots & k_{eq_n} \end{bmatrix} \tag{2.62}$$

$$\{X\} = \{x_s, \theta_s, x_{r_1}, x_{r_2}, \cdots, x_{r_n}\} \tag{2.63}$$

where $m_s{}'$ is the summation of the mass of the structure and the total non-participating fluid mass, $\sum m_{o_i}$; I' is the summation of the moment of inertia of the structure and the additional moment of inertia from the non-participating fluid mass, ${m_{o_i}}{y_i}^2$. The modifications made here allow the use of the equivalent mechanical model for a TLD developed by Tait (2008).

2.6 Verification of Numerical Optimization Technique

The equations described perviously and the mechanical model developed in this chapter are utilized for numerical studies, which include torsionally coupled systems installed with TMDs under harmonic excitation and torsionally coupled systems equipped with TMDs or TLDs under random excitation. Numerical simulations are performed by employing MATLAB(r2007b) optimization toolboxes (fminimax and fmincon) such that the optimal parameters, which include the tuning ratio values,

damping ratio values and mass ratio values are obtained by minimizing the targeted response parameter. The fminimax toolbox is employed to target the peak response of the system whereas the fmincon toolbox is utilized to reduce the overall vibration energy of the system which is related to the area bounded by the mechanical admittance function.

The optimization toolbox fmincon is employed to minimize the area bounded by the mechanical admittance function when a structure is subjected to random excitation. The fmincon optimization toolbox is able to find a minimum of a constrained nonlinear multivariable function. The area bounded by the mechanical admittance function is expressed as an input function and solved numerically by inputing an initial estimate of the absorbers parameters. By imposing a convergent criterion to the optimization toolbox, the area bounded by the mechanical admittance function is minimized such that the corresponding absorbers parameters and the minimized response are returned. The optimization toolbox was verified by comparing the absorber parameters and the minimized response obtained with results obtained by Asami *et al.* (2002). The tuning ratio and the damping ratio values for a two-degree-of-freedom undamped structure-TMD system with a mass ratio value of $\mu = 0.01$ were found to be 0.932 and 0.153, respectively, which match closed-form values obtained by Asami *et al.* (2002).

The optimization toolbox fminimax is employed to minimize the peak response on the frequency response function plot when a structure is subjected to harmonic excitation. The fminimax optimization toolbox minimizes the worst-case value of a set of multivariable function starting at an initial estimate. The maximum peak

response is solved numerically by inputing an initial estimate of the absorbers' parameters and expressed as an input function. By imposing a convergent criterion to the optimization toolbox, the maximum peak response is minimized such that the corresponding absorbers parameters and the minimized peak response are returned. The optimization toolbox was verified by comparing the absorber parameters and the minimized response obtained with the result obtained by Asami *et al.* (2002). The optimal tuning ratio and the damping ratio values for a two-degree-of-freedom undamped structure-TMD system with a mass ratio of $\mu = 0.01$ were found to be 0.909 and 0.185, respectively, which match closed-form values with those obtained by Asami *et al.* (2002).

2.7 Chapter Figures

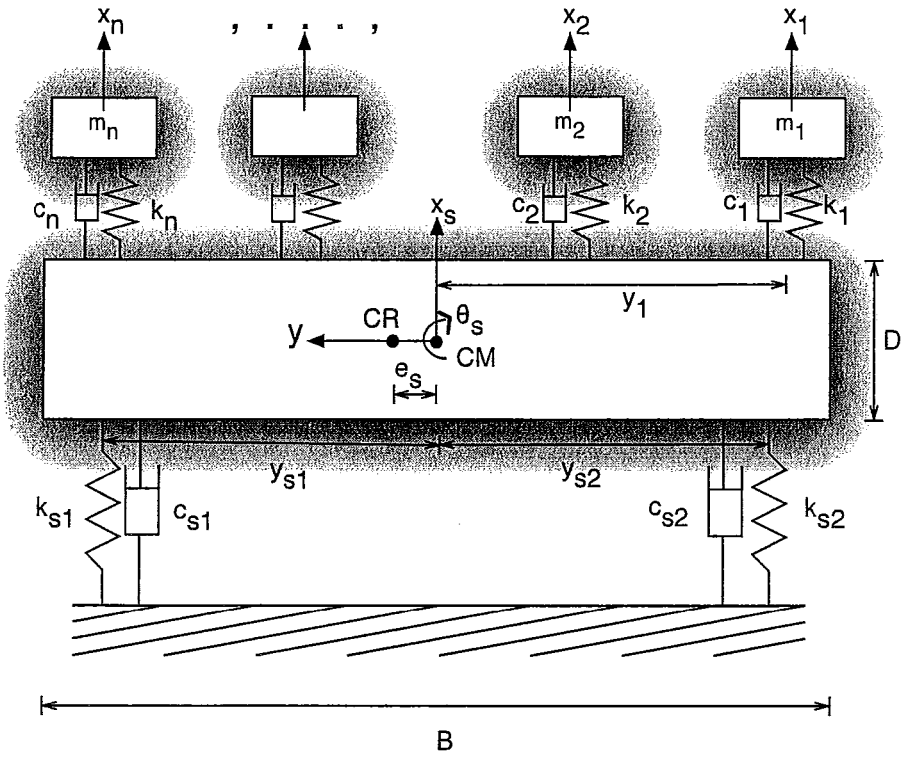

Figure 2.1: A Schematic of Torsionally Coupled System Equipped with TMDs

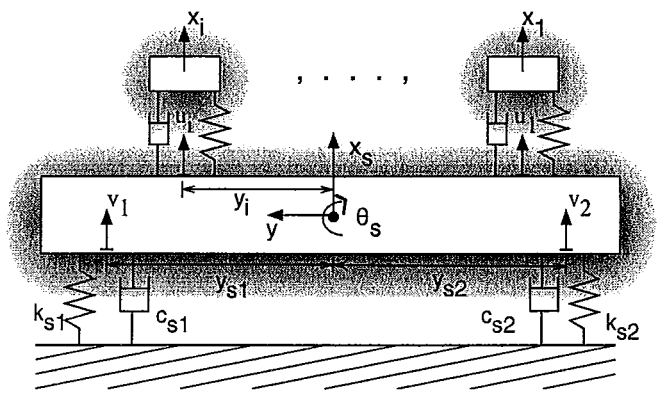

Figure 2.2: Symbolic Explanation for the Development of Equations of Motion

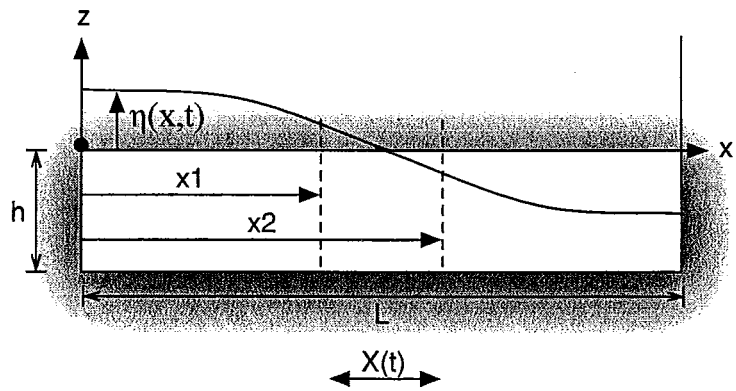

Figure 2.3: A Schematic of a Rectangular TLD Equipped with Damping Screens

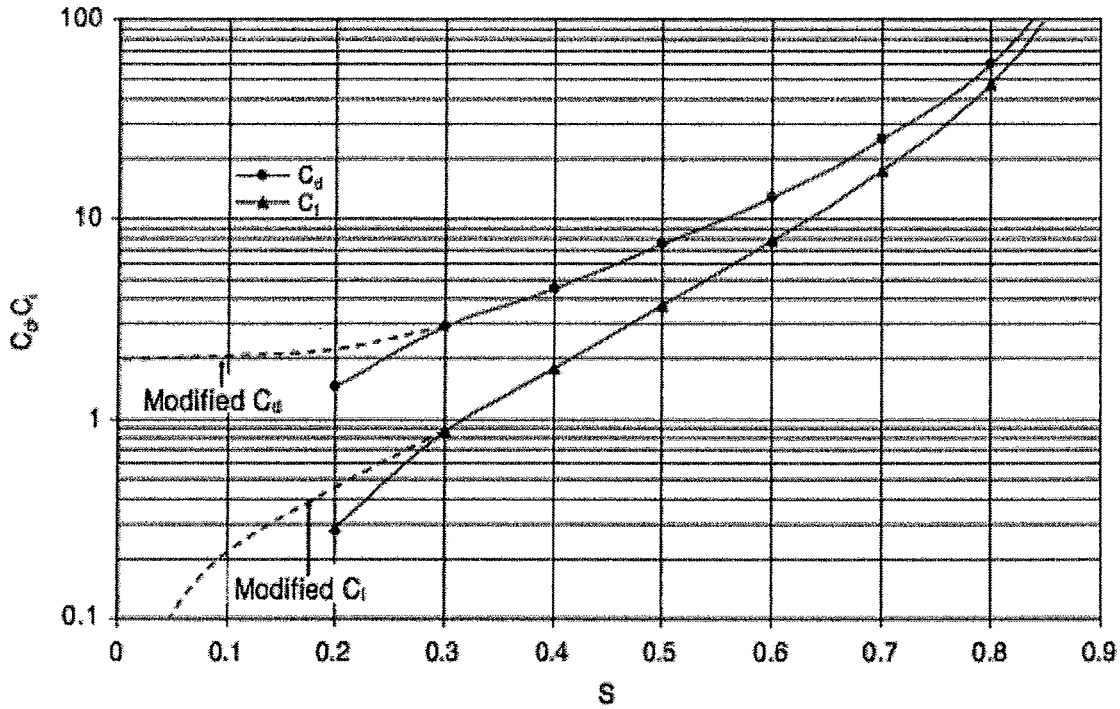

Figure 2.4: Relationship between C_c, C_l and S
(taken from Tait *et al.*, 2005)

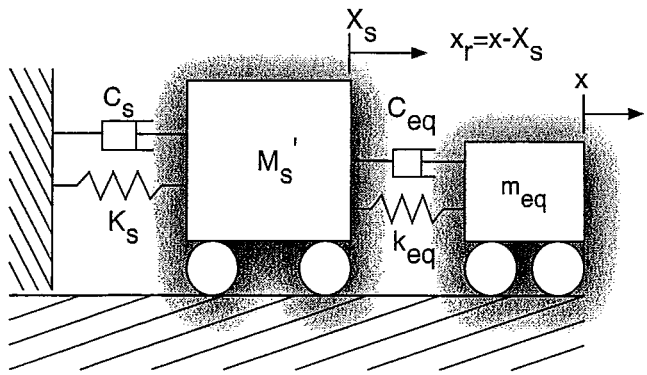

Figure 2.5: Equivalent TMD Model

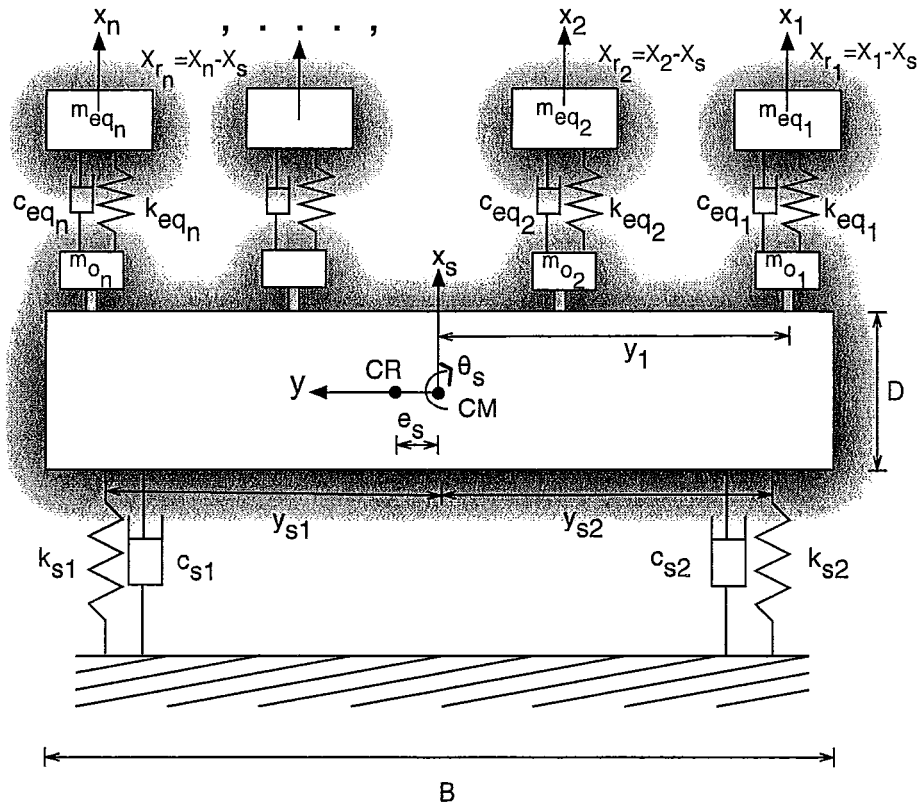

Figure 2.6: A Schematic of the Equivalent Mechanical Model of Torsionally Coupled System Equipped with TLDs

Chapter 3

Torsionally Coupled Structures Equipped with TMD(s) subjected to Harmonic Excitation

3.1 Introduction

This chapter reports on an investigation into the response behavior of torsionally coupled systems, equipped with multiple TMDs, under harmonic excitation. The numerical study is divided into two parts. Part 1 investigates structures with equal modal damping ratio values of 2% in both modes of vibration. Part 2 investigates structures with unequal modal damping ratio values such that two peaks of equal amplitude appear in the frequency response function plot of each structure considered (without the presence of dampers). The uncoupled frequency ratio values are selected to be 0.5, 0.7, 0.8, 1.0 1.2 and 1.3 for Part 1. For Part 2, uncoupled frequency ratio values of 0.8, 1.0 and 1.2 are considered.

The response parameter of interest, which is used as the objective function in the optimization program, is first introduced. Next, results from the numerical study conducted on structures with equal modal damping ratio values and equal modal peak amplitude values equipped with various TMD arrangements are presented. Finally, the efficiency of the proposed TMD arrangements for both Part 1 and Part 2 is evaluated and discussed.

3.2 Minimization of Response Parameter and Performance Indices

3.2.1 Response Parameter of Interest

In this chapter, the excitation force acting on the structure is modelled as a harmonic force

$$f(t) = f_o e^{i\omega t} \tag{3.1}$$

where ω is the forcing frequency, f_o is the amplitude of excitation and $i = \sqrt{-1}$. The corresponding steady state response of the system can be obtained by solving the equations of motion of the system (see Equation 2.18). The maximum dynamic response (maximum displacement) of the building, which this study focuses on, occurs at the building corners. The corner displacements are expressed as

$$x_{c_1,c_2} = x_s \pm \theta_s \frac{B}{2} \tag{3.2}$$

where B is the length of the structure (see Figure 2.1), x_s and θ_s are the structure's translational and rotational (torsional) motions, respectively. Thus, the dynamic response represents the maximum displacement that the building experiences.

3.2.2 Performance Indices

The maximum displacement serves as the objective function, which is minimized by utilizing MATLAB (r2007b) optimization toolbox (fminimax) such that the lowest peak response is obtained. This numerical optimization technique was previously verified in Chapter 2. In addition, a numerical searching technique, which involves inputing a wide range of tuning ratio and damping ratio values to study the structural response, is used to confirm the results obtained from the optimization toolbox (fminimax) in MATLAB (r2007b) are the lowest response values that can be obtained.

The dynamic response is normalized by the static displacement

$$\delta_{st} = f_o/k_s \tag{3.3}$$

where k_s is defined as $k_{s1} + k_{s2}$, at the CM of the main system and is defined as the dynamic magnification factor (DMF)

$$R = \frac{Dynamic\ Response\ of\ the\ Main\ Structure\ with\ TMD(s)}{\delta_{st}} \tag{3.4}$$

In order to evaluate the effectiveness of the proposed TMD configurations, a response reduction factor is introduced and is defined as the ratio of the peak dynamic response of the structure equipped with TMD(s) to the peak dynamic response of the structure

without TMD(s)

$$R_o = \frac{Dynamic\ Response\ of\ the\ Main\ Structure\ with\ TMD(s)}{Dynamic\ Response\ of\ the\ Main\ Structure\ without\ TMD(s)} \quad (3.5)$$

Therefore, the response reduction factor, R_o, indicates the effectiveness of the TMD configuration. A value less then unity indicates that TMD configuration is effective for vibration control. The efficiency, ψ, is the parameter used to compare the performance of different TMD configurations and is defined as

$$\psi = 1 - R_o \quad (3.6)$$

The forcing frequency ratio is defined as ratio of the forcing frequency to the uncoupled translational frequency

$$\beta = \frac{\omega}{\omega_s} \quad (3.7)$$

Note that the forcing frequency ratio differs from that of α previously defined in Chapter 1.

3.3 Study of Structures with Equal Modal Damping Ratio Values

The frequency response function plots of the structures considered in this study (without TMD(s)), are shown in Figure 3.1 and the corresponding undamped mode shapes are shown in Figures 3.2 to 3.7. The peak dynamic response values and

undamped mode shapes are given in Table 3.1. Listed below are the structure-TMD configurations considered in this study

1. - Single TMD Configuration;
2. - Two Identical TMDs Configuration;
3. - Two Different TMDs Configuration;
4. - Four TMDs (Approach-I) Configuration;
5. - Four TMDs (Approach-II) Configuration.

For each TMD configuration, two total mass ratio values, $\mu = 0.01$ and $\mu = 0.02$, are considered in order to investigate the influence of this parameter on the dynamic response behavior of the systems investigated.

3.3.1 Single TMD Configuration

Typically, a single TMD is placed at the centre of mass of a structure which only responds in translational motion (i.e. no torsional motion). This section investigates the influence of the location of a single TMD on a structure with combined translational and torsional response motion. The following seven TMD locations for each of the six uncoupled frequency ratios considered in this study are listed below (see Figure 3.8).

1. $y_1 = -B/2$;
2. $y_1 = -B/3$;
3. $y_1 = -B/6$;

4. $y_1 = 0$;

5. $y_1 = B/6$;

6. $y_1 = B/3$;

7. $y_1 = B/2$.

3.3.1.1 Single TMD Results - Harmonic

The rationale for placing a TMD at various locations, other than at the centre of mass of the structure, is to minimize the torsional response component. Frequency response function plots determined from the numerical optimization process for four different uncoupled frequency ratios are shown in Figure 3.9. The frequency response function plots shown correspond to TMD locations where maximum and minimum efficiency was found to occur. In addition, the frequency response function plot corresponding to the centre of mass TMD location is also shown. The remaining frequency response function plots corresponding to other uncoupled frequency ratios and TMD locations can be found in Appendix A.

Interesting dynamic response behavior characteristics can be observed from the frequency response function plots shown in Figure 3.9. For example, for $\omega_\theta/\omega_s = 0.8$ and 1.0, a double peak occurs on the lower frequency mode at the location where minimum efficiency is achieved. This occurs as a result of the coupling between modes 1 and 2 and the lower frequency mode having a significant torsional response component.

Response performance indices are summarized in Figures 3.10 to 3.16. Figures 3.10 and 3.11 show the minimized response (R) for different TMD locations for $\mu =$

0.01 and $\mu = 0.02$, respectively. It can be observed from Figures 3.10 and 3.11 that placing the TMD at the centre of mass does not result in the lowest response of the system for a given ω_θ/ω_s ratio value. In fact, this location results in the minimum efficiency for the torsionally flexible structures ($\omega_\theta/\omega_s = 0.5$ and 0.7). It can also be observed from these two figures that for ω_θ/ω_s of 0.8 and 1.0, the dynamic response is sensitive to TMD location relative to other ω_θ/ω_s ratios. This can be concluded from the large variation in R obtained for different TMD locations within each ω_θ/ω_s ratio (see Figures 3.10 and 3.11). This sensitivity to TMD location is due to the strong coupling between modes. This coupling between modes causes the response of one mode to be significantly influenced by the contribution from the other mode. Also, as the TMD location is modified, the response of the two modes change. Thus, the change in response, due to a change in TMD location, is amplified due to the strong coupling. As a result, the response becomes sensitive to TMD location. Finally, Figures 3.10 and 3.11 show that the torsionally stiff structures considered in this study are less sensitive to TMD location. The reduction in sensitivity to TMD location is a result of the negligible torsional contribution to the overall dynamic response of the structure.

From Figure 3.12, the influence of TMD location for each ω_θ/ω_s ratio can be readily observed. For ω_θ/ω_s=0.5, which is the most torsionally flexible structure considered in this study, placing a single TMD at the centre of mass results in the highest response reduction factor (R_o), which indicates the lowest effectiveness. For the strongly torsionally coupled system (i.e. ω_θ/ω_s=1.0), the highest response reduction factor was found to occur at $B/3$ and not at the centre of mass. This highlights the importance of considering TMD location during the design of a strongly

torsionally coupled system. For the torsionally stiff structures, the highest response reduction factor occurs at $B/2$. This is due to the reduced motion experienced by the TMD in mode 1 (see Figures 3.6 and 3.7).

In Figure 3.12, focusing on the torsionally stiff structures (i.e. $\omega_\theta/\omega_s = 1.2$ and 1.3), a clear trend can be observed in the reduction in response for $\omega_\theta/\omega_s = 1.3$ as the TMD is moved from $-B/2$ to $B/2$ for both mass ratio values. However, for $\omega_\theta/\omega_s = 1.2$ and a mass ratio value of 0.02, a different trend is observed. In order to verify the optimized results, a parametric study is conducted to investigate the response behavior of $\omega_\theta/\omega_s = 1.2$. This study involves utilizing the optimal tuning parameters obtained from the literature to target the response of mode 1 (the translational dominant mode). The TMD is located at the centre of mass and mass ratio values of 0.01 and 0.02 are considered. The frequency response function plots for the two mass ratio values along with the peak response values are shown in Figures 3.13 and 3.14. It can be observed from these two figures that the response in mode 2 is insensitive to the change in mass ratio value. These findings are in agreement with the results obtained utilizing MATLAB (r2007b) to target the response of the entire system.

Figures 3.15 and 3.16 show the minimum and maximum efficiency for each ω_θ/ω_s ratio with corresponding TMD location. It can be observed that the lowest TMD efficiency is obtained for the torsionally flexible structures. As the structures become more torsionally stiff, it is found that the efficiency increases. However, the efficiency reduces for the strongly torsionally coupled system. The efficiency is found to increase with increased mass ratio for all uncoupled frequency ratios investigated in this study.

3.3.2 Two Identical TMDs Configuration

This section discusses the dynamic response of structures equipped with two identical TMDs. The two identical TMDs have the same mass ratio, tuning ratio and damping ratio values. The locations of the paired TMDs are as follows (see Figure 2.1)

1. $y_1 = -B/2$, $y_2 = B/2$;
2. $y_1 = -B/3$, $y_2 = B/3$;
3. $y_1 = -B/6$, $y_2 = B/6$.

3.3.2.1 Two Identical TMDs Results - Harmonic

Frequency response function plots for ω_θ/ω_s = 0.5, 0.8, 1.0 and 1.2, respectively, are shown in Figure 3.17. The remaining frequency response function plots can be found in Appendix B. It is noted that for this particular TMD configuration, a double peak in mode 1, which was found for the single TMD configuration, does not occur in ω_θ/ω_s ratio values of 0.8 and 1.0. In addition, the maximum peak amplitude corresponding to mode 1 is significantly less for the strongly torsionally coupled system equipped with two identical TMDs compared to the same system equipped with a single TMD.

The plots of the dynamic magnification factor for all uncoupled frequency ratios and TMD location are shown in Figure 3.18 for μ=0.01 and Figure 3.19 for μ=0.02. Results indicate that strongly coupled systems (ω_θ/ω_s = 0.8 and 1.0) are not as sensitive to TMD location when equipped with two identical TMDs. Furthermore, as the structure becomes torsionally stiff (i.e. ω_θ/ω_s = 1.2 and 1.3), the dynamic

response converges within each ω_θ/ω_s ratio, even when the TMDs locations are adjusted. This is a result of the insignificant torsional response when the structure is torsionally stiff, and unlike a single TMD, the two identical TMDs do not induce any additional torsional motion.

Figure 3.20 shows the response reduction factor for all six uncoupled frequency ratios investigated. For all cases, the lowest response reduction factor was obtained when the paired TMDs were placed at $y_1 = -B/2$ and $y_2 = B/2$. Thus, placing the two identical TMDs at the maximum distance from the centre of mass gives the lowest dynamic response. This is in agreement with research finding by Lin *et al.* (1999). Finally, it is noted that torsionally stiff systems are insensitive to TMD location for this configuration.

Figures 3.21 to 3.22 show the maximum and minimum efficiency values for this TMD configuration. These figures confirm that greater efficiency is achieved as the TMDs are placed further apart. It can also be observed that increasing the mass ratio increases the efficiency independent of TMD location. This configuration is inefficient for torsionally flexible systems and most efficient for strongly torsionally coupled system.

3.3.3 Two Different TMDs Configuration

This section investigates the response behavior of torsionally coupled systems equipped with two different TMDs. In this configuration, the two TMDs have different mass ratio, tuning ratio and damping ratio values. However, the total mass ratio values considered are $\mu = 0.01$ and $\mu = 0.02$.

3.3.3.1 Two Different TMDs Results - Harmonic

The frequency response function plots for this configuration, shown in Figure 3.23, are significantly different than those obtained for the two previous TMD configurations considered. It is evident from the double peaks occurring in both mode 1 and 2, for the torsionally flexible and strongly torsionally coupled systems, that one of the TMDs is tuned to mode 1 while the other is tuned around to mode 2. This highlights the benefit of employing two independent TMDs. The remaining frequency response function plots can be found in Appendix C.

Figures 3.24 and 3.25 show the dynamic magnification factor for two different TMDs configuration having total mass ratio values of $\mu = 0.01$ and $\mu = 0.02$, respectively. The two different TMDs configuration is found to be significantly less sensitive to TMD location for the strongly torsionally coupled system compared to two identical TMDs configuration. This is a direct result of the ability to target both modes, 1 and 2, simultaneously. However, the dynamic magnification factor does not converge to a unique value for the torsionally stiff structures as rapidly as that of the two identical TMDs configuration. This is due to the fact that the unequal TMDs masses, for the case with two different TMDs, induce additional torsional motion to the system.

The influence of TMD location on the response reduction factor is shown in Figure 3.26. The trends are similar to those of the two identical TMDs configuration. However, inspection of Figures 3.27 and 3.28 highlight the robustness of this configuration. It can be seen that the maximum efficiency remains relatively constant over a range of uncoupled frequency ratios. For this particular configuration, significant reduced efficiency occurs for both the torsionally flexible and torsionally stiff systems.

3.3.4 Four TMDs Configuration

3.3.4.1 Approach-I

Numerical simulation results for structures equipped with four TMDs are presented in this section. In Approach-I, the four TMDs, which all have the same mass ratio value (i.e. $\mu_1 = \mu_2 = \mu_3 = \mu_4$), are grouped such that two TMDs form a pair of TMDs located opposite one another with the same tuning ratio and damping ratio values. Thus, a total of two pairs of identical TMDs are used. For instance, TMD-1, located at $-B/2$ is paired with TMD-3, located at $B/2$, having the same properties, mass ratio, tuning ratio and damping ratio values (i.e. $\nu_1 = \nu_3$; $\zeta_1 = \zeta_3$; $\nu_2 = \nu_4$ and $\zeta_2 = \zeta_4$). However, the non-paired TMDs have different tuning ratio and damping ratio values (i.e. $\nu_1 \neq \nu_2$ and $\zeta_1 \neq \zeta_2$). The arrangement of the TMDs considered are as follows (see Figure 2.1)

1. $y_{1,2} = -B/2$, $y_{3,4} = B/2$;
2. $y_{1,2} = -B/3$, $y_{3,4} = B/3$;
3. $y_{1,2} = -B/6$, $y_{3,4} = B/6$.

3.3.4.2 Approach-I Results - Harmonic

Inspection of the frequency response function plots in Figure 3.29 show that the two double peak modes observed for the two different TMDs configuration does not occur for this configuration. This is a result of enforcing the same mass ratio for all TMDs. The remaining frequency response function plots corresponding to the other uncoupled frequency ratios considered are shown in Appendix D.

The dynamic magnification factors for both mass ratio values investigated are shown in Figures 3.30 and 3.31. Similar to the case of two identical TMDs, the dynamic magnification factor converges for the torsionally stiff structures. The sensitivity to TMD location for the strongly torsionally coupled system is found to be greater for this configuration than for the two identical TMDs configuration. Again, similar trends are found for the response reduction factor, shown in Figure 3.32, as those observed for both two identical and two different TMD configurations. The efficiency plots shown in Figures 3.33 and 3.34 indicate this configuration is most efficient in the strongly torsionally coupled systems.

3.3.4.3 Approach-II

Numerical simulation results for a structure equipped with four TMDs (Approach-II) are presented in this section. The difference between Approach-I and the Approach-II is the difference in TMD mass ratio values. The mass ratio values of the paired TMDs located opposite one another are equivalent, however, their mass ratio values are not the same as the other paired TMDs. For instance, the mass ratio value of TMD-1 is equal to TMD-3 and the mass ratio value of TMD-2 is equal to TMD-4 (i.e. $\mu_1 = \mu_3$ and $\mu_2 = \mu_4$). Note that the mass ratio value of TMD-1 is not the same as that of TMD-2 (i.e. $\mu_1 \neq \mu_2$). However, the summation of the mass ratio values for the two paired TMDs is equal to the total mass ratio values considered (i.e. 0.01 and 0.02). The tuning ratio and the damping ratio relationship of the TMDs are the same as in Approach I. The TMD locations selected are the same as that for Approach I.

3.3.4.4 Approach-II Results - Harmonic

The frequency response function plots observed in Figure 3.35 are found to differ from those obtained for Approach I but are similar to that of two different TMDs configuration. This is a result of allowing the mass ratio values of the TMDs to be varied. Thus, each of the TMDs can be optimally tuned to target the response of the two modes. The remaining frequency response function plots can be found in Appendix E corresponding to this TMD configuration. Observing the dynamic magnification factors in Figures 3.36 and 3.37, the response reduction factors in Figure 3.38 and the maximum and minimum efficiency obtained in Figures 3.39 and 3.40, similar trends can be observed as compared to Approach I. Although both approaches perform approximately the same when the structure is torsionally stiff, as the structure makes a transition from strongly torsionally coupled to torsionally flexible, Approach II performs slightly better than Approach I. This further validates that a more efficient system can be obtained when greater freedom is permitted in selecting the TMD design parameters. This finding is in agreement with previous research finding by Singh *et al.* (2002).

3.3.5 Evaluation of Different TMD Configurations

Frequency response function plots corresponding to TMD locations that result in maximum efficiency for each configuration are presented in Figure 3.41. These frequency response function plots clearly indicate that the two different TMDs configuration is most effective in simultaneously reducing both modes 1 and 2. As stated previously, this response behavior occurs as this configuration allows a TMD to be tuned around mode. This is evident for the torsionally stiff and strongly torsionally

coupled systems. For the torsionally stiff structures considered in this study, mode 1 amplitude is significantly greater than mode 2. Thus, for these two torsionally stiff systems, both TMDs target mode 1. The four TMDs, Approach II, produces similar frequency response function plots. However, the constrains on the mass of the paired TMDs (i.e $\mu_1 = \mu_3$ and $\mu_2 = \mu_4$) reduces this configuration efficiency compared to two different TMDs configuration. The additional mass constraints placed on Approach I, (i.e $\mu_1 = \mu_3 = \mu_2 = \mu_4$) further reduces the efficiency of the four TMDs configuration. It should be noted, however, that all configurations lead to a reduction in the response of the original uncontrolled system.

Figures 3.42 and 3.43 compare the maximum efficiency achieved for five configurations investigated. It can be observed that at least two TMDs are required to reduce the dynamic response of the strongly torsionally coupled system. This is due to the mass coupling term generated by a single TMD do not aid in reducing the response effectively when two modes are strongly coupled. Also, at least two different tuning ratios are required to suppress the dynamic response of the torsionally flexible structures effectively. This is due to the strong torsional motion associated with the structures. Thus, the two TMDs (or paired TMDs) can be tuned differently such that one can be tuned to target mode 1 and the other can be tuned to target mode 2. As for the torsionally stiff structures, the dynamic response is insensitive to the five configurations that have been considered. It is evident that a single TMD is inefficient in reducing the response of strongly torsionally coupled system. Also, as expected, the efficiency of the TMD increases as the mass ratio value is increased. It can also be observed that the efficiency of the TMD configurations can be categorized according to the nature of the structures, which are torsionally flexible, strongly coupled and

torsionally stiff. For the torsionally flexible structures (i.e. $\omega_\theta/\omega_s = 0.5$, 0.7 and 0.8), the descending order of efficiency is as follow,

1. Two Different TMDs
2. Four TMDs
3. Single TMD
4. Two Identical TMDs

whereas for the case of the strongly torsionally coupled structure

1. Two Different TMDs
2. Four TMDs
3. Two Identical TMDs
4. Single TMD

For cases when the structures are torsionally stiff (i.e. $\omega_\theta/\omega_s = 1.2$ and 1.3), the descending order of efficiency is

1. Two Different TMDs
2. Single TMD
3. Four TMDs
4. Two Identical TMDs

In all cases, the two different TMDs configuration is the most efficient configuration considered in this study.

3.3.6 Optimal TMD Parameters - Harmonic

For the six uncoupled frequency ratios considered, the optimal parameters corresponding to the TMD location resulting in maximum efficiency are given in Tables 3.2 and 3.3. The parameters optimized for each mass ratio are the tuning ratio and the TMD damping ratio. The optimal parameters determined for all other locations considered for each uncoupled frequency ratio investigated can be found in Appendix A to Appendix E.

3.4 Study of Structures with Equal Modal Peak Amplitude Values

This section investigates the dynamic response of structures with unequal modal damping ratio values such that the modal peak amplitude values of mode 1 and mode 2 are equal. The two peaks in the frequency response function plot are adjusted to the same amplitude by manipulating the damping parameters, c_{s1} and c_{s2}. The damping ratio value in each mode of vibration after adjusting c_{s1} and c_{s2} deviates less than 0.5% from the original damping ratio value of (2%). The uncoupled frequency ratios investigated are 0.8, 1.0 and 1.2. The objective of the study is to investigate the response behavior of structure-TMD systems having equal modal peak amplitude values and compare this response behavior to that of structures having equally damped modes. The same structure-TMD configuration, TMD locations and two mass ratio values were investigated in this study. Frequency response function plots of the structures without TMD(s) are shown in Figure 3.44. The undamped mode shapes corresponding to these three structures are shown in Figures 3.4, 3.5

and 3.6 corresponding to $\omega_\theta/\omega_s = 0.8$, 1.0 and 1.2 respectively. The peak response and modal damping values are presented in Table 3.4.

3.4.1 Single TMD Results - Harmonic

The dynamic response of the structures equipped with a single TMD are first investigated. The TMD locations are selected to match the previous study for structures with equal modal damping ratio values equipped with a single TMD. Consistent with previous study, the response behavior for two different mass ratio values ($\mu = 0.01$ and $\mu = 0.02$) was also considered.

Comparing Figure 3.45 to Figure 3.9, it is evident the frequency response function plots corresponding to the torsionally coupled systems differ significantly. This is a result of both modes having the same influence on the response, unlike the previous case where a dominant mode (mode 1) was clearly evident. Additional frequency response function plots corresponding to this TMD configuration can be found in Appendix F.

Inspection of the dynamic magnification factor given in Figures 3.46 and 3.47, shows that for the single TMD configuration the torsionally stiff structures are found to be sensitive to TMD location unlike that of equally damped structures. Again, this is due to the increased level of torsional response for the structures having equal modal peak amplitude values.

The response reduction factor plots for this TMD configuration are shown in Figure 3.48. The shape of the response reduction factor plots are different than those for the structures having equal modal damping values. For example, the response plot, corresponding to $\omega_\theta/\omega_s = 0.8$ mirrors that of $\omega_\theta/\omega_s = 1.2$. In addition, the plot

corresponding to the strongly torsionally coupled system indicates that there are now two TMD locations where a single TMD is ineffective. For the torsionally flexible systems, the optimal location is found to be at $B/2$ whereas for the torsionally stiff systems, the optimal location is at $-B/2$. Interestingly, for the strongly torsionally coupled system, the optimal location is either at $B/2$ or $-B/2$. Comparing Figures 3.48 and 3.12, it is evident that the structural response patterns have changed as a result of modifying the modal damping of the structure. Thus, the dynamic response behavior appears to be sensitive to small changes in structural damping. This sensitivity to structural damping appears to contradict previous research findings. Warburton and Ayorinde (1980) have shown that the damping in a lightly damped structure can be completely neglected without influencing optimized TMD performance. However, this previous research focused on targeting a single mode whereas this study focuses on reducing the response of a coupled structure. In this single TMD configuration, only one tuning ratio value can be selected to reduce the response of the coupled system. Thus, the TMD is either tuned to one of the modes of the structure or tuned to a frequency falls in between the natural frequencies of the structure. As a result, either one mode is neglected or the TMD is mistuned to both modes (i.e. the reduction in response in both modes is not as significant as that obtained from tuning the TMD to reduce the response of a single mode). Thus, a slight adjustment in the modal damping ratio values results in signifiant changes in the frequency response of the optimized system.

The efficiency plots, shown in Figures 3.49 and 3.50, indicate the lowest efficiency occurs for the strongly torsionally coupled system. Furthermore, for this particular uncoupled frequency ratio, as the mass ratio is increased, the location

resulting in maximum efficiency changes from $B/2$ to $-B/2$.

It can been seen in Figure 3.51 that for the damping ratio values and ω_θ/ω_s ratios considered, a single TMD is more efficient in reducing the dynamic response of the torsionally coupled structures with equal damping ratio values. As mentioned previously, for the case of a structure with equal damping ratio values, the TMD can be tuned around the largest contributing mode, which is not the case for a structure with equal modal peak amplitude values. Thus, a single TMD is more efficient in reducing the response of a structure which has two modes that contribute unequally to the total response.

3.4.2 Two Identical TMDs Results - Harmonic

This section presents the dynamic response of torsionally coupled structures with equal modal peak amplitude values equipped with two identical TMDs. The TMD locations examined in this section for ω_θ/ω_s =0.8, 1.0 and 1.2 are the same as those investigated in Section 3.3.2.

Figure 3.52 shows the frequency response function plots for the three uncoupled frequency ratios investigated. The remaining frequency response function plots corresponding to other TMD locations can be found in Appendix G. The shape of frequency response function plots for $\omega_\theta/\omega_s = 0.8$ and 1.0 are found to be similar to those corresponding to the structures with matching ω_θ/ω_s ratio values having equal modal damping values (see Figure 3.17). As for the torsionally stiff structure (i.e $\omega_\theta/\omega_s = 1.2$), the frequency response function plot was found to be different than that corresponding to the structure with equal modal damping ratio values. For the case of equal modal damping ratio values, the two TMDs are always tuned to the

dominant mode whereas for the case of equal modal peak amplitude values, the two TMDs are tuned to target the system when they are at $\pm B/6$ and $\pm B/3$. However, when the TMDs are placed at $\pm B/2$, they are tuned to the fundamental mode (mode 1) as they are spaced sufficient far apart to reduce the torsional response introduced by mode 2.

Inspection of Figures 3.53 and 3.54, which show the dynamic magnification factor for mass ratio of $\mu = 001$ and $\mu = 0.02$, respectively, reveal that the response does not converge for ω_θ/ω_s =1.2. The reason these curves do not converge, unlike those for equal modal damping, is due to the increased amplitude of mode 2 (see Figure 3.44), which has a significantly large torsional response component (see Figure 3.6). This plot also shows that even for the torsionally stiff system (ω_θ/ω_s=1.2), if the second mode has a large torsional response component and contributes to the response, the structure will be sensitive to TMD location.

For this particular TMD configuration, the lowest response reduction factor (see Figure 3.55) is achieved when the TMDs are placed at $\pm B/2$ for all ω_θ/ω_s ratios considered. Figures 3.56 and 3.57 show this system is most efficient for the strongly torsionally coupled system. This is similar to the case of a structure with equal modal damping ratio values equipped with two identical TMDs. As shown in Figure 3.58, for both structural configurations, the efficiency is increased as the mass ratio is increased. Again, the lowest efficiency was found for structures having equal modal peak amplitude values. This is due to the fact that, for the case with equal damping ratio values, the two TMDs can target the largest contributing mode, which is in contrast to the structures with unequal damping ratio values.

3.4.3 Two Different TMDs Results - Harmonic

The dynamic response of the torsionally coupled structures with equal modal peak amplitude values equipped with two different TMDs are presented in this section. The TMD configuration and TMD locations studied in this section, for ω_θ/ω_s=0.8, 1.0 and 1.2, are the same as those investigated in Section 3.3.3.

Similar to the two identical TMDs configuration, the frequency response function plot corresponding to ω_θ/ω_s =1.2 differs due to the increase amplitude of mode 2. It is evident from Figure 3.59 that one TMD is tuned to mode 1 while the other is tuned to mode 2. This is not the case for ω_θ/ω_s =1.2 having equal modal damping ratio values (see Figure 3.23) where both TMDs where tuned to mode 1. This is confirmed by comparing the optimal tuning ratio values obtained for these two system. For the maximum efficiency location (i.e. ±B/2), corresponding to the equal modal peak amplitude values structure, the tuning ratio values bracket both mode 1 and mode 2. However, for the equal modal damping structure case, the tuning ratio values only bracket mode 1. The remaining frequency response function plots corresponding to this TMD configuration can be found in Appendix H.

The dynamic magnification factor (see Figures 3.60 and 3.61) for this particular configuration is very similar to that found for the structure having equal damping ratio values. This highlights the flexibility of this particular configuration as it is capable of being tuned to one or both modes.

The response reduction factor plots shown in Figure 3.62 have similar trends as those in Figure 3.26 for all three uncoupled frequency ratios. The location that results in the lowest response reduction factor is at $\pm B/2$ for all three uncoupled frequency ratio values.

Inspection of Figures 3.63 and 3.64 indicate that this TMD configuration is less sensitive to TMD location than that of the two identical TMDs configuration. For example, for a mass ratio of 0.02, the difference in maximum and minimum efficiency for two identical TMDs is approximately a factor of 2. However, for two different TMDs, it is approximately 1.25.

Figure 3.65 compares the efficiency of the two different TMDs configuration for the cases of equal modal damping ratio and equal modal peak amplitude. Again, the efficiency is found to be lower for structures having equal modal peak amplitude for all three uncoupled frequency ratio considered. This configuration is best suited for the torsionally flexible and the strongly torsionally coupled structures.

3.4.4 Four TMDs Results - Harmonic

The dynamic response of the torsionally coupled structures with equal modal peak amplitude values, corresponding to Approach I and II, is presented in this section. These TMD configurations have previously been described in Section 3.3.4.

3.4.4.1 Approach I Results - Harmonic

The frequency response function plots for ω_θ/ω_s =0.8, 1.0 and 1.2 are shown in Figure 3.66, while the remaining frequency response function plots are shown in Appendix I. Similar to the case of two identical TMDs, the frequency response function plots for the strongly torsionally coupled and the torsionally stiff structures do not show significant change in shape when the modal damping ratio values are modified. However, the frequency response function plots for the torsionally stiff structure are affected by a change in modal damping. This changed in the frequency response

function plots as mentioned for the two TMDs configuration is a result of an increase in the amplitude of mode 2 which has a strong torsional component. Owing to the increase in amplitude of mode 2, one pair of TMDs remains tuned to mode 1. However, the second paired is now tuned to between mode 1 and mode 2. When equal modal damping was presented in the structure, both pairs of TMDs, were tuned to mode 1. This change in tuning ratio values are responsible for modifying the frequency response function plot.

Comparing Figures 3.67 and 3.68 to 3.30 and 3.31, it can be concluded, for the structures investigated, the torsionally flexible structure with equal damping is more sensitive to TMD location whereas the torsionally stiff structure with equal modal peak amplitude is more sensitive to TMD location. Again, inspection of Figures 3.1 and 3.44 can be utilized to explained this behavior. For $\omega_\theta/\omega_s = 0.8$, the structure with equal modal damping ratio values is found to have a large peak amplitude corresponding to mode 1, which has a large torsional response component. This modal amplitude is reduced relative to mode 2 for the case with equal modal peak amplitude values. In other words, the mode that has the largest torsional component has been reduced relative to the mode having the largest translational component. The opposite is found to occur for $\omega_\theta/\omega_s = 1.2$. Here, mode 1, which has the largest modal amplitude for the structure with equal damping, has a large translational response component. For the case of equal modal peak amplitude values, mode 2, which has a significant torsional response component, is increased relative to mode 1. In order words, increase torsional response is introduced. Therefore, the torsionally stiff and flexible systems are less sensitive to TMD locations when the peak amplitude of the torsionally dominant mode is reduced.

The response reduction factors shown in Figure 3.69 shows similar trends for all three ω_θ/ω_s ratio values. The highest reduction factor is found at $\pm B/6$. As with the previous two configurations, the most effective location is at $\pm B/2$.

The maximum and minimum efficiency plots are shown in Figures 3.70 and 3.71. Similar to the two TMDs configurations, the system has the highest efficiency for the strongly torsionally coupled structure. Finally, Figure 3.72 compares the efficiency of the Four different TMDs, Approach I, configuration for the cases of equal damping ratio values and equal modal peak amplitude values. Again, the efficiency is found to be lower for structures having equal modal peak amplitude values for all three uncoupled frequency ratios considered.

3.4.4.2 Approach II Results - Harmonic

The TMD arrangement and locations match those introduced in section 3.3.4. The frequency response function plots in Figure 3.73 show the response behavior is similar to that found when the structures have equal modal damping ratio values. As with Approach I, the most significant change occurs for ω_θ/ω_s =1.2, which has been previously explained.

The dynamic magnification factors and response reduction factors shown for all three ω_θ/ω_s ratio values can be found in Figures 3.74 to 3.76. As with Approach I, the TMD location that results in the lowest reduction factor is at $\pm B/2$.

The minimum and maximum efficiency plots are shown in Figures 3.77 and 3.78. Similar to Approach I, maximum efficiency is found for the strongly torsionally coupled system. Finally, the maximum efficiency obtained for structures with equal modal peak amplitude values is compared to that of structures with equal damping

ratio values in Figure 3.79. It is found that, for this particular configuration, higher efficiencies are achieved for structures with equal modal damping ratio values. In addition, as mass ratio value is increased, the efficiency is increased for all three uncoupled frequency ratios considered.

3.4.5 Evaluation of Different TMD Configurations

Frequency response function plots corresponding to TMD locations resulting in maximum efficiency for each TMD configuration are shown in Figure 3.80. It is evident that two different TMDs configuration is most effective configuration considered. These plots highlight how different configurations influence the frequency response of the structures. For all TMD configurations considered, the TMD(s) reduced the uncontrolled response.

Figures 3.81 and 3.82 show the maximum efficiency achieved for all five TMD configurations for $\mu = 0.01$ and $\mu = 0.02$, respectively. It can be observed from these figures, for four TMDs configurations, that the maximum efficiency is found to be approximately the same for Approach I and II for the torsionally stiff structures. Approach II, however, has higher maximum efficiency values for the torsionally flexible structures. Also, from these figures, the efficiency for different TMD configurations can be determined. For the torsionally flexible structure (i.e. $\omega_\theta/\omega_s = 0.8$), the descending order of efficiency is as follow,

1. Two Different TMDs
2. Four TMDs
3. Single TMD

4. Two Identical TMDs

whereas for the case of the strongly torsionally coupled structure

1. Two Different TMDs
2. Four TMDs
3. Two Identical TMDs
4. Single TMD

For cases when the structure is torsionally stiff (i.e. $\omega_\theta/\omega_s = 1.2$), the descending order of efficiency is

1. Two Different TMDs
2. Single TMD
3. Four TMDs
4. Two Identical TMDs

Also, as with the case of the structure with equal modal damping ratio values, at least two TMDs are required to suppress the response of the strongly torsionally coupled system and two tuning ratio values are required to reduce the response of the torsionally flexible structure effectively.

3.4.6 Optimal TMD Parameters

For the three uncoupled frequency ratios considered, the optimal parameters corresponding to the TMD location resulting in maximum efficiency are given in

Tables 3.5 and 3.6. The parameters optimized for each mass ratio are the tuning ratio and the TMD damping ratio. The optimal parameters determined for all other locations considered for each uncoupled frequency ratio investigated can be found in Appendix F to Appendix J.

3.5 Dynamic Response and TMD Location

This section discusses the relationship between the dynamic response and the TMD location. This is accomplished by using the concept of generalized mass ratio values to investigate the influence of TMD location on the dynamic response of the torsionally coupled structures.

3.5.1 Generalized Mass Ratio Values

Calculation of the generalized mass ratio values can be accomplished using the mode shapes of the structure, ϕ_n, the mass matrix of the structure, M_s, and TMD mass matrix, M_{tmd}. Note that the subscript n represents the structural mode of interests. The mode shapes of the structure can be calculated by solving the following eigenvalue problem (Chopra, 2000)

$$[K_s - {\omega_n}^2 M_s]\phi_n = 0 \tag{3.8}$$

The stiffness of the structure, K_s, and the mass matrix of a torsionally coupled structure can be expressed as follows

$$[M_s] = \begin{bmatrix} m_s & 0 \\ 0 & m_s r^2 \end{bmatrix} \tag{3.9}$$

$$[K_s] = \begin{bmatrix} k_{s1} + k_{s2} & k_{s1}y_{s1} - k_{s2}y_{s2} \\ k_{s1}y_{s1} - k_{s2}y_{s2} & k_{s1}{y_{s1}}^2 + k_{s2}{y_{s2}}^2 \end{bmatrix} \tag{3.10}$$

The TMD mass matrix can be calculated by transferring the mass of the TMD back to the centre of mass of the structure. This can be achieved by direct equilibrium method, in which a unit acceleration is imposed on each degree-of-freedom, and the mass influence coefficients determined. The derivation of the mass matrix of a single TMD is represented in Figure 3.83. The TMD mass matrix is found to be

$$[M_{tmd}] = \begin{bmatrix} m_1 & -m_1 e_{x1} \\ -m_1 e_{x1} & m_1 {e_{x1}}^2 \end{bmatrix} \tag{3.11}$$

With the mode shapes, mass matrix of the structure and TMD mass matrix calculated, the generalized mass ratio value of a specific mode can be calculated as

$$\mu_n{}^* = \frac{{m_{tmd_n}}^*}{{m_{s_n}}^*} \tag{3.12}$$

where the generalized mass of the TMD, ${m_{tmd_n}}^*$, and the generalized mass the structure ${m_{s_n}}^*$ are expressed as

$$ {m_{tmd_n}}^* = \{\phi_n\}^T [M_{tmd}] \{\phi_n\} \tag{3.13} $$

and

$$ {m_{s_n}}^* = \{\phi_n\}^T [M_s] \{\phi_n\} \tag{3.14} $$

respectively. The generalized mass ratio values obtained from Equation 3.12 can be used to investigate the relationship between the dynamic response and TMD location. Note that the generalized mass ratio values are employed here as a way of qualitatively predicting the effectiveness of a TMD at different locations. However, this approximation can provide a great deal of insight regarding the least and the most effective TMD locations.

3.5.2 Relationship between Generalized Mass Ratio and Dynamic Response

The generalized mass ratio values for structures equipped with a single TMD are calculated and plotted in Figures 3.84 ($\mu = 0.01$) and 3.85 ($\mu = 0.02$) for different TMD locations. The generalized mass ratio values for each mode are shown in Appendix A, Tables A.7 to A.12.

3.5.2.1 Structures with Equal Modal Peak Amplitude Values

A discussion on structures with equal modal peak amplitude values is first presented. In order to reduce the response effectively, it is necessary to provide sufficient generalized mass ratio values in both modes. Observing Figures 3.84 and 3.85, for $\omega_\theta/\omega_s = 0.8$, it can be seen that a low generalized mass ratio value is obtained in mode 1 when a TMD is placed at $B/6$. Thus, it is expected that this would be an ineffective location to place a single TMD. In addition, it can be concluded from the generalized mass ratio values presented in Figures 3.84 and 3.85 that the second least effective location is at the centre of mass of the structure (i.e. $y_1 = 0$). At TMD location $B/2$, relatively large generalized mass ratio values are obtained for both modes. Thus, it can be postulated that $B/2$ is the most effective TMD location for this uncoupled frequency ratio. As for $\omega_\theta/\omega_s = 1.2$, based on observations, the least and second least effective locations are at $-B/6$ and the centre of mass of the structure (i.e. $y_1 = 0$), respectively. The most effective location to place a single TMD is at $-B/2$ as high generalized mass ratio values are obtained for both modes at this location. The above observations drawn from Figures 3.84 and 3.85 are found to agree with the results obtained from the numerical simulations.

As for the strongly torsionally coupled system (i.e. $\omega_\theta/\omega_s = 1.0$), a symmetric shape in the generalized mass ratio values plot can be observed. It can be concluded from the plots that both $B/2$ and $-B/2$ are very effective locations to place a single TMD as high generalized mass ratio values can be obtained for one of the modes. Also, it can be observed that $-B/3$ and $B/3$ are ineffective locations to place a single TMD. This is due to the fact that a small generalized mass ratio value is obtained for one of the modes.

3.5.2.2 Structures with Equal Modal Damping Ratio Values

A discussion on structures with equal modal damping ratio values equipped with a single TMD are presented in this section. As shown in Figure 3.1, a structure with equal damping ratio values, does not have equal modal peak amplitude values. Thus, in order to utilize the generalized mass ratio values to predict the most effective TMD locations it is necessary to first understand how the structure behaves without TMD(s). Therefore, the frequency response function plots of structures without any TMD(s) (see Figure 3.1), need to be considered along with the plots of generalized mass ratio values. Although it is more challenging to predict the response of structures with equal modal damping ratio equipped with a single TMD, a general indication of the least and most effective locations can be obtained.

For $\omega_\theta/\omega_s = 0.5$, it can be seen from the frequency response function plots that the peak values of mode 1 and mode 2 are similar (see Figure 3.1). Thus, it is expected that locations resulting in relatively low generalized mass ratio values in either mode 1 or 2 will result in poor performance. Based on Figures 3.84 and 3.85, it can been seen that the centre of mass of the structure and location $B/6$ are locations resulting in low generalized mass ratio values in mode 1. Thus, it is expected that the amount of reduction in response at these two locations will be less than that obtained for other locations. Based on the generalized mass values, it is expected that placing a single TMD at location $B/2$ will result in the highest efficiency.

For ω_θ/ω_s ratio $= 0.7$, it can be seen from the frequency response function plots in Figure 3.1 that the peak amplitude of mode 2 is larger than mode 1. Thus, it is expected that at location $B/2$, where the highest generalized mass ratio value is obtained in mode 2, will result in the maximum efficiency. However, at location $B/6$

and at the centre of mass of the structure, negligible generalized mass ratio values are obtained in the mode 1 also resulting in low TMD efficiency.

For $\omega_\theta/\omega_s = 0.8$, it can be seen that mode 1 has a higher peak amplitude (see Figure 3.1). Thus, based on Figures 3.84 and 3.85, it can be expected that the least efficient TMD location is at $B/6$ since the generalized mass ratio value is negligible at this location for mode 1. As for the most efficient TMD location, it is expected to occur at $B/2$ as large generalized mass ratio values are obtained for both modes.

For the strongly torsionally coupled system (i.e. $\omega_\theta/\omega_s = 1.0$), mode 1 has the largest peak amplitude (see Figure 3.1). From Figures 3.84 and 3.85, the lowest efficiency is expected to occur when the TMD is placed at $B/3$. Since a very large generalized mass ratio value is obtained for mode 1 at $-B/2$, maximum efficiency is expected if the TMD is placed at this location.

For the torsionally stiff structures (i.e. $\omega_\theta/\omega_s > 1.0$), mode 1 has the largest peak amplitude value (see Figure 3.1). Thus, the most efficient location to place a single TMD is expected to be $-B/2$. The least effective location is expected to be $B/2$ as a small generalized mass ratio value is obtained for mode 1 at this location.

The above observations drawn from Figures 3.84 and 3.85 are found to be consistent with the results obtained from the numerical simulations utilizing MATLAB (r2007b). In general, generalized mass ratio plots can be used as a simple design tool allowing the designer to quickly evaluate efficient TMD locations and the method can be applied for multiple TMDs systems. Chapter 5 investigates this technique in more detail.

3.6 Summary and Conclusions

This chapter presents the results of torsionally coupled systems with equal modal damping ratio values, and equal modal peak amplitude values under harmonic excitation. Different TMD configurations are utilized to study the dynamic response of the structure-TMD systems. The following conclusions are summarized for the particular types of structures that have been considered:

- The efficiency of different TMD configurations can be categorized according to the nature of the structures; i.e., torsionally flexible, strongly torsionally coupled and torsionally stiff.

- The dynamic response for $\omega_\theta/\omega_s = 0.8$, 1.0 and 1.2 was found to be sensitive to the structural damping which is in contrast to previous finding by Warburton and Ayorinde (1980). This is due to the differing objectives in the optimization criterion. This study focused on optimizing the response of the entire system whereas the research by Warburton and Ayorinde (1980) focused on optimizing the response of a single-degree-of-freedom primary structure.

- TMD(s) efficiency can be maximized by locating the absorbers at the edge(s) of the structures as this provides the greatest mass coupling terms and mass moment of inertia.

- The two different TMDs configuration was found to be the most efficient configuration for all the torsionally coupled structures as each of the TMDs, with their own unique mass ratio, can be tuned to a particular mode.

- The efficiency of a single TMD configuration was found to approach that of the

two different TMDs configuration for the torsionally stiff structures.

- The design of single TMD without considering the torsional motion can be justified for the torsionally stiff structures with equal modal damping ratio values. This is a result of the response motion being dominated by the translational motion.

- The response behavior and TMD location resulting in maximum and minimum efficiency of the torsionally coupled structures equipped with a single TMD can be predicted using the generalized mass ratio values plot.

- A single TMD was not efficient in reducing the response of the strongly torsionally coupled system. Therefore, TMD configuration is an important parameter which should be considered in the design of TMDs for strongly torsionally coupled structure.

- The efficiency of the single TMD configuration was found to exceed that of the two identical TMDs configuration except for the strongly torsionally coupled structure case. This can be attributed to the mass coupling term generated by a single DVA that aids in reducing the response when two modes are well separated.

- The additional mass constraint placed on the four TMD configurations (Approach I and II) limited the efficiency in this configuration for the torsionally coupled structures as compared to that of the two different TMDs configuration. The four TMDs configuration (Approach II) was found to be more efficient in reducing the response of the torsionally flexible structures compared to that of

Approach I. This indicates the importance of minimizing the constraints placed on selecting TMDs parameters.

- The TMD configurations considered are more efficient in reducing the response of structures with equal damping ratio values than structures with equal modal peak amplitude values. For the case of equal modal peak amplitude, the total response is equally comprised of both modes. As a result, the TMDs are not as efficient in reducing the system peak amplitude as it cannot be tuned to a dominant mode.

- At least two TMDs are required to reduce the dynamic response effectively of the strongly torsionally coupled system since the mass coupling term generated by a single TMD does not aid in reducing the response when two modes are strongly coupled.

- At least two tuning ratios are required to suppress the dynamic response effectively for the torsionally flexible structures as the mass moment of inertia generated by the TMDs tuned to the torsionally dominant mode do not aid in suppressing the response of the higher frequency translational mode.

- For TMD configurations where only one tuning ratio can be employed (a single TMD and two identical TMDs configurations), tuning the TMD(s) around the translation dominant mode can reduce the response of the torsionally dominant mode in the torsionally stiff structures as a result of the inertia forces generated by the TMD(s).

- All TMD configurations considered were able to attenuate the uncontrolled dynamic response and the efficiency for each configuration was found to increase

as the mass ratio was increased.

3.7 Chapter Tables

ω_θ/ω_s	R	Mode 1		Mode 2	
0.5	34.01	$\{1$	$-1.5161\}^T$	$\{1$	$0.0615\}^T$
0.7	34.83	$\{1$	$-1.1067\}^T$	$\{1$	$0.0867\}^T$
0.8	40.83	$\{1$	$-0.8350\}^T$	$\{1$	$0.1150\}^T$
1.0	40.89	$\{1$	$-0.3098\}^T$	$\{1$	$0.3098\}^T$
1.2	27.34	$\{1$	$-0.0981\}^T$	$\{1$	$0.9781\}^T$
1.3	25.61	$\{1$	$-0.0664\}^T$	$\{1$	$1.4464\}^T$

Table 3.1: DMF of Structures without DVA(s) and the Undamped Mode Shapes

ω_θ/ω_s	y_1	y_2	y_3	y_4	μ_1	μ_2	μ_3	μ_4	ν_1	ν_2	ν_3	ν_4	ζ_1	ζ_2	ζ_3	ζ_4	R
Single TMD																	
0.5	$B/2$				0.01				0.6231				0.4486				24.8824
0.7	$B/2$				0.01				0.8702				0.1936				17.9840
0.8	$B/2$				0.01				0.8206				0.1351				16.9127
1.0	$-B/2$				0.01				0.9728				0.0507				20.2683
1.2	$-B/2$				0.01				0.9645				0.0939				9.9085
1.3	$-B/2$				0.01				0.9727				0.0863				9.7155
Two Identical TMDs																	
0.5	$-B/2$	$B/2$			0.005	0.005			0.7139	0.7139			0.3981	0.3981			26.3921
0.7	$-B/2$	$B/2$			0.005	0.005			0.9329	0.9329			0.1696	0.1696			19.7885
0.8	$-B/2$	$B/2$			0.005	0.005			0.8609	0.8609			0.1750	0.1750			18.6698
1.0	$-B/2$	$B/2$			0.005	0.005			0.9305	0.9305			0.1050	0.1050			14.3146
1.2	$-B/2$	$B/2$			0.005	0.005			0.9638	0.9638			0.0681	0.0681			11.5974
1.3	$-B/2$	$B/2$			0.005	0.005			0.9710	0.9710			0.0659	0.0659			11.0429
Two Different TMDs																	
0.5	$-B/2$	$B/2$			0.0044	0.0056			0.4541	1.0022			0.0725	0.0603			12.2132
0.7	$-B/2$	$B/2$			0.0018	0.0082			0.6505	0.9966			0.0488	0.0758			10.6199
0.8	$-B/2$	$B/2$			0.0031	0.0069			0.7396	0.9948			0.0618	0.0753			10.3127
1.0	$-B/2$	$B/2$			0.0074	0.0026			0.9015	1.0525			0.0998	0.0611			10.5584
1.2	$-B/2$	$B/2$			0.0093	0.0007			0.9590	1.0193			0.0859	0.0171			9.7675
1.3	$-B/2$	$B/2$			0.0089	0.0011			0.9641	1.0251			0.0756	0.0217			9.5021
Four TMDs (Approach-I)																	
0.5	$-B/2$	$-B/2$	$B/2$	$B/2$	0.0025	0.0025	0.0025	0.0025	0.4577	1.0081	0.4577	1.0081	0.1032	0.0477	0.1032	0.0477	14.5448
0.7	$-B/2$	$-B/2$	$B/2$	$B/2$	0.0025	0.0025	0.0025	0.0025	0.6870	1.0141	0.6870	1.0141	0.1729	0.0481	0.1729	0.0481	14.3540
0.8	$-B/2$	$-B/2$	$B/2$	$B/2$	0.0025	0.0025	0.0025	0.0025	0.7498	1.0178	0.7498	1.0178	0.0918	0.0501	0.0918	0.0501	12.7260
1.0	$-B/2$	$-B/2$	$B/2$	$B/2$	0.0025	0.0025	0.0025	0.0025	0.8944	1.0085	0.8944	1.0085	0.0587	0.0804	0.0587	0.0804	12.9243
1.2	$-B/2$	$-B/2$	$B/2$	$B/2$	0.0025	0.0025	0.0025	0.0025	0.9326	0.9994	0.9326	0.9994	0.0445	0.0468	0.0445	0.0468	10.7439
1.3	$-B/2$	$-B/2$	$B/2$	$B/2$	0.0025	0.0025	0.0025	0.0025	0.9406	1.0055	0.9406	1.0055	0.0434	0.0462	0.0434	0.0462	10.2450
Four TMDs (Approach-I)																	
0.5	$-B/2$	$-B/2$	$B/2$	$B/2$	0.0019	0.0031	0.0019	0.0031	0.4569	1.0067	0.4569	1.0067	0.0602	0.0511	0.0602	0.0511	13.7374
0.7	$-B/2$	$-B/2$	$B/2$	$B/2$	0.0042	0.0008	0.0042	0.0008	1.0084	0.6520	1.0084	0.6520	0.0617	0.0393	0.0617	0.0393	12.5776
0.8	$-B/2$	$-B/2$	$B/2$	$B/2$	0.0018	0.0032	0.0018	0.0032	0.7441	1.0146	0.7441	1.0146	0.0562	0.0565	0.0562	0.0565	12.1313
1.0	$-B/2$	$-B/2$	$B/2$	$B/2$	0.0046	0.0004	0.0046	0.0004	0.9102	1.0848	0.9102	1.0848	0.0805	0.0271	0.0805	0.0271	12.4069
1.2	$-B/2$	$-B/2$	$B/2$	$B/2$	0.0026	0.0024	0.0026	0.0024	0.9333	1.0001	0.9333	1.0001	0.0459	0.0455	0.0459	0.0455	10.7430
1.3	$-B/2$	$-B/2$	$B/2$	$B/2$	0.0026	0.0024	0.0026	0.0024	0.9410	1.0062	0.9410	1.0062	0.0439	0.0448	0.0439	0.0448	10.2442

Table 3.2: Optimal TMD Parameters for Torsionally Coupled Systems (Equal Modal Damping Ratio Values) subjected to Harmonic Excitation (μ=0.01)

ω_θ/ω_s	y_1	y_2	y_3	y_4	μ_1	μ_2	μ_3	μ_4	ν_1	ν_2	ν_3	ν_4	ζ_1	ζ_2	ζ_3	ζ_4	R
Single TMD																	
0.5	$B/2$				0.01				0.5913				0.4483				20.2962
0.7	$B/2$				0.01				0.8346				0.2135				13.4953
0.8	$B/2$				0.01				0.8331				0.1499				11.7144
1.0	$-B/2$				0.01				0.9321				0.0439				16.9398
1.2	$-B/2$				0.01				0.9541				0.1356				7.8849
1.3	$-B/2$				0.01				0.9624				0.1220				7.7362
Two Identical TMDs																	
0.5	$-B/2$	$B/2$			0.01	0.01			0.6673	0.6673			0.4300	0.4300			22.4252
0.7	$-B/2$	$B/2$			0.01	0.01			0.8896	0.8896			0.2066	0.2066			16.0920
0.8	$-B/2$	$B/2$			0.01	0.01			0.8689	0.8689			0.1881	0.1881			14.2750
1.0	$-B/2$	$B/2$			0.01	0.01			0.9169	0.9169			0.1317	0.1317			10.2648
1.2	$-B/2$	$B/2$			0.01	0.01			0.9533	0.9533			0.0951	0.0951			9.1786
1.3	$-B/2$	$B/2$			0.01	0.01			0.9601	0.9601			0.0926	0.0926			8.7905
Two Different TMDs																	
0.5	$-B/2$	$B/2$			0.0091	0.0109			0.4426	0.9910			0.1007	0.0800			9.5900
0.7	$-B/2$	$B/2$			0.0035	0.0165			0.6351	0.9748			0.0639	0.1021			8.1758
0.8	$-B/2$	$B/2$			0.0040	0.0160			0.7200	0.9607			0.0662	0.1062			7.9427
1.0	$-B/2$	$B/2$			0.0140	0.0060			0.8873	1.0290			0.1407	0.0871			8.2085
1.2	$-B/2$	$B/2$			0.0176	0.0024			0.9413	1.0285			0.1131	0.0319			7.6262
1.3	$-B/2$	$B/2$			0.0171	0.0029			0.9467	1.0333			0.1011	0.0367			7.4374
Four TMDs (Approach-I)																	
0.5	$-B/2$	$-B/2$	$B/2$	$B/2$	0.0050	0.0050	0.0050	0.0050	0.4478	1.0024	0.4478	1.0024	0.1334	0.0654	0.1334	0.0654	11.5043
0.7	$-B/2$	$-B/2$	$B/2$	$B/2$	0.0050	0.0050	0.0050	0.0050	0.6755	1.0081	0.6755	1.0081	0.1930	0.0669	0.1930	0.0669	11.1389
0.8	$-B/2$	$-B/2$	$B/2$	$B/2$	0.0050	0.0050	0.0050	0.0050	0.7420	1.0107	0.7420	1.0107	0.1258	0.0693	0.1258	0.0693	10.0200
1.0	$-B/2$	$-B/2$	$B/2$	$B/2$	0.0050	0.0050	0.0050	0.0050	0.8717	0.9981	0.8717	0.9981	0.0802	0.0950	0.0802	0.0950	9.3493
1.2	$-B/2$	$-B/2$	$B/2$	$B/2$	0.0050	0.0050	0.0050	0.0050	0.9119	1.0025	0.9119	1.0025	0.0625	0.0657	0.0625	0.0657	8.4081
1.3	$-B/2$	$-B/2$	$B/2$	$B/2$	0.0050	0.0050	0.0050	0.0050	0.9196	1.0084	0.9196	1.0084	0.0595	0.0639	0.0595	0.0639	8.0681
Four TMDs (Approach-II)																	
0.5	$-B/2$	$-B/2$	$B/2$	$B/2$	0.0041	0.0059	0.0041	0.0059	0.4476	1.0002	0.4476	1.0002	0.0870	0.0701	0.0870	0.0701	10.9467
0.7	$-B/2$	$-B/2$	$B/2$	$B/2$	0.0018	0.0082	0.0018	0.0082	0.6380	0.9984	0.6380	0.9984	0.0571	0.0847	0.0571	0.0847	9.8579
0.8	$-B/2$	$-B/2$	$B/2$	$B/2$	0.0032	0.0068	0.0032	0.0068	0.7265	1.0035	0.7265	1.0035	0.0724	0.0803	0.0724	0.0803	9.4520
1.0	$-B/2$	$-B/2$	$B/2$	$B/2$	0.0097	0.0003	0.0097	0.0003	0.9026	1.0937	0.9026	1.0937	0.1151	0.0291	0.1151	0.0291	9.4444
1.2	$-B/2$	$-B/2$	$B/2$	$B/2$	0.0053	0.0047	0.0053	0.0047	0.9131	1.0044	0.9131	1.0044	0.0639	0.0636	0.0639	0.0636	8.4063
1.3	$-B/2$	$-B/2$	$B/2$	$B/2$	0.0053	0.0047	0.0053	0.0047	0.9212	1.0101	0.9212	1.0101	0.0623	0.0626	0.0623	0.0626	8.0667

Table 3.3: Optimal TMD Parameters for Torsionally Coupled Systems (Equal Modal Damping Ratio Values) subjected to Harmonic Excitation (μ=0.02)

ω_θ/ω_s	R	Translational Damping	Torsional Damping
0.8	28.03	2.01%	1.84%
1.0	33.35	1.79%	2.41%
1.2	19.18	2.13%	2.49%

Table 3.4: DMF and Damping Ratio Values of Structures with Equal Modal Peak Amplitude Values without DVAs subjected to Harmonic Excitation

ω_θ/ω_s	y_1	y_2	y_3	y_4	μ_1	μ_2	μ_3	μ_4	ν_1	ν_2	ν_3	ν_4	ζ_1	ζ_2	ζ_3	ζ_4	R
Single TMD																	
0.8	$B/2$				0.01				0.8543				0.1519				16.1430
1.0	$B/2$				0.01				0.9744				0.0272				21.9203
1.2	$-B/2$				0.01				0.9847				0.0993				9.5201
Two Identical TMDs																	
0.8	$-B/2$	$B/2$			0.005	0.005			0.9082	0.9082			0.1582	0.1582			17.9893
1.0	$-B/2$	$B/2$			0.005	0.005			0.9524	0.9524			0.1117	0.1117			15.0529
1.2	$-B/2$	$B/2$			0.005	0.005			0.9646	0.9646			0.0805	0.0805			10.0508
Two Different TMDs																	
0.8	$-B/2$	$B/2$			0.0024	0.0076			0.7401	0.9975			0.0542	0.0791			10.0444
1.0	$-B/2$	$B/2$			0.0064	0.0036			0.9024	1.0490			0.0951	0.0700			10.4551
1.2	$-B/2$	$B/2$			$9.969E^{-3}$	$0.308E^{-4}$			0.9684	1.2306			0.0984	0.0083			8.8048
Four TMDs (Approach-I)																	
0.8	$-B/2$	$-B/2$	$B/2$	$B/2$	0.0025	0.0025	0.0025	0.0025	0.7641	1.0197	0.7641	1.0197	0.1134	0.0503	0.1134	0.0503	12.9891
1.0	$-B/2$	$-B/2$	$B/2$	$B/2$	0.0025	0.0025	0.0025	0.0025	0.8972	1.0394	0.8972	1.0394	0.0593	0.0766	0.0593	0.0766	12.6124
1.2	$-B/2$	$-B/2$	$B/2$	$B/2$	0.0025	0.0025	0.0025	0.0025	1.0069	0.9467	1.0069	0.9467	0.0817	0.0584	0.0817	0.0584	9.9441
Four TMDs (Approach-II)																	
0.8	$-B/2$	$-B/2$	$B/2$	$B/2$	0.0038	0.0012	0.0038	0.0012	1.0140	0.7425	1.0140	0.7425	0.0612	0.0473	0.0612	0.0473	11.9315
1.0	$-B/2$	$-B/2$	$B/2$	$B/2$	0.0011	0.0039	0.0011	0.0039	1.0777	0.9061	1.0777	0.9061	0.0416	0.0749	0.0416	0.0749	12.0331
1.2	$-B/2$	$-B/2$	$B/2$	$B/2$	0.0007	0.0043	0.0007	0.0043	0.9343	0.9812	0.9343	0.9812	0.0380	0.0824	0.0380	0.0824	9.8983

Table 3.5: Optimal TMD Parameters for Torsionally Coupled Systems (Equal Modal Peak Amplitude Values) subjected to Harmonic Excitation (μ=0.01)

ω_θ/ω_s	y_1	y_2	y_3	y_4	μ_1	μ_2	μ_3	μ_4	ν_1	ν_2	ν_3	ν_4	ζ_1	ζ_2	ζ_3	ζ_4	R
Single TMD																	
0.8	$B/2$				0.01				0.8545				0.1569				11.2650
1.0	$-B/2$				0.01				0.9456				0.0330				18.9525
1.2	$-B/2$				0.01				0.9601				0.1346				7.2453
Two Identical TMDs																	
0.8	$-B/2$	$B/2$			0.01	0.01			0.8978	0.8978			0.1801	0.1801			13.7968
1.0	$-B/2$	$B/2$			0.01	0.01			0.9341	0.9341			0.1316	0.1316			10.6272
1.2	$-B/2$	$B/2$			0.01	0.01			0.9539	0.9539			0.0970	0.0970			8.1242
Two Different TMDs																	
0.8	$-B/2$	$B/2$			0.0033	0.0167			0.7205	0.9682			0.0619	0.1067			7.7191
1.0	$-B/2$	$B/2$			0.0127	0.0073			0.8893	1.0260			0.1364	0.0947			8.1416
1.2	$-B/2$	$B/2$			0.0160	0.0040			0.9434	1.0308			0.1085	0.0594			7.0838
Four TMDs (Approach-I)																	
0.8	$-B/2$	$-B/2$	$B/2$	$B/2$	0.0050	0.0050	0.0050	0.0050	0.7551	1.0129	0.7551	1.0129	0.1444	0.0702	0.1444	0.0702	10.1305
1.0	$-B/2$	$-B/2$	$B/2$	$B/2$	0.0050	0.0050	0.0050	0.0050	0.8750	1.0220	0.8750	1.0220	0.0795	0.0929	0.0795	0.0929	9.2468
1.2	$-B/2$	$-B/2$	$B/2$	$B/2$	0.0050	0.0050	0.0050	0.0050	1.0040	0.9116	1.0040	0.9116	0.0688	0.0649	0.0688	0.0649	7.5229
Four TMDs (Approach-II)																	
0.8	$-B/2$	$-B/2$	$B/2$	$B/2$	0.0077	0.0023	0.0077	0.0023	1.0026	0.7245	1.0026	0.7245	0.0850	0.0631	0.0850	0.0631	9.3400
1.0	$-B/2$	$-B/2$	$B/2$	$B/2$	0.0087	0.0013	0.0087	0.0013	0.8971	1.0842	0.8971	1.0842	0.1076	0.0493	0.1076	0.0493	9.1009
1.2	$-B/2$	$-B/2$	$B/2$	$B/2$	0.0051	0.0049	0.0051	0.0049	0.9119	1.0043	0.9119	1.0043	0.0653	0.0687	0.0653	0.0687	7.5228

Table 3.6: Optimal TMD Parameters for Torsionally Coupled Systems (Equal Modal Peak Amplitude Values) subjected to Harmonic Excitation (μ=0.02)

3.8 Chapter Figures

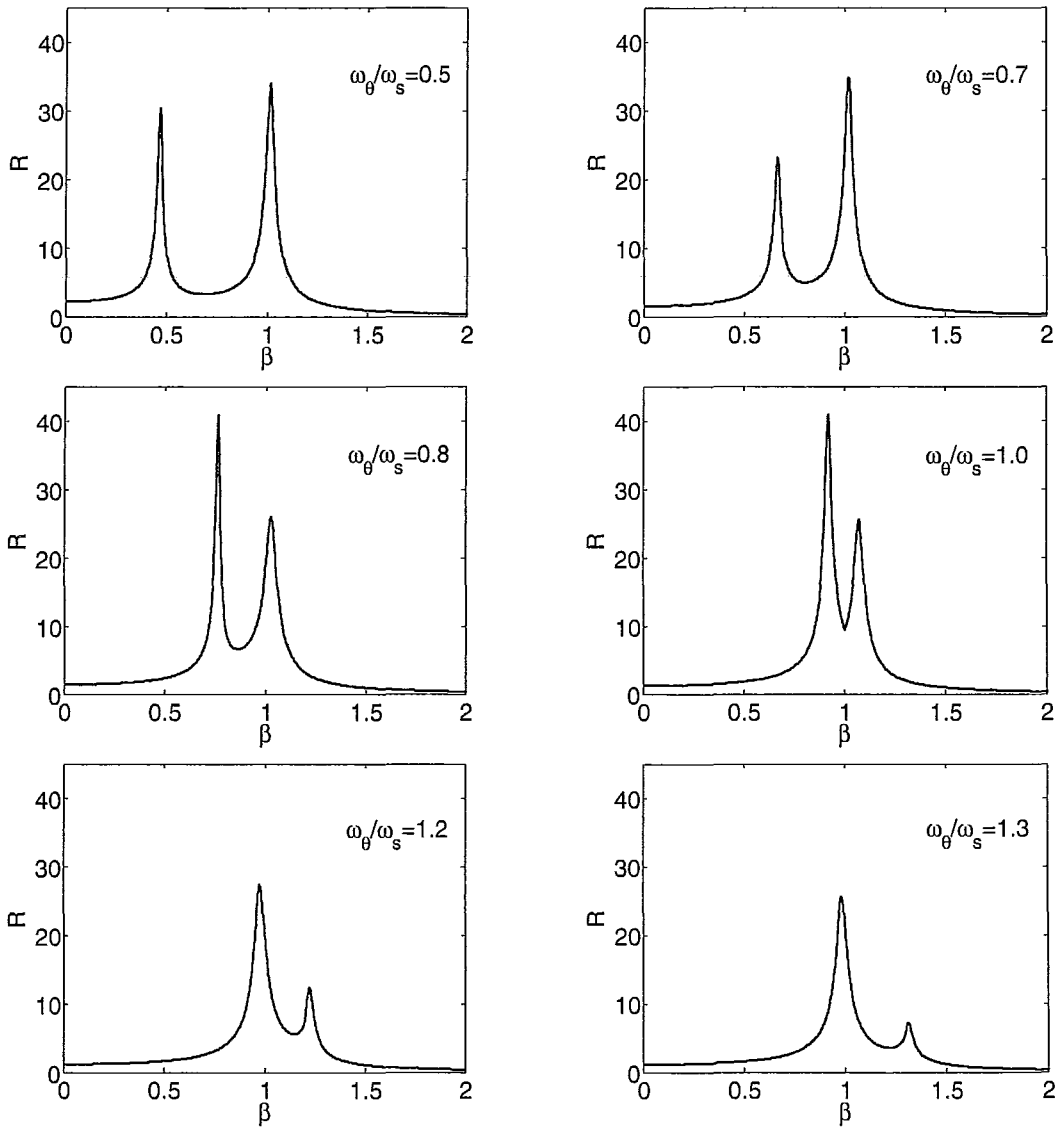

Figure 3.1: Frequency Response Function Plots of Structures with Equal Modal Damping Ratio Values without DVA subjected to Harmonic Excitation

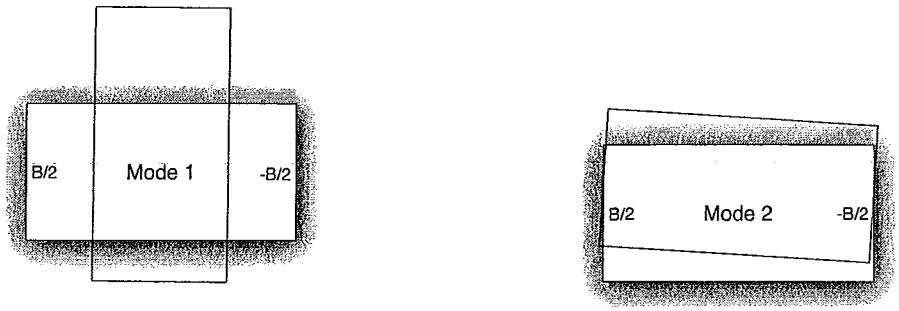

Figure 3.2: Undamped Mode Shapes for Structure with $\omega_\theta/\omega_s = 0.5$

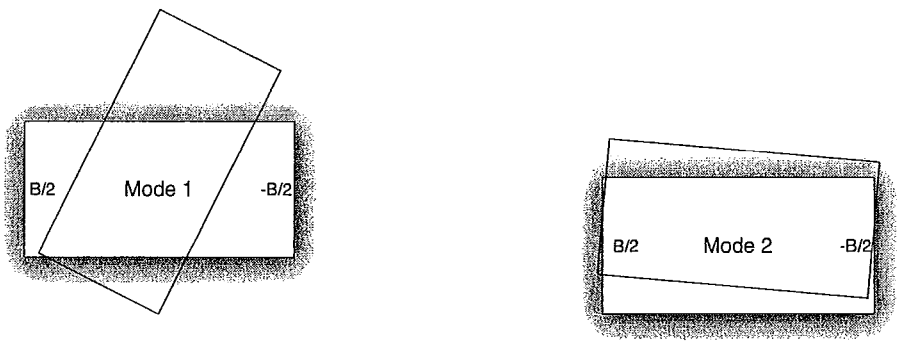

Figure 3.3: Undamped Mode Shapes for Structure with $\omega_\theta/\omega_s = 0.7$

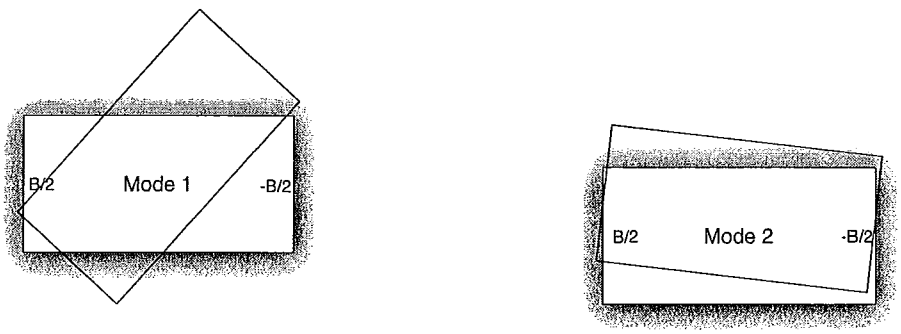

Figure 3.4: Undamped Mode Shapes for Structure with $\omega_\theta/\omega_s = 0.8$

Figure 3.5: Undamped Mode Shapes for Structure with $\omega_\theta/\omega_s = 1.0$

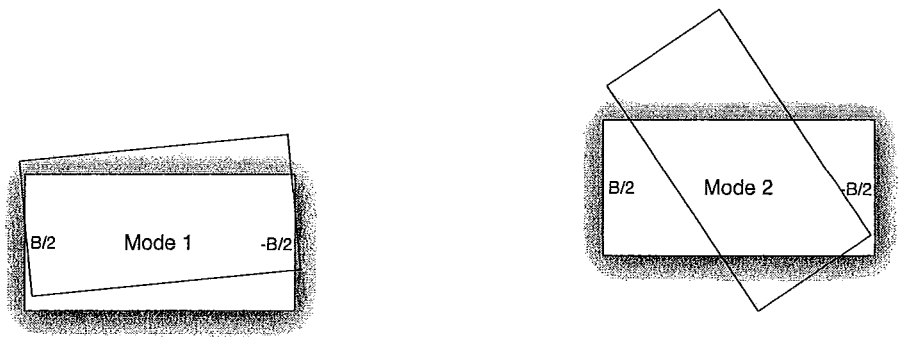

Figure 3.6: Undamped Mode Shapes for Structure with $\omega_\theta/\omega_s = 1.2$

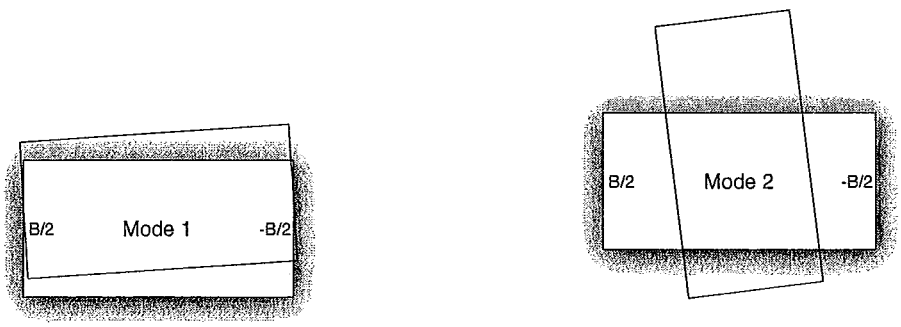

Figure 3.7: Undamped Mode Shapes for Structure with $\omega_\theta/\omega_s = 1.3$

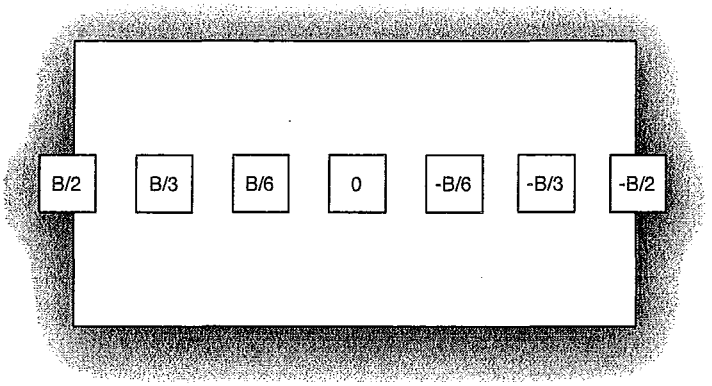

Figure 3.8: Single TMD Location Description

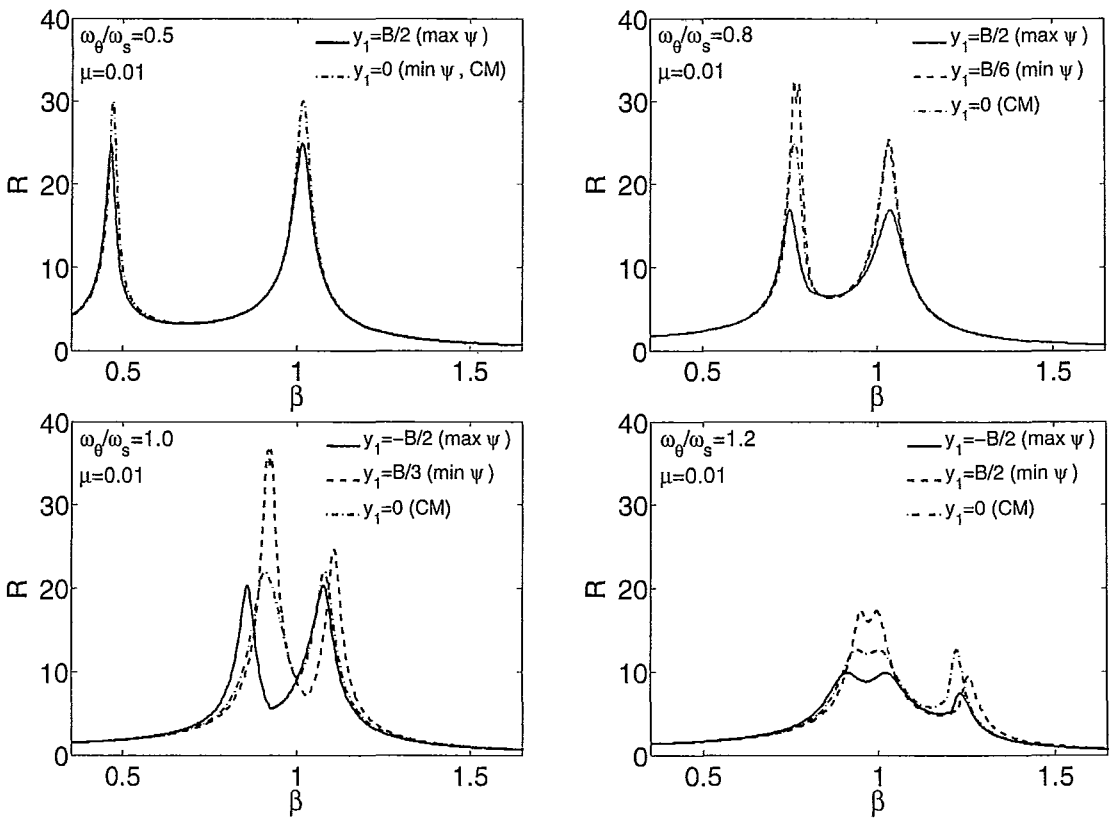

Figure 3.9: Frequency Response Function Plots (Equal Modal Damping Ratio Values - Single TMD Configuration)

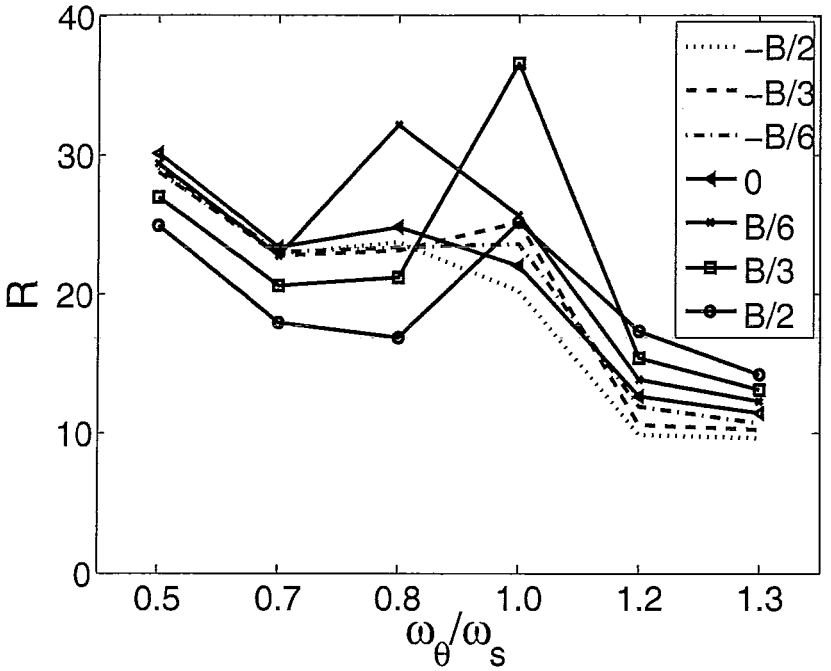

Figure 3.10: DMF of Structures with Equal Modal Damping Ratio Values Equipped with Single TMD ($\mu = 0.01$) subjected to Harmonic Excitation

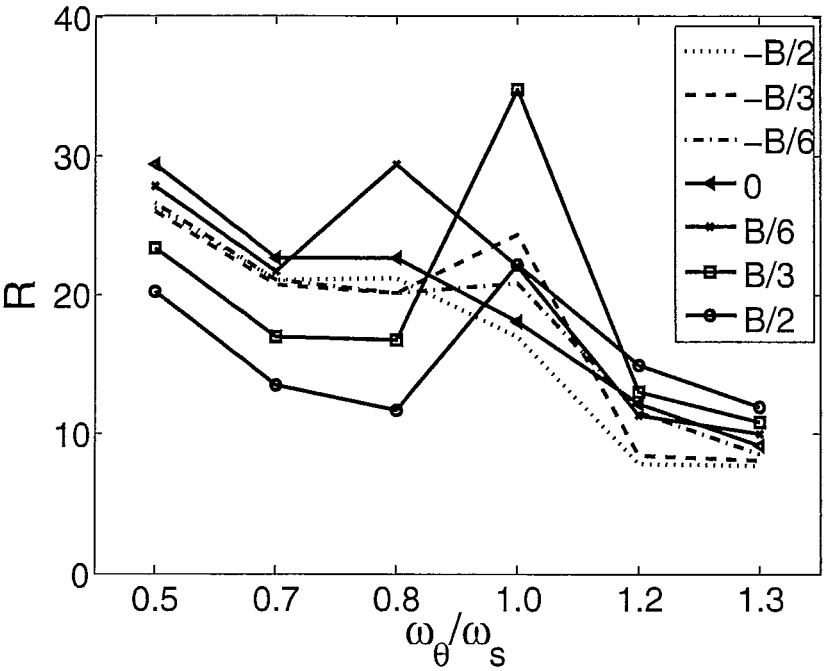

Figure 3.11: DMF of Structures with Equal Modal Damping Ratio Values Equipped with Single TMD ($\mu = 0.02$) subjected to Harmonic Excitation

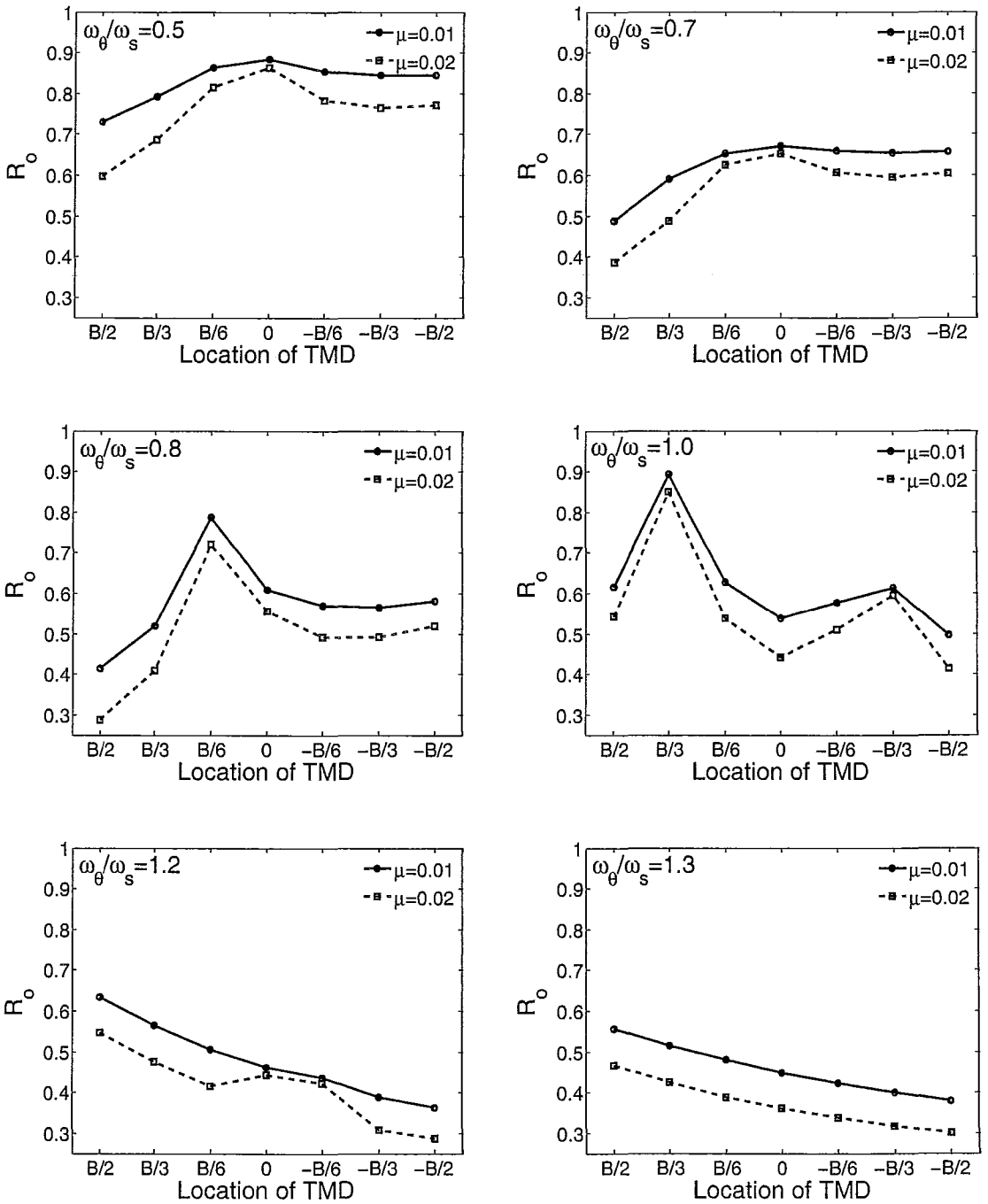

Figure 3.12: Response Reduction Factors for Structures with Equal Modal Damping Ratio Values Equipped with Single TMD subjected to Harmonic Excitation

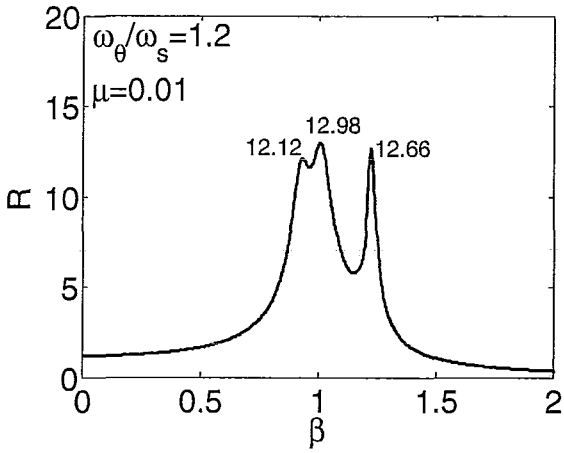

Figure 3.13: Frequency Response Function Plot of Structures Equipped with Single TMD ($\mu = 0.01$) using Optimal Parameters from Literature

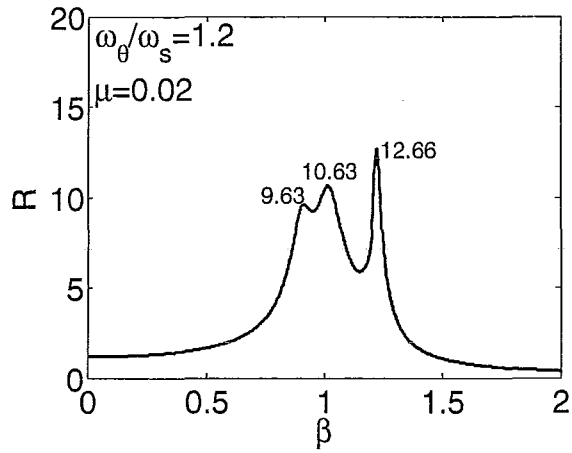

Figure 3.14: Frequency Response Function Plot of Structures Equipped with Single TMD ($\mu = 0.02$) using Optimal Parameters from Literature

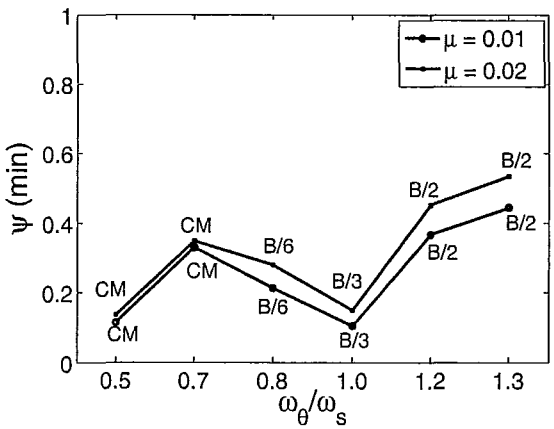

Figure 3.15: Minimum Efficiency Obtained for a Single TMD subjected to Harmonic Excitation

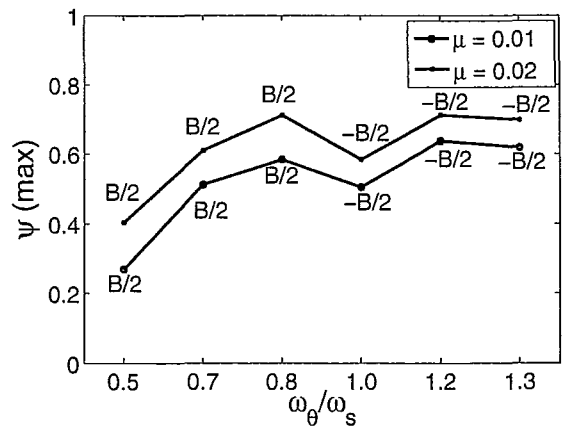

Figure 3.16: Maximum Efficiency Obtained for a Single TMD subjected to Harmonic Excitation

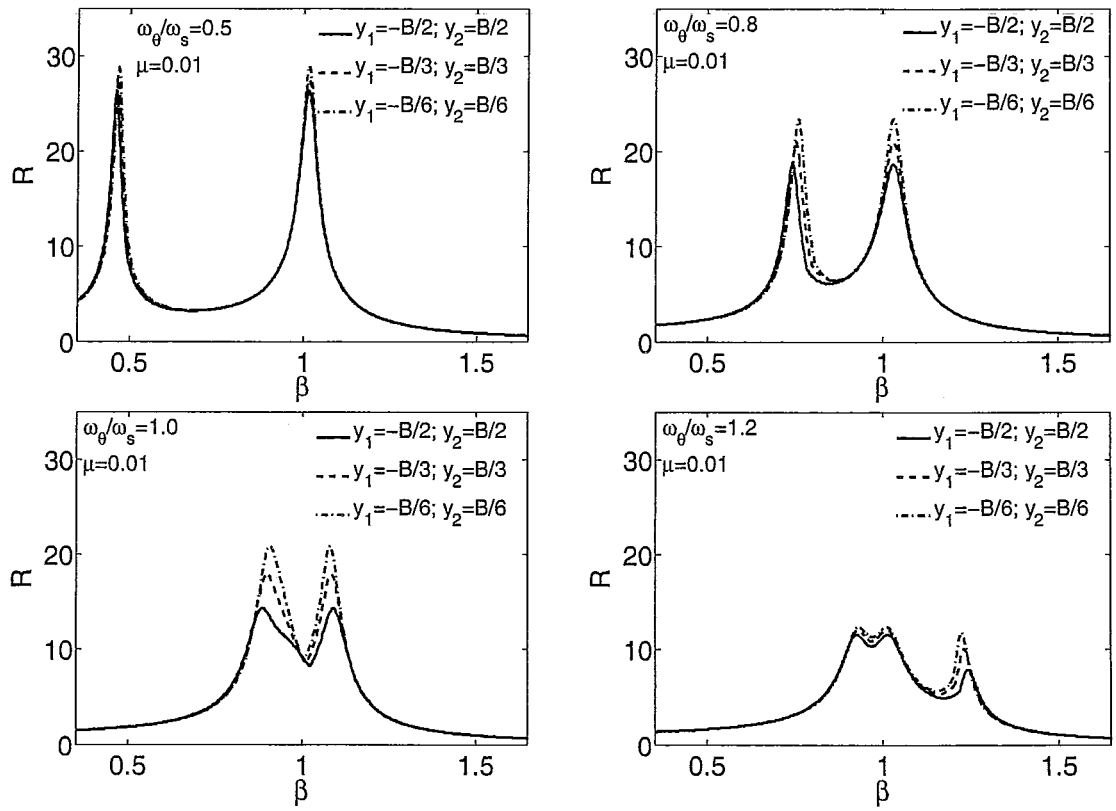

Figure 3.17: Frequency Response Function Plots (Equal Modal Damping Ratio Values - Two Identical TMDs Configuration)

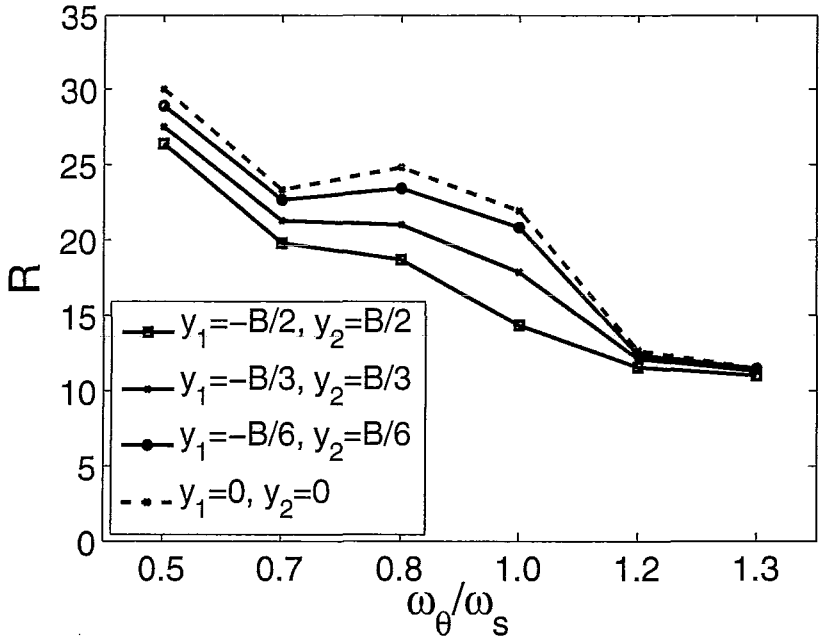

Figure 3.18: DMF of Structures with Equal Modal Damping Ratio Values Equipped with Two Identical TMDs ($\mu = 0.01$) subjected to Harmonic Excitation

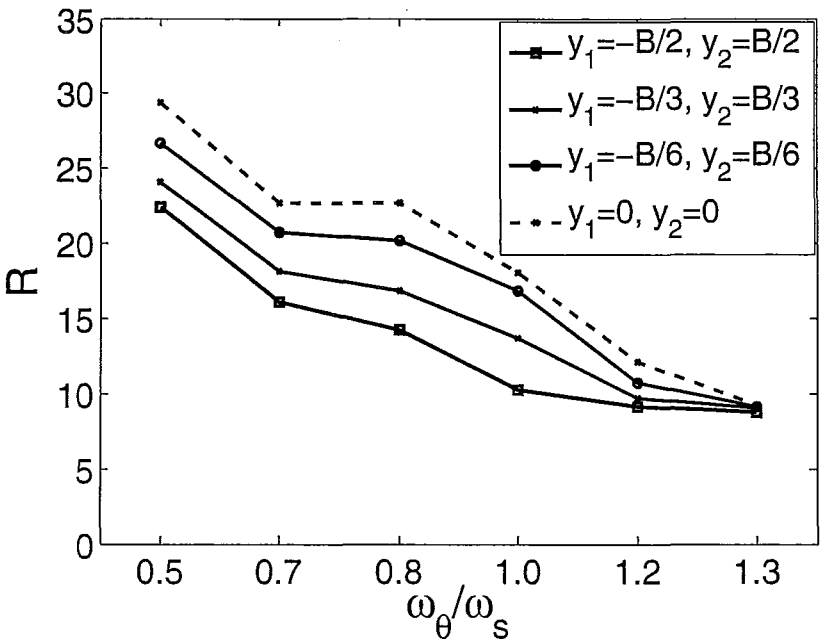

Figure 3.19: DMF of Structures with Equal Modal Damping Ratio Values Equipped with Two Identical TMDs ($\mu = 0.02$) subjected to Harmonic Excitation

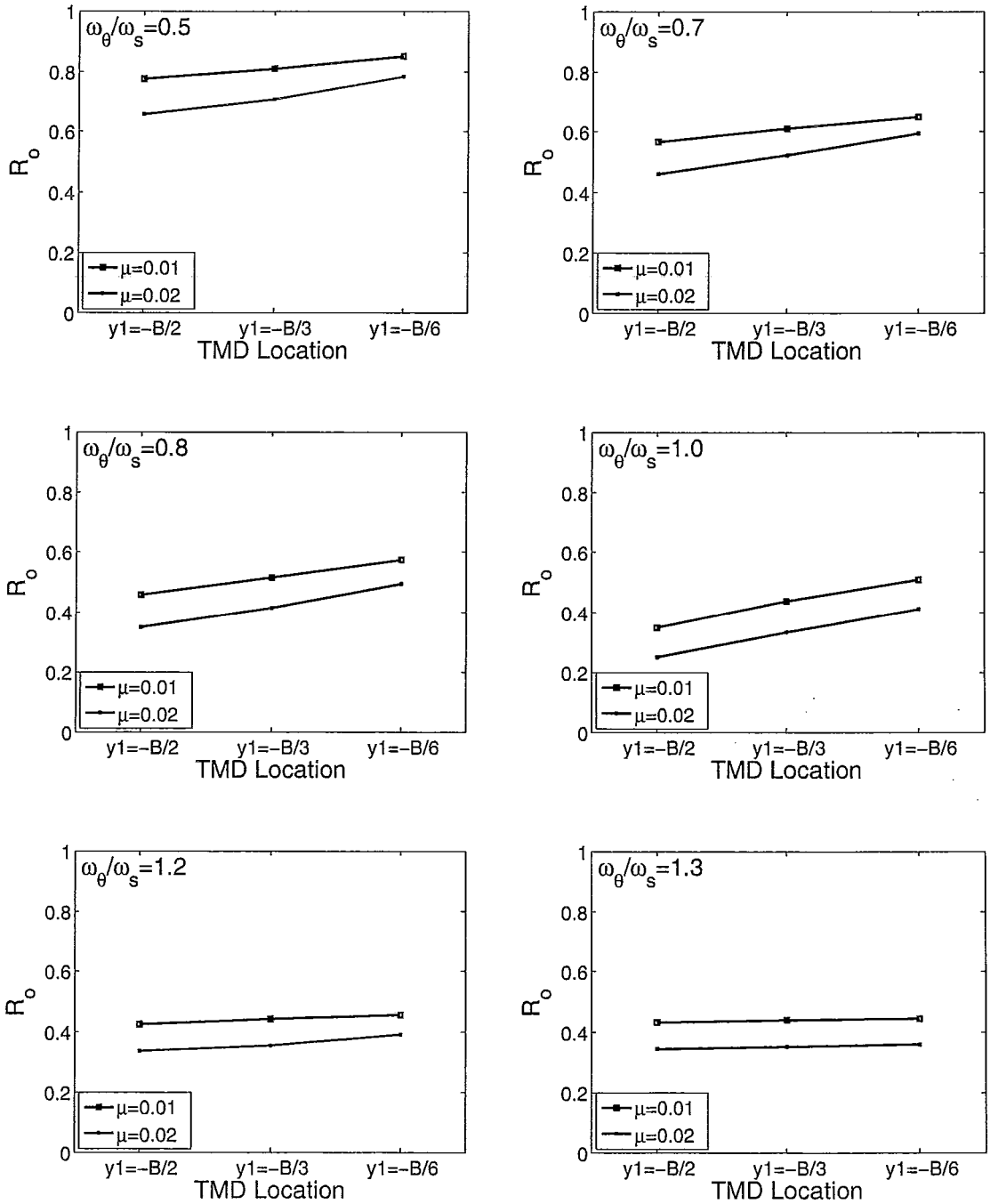

Figure 3.20: Response Reduction Factors for Structures with Equal Modal Damping Ratio Values Equipped with Two Identical TMDs subjected to Harmonic Excitation

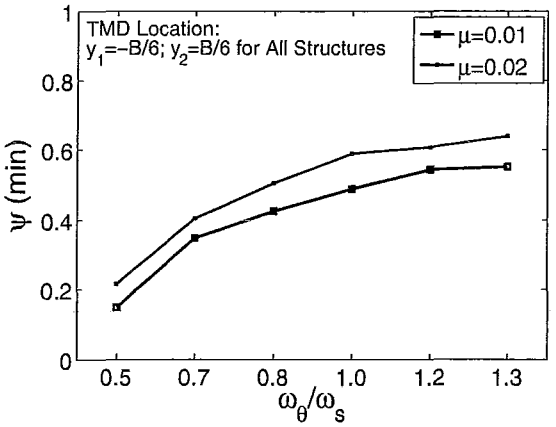

Figure 3.21: Minimum Efficiency Obtained for Two Identical TMDs subjected to Harmonic Excitation

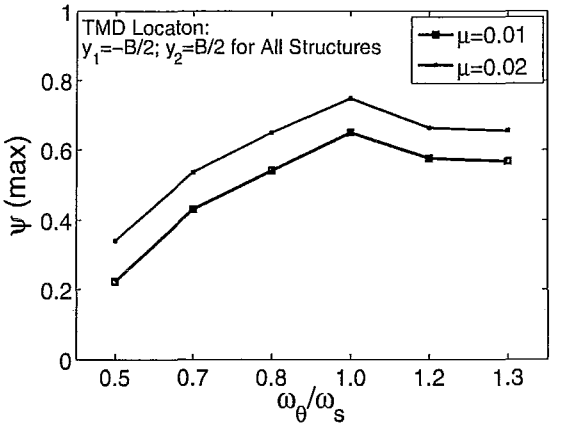

Figure 3.22: Maximum Efficiency Obtained for Two Identical TMDs subjected to Harmonic Excitation

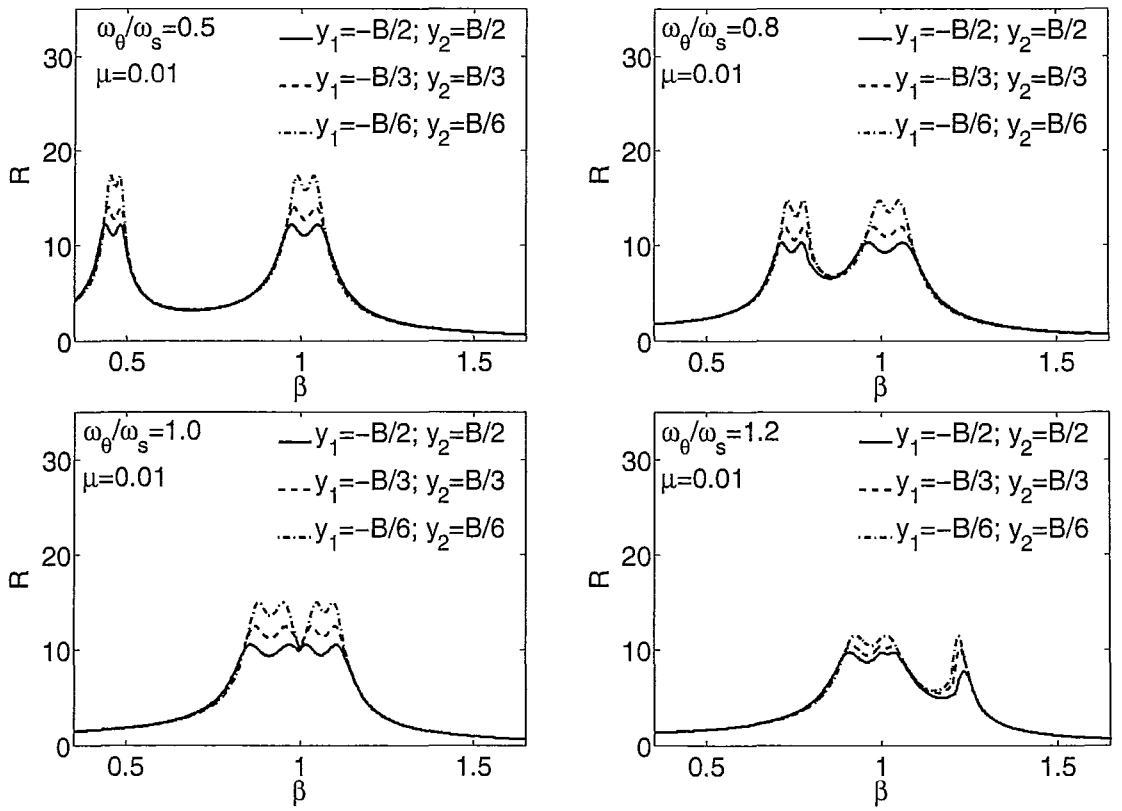

Figure 3.23: Frequency Response Function Plots (Equal Modal Damping Ratio Values - Two Different TMDs Configuration)

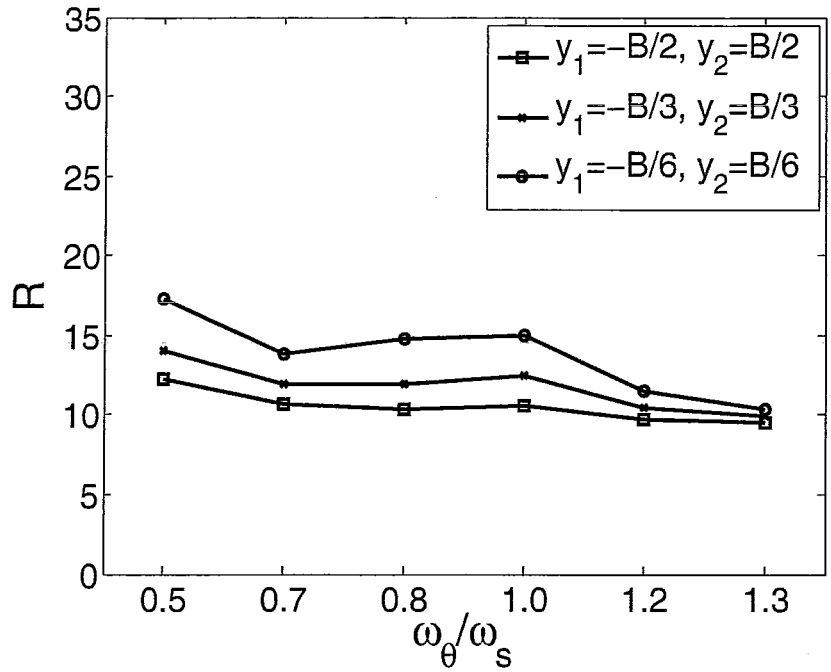

Figure 3.24: DMF of Structures with Equal Modal Damping Ratio Values Equipped with Two Different TMDs ($\mu = 0.01$) subjected to Harmonic Excitation

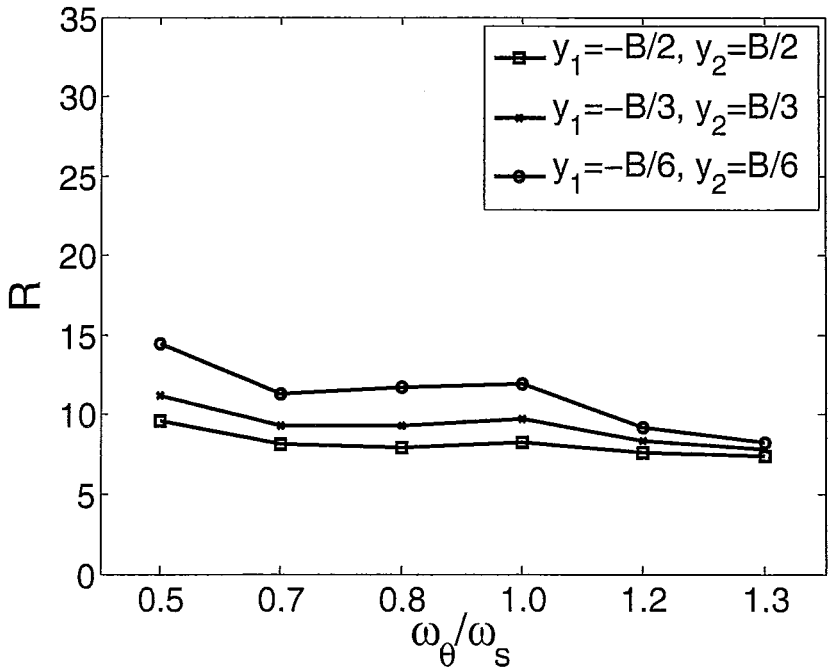

Figure 3.25: DMF of Structures with Equal Modal Damping Ratio Values Equipped with Two Different TMDs ($\mu = 0.02$) subjected to Harmonic Excitation

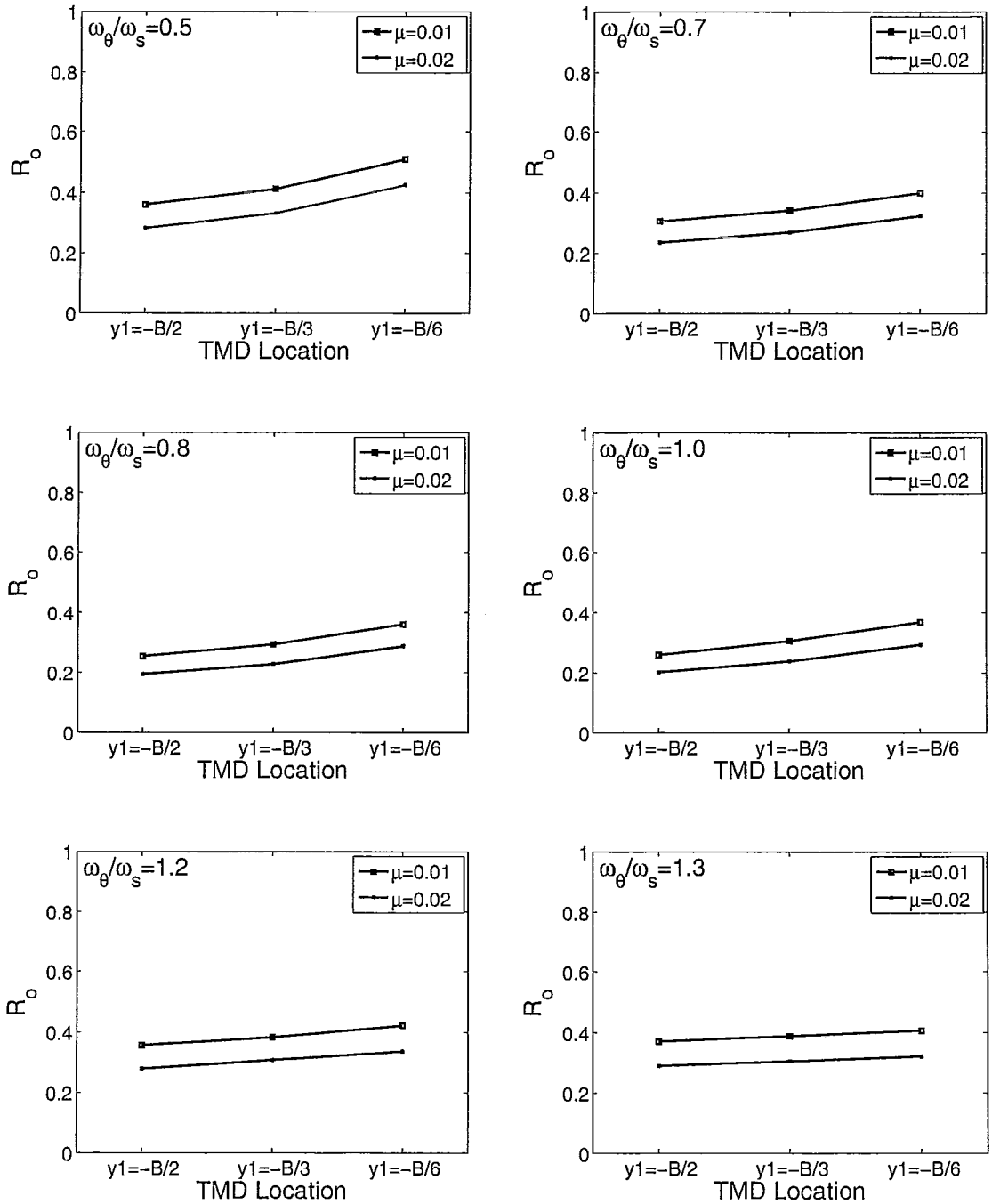

Figure 3.26: Response Reduction Factors for Structures with Equal Modal Damping Ratio Values Equipped with Two Different TMDs subjected to Harmonic Excitation

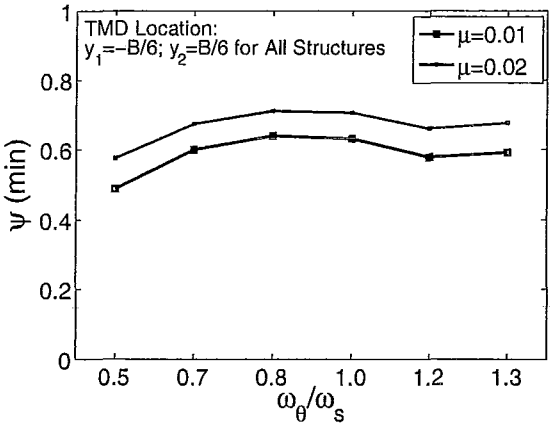

Figure 3.27: Minimum Efficiency Obtained for Two Different TMDs subjected to Harmonic Excitation

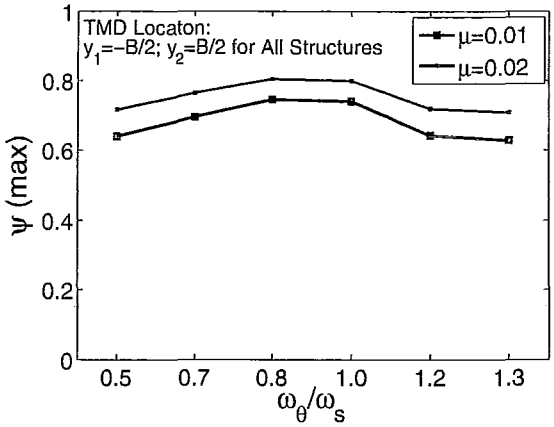

Figure 3.28: Maximum Efficiency Obtained for Two Different TMDs subjected to Harmonic Excitation

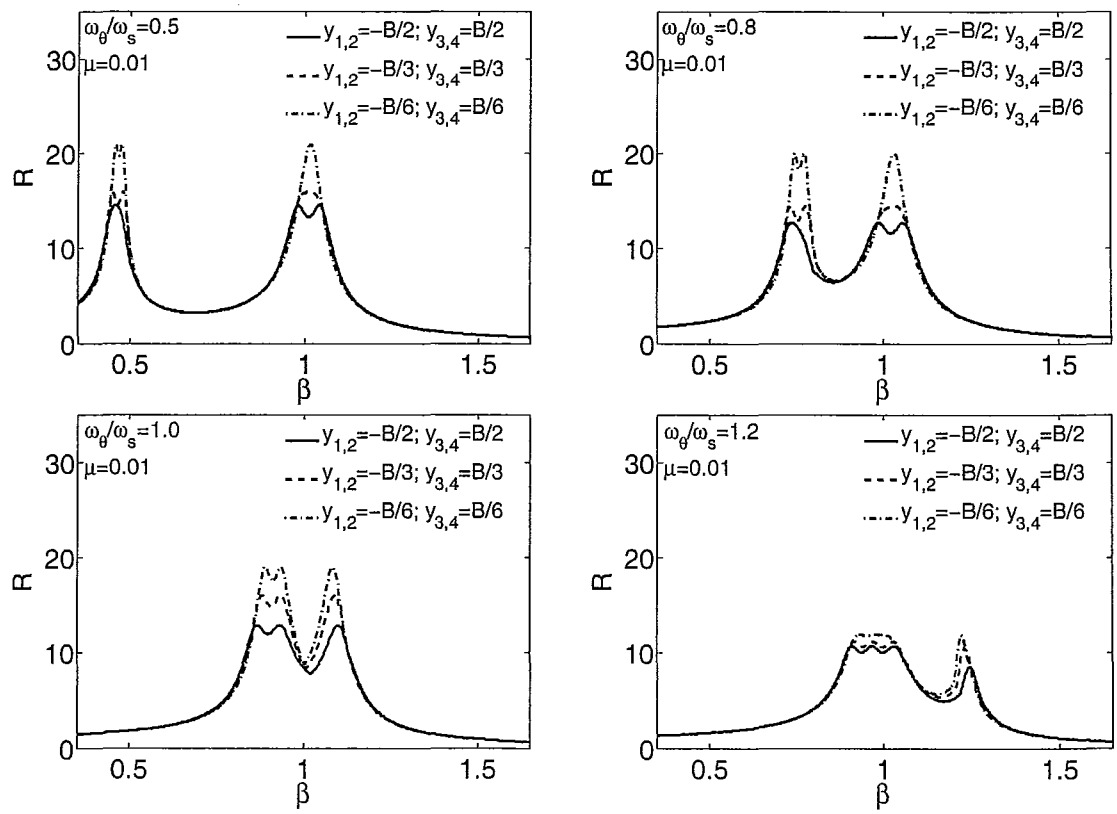

Figure 3.29: Frequency Response Function Plots (Equal Modal Damping Ratio Values - Four TMDs Configuration Approach-I)

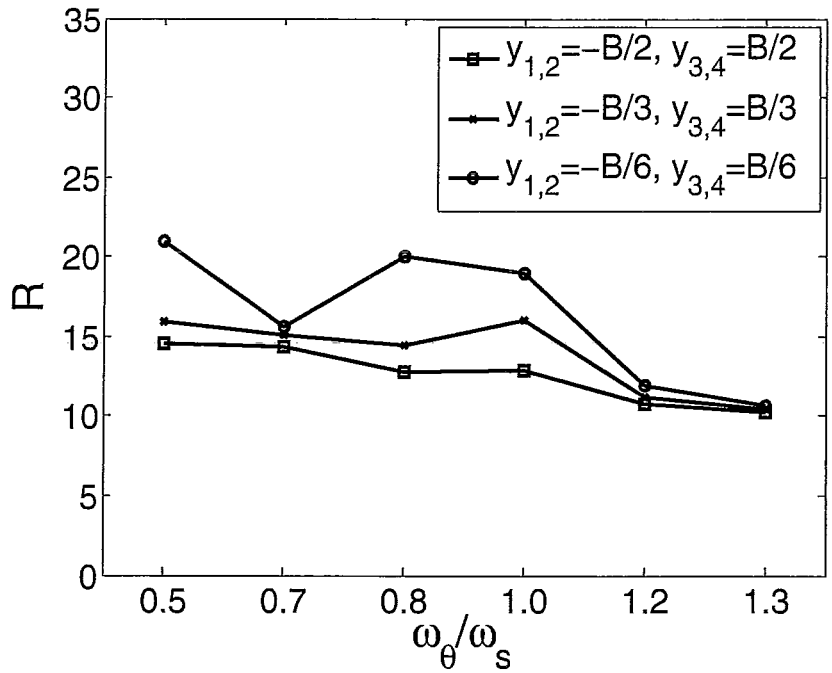

Figure 3.30: DMF of Structures Equipped with Four TMDs ($\mu = 0.01$) (Approach-I) subjected to Harmonic Excitation

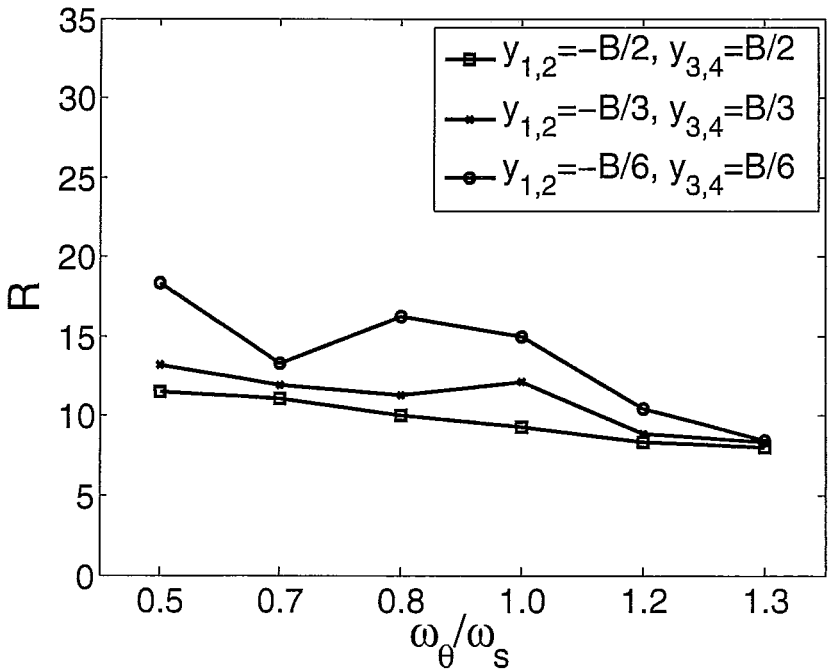

Figure 3.31: DMF of Structures Equipped with Four TMDs ($\mu = 0.02$) (Approach-I) subjected to Harmonic Excitation

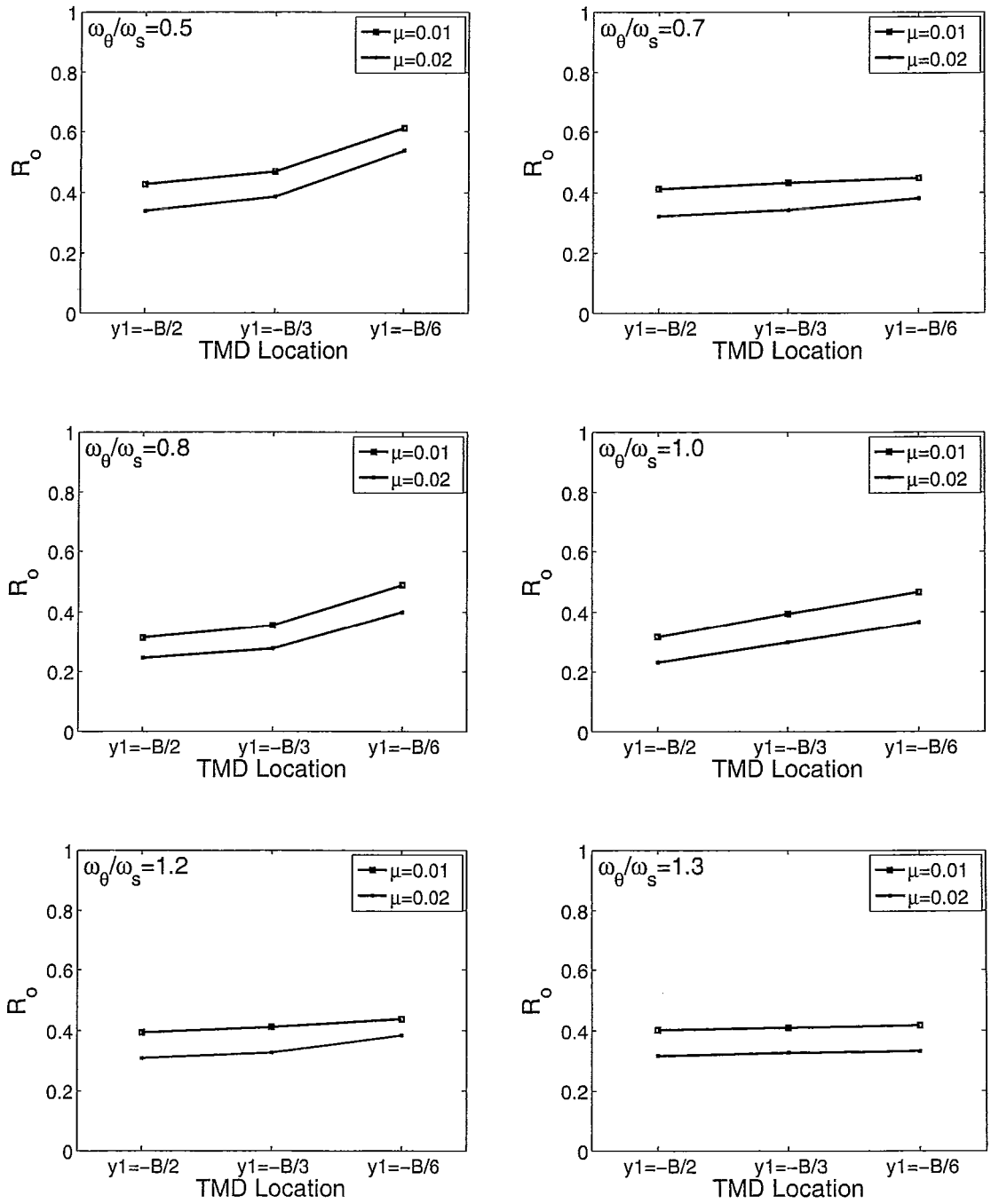

Figure 3.32: Response Reduction Factors for Structures with Equal Modal Damping Ratio Values Equipped with Four TMDs (Approach-I) subjected to Harmonic Excitation

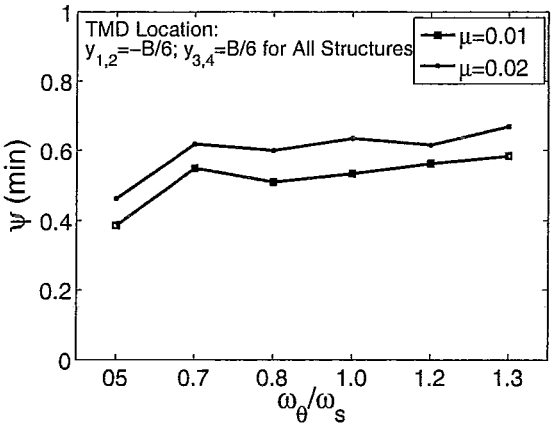

Figure 3.33: Minimum Efficiency Obtained for Four TMDs (Approach-I) subjected to Harmonic Excitation

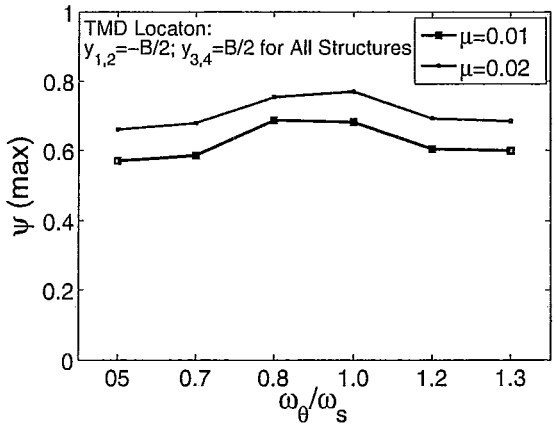

Figure 3.34: Maximum Efficiency Obtained for Four TMDs (Approach-I) subjected to Harmonic Excitation

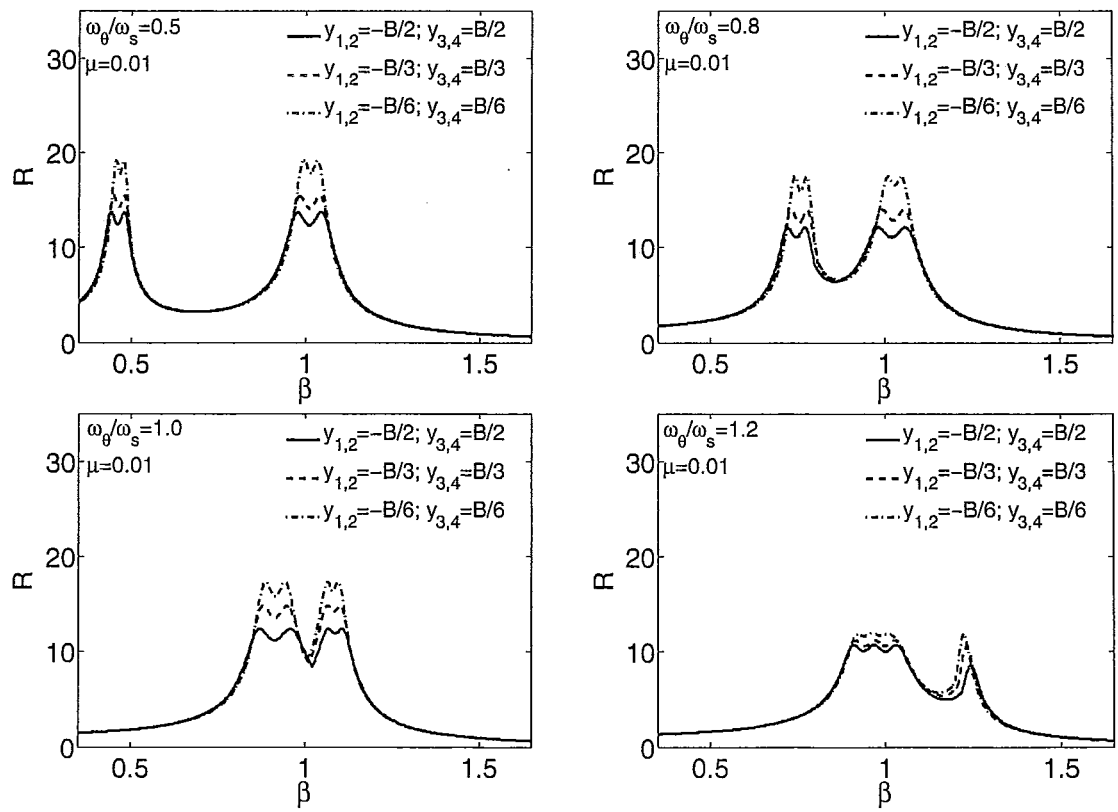

Figure 3.35: Frequency Response Function Plots (Equal Modal Damping Ratio Values - Four TMDs Configuration Approach-II)

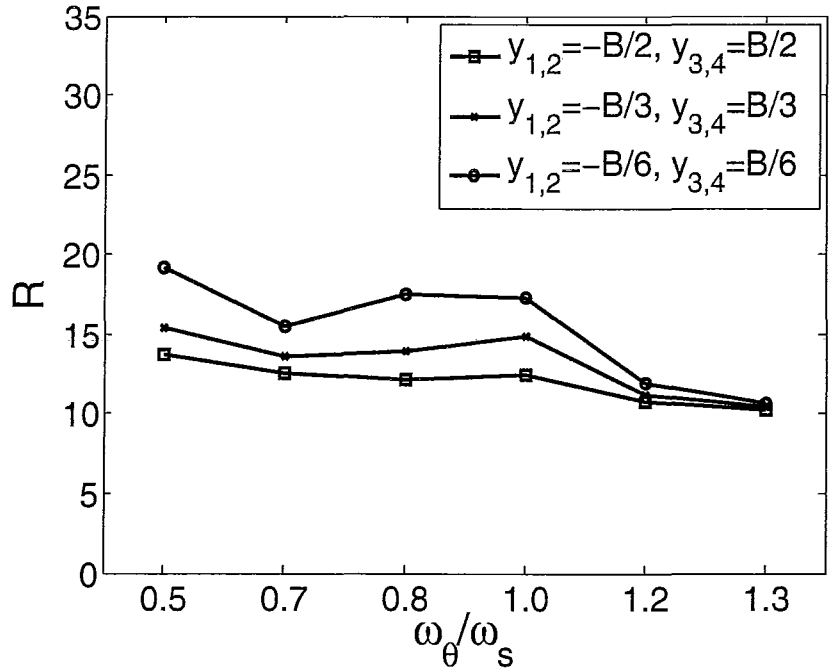

Figure 3.36: DMF of Structures with Equal Modal Damping Ratio Values Equipped with Four TMDs ($\mu = 0.01$) (Approach-II) subjected to Harmonic Excitation

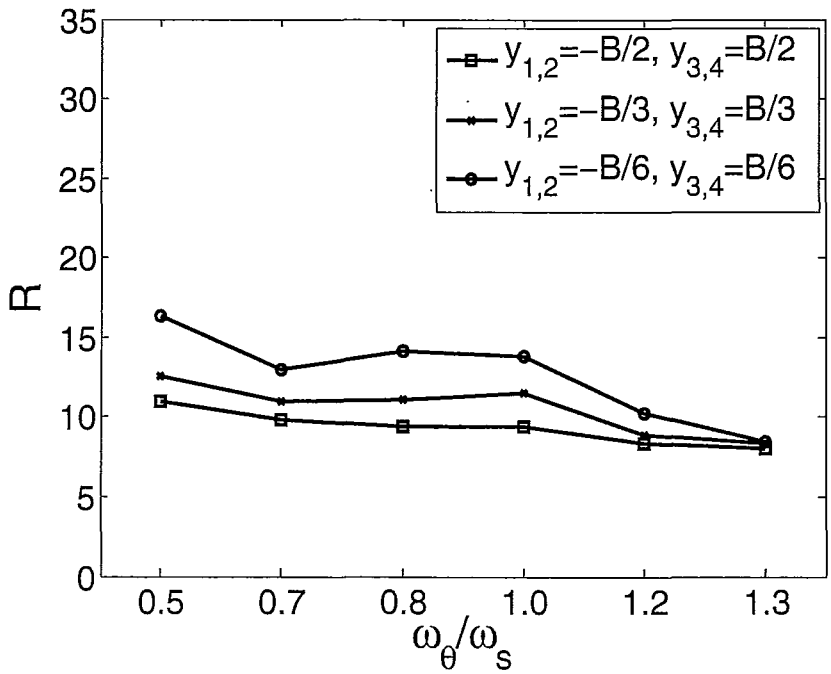

Figure 3.37: DMF of Structures with Equal Modal Damping Ratio Values Equipped with Four TMDs ($\mu = 0.02$) (Approach-II) subjected to Harmonic Excitation

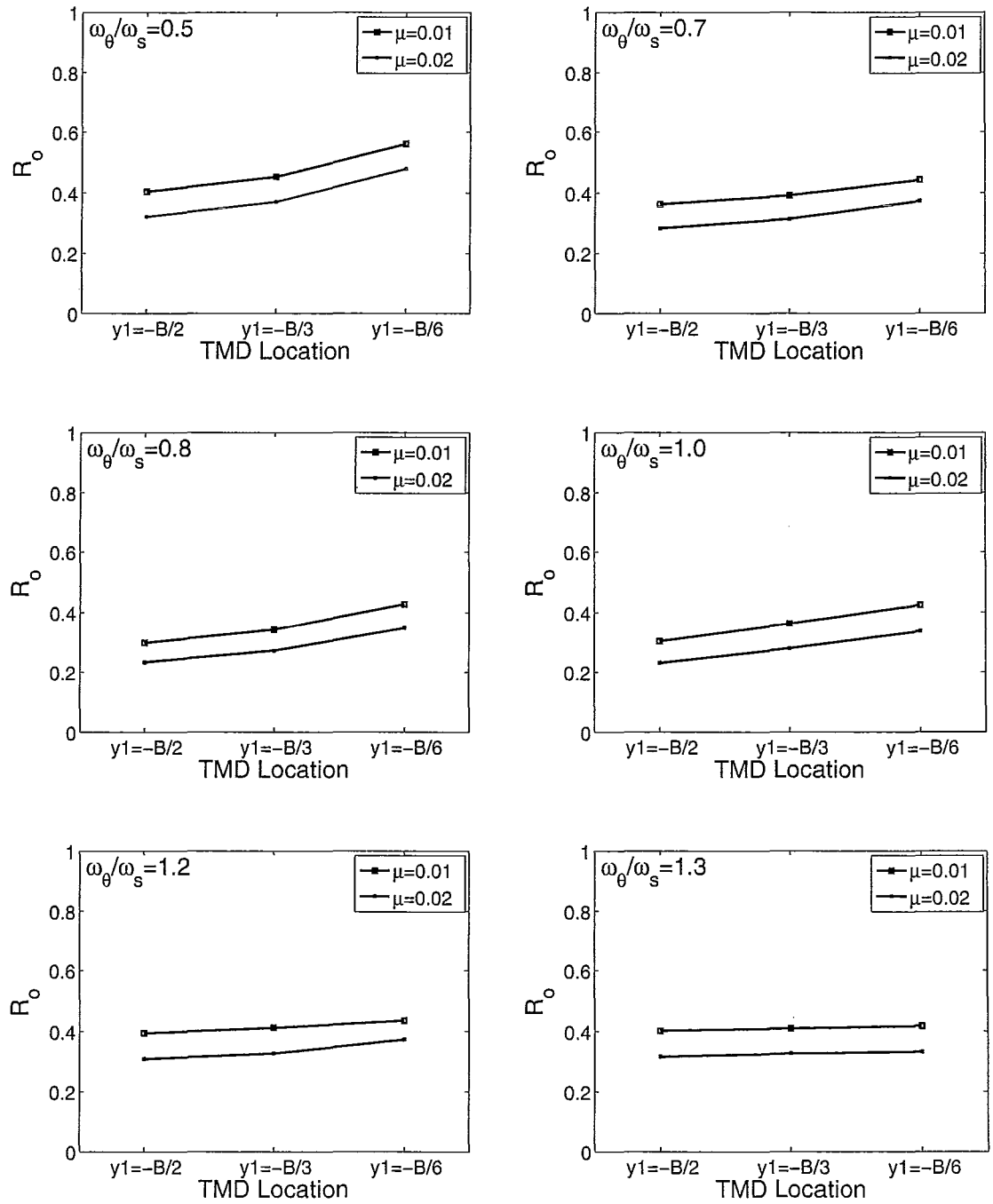

Figure 3.38: Response Reduction Factors for Structures with Equal Modal Damping Ratio Values Equipped with Four TMDs (Approach-II) subjected to Harmonic Excitation

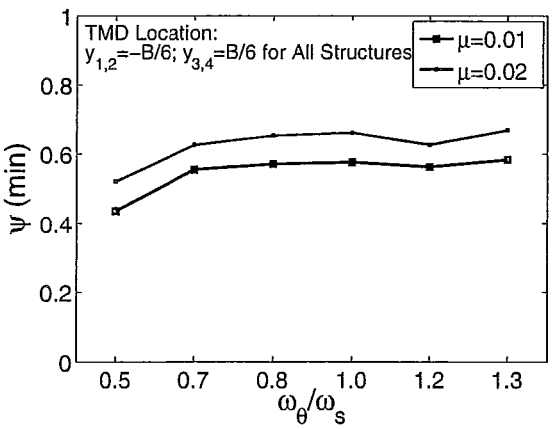

Figure 3.39: Minimum Efficiency Obtained for Four TMDs (Approach-II) subjected to Harmonic Excitation

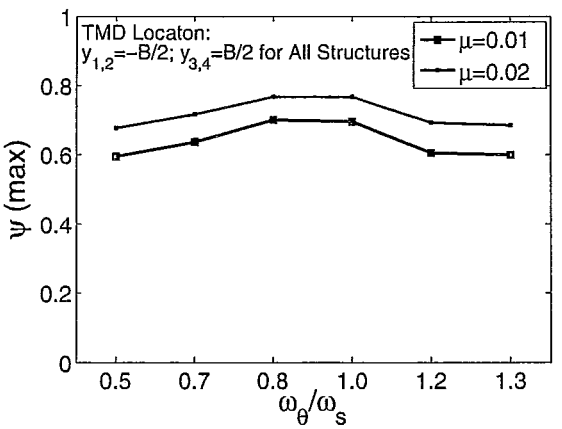

Figure 3.40: Maximum Efficiency Obtained for Four TMDs (Approach-II) subjected to Harmonic Excitation

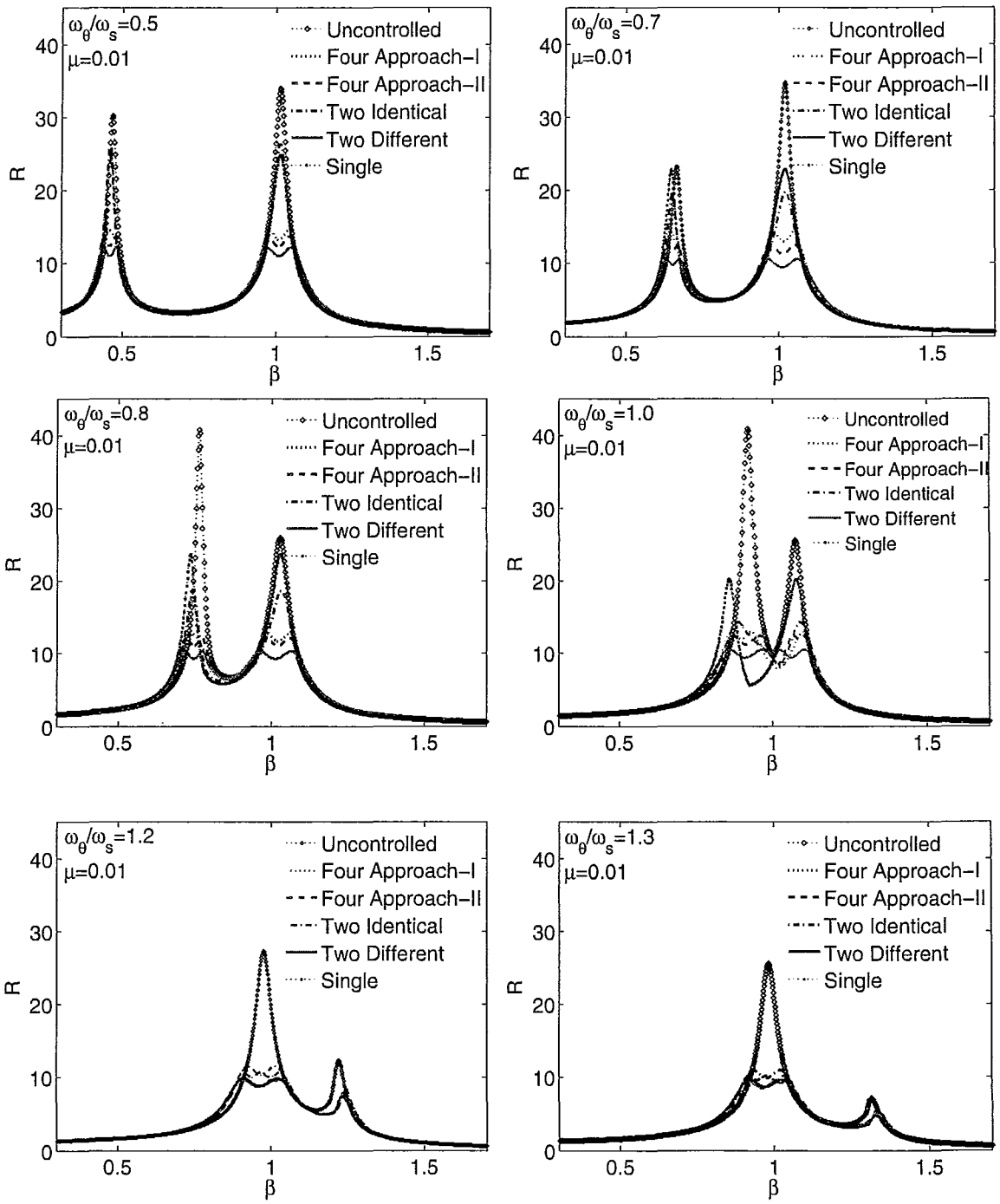

Figure 3.41: Frequency Response Function Plots of Structures with Equal Modal Damping Ratio Values with Maximum TMD(s) Efficiency Location

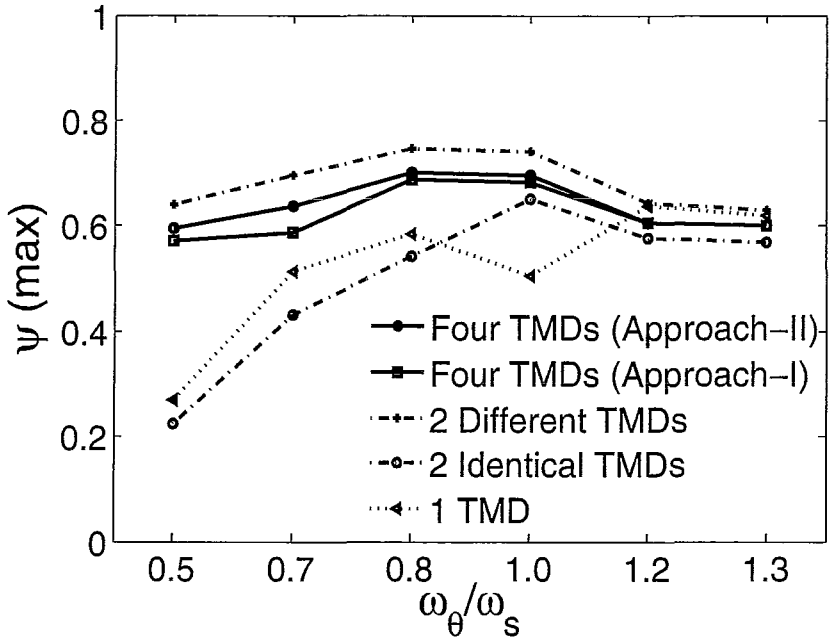

Figure 3.42: Maximum Efficiency for Different Arrangements of TMDs ($\mu = 0.01$)

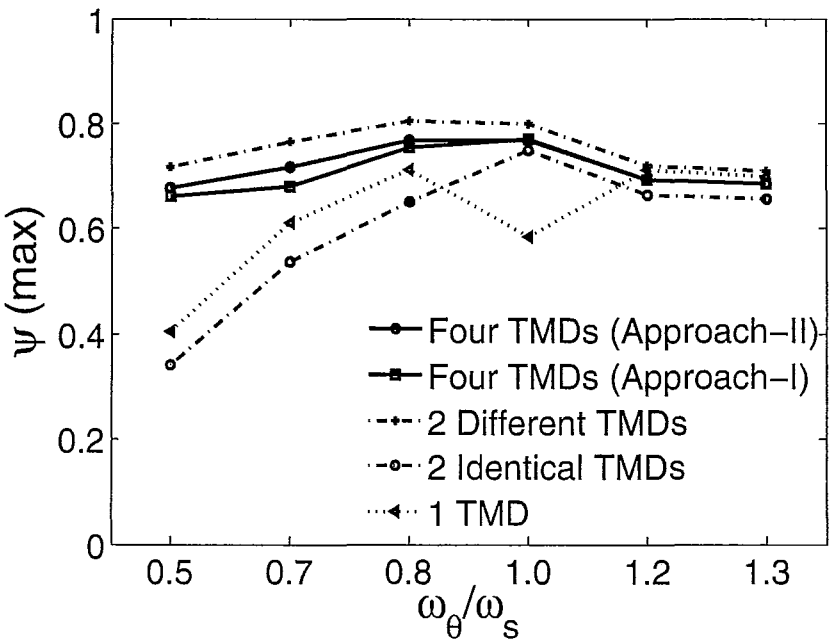

Figure 3.43: Maximum Efficiency for Different Arrangements of TMDs ($\mu = 0.02$)

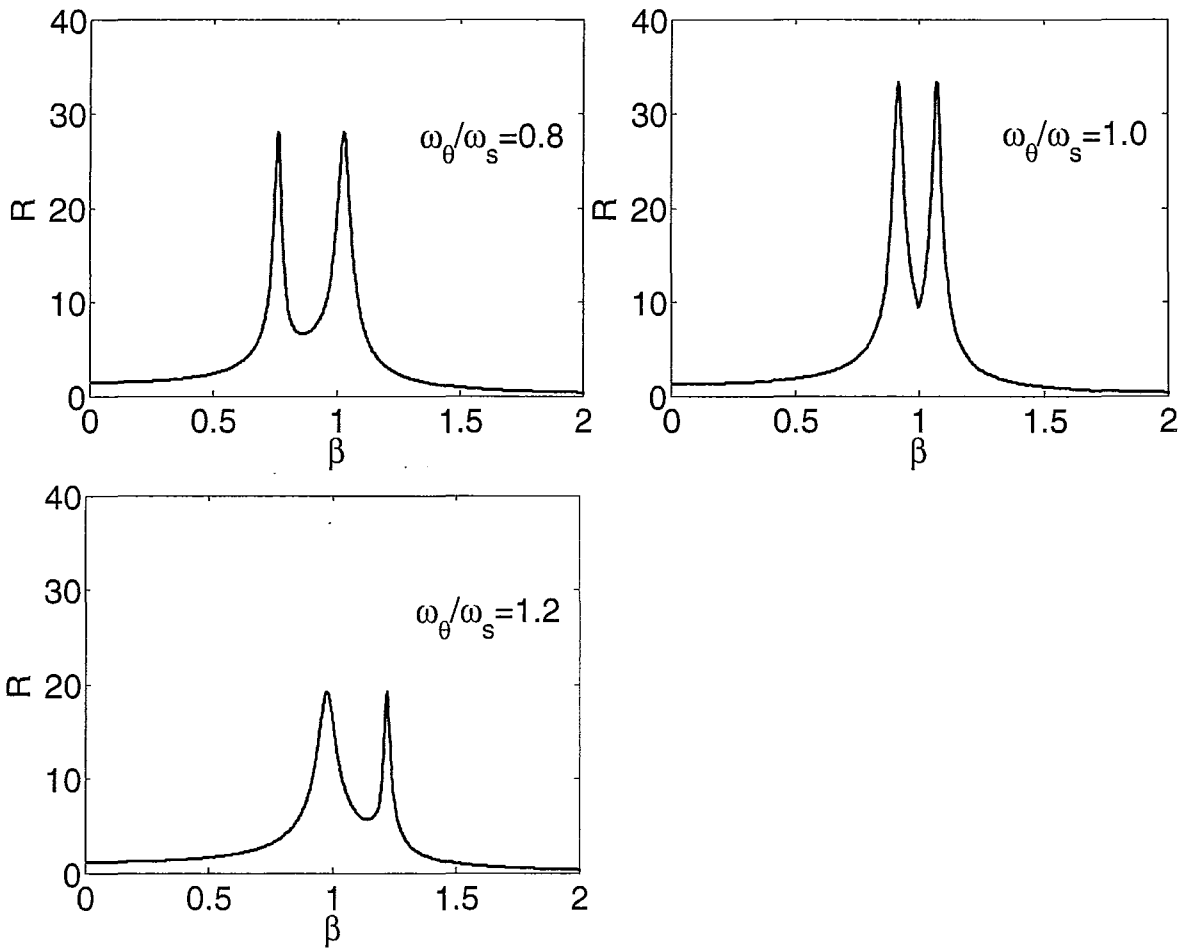

Figure 3.44: Frequency Response Function Plots of Structures with Equal Modal Peak Amplitude Values without DVA subjected to Harmonic Excitation

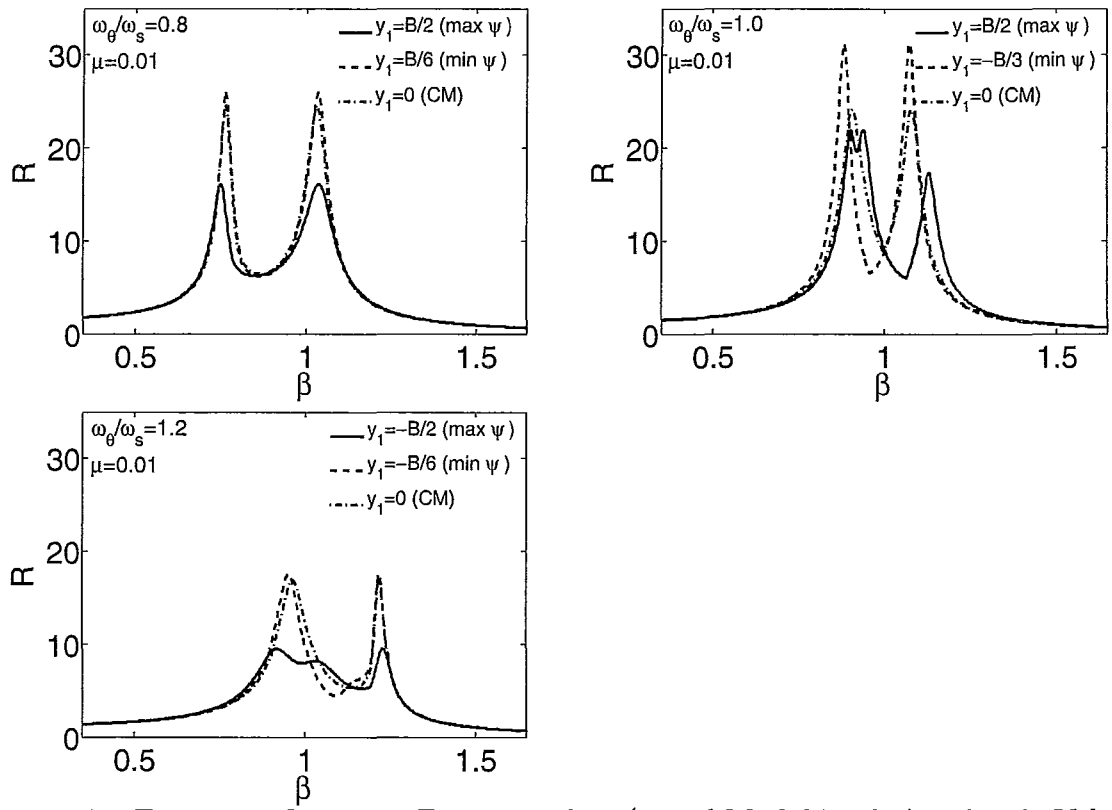

Figure 3.45: Frequency Response Function Plots (Equal Modal Peak Amplitude Values - Single TMD Configuration)

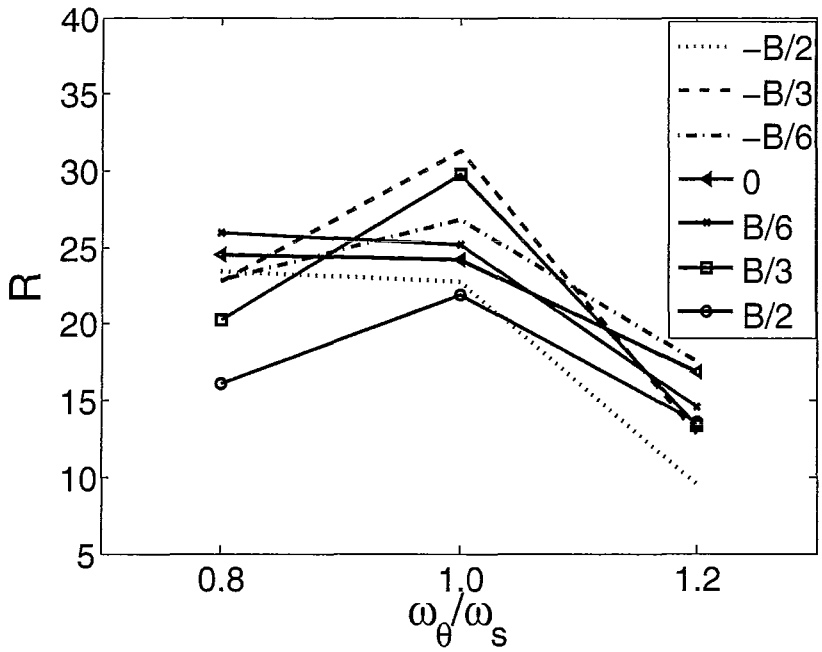

Figure 3.46: DMF of Structures with Equal Modal Peak Amplitude Values Equipped with Single TMD ($\mu = 0.01$) subjected to Harmonic Excitation

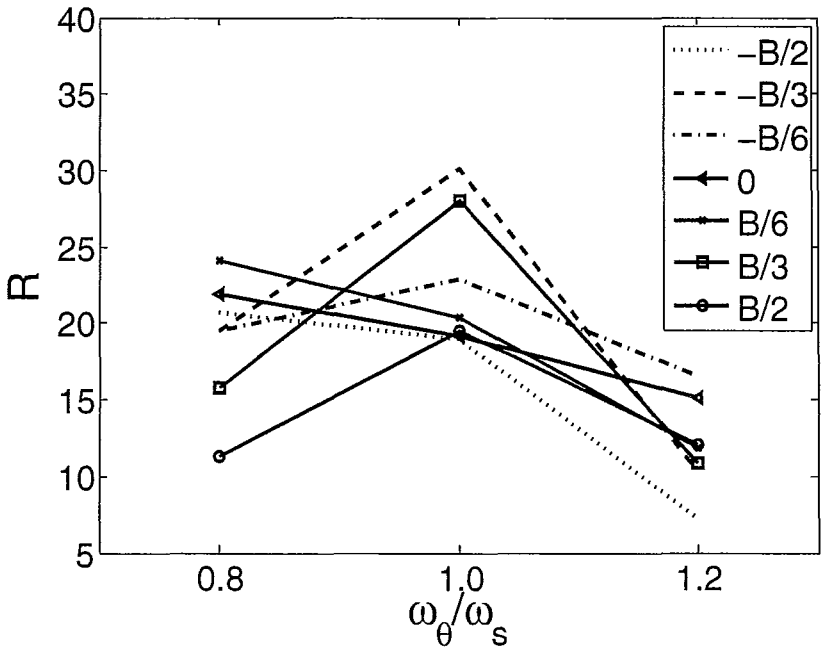

Figure 3.47: DMF of Structures with Equal Modal Peak Amplitude Values Equipped with Single TMD ($\mu = 0.02$) subjected to Harmonic Excitation

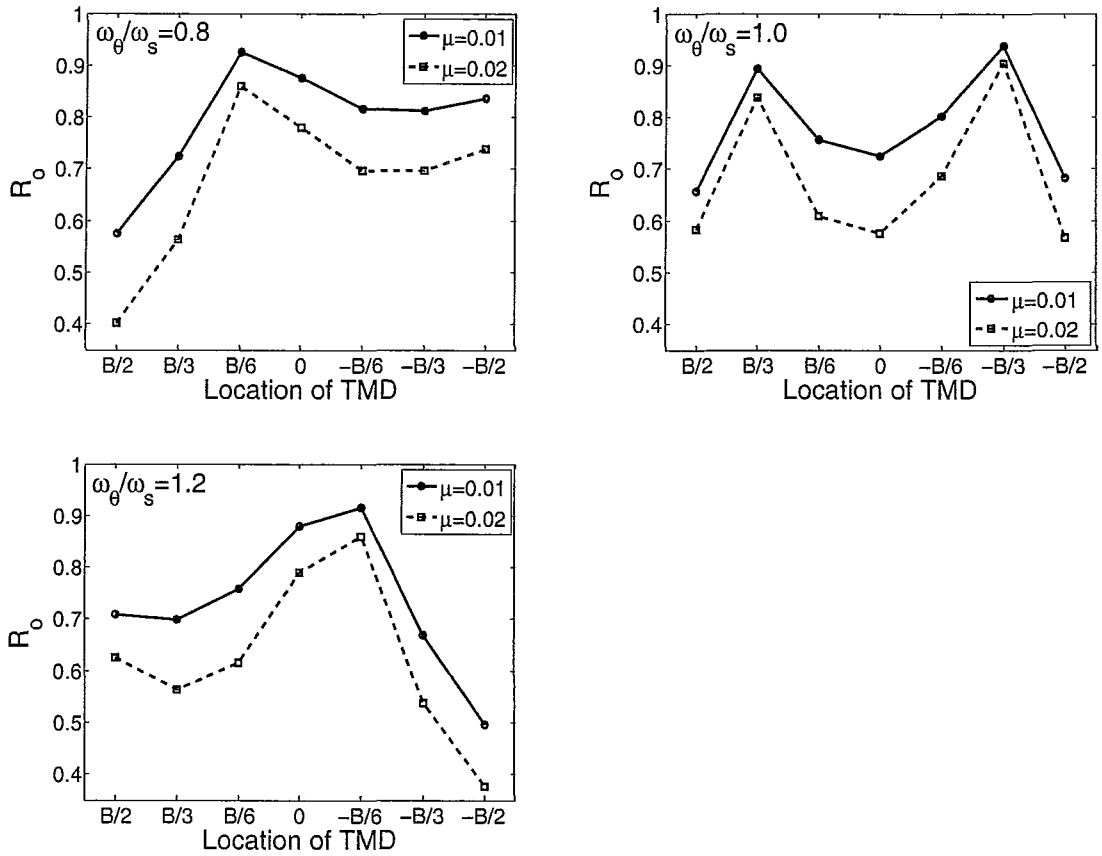

Figure 3.48: Response Reduction Factors for Structures with Equal Modal Peak Amplitude Values Equipped with Single TMD subjected to Harmonic Excitation

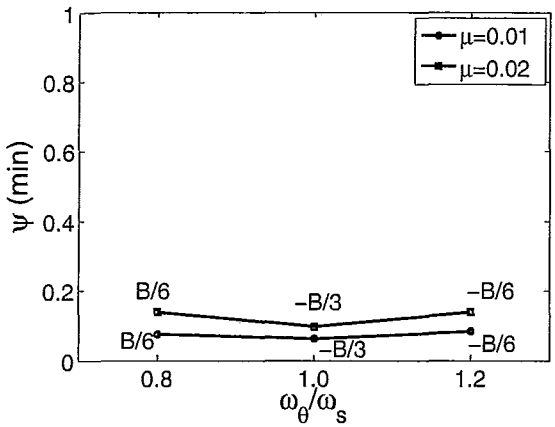

Figure 3.49: Minimum Efficiency Obtained for Structures with Equal Modal Peak Amplitude Values Equipped with Single TMD subjected to Harmonic Excitation

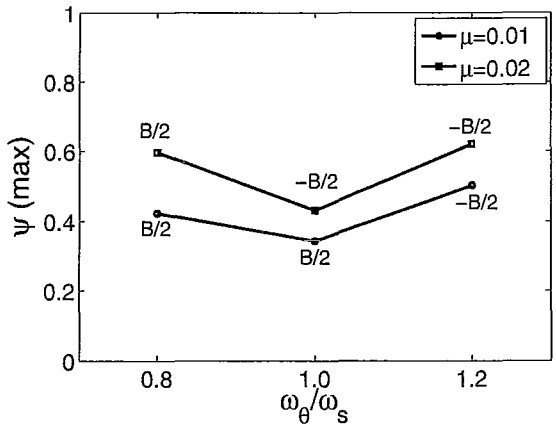

Figure 3.50: Maximum Efficiency Obtained for Structures with Equal Modal Peak Amplitude Values Equipped with Single TMD subjected to Harmonic Excitation

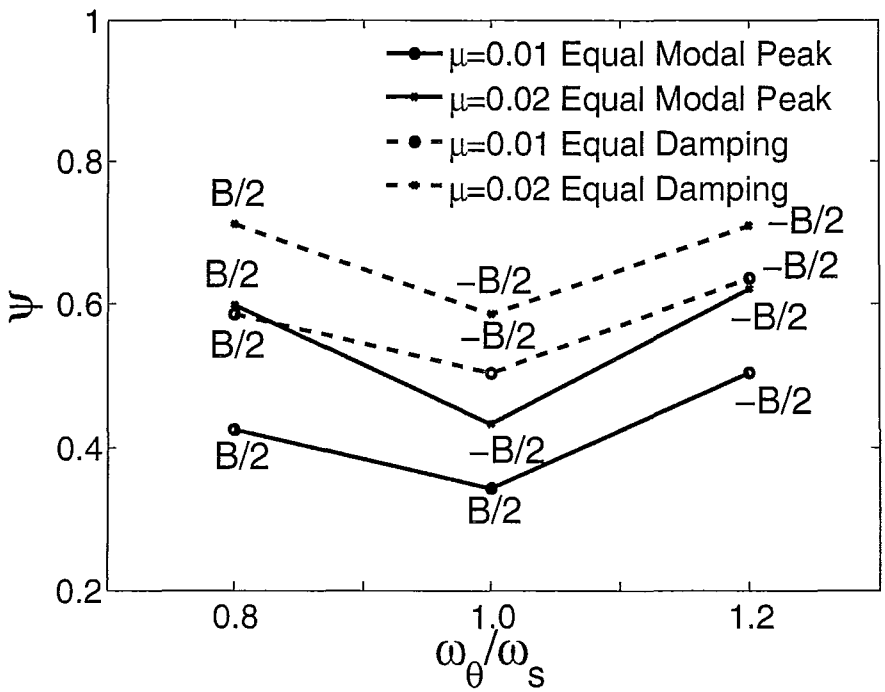

Figure 3.51: Maximum Efficiency Comparison between Structures with Equal Modal Damping Ratio and Equal Modal Peak Amplitude Equipped with Single TMD subjected to Harmonic Excitation

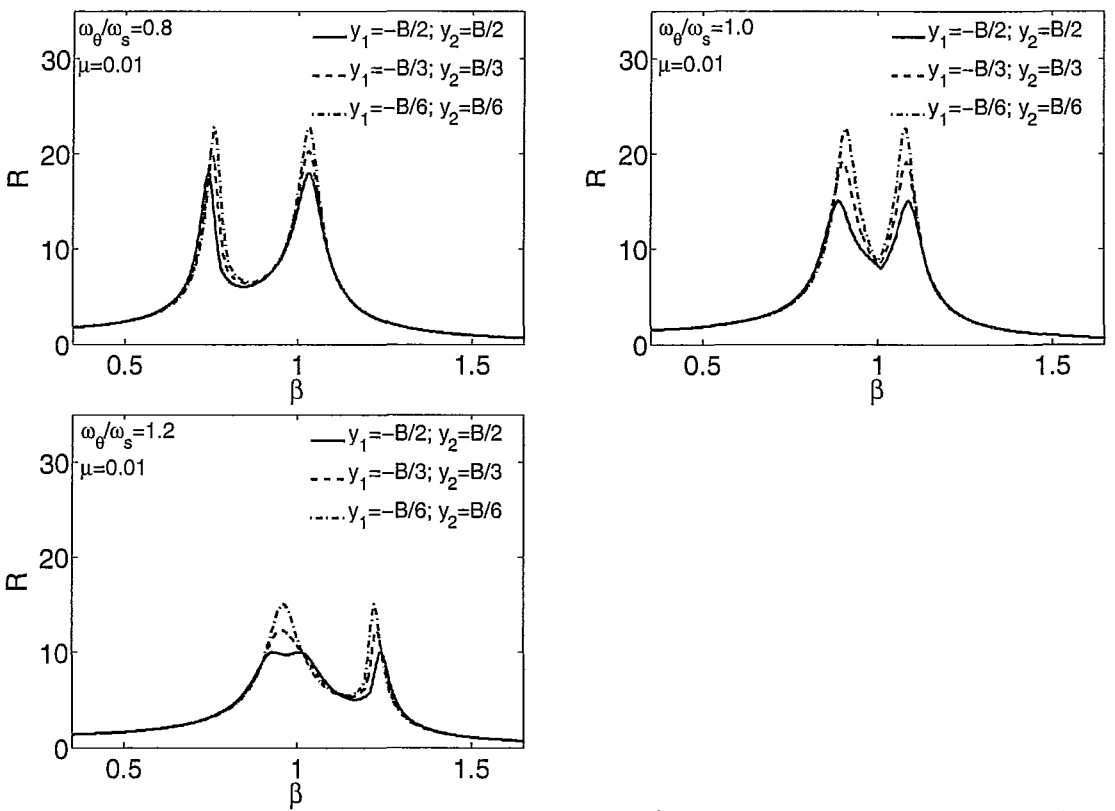

Figure 3.52: Frequency Response Function Plots (Equal Modal Peak Amplitude - Two Identical TMDs Configuration)

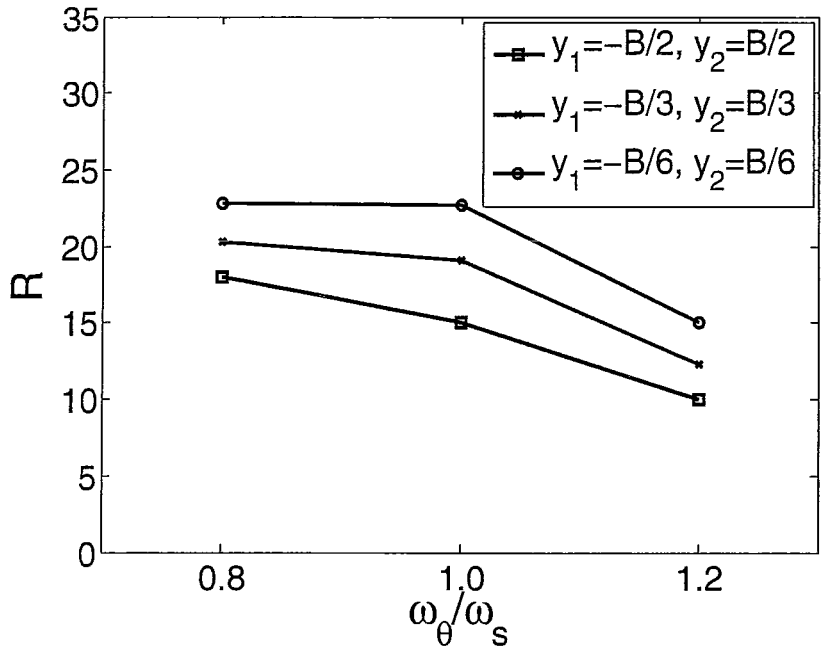

Figure 3.53: DMF for Structures with Equal Modal Peak Amplitude Values Equipped with Two Identical TMDs ($\mu = 0.01$) subjected to Harmonic Excitation

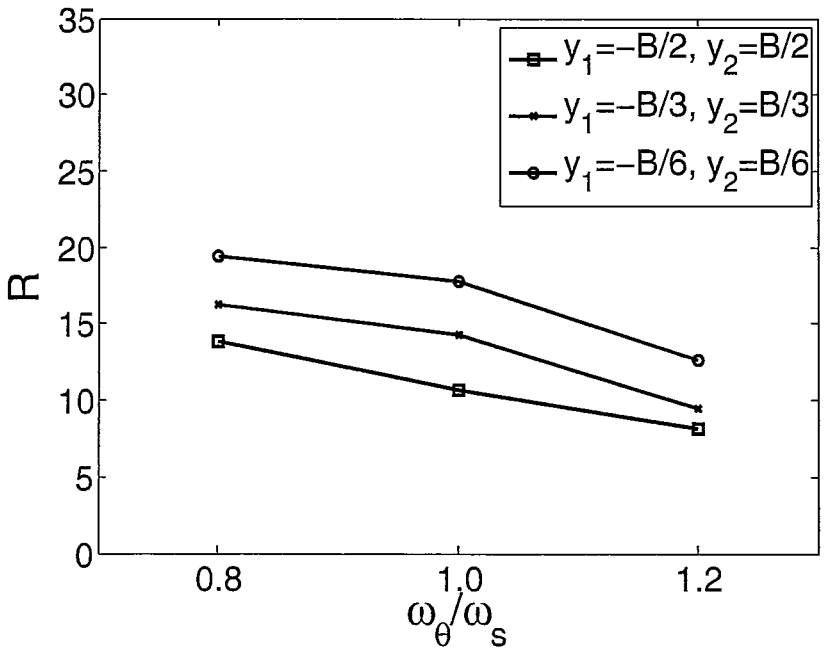

Figure 3.54: DMF for Structures with Equal Modal Peak Amplitude Values Equipped with Two Identical TMDs ($\mu = 0.02$) subjected to Harmonic Excitation

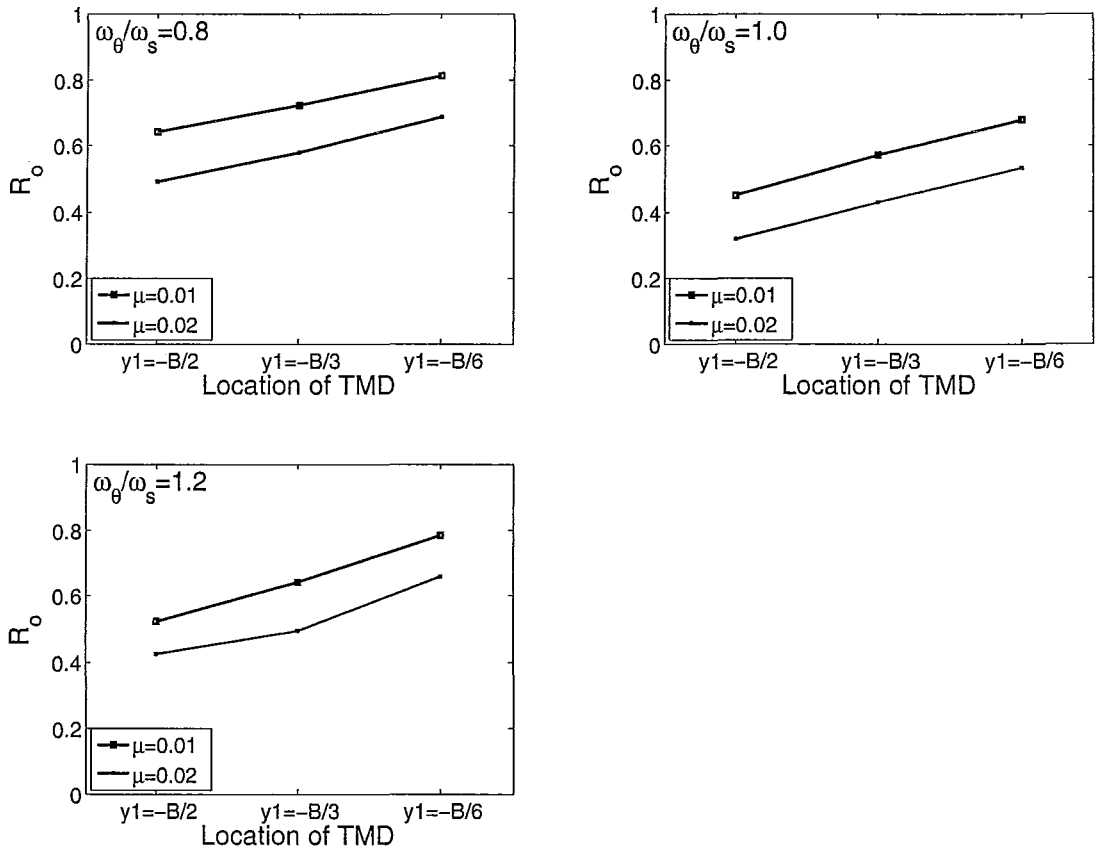

Figure 3.55: Response Reduction Factors of Structures with Equal Modal Peak Amplitude Values Equipped with Two Identical TMDs subjected to Harmonic Excitation

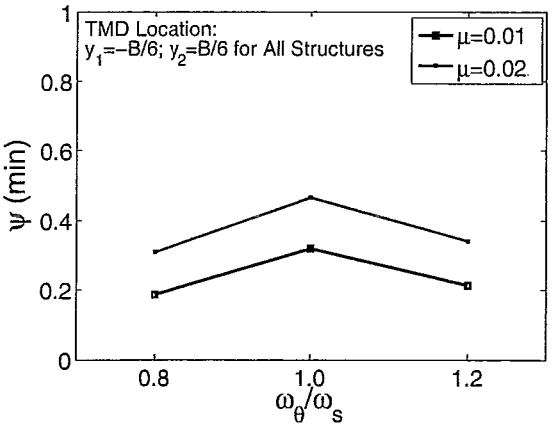

Figure 3.56: Minimum Efficiency Obtained for Structures with Equal Modal Peak Values Equipped with Two Identical TMDs subjected to Harmonic Excitation

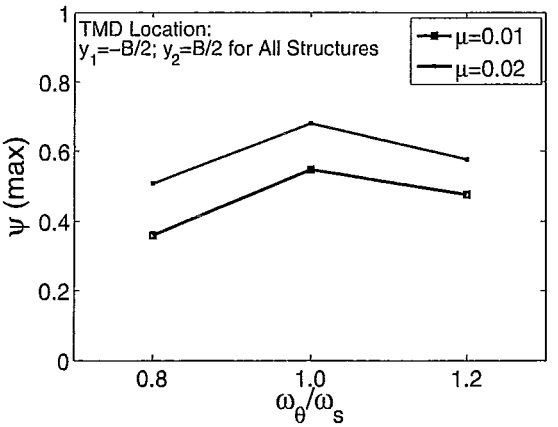

Figure 3.57: Maximum Efficiency Obtained for Structures with Equal Modal Peak Values Equipped with Two Identical TMDs subjected to Harmonic Excitation

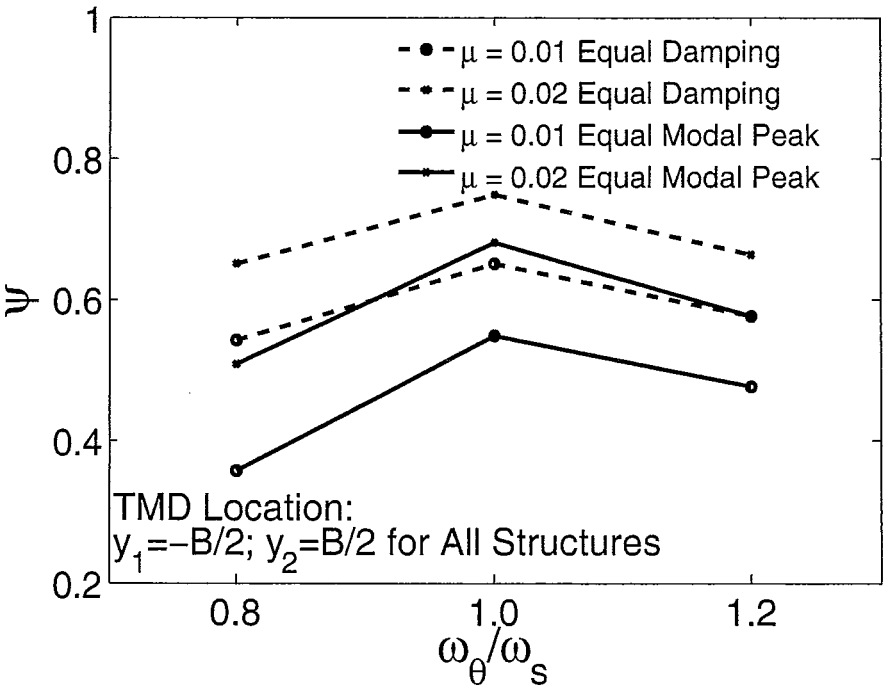

Figure 3.58: Maximum Efficiency Comparison between Structures with Equal Modal Damping Ratio and Equal Modal Peak Amplitude Equipped with Two Identical TMDs subjected to Harmonic Excitation

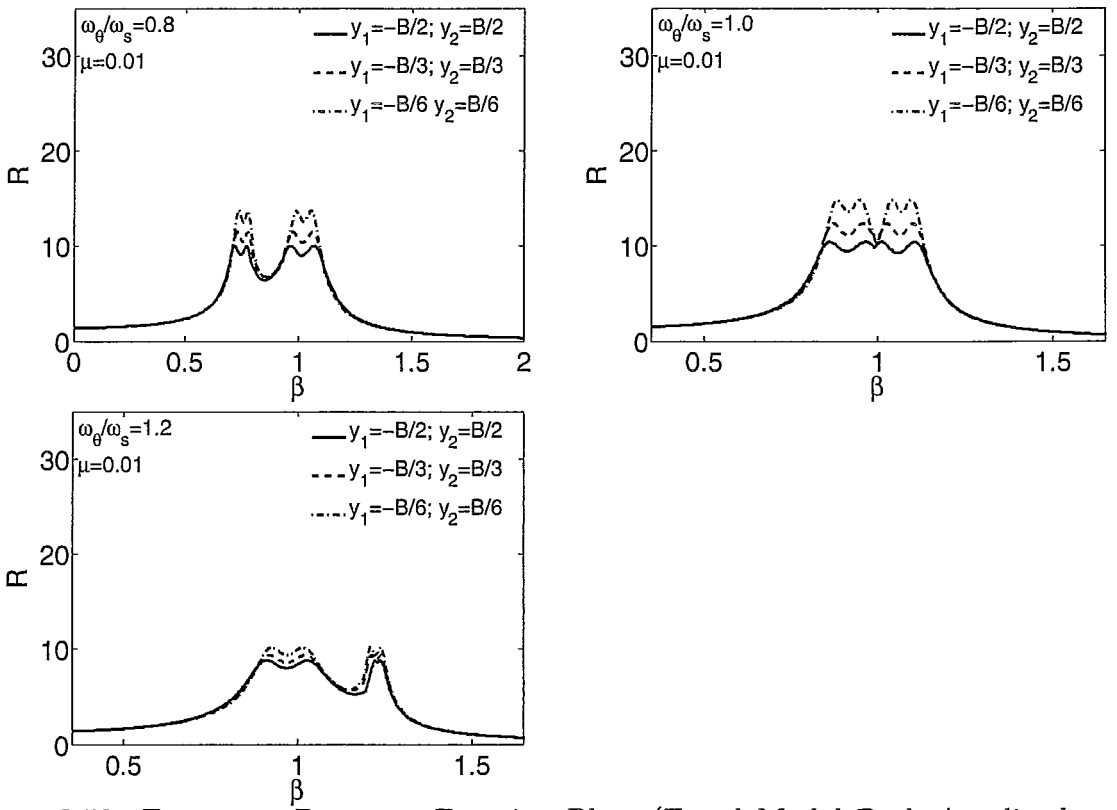

Figure 3.59: Frequency Response Function Plots (Equal Modal Peak Amplitude - Two Different TMDs Configuration)

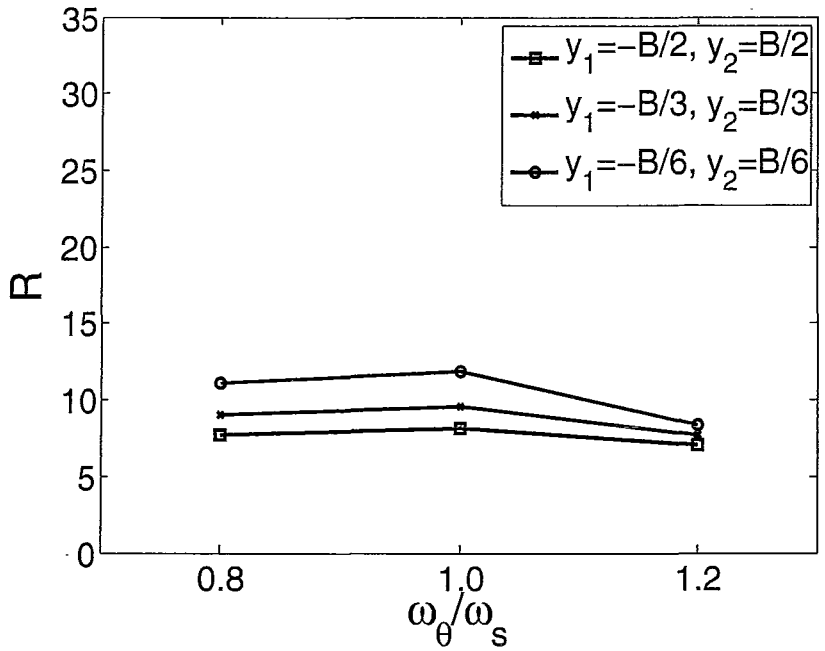

Figure 3.60: DMF of Structures with Equal Modal Peak Amplitude Values Equipped with Two Different TMDs ($\mu = 0.01$) subjected to Harmonic Excitation

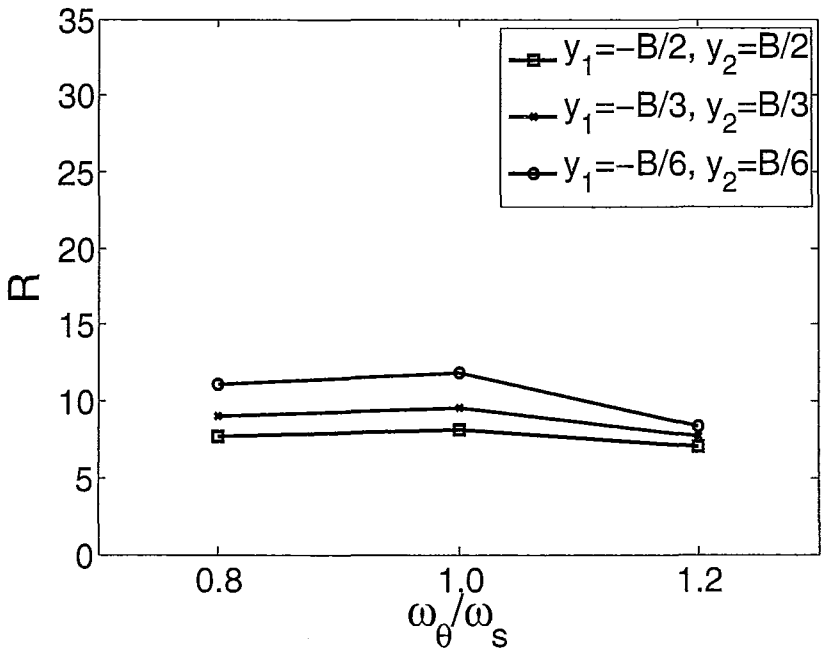

Figure 3.61: DMF of Structures with Equal Modal Peak Amplitude Values Equipped with Two Different TMDs ($\mu = 0.02$) subjected to Harmonic Excitation

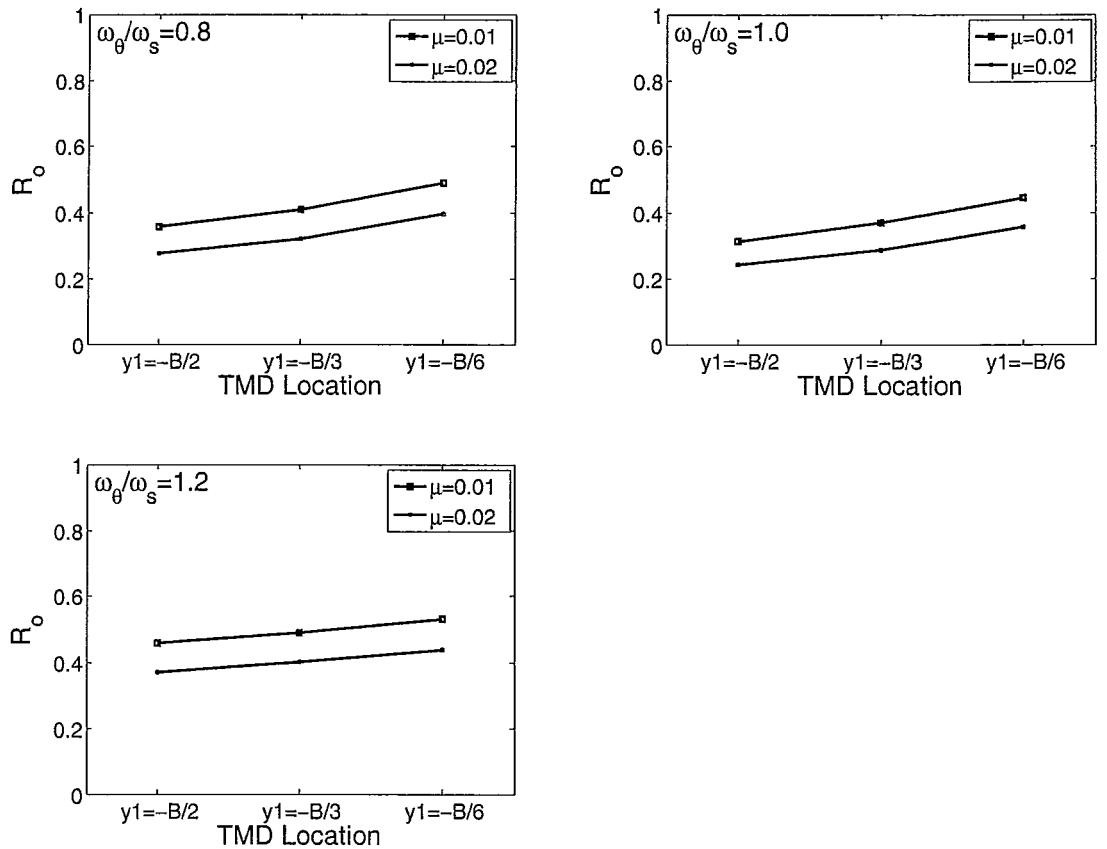

Figure 3.62: Response Reduction Factor for Structures with Equal Modal Peak Amplitude Values Equipped with Two Different TMDs subjected to Harmonic Excitation

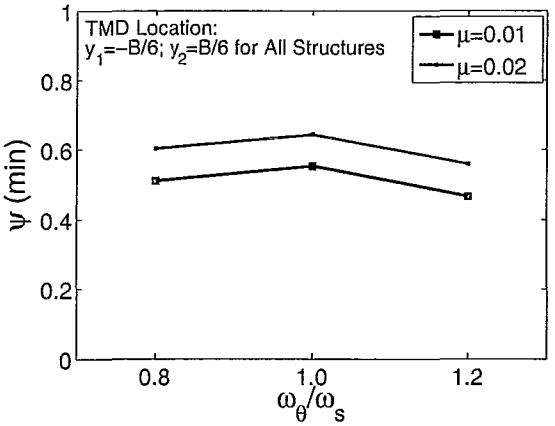

Figure 3.63: Minimum Efficiency Obtained for Structures with Equal Modal Peak Values Equipped with Two Different TMDs subjected to Harmonic Excitation

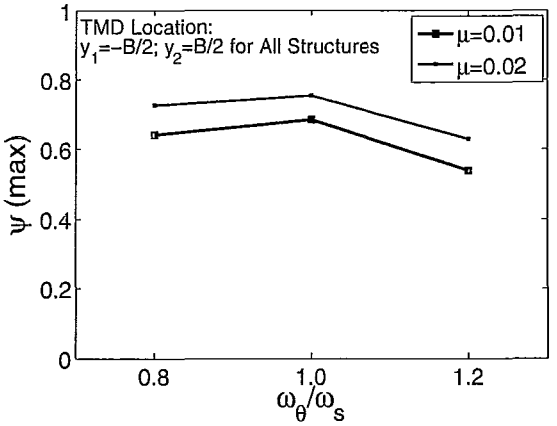

Figure 3.64: Maximum Efficiency Obtained for Structures with Equal Modal Peak Values Equipped with Two Different TMDs subjected to Harmonic Excitation

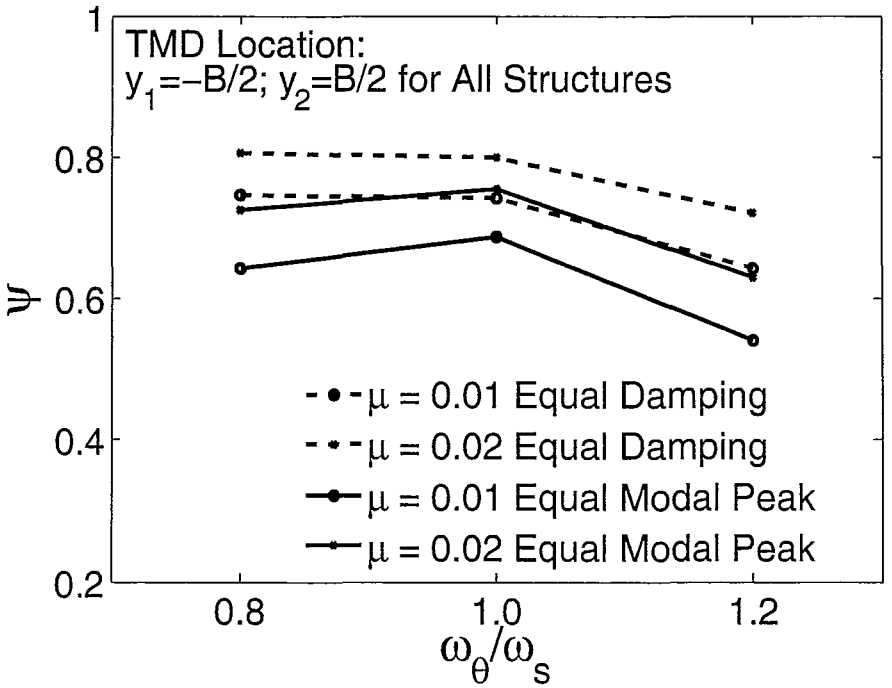

Figure 3.65: Maximum Efficiency Comparison between Structures with Equal Modal Damping Ratio and Equal Modal Peak Amplitude Equipped with Two Different TMDs subjected to Harmonic Excitation

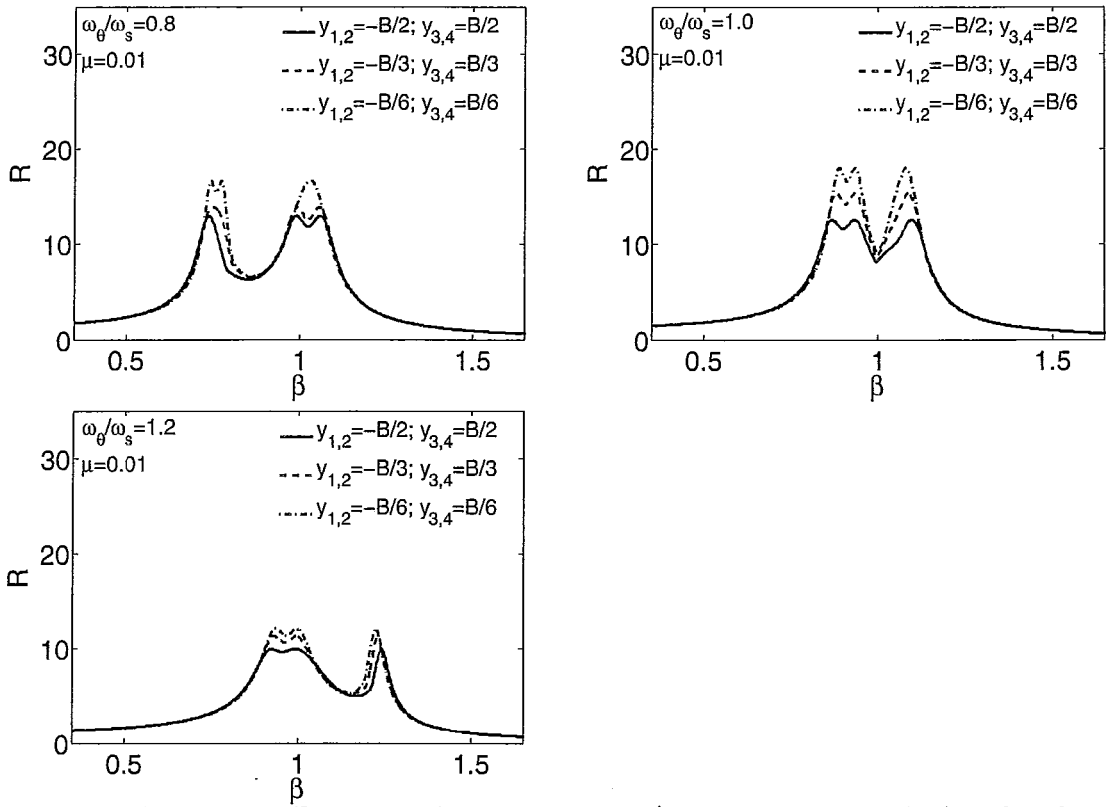

Figure 3.66: Frequency Response Function Plots (Equal Modal Peak Amplitude - Four TMDs Configuration (Approach-I))

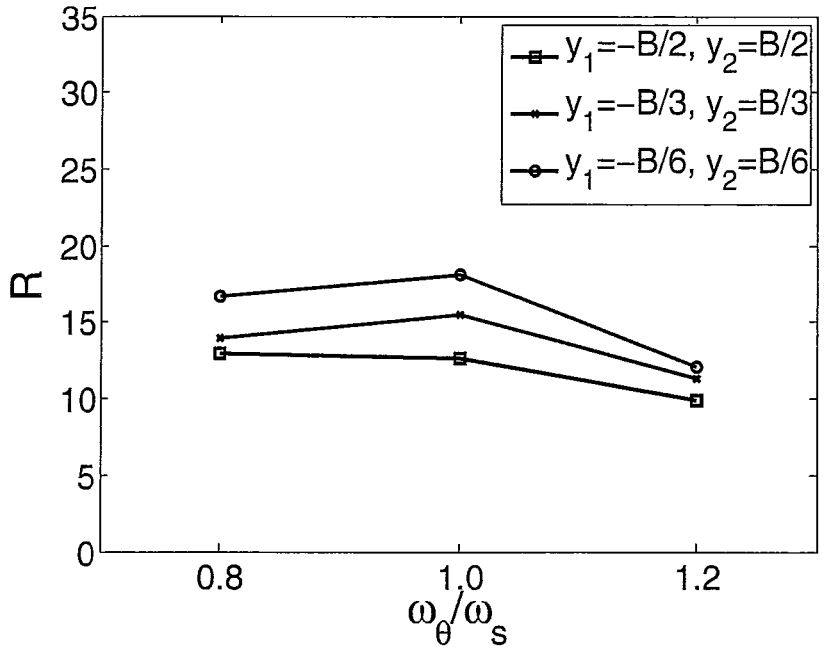

Figure 3.67: DMF of Structures with Equal Modal Peak Amplitude Values Equipped with Four TMDs ($\mu = 0.01$) (Approach-I) subjected to Harmonic Excitation

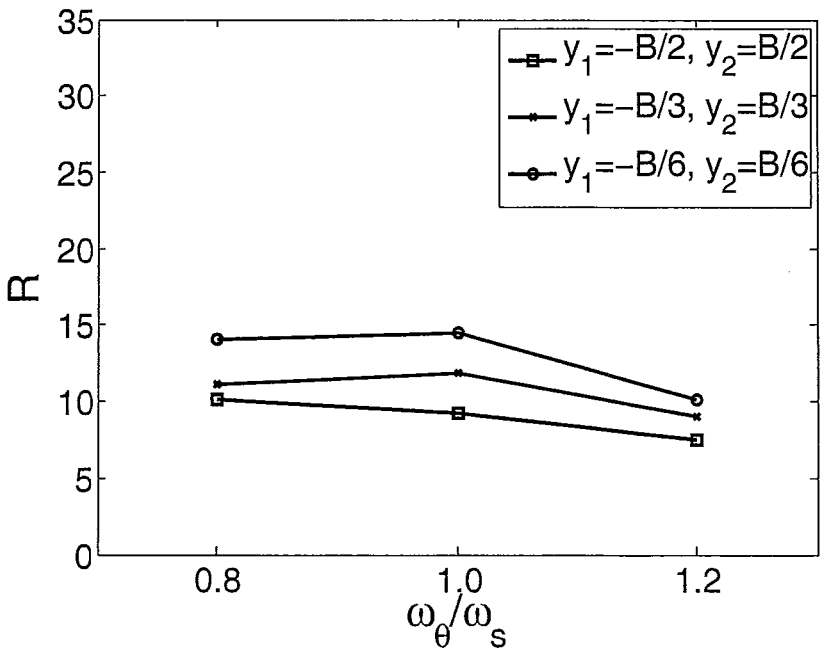

Figure 3.68: DMF of Structures with Equal Modal Peak Amplitude Values Equipped with Four TMDs ($\mu = 0.02$) (Approach-I) subjected to Harmonic Excitation

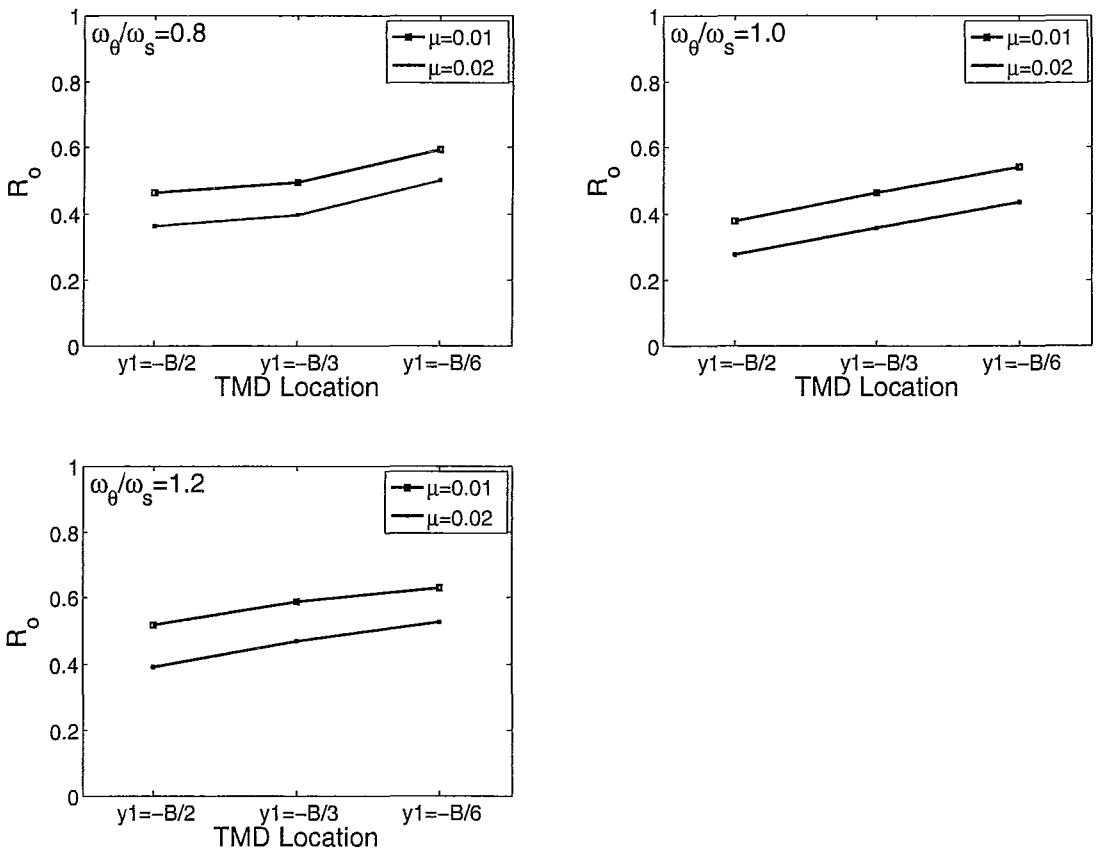

Figure 3.69: Response Reduction Factor for Structures with Equal Modal Peak Amplitude Values Equipped with Four TMDs (Approach-I) subjected to Harmonic Excitation

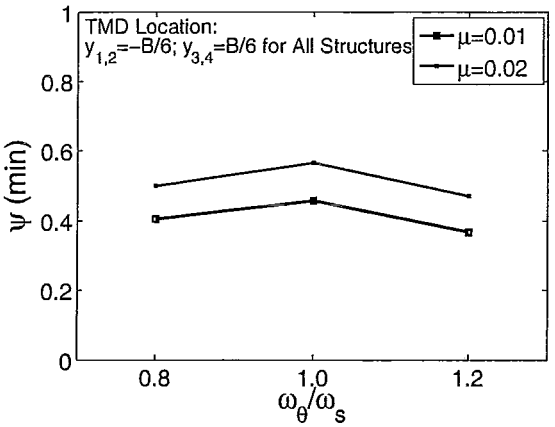

Figure 3.70: Minimum Efficiency Obtained for Structures with Equal Modal Peak Values Equipped with Four TMDs (Approach I) subjected to Harmonic Excitation

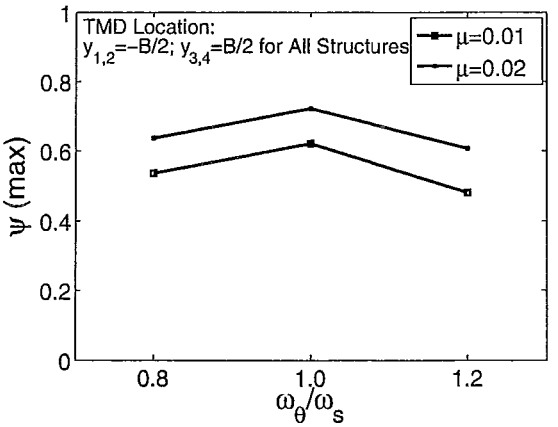

Figure 3.71: Maximum Efficiency Obtained for Structures with Equal Modal Peak Values Equipped with Four TMDs (Approach I) subjected to Harmonic Excitation

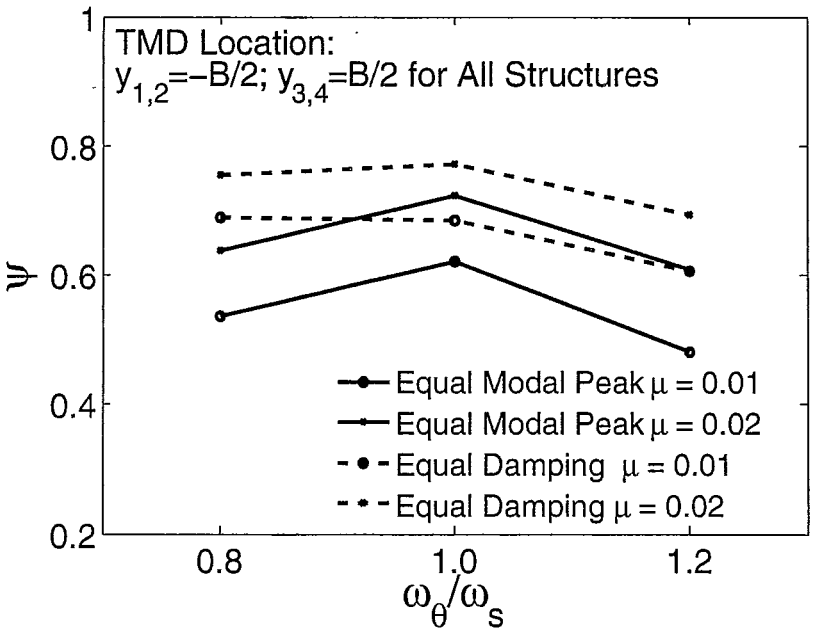

Figure 3.72: Maximum Efficiency Comparison between Structures with Equal Modal Damping Ratio and Equal Modal Peak Amplitude Equipped with Four TMDs (Approach-I) subjected to Harmonic Excitation

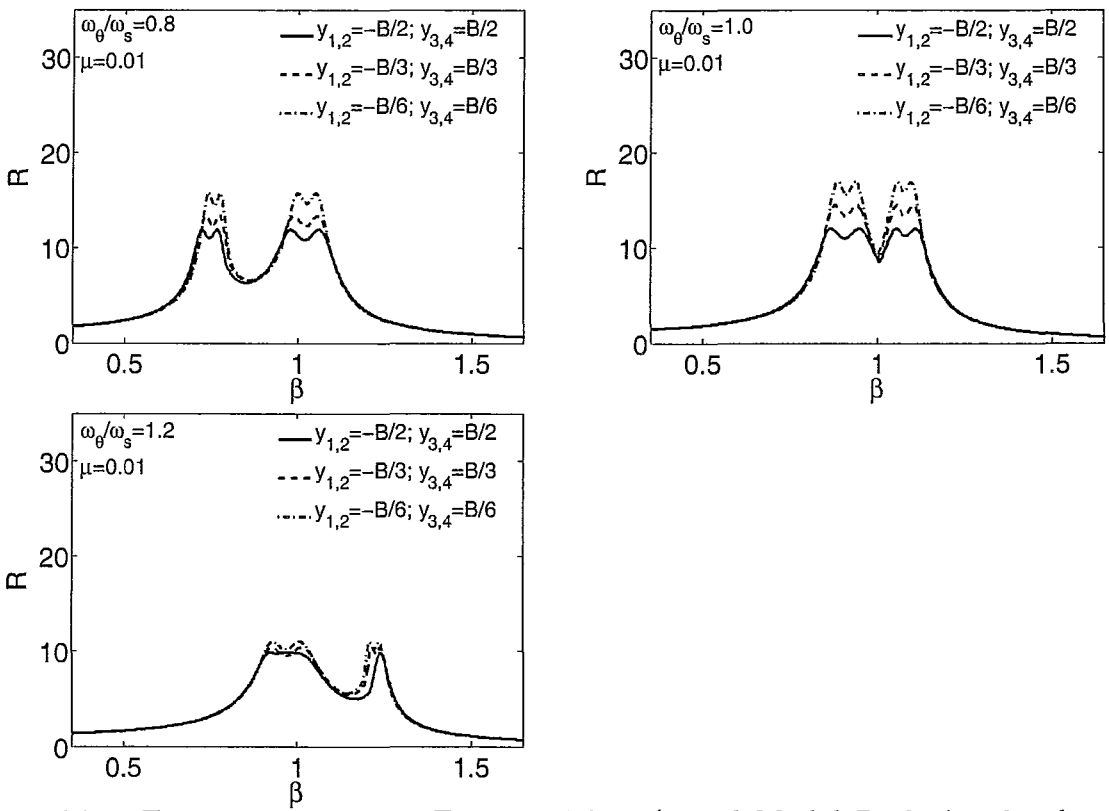

Figure 3.73: Frequency Response Function Plots (Equal Modal Peak Amplitude - Four TMDs Configuration (Approach-II))

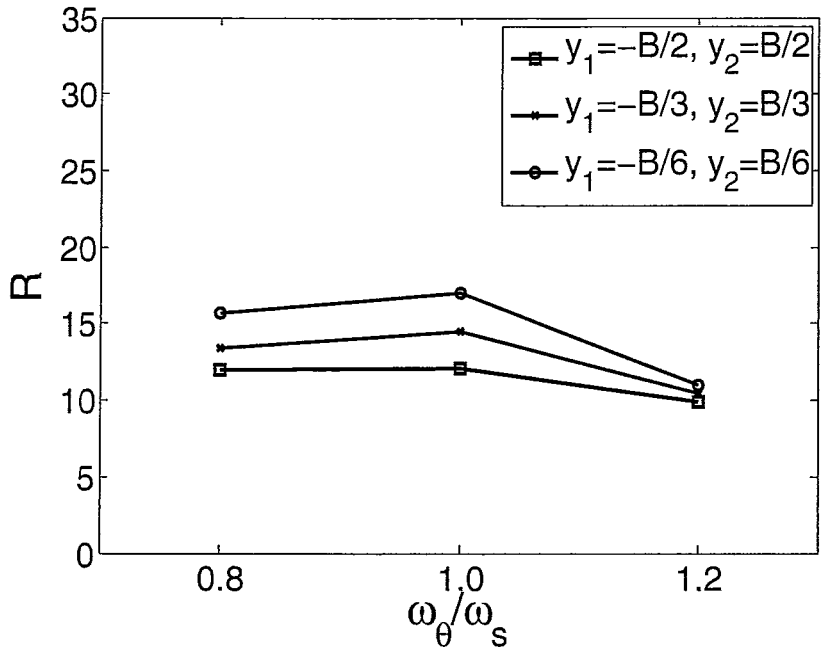

Figure 3.74: DMF of Structures with Equal Modal Peak Amplitude Values Equipped with Four TMDs ($\mu = 0.01$) (Approach-II) subjected to Harmonic Excitation

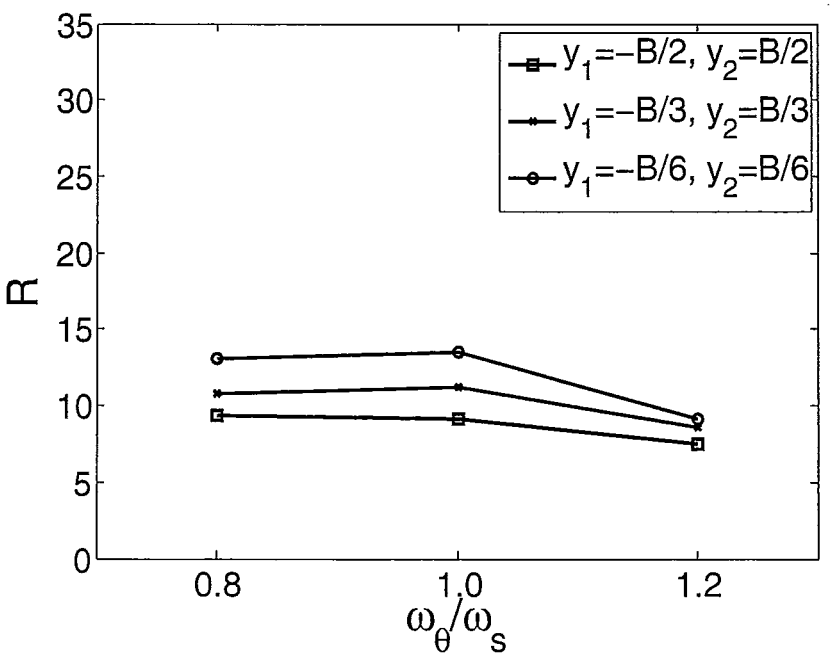

Figure 3.75: DMF of Structures with Equal Modal Peak Amplitude Values Equipped with Four TMDs ($\mu = 0.02$) (Approach-II) subjected to Harmonic Excitation

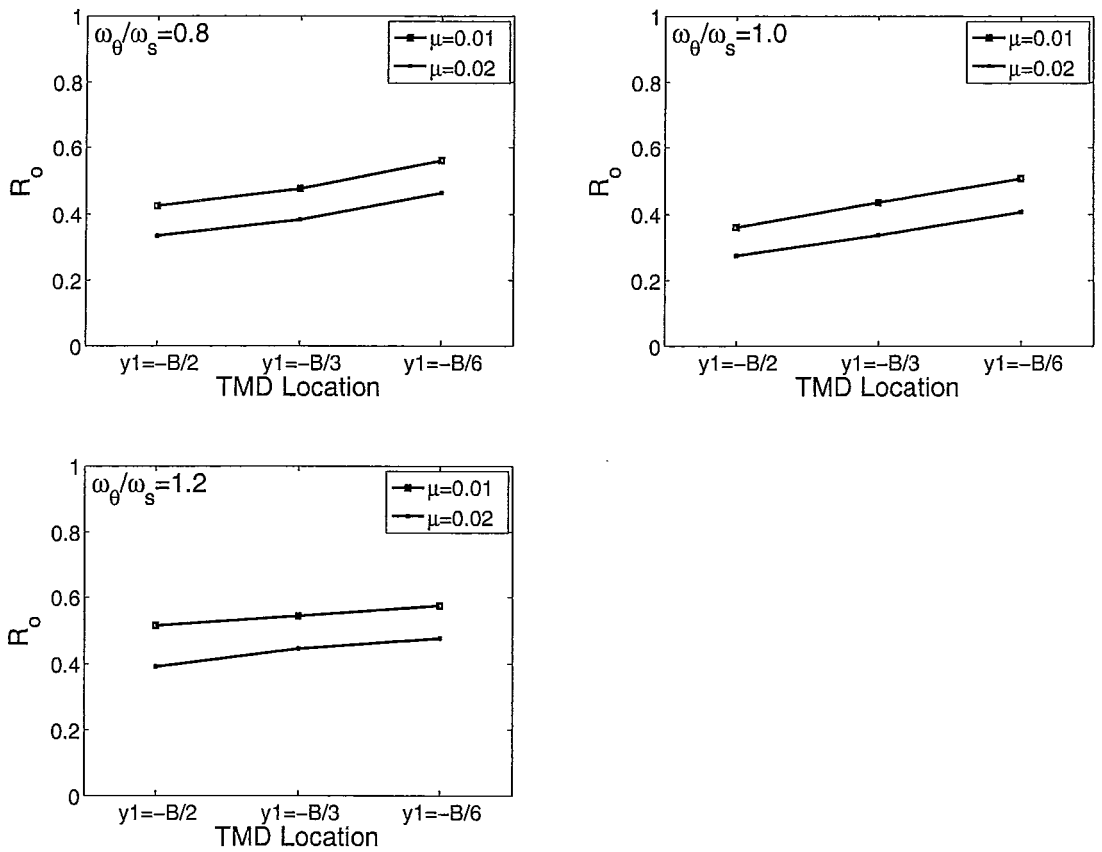

Figure 3.76: Response Reduction Factors for Structures with Equal Modal Peak Amplitude Values Equipped with Four TMDs (Approach-II) subjected to Harmonic Excitation

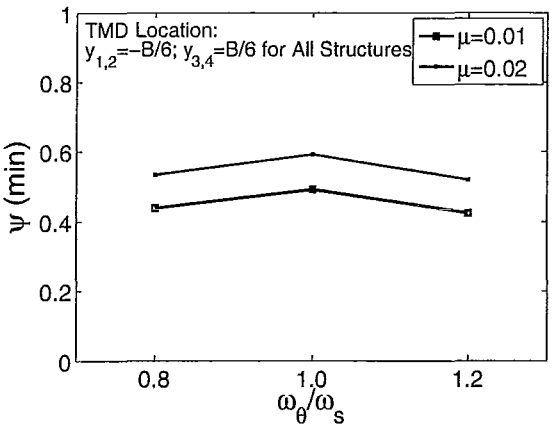

Figure 3.77: Minimum Efficiency for Structures with Equal Modal Peak Amplitude Values Equipped with Four TMDs (Approach II) subjected to Harmonic Excitation

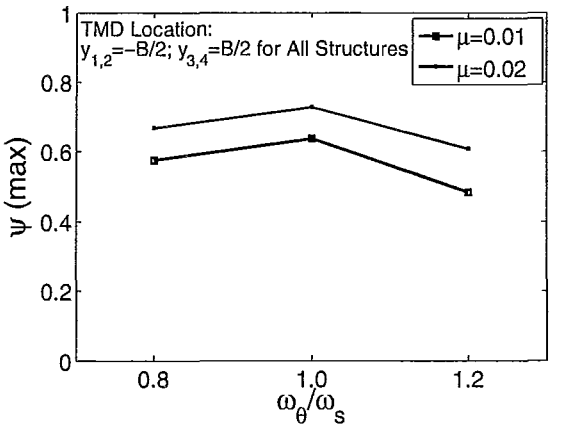

Figure 3.78: Maximum Efficiency for Structures with Equal Modal Peak Amplitude Values Equipped with Four TMDs (Approach II) subjected to Harmonic Excitation

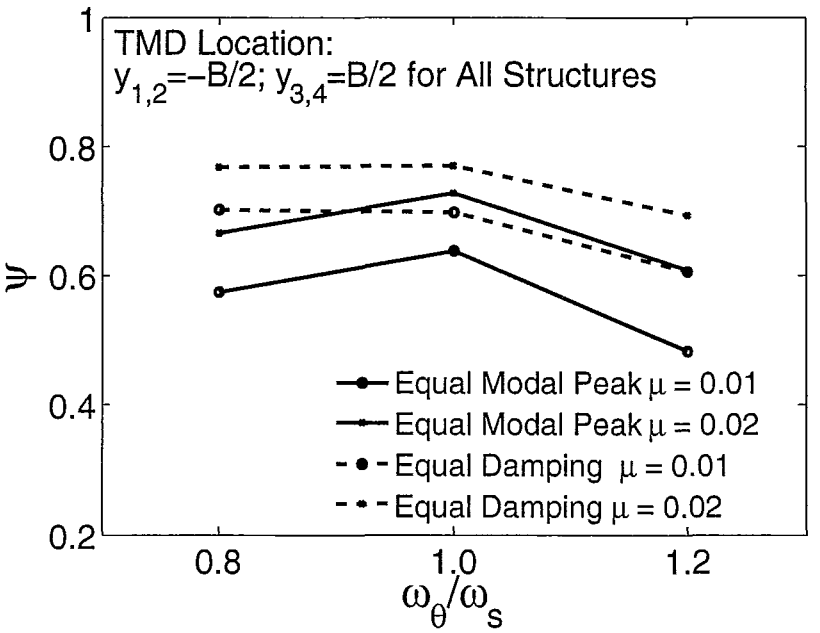

Figure 3.79: Maximum Efficiency Comparison between Structures with Equal Modal Damping Ratio and Equal Modal Peak Amplitude Equipped with Four TMDs (Approach-II) subjected to Harmonic Excitation

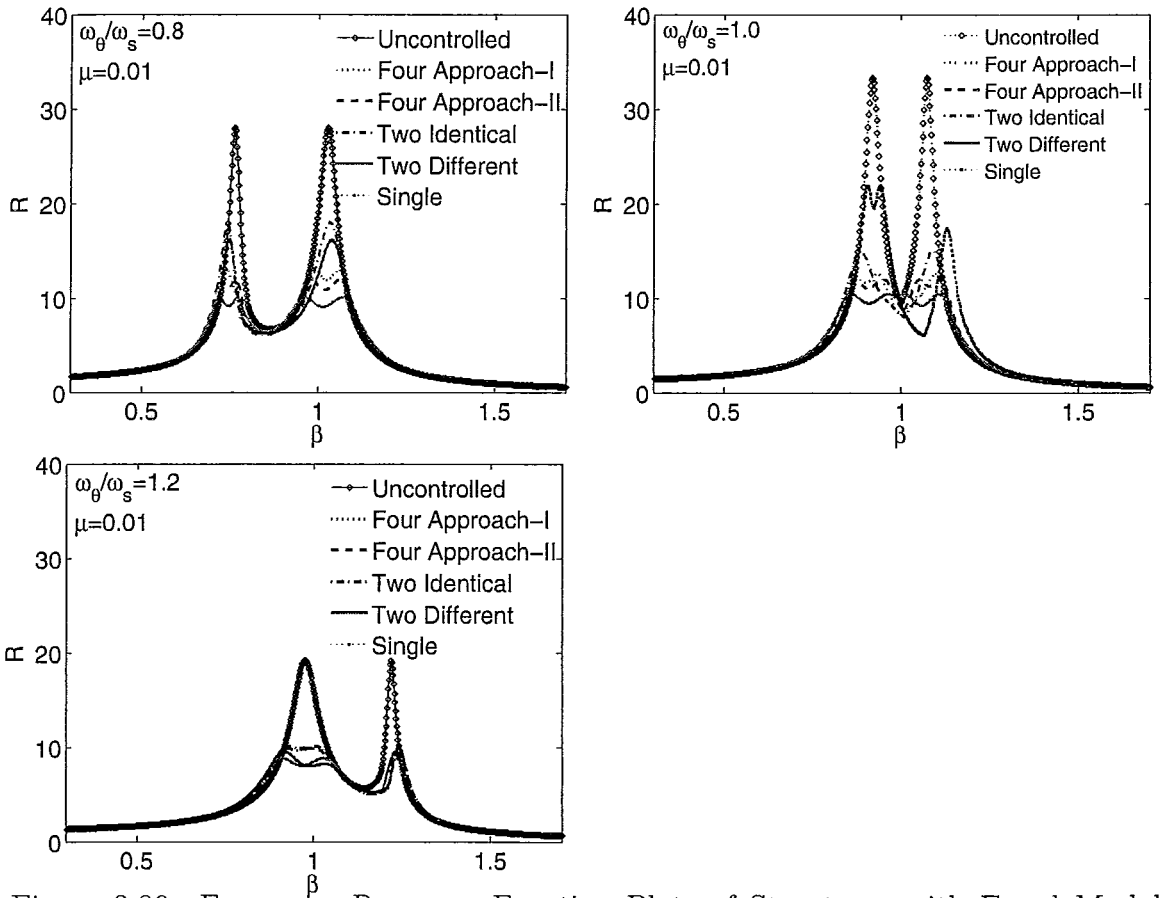

Figure 3.80: Frequency Response Function Plots of Structures with Equal Modal Peak Amplitude Values with Maximum TMD(s) Efficiency Location

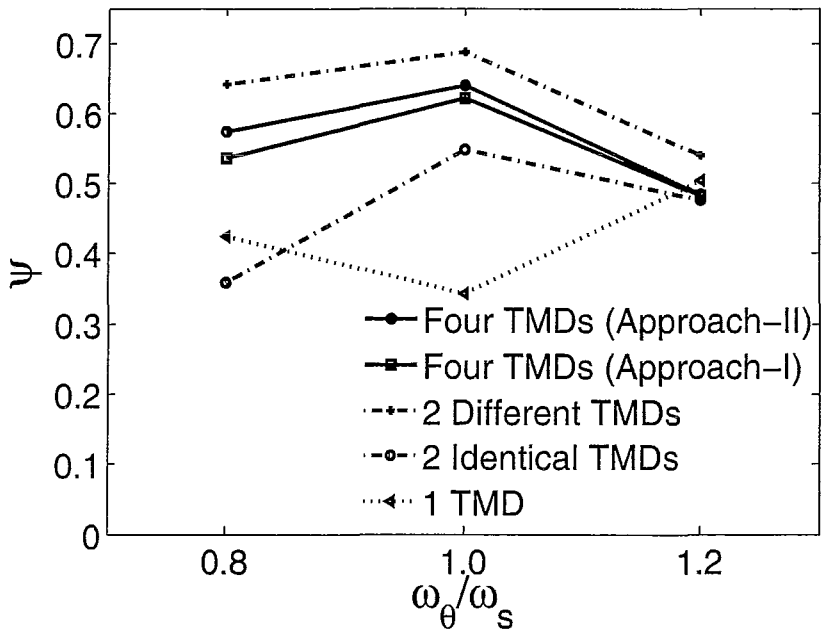

Figure 3.81: Maximum Efficiency for Different Arrangements of TMDs ($\mu = 0.01$) for Structures with Equal Modal Peak Amplitude Values

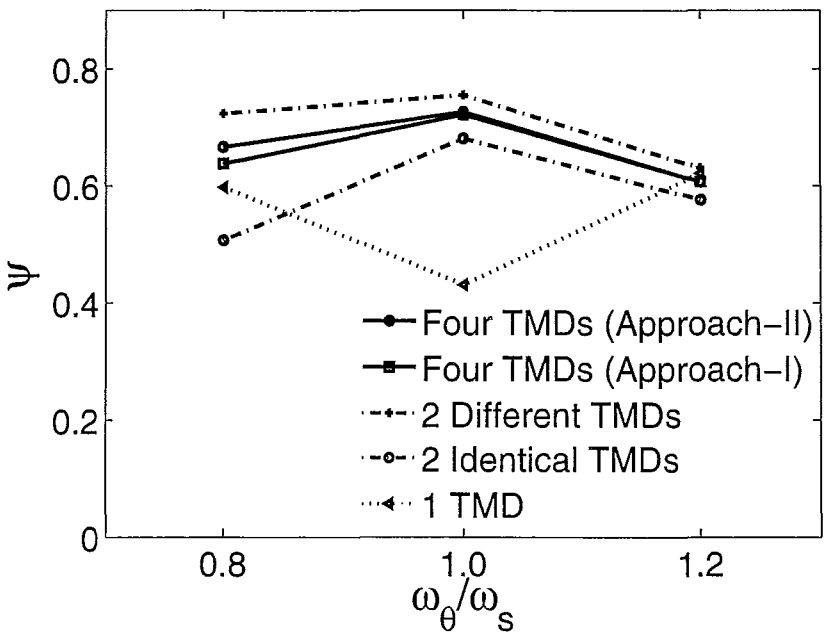

Figure 3.82: Maximum Efficiency for Different Arrangements of TMDs ($\mu = 0.02$) for Structures with Equal Modal Peak Amplitude Values

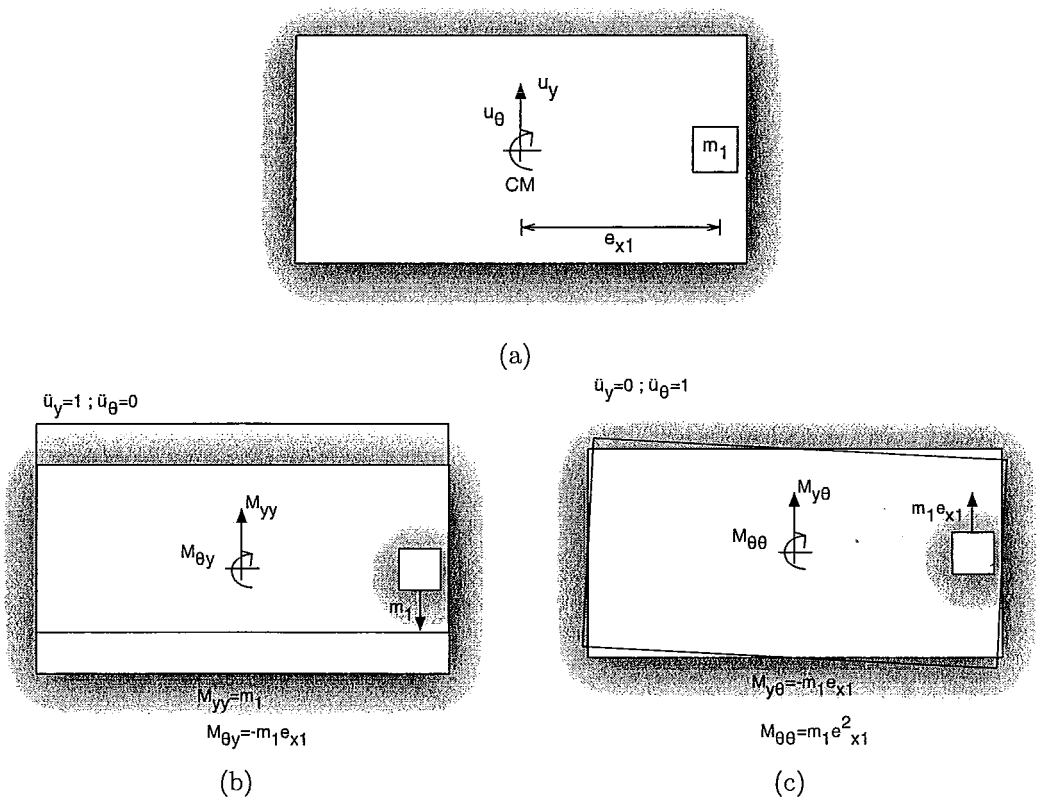

Figure 3.83: Development of TMD Mass Matrix (Single TMD) (a), (b) and (c)

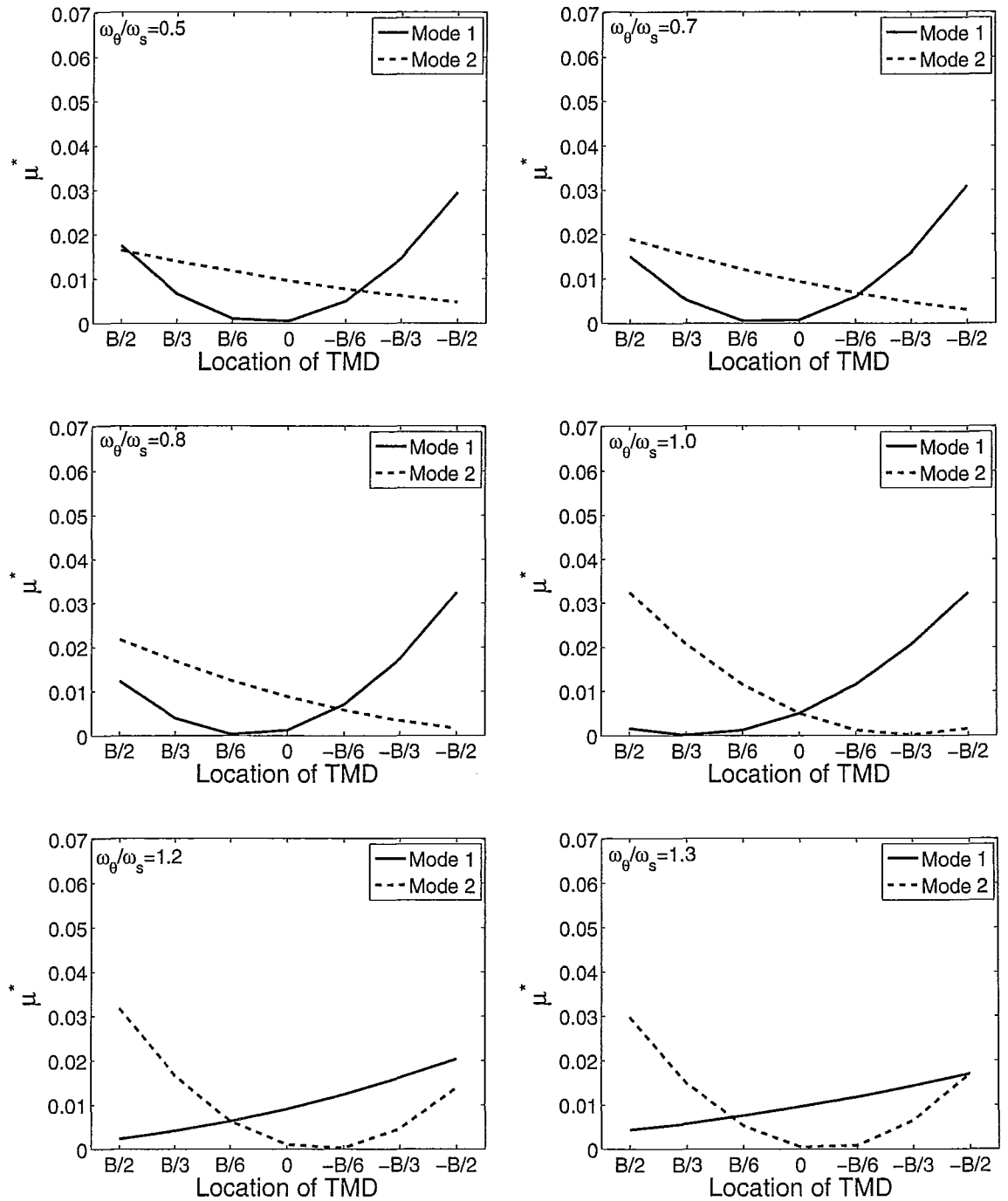

Figure 3.84: Generalized Mass Ratio Values of Structures Equipped with a Single TMD ($\mu = 0.01$)

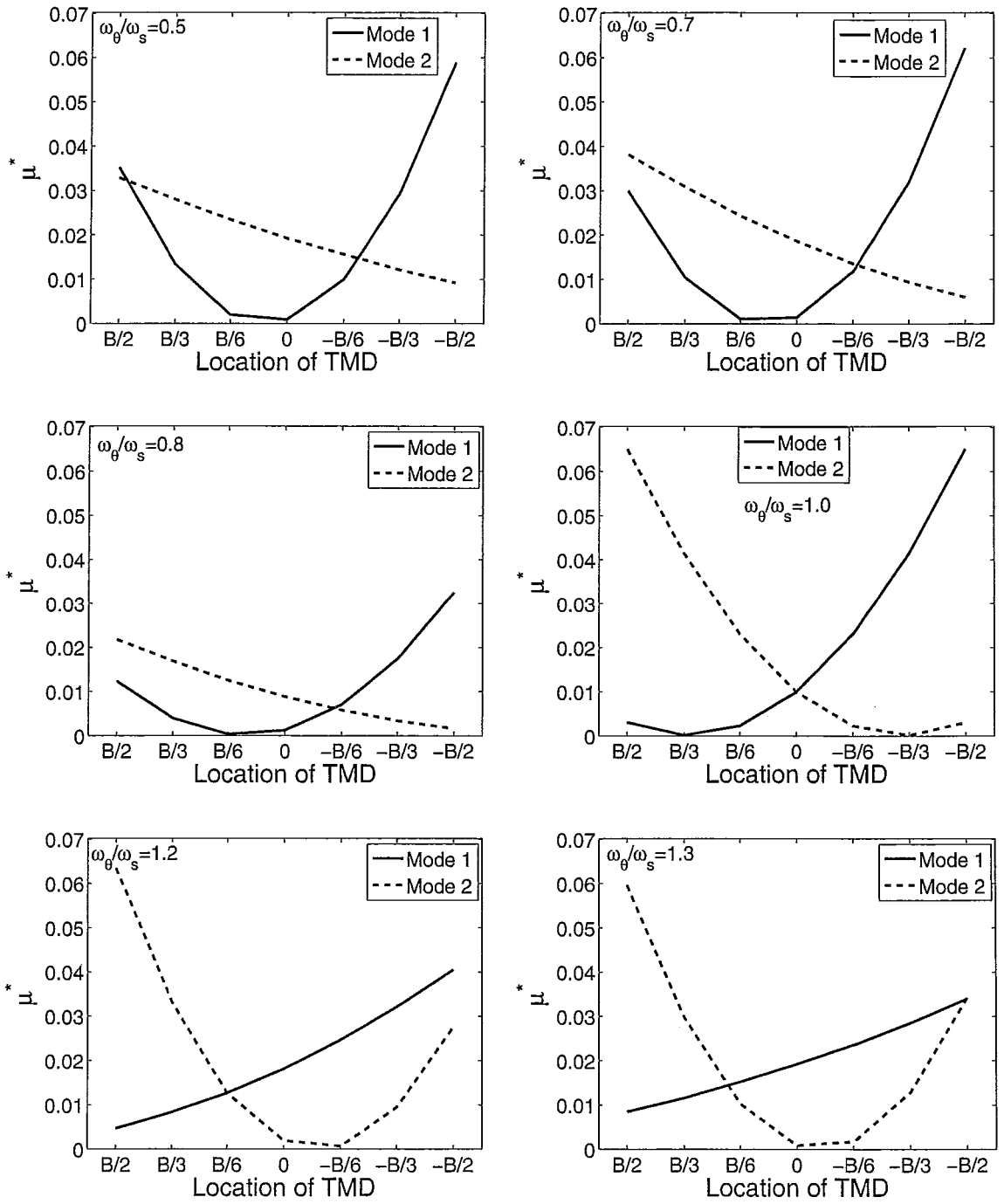

Figure 3.85: Generalized Mass Ratio Values of Structures Equipped with a Single TMD ($\mu = 0.02$)

Chapter 4

Torsionally Coupled Structures Equipped with DVA(s) subjected to Random Excitation

4.1 Introduction

This chapter investigates the dynamic response behavior of torsionally coupled structures equipped with DVA(s) subjected to random excitation. Structures with uncoupled frequency ratio values of 0.5, 0.7, 0.8, 1.0, 1.2 and 1.3 are investigated in this study. The structures are assumed to have equal damping ratio values of 2% in both modes. The response parameter of interest, which is minimized to obtain the optimal DVA(s) parameters, is first introduced. Part 1 of this chapter investigates the performance of various TMD configurations while Part 2 investigates the response behavior of torsionally coupled structures equipped with TLDs utilizing the equivalent mechanical model developed by Tait (2008). Subsequently, the efficiency of the DVA

configurations are evaluated and compared for a given structure.

A total of five different TMD configurations are considered for each uncoupled frequency ratio value. In addition, for each TMD configuration, the influence of TMD location is investigated. The efficiency of the TMD configurations are evaluated and compared for each uncoupled frequency ratio considered.

A similar study is carried out to investigate the response behavior of same torsionally coupled structures equipped with TLD(s). A total of five TLD configurations were also investigated and the same absorber locations employed.

4.2 Minimization of Response Parameter and Performance Indices

4.2.1 Response Parameter of Interest

In this chapter, the external force is modelled as a random white noise excitation with constant spectral density, S_o. The objective function, which is the maximum mean square corner displacement, $\sigma^2_{x_c}$, can be expressed as

$$\sigma^2_{x_c} = S_o \int_{-\infty}^{\infty} |X(\omega)|^2 \, d\omega \tag{4.1}$$

where $|X(\omega)|$ is the mechanical admittance function of the system corner displacement that is obtained using the equations of motion (Equation 2.18) and Equation 3.2. As the structure-DVA systems considered are subjected to random excitation, which contains infinitely many frequencies, the H_2 optimization criterion is employed. As discussed in Chapter 1, the objective of this optimization criterion is to minimize

the objective function, $\sigma^2_{x_c}$. As the systems investigated in this study are subjected to white noise excitation, this implies that the area under the mechanical admittance function is minimized. Therefore, the optimal DVA parameters are obtained by minimizing the integral in Equation 4.1.

4.2.2 Performance Indices

The response parameter of interest for the case of random excitation is the root mean square (RMS) corner displacement. This is expressed as

$$\sigma_{x_c} = \sqrt{S_o \int_{-\infty}^{\infty} |X(\omega)|^2 \, d\omega} \tag{4.2}$$

To evaluate the effectiveness of the DVA(s), a response reduction factor, R_o, is introduced as follow

$$R_o = \frac{RMS\ of\ Structure\ with\ DVAs}{RMS\ of\ Structure\ without\ DVAs} \tag{4.3}$$

The ratio R_o is a measure of the effectiveness of the DVA configuration being investigated. A value less then unity indicates that absorber configuration is effective for vibration control. The efficiency, ψ, is the parameter used in this study to compared the performance of different DVA configurations and is expressed as $\psi = 1 - R_o$.

4.3 Study of Structures with Equal Modal Damping Ratio Values Equipped with TMD(s)

This section presents a numerical study of torsionally coupled structures with and without TMD(s) subjected to white noise random excitation. The TMD arrangements and locations are selected to match the configurations previously investigated under harmonic excitation. Total mass ratio values of 1% and 2% are again considered. The mechanical admittance function plots for the six uncoupled frequency ratios studied are shown in Figure 4.1, with the corresponding undamped mode shapes provided in Figures 3.2 to 3.7. Also shown in each plot is the percentage contribution to the total variance of the maximum corner response as a function of the forcing frequency ratio. This identifies the amount each mode contributes to the total variance or the area bounded by the mechanical admittance function, $\sigma^2_{x_c}$. The normalized RMS corner response values for the torsionally coupled structures considered in this study are given in Table 4.1.

4.3.1 Single TMD Results - Random

This section presents results obtained for torsionally coupled structures equipped with a single TMD subjected to random excitation. Mechanical admittance function plots corresponding to TMD locations resulting in maximum and minimum efficiency and at the centre of mass are shown in Figure 4.2. For the torsionally flexible structure ($\omega_\theta/\omega_s = 0.5$) selected in this study, the percentage that mode 1 and mode 2 contribute to the total variance can be determined from Figure 4.1. It is observed that approximately 35% of the total variance can be attributed to mode 1 and 65%

of the total variance attributed to mode 2. As approximately two-thirds of the total variance is related to mode 2, it is expected that the optimized single TMD would be tuned around this dominant mode. This is confirmed by the mechanical admittance function plot shown in Figure 4.2 for $\omega_\theta/\omega_s = 0.5$. Notice that for all TMD locations considered, mode 2 maintains a double peak response indicating the TMD is tuned to this mode. For the case of $\omega_\theta/\omega_s = 0.8$, mode 1 and mode 2 contribute approximately equally to the total variance (see Figure 4.1). Inspection of the mechanical admittance function plots corresponding to this uncoupled frequency ratio reveals two tuning strategies are employed. The tuning strategy employed depends on the TMD location. For the minimum efficiency case, which corresponds to the centre of mass location, the TMD is tuned to mode 2, which is dominated by translational motion (see Figure 3.4). This tuning strategy is employed as the TMD is ineffective in reducing torsional motion at this location. However, when the TMD is placed at $B/2$, which corresponds to the location resulting in maximum TMD efficiency, the optimal tuning ratio is found to lie between mode 1 and mode 2. This tuning strategy is employed as the TMD is effective in reducing both translational motion and torsional motion at this location. Thus, the optimized TMD at this location is effective in reducing the response of both modes 1 and 2 simultaneously. For the strongly torsionally coupled structure, approximately 65% of the total variance is related to mode 1 and the remaining 35% to mode 2. However, it is important to note that there is strong coupling between modes 1 and 2. The optimal TMD tuning ratio value obtained indicates the TMD is tuned around mode 1, which is expected as a large percentage of the total variance is contributed by mode 1. The mode shapes found in Figure 3.5 show that, for mode 1, location $-B/2$ experiences the largest

response motion. This can be employed to explain why TMD location, $-B/2$, results in maximum efficiency. The mechanical admittance function plots shown in Figure 4.1 for $\omega_\theta/\omega_s = 1.2$, indicate that over 85% of the variance can be attributed to mode 1 (translational motion dominated response). As a result, the TMD is tuned to target this mode for all the TMD locations considered. The remaining mechanical admittance function plots for this TMD configuration are found in Appendix K. It is evident that by determining the level each of the structural modes contributes to the total variance the tuning strategy employed to optimize the TMD can be predicted.

The normalized RMS corner response value shown in Figures 4.3 and 4.4 indicate that the torsionally flexible ($\omega_\theta/\omega_s = 0.5$ and 0.7) and torsionally stiff ($\omega_\theta/\omega_s = 1.2$ and 1.3) structures are less sensitive to TMD location compared to the strongly torsionally coupled case. This is again a result of the modal contribution to the total variance. For both the torsionally flexible and torsionally stiff structures the translational mode is the dominant mode, resulting in reduced sensitivity to TMD location.

From Figure 4.5, which shows the response reduction factor plot of all six uncoupled frequency ratio values, it is found that, for the torsionally flexible structures the lowest reduction factor occurs when the TMD is placed at $B/2$ whereas for torsionally stiff structures, the lowest response reduction factor occurs when the TMD is placed at $-B/2$. The location resulting in maximum efficiency can be explained using the mode shapes plotted in Figures 3.2 and 3.3 for torsionally flexible structures and Figures 3.6 and 3.7 for the torsionally stiff structures. As stated above, for both the torsionally flexible and torsionally stiff structures, the dominant mode is the translational mode. Inspection of Figures 3.2 and 3.3 show that the largest corner

response corresponding to this translational mode (mode 2) of the torsionally flexible structures occurs at $B/2$. Conversely, Figures 3.6 and 3.7 show that the largest corner response occurs at $-B/2$ in the translational mode (mode 1) of the torsionally stiff structures. Maximum TMD efficiency is expected to occur when the TMD location coincides with the largest corner displacement location. This is confirmed from the response reduction factor plots in Figure 4.5.

Minimum and maximum efficiency values and corresponding TMD locations are shown in Figures 4.6 and 4.7. As expected, an increase in the mass ratio value results in the higher efficiency. For the TMD locations investigated, the lowest maximum efficiency corresponded to the torsionally flexible system ($\omega_\theta/\omega_s = 0.5$).

4.3.2 Two Identical TMDs Results - Random

The mechanical admittance function plots for the two identical TMDs configuration are shown in Figure 4.8. For the torsionally flexible and torsionally stiff structures ($\omega_\theta/\omega_s = 0.5$ and 1.2, respectively), the mechanical admittance function plots are found to remain relatively constant for all TMD locations considered. This is due to the fact that for all TMD locations considered the TMDs are always tuned to the translationally dominant mode which does not have a significant torsional response component. For ω_θ/ω_s =0.8, unlike that of the single TMD configuration, the two identical TMDs configuration is found to be tuned to around mode 1 (torsional motion dominated, see Figure 3.4) when the system is optimized. A different tuning strategy is employed for this TMD configuration. As both modes contribute equally to the total variance a single TMD, which is more effective in reducing translational motion, is tuned to the translational mode (mode 2). However, two identical

TMDs are effective in reducing torsional motion. As a result this TMD configuration is tuned to the torsional mode (mode 1). For the case of the strongly torsionally coupled system, the TMDs are tuned in between modes 1 and 2.

The normalized RMS corner response plots shown in Figures 4.9 and 4.10 indicate that the strongly torsionally coupled system is sensitive to TMD location, whereas the torsionally stiff and flexible systems are significantly less sensitive to TMD location. This is confirmed by inspection of the response reduction factor plots in Figure 4.11. For the case of $\omega_\theta/\omega_s = 0.5$ and 1.3, the response reduction factors remain nearly constant for all TMD locations. Note that for all uncoupled frequency ratio considered, the lowest response reduction factor occurs when the TMDs are placed at the edges ($\pm B/2$) of the structure.

The minimum and maximum efficiency plots shown in Figures 4.12 and 4.13 indicate that for the two identical TMDs configuration the greatest maximum efficiency is obtained for the strongly torsionally coupled structure. The lowest maximum efficiency is obtained for the torsionally flexible structure ($\omega_\theta/\omega_s = 0.5$).

4.3.3 Two Different TMDs Results - Random

For this particular two TMDs configuration, significant differences in mechanical admittance function plots (see Figure 4.14) are found compared to the two identical TMDs configuration. For all four mechanical admittance function plots shown, it is evident that one TMD is tuned to mode 1 and one TMD is tuned to mode 2. As two different TMDs are employed in this configuration, each TMD has a unique mass ratio value. The TMD with the larger mass ratio value is found to be tuned to the mode that is the largest contributor to the total variance. For example, for ω_θ/ω_s

= 0.7, about 70% of the total variance can be attributed to mode 2. It is therefore expected that the TMD tuned to mode 2 will have a larger mass ratio value. This relationship is confirmed (see Tables 4.2 and 4.3) for all uncoupled frequency ratios considered. For the torsionally flexible structures (ω_θ/ω_s = 0.5 and 0.8) considered, it can also be observed that there is a rapid change in peak heights in the torsional dominant mode (mode 1) due to a change in TMD location. This indicates that the response of the torsional dominant mode is sensitive to TMD location.

The normalized RMS corner response plots in Figures 4.15 and 4.16 show that the torsionally stiff coupled systems are less sensitive to TMD location as compared to the other systems. However, it can also be observed, by comparing Figures 4.15 and 4.16 to 4.9 and 4.10, that the torsionally flexible systems are more sensitive to TMD location for the two different TMDs configuration than that of the two identical TMDs configuration. This is a direct result of targeting the torsional dominant mode and the additional torsional motion induced due to the unequal masses for the case of two different TMDs configuration. Also, compared to the other systems the response reduction factors shown in Figure 4.17 indicate that the lowest response reduction factor occurs when the TMDs are placed at the edges ($\pm B/2$) of the structure.

Similar to the case of two identical TMDs, the maximum and minimum efficiency plots in Figures 4.18 and 4.19 corresponded to the TMD locations of $\pm B/2$ and $\pm B/6$, respectively. The maximum efficiency plot indicates that this configuration is most efficient when applied to the strongly torsionally coupled system.

4.3.4 Four TMDs Results - Random

4.3.4.1 Approach I Results - Random

The mechanical admittance function plots shown in Figure 4.20, corresponding to this TMD configuration, indicate that the paired TMDs are tuned to each mode for the torsionally flexible and the strongly torsionally coupled systems. However, for the torsionally stiff systems, both sets of paired TMDs, are tuned to mode 1. Again. this occurs as mode 1 contributes over 85% of the total variance for the torsionally stiff structures. The remaining mechanical admittance function plots corresponding to other uncoupled frequency ratio can be found in Appendix N.

Inspection of the normalized RMS corner response plots shown in Figures 4.21 and 4.22 for the four TMDs configuration (Approach I) indicate that the torsionally stiff systems (ω_θ/ω_s = 1.2 and 1.3) are less sensitive to TMD location compared to the other uncoupled frequency ratios. This sensitivity to the TMD location is found to be less than that of the two different TMDs configuration. Again, this is attributed to the fact that the sets of paired TMDs remain tuned to mode 1 for all locations considered in this configuration for the torsionally stiff structures. As with two identical and two different TMDs configurations, the lowest response reduction factor occurs when the TMD are located at $\pm B/2$. The efficiency plots in Figures 4.24 and 4.25 show that the largest maximum efficiency is achieved for the strongly torsionally coupled system and the maximum efficiency is found to be approximately the same for the torsionally stiff and torsionally flexible systems.

4.3.4.2 Approach II Results - Random

The mechanical admittance function plots (see Figure 4.26) for Approach II are found to be very similar to those of Approach I. Additionally, similar normalized RMS corner response values and trends shown in Figures 4.27 and 4.28 are also found to exist between Approach I and II. The lowest response reduction factors (see Figure 4.29) are found to occur at $\pm B/2$, which is in agreement with the other multiple TMDs configurations considered. The minimum and maximum efficiency for all uncoupled frequency ratios investigated are shown in Figures 4.30 and 4.31. The largest maximum efficiency is found to occur for the strongly torsionally coupled system, which is consistent with Approach I.

4.4 Evaluation of Different TMD Configurations

Mechanical admittance function plots corresponding to maximum efficiency TMD location for the six uncoupled frequency ratios investigated are shown in Figure 4.32. This figure highlights the different optimized tuning strategies employed, and resulting frequency response behavior, which are dependent on the TMD configuration selected.

Figures 4.33 and 4.34 compare the maximum efficiency obtained for the different TMD configurations, considered for $\mu = 0.01$ and $\mu = 0.02$, respectively. The two different TMDs configuration resulted in the highest efficiency for all the uncoupled frequency ratios considered. The single TMD configuration is found to be the least efficient configuration for the strongly torsionally couple system. This is due to the mass coupling term generated by a single TMD do not aid in reducing

the response effectively when two modes are strongly coupled. However, it results in approximately the same efficiency as the two different TMDs configuration for the torsionally stiff structures. Thus, the single TMD configuration is suitable for the torsionally stiff structures. The maximum efficiency of the two identical TMDs configuration is found to exceed that of single TMD configuration only for the strongly torsionally coupled system case. The efficiency of the four TMDs configuration (Approach I and II) was found to be lower than that obtained for the two different TMDs configuration even though both configurations are capable of targeting both modes simultaneously. This is due to the additional mass ratio constraints placed on the four TMDs configuration. Furthermore, for the four TMDs configuration, Approach II was found to be more efficient than Approach I for the torsionally flexible structures. This is due to the released constraint enforced on the mass ratio values. It can be observed from these plots that at least two TMDs are required to effectively suppress the response of the strongly torsionally coupled system. As expected, for all configurations, the maximum efficiency is increased as the mass ratio is increased.

4.4.1 Optimal TMD Parameters - Random

For the six uncoupled frequency ratios considered, the optimal parameters corresponding to the TMD location resulting in maximum efficiency are given in Tables 4.2 and 4.3. The parameters optimized for each mass ratio are the tuning ratio and the TMD damping ratio. The tuning strategy employed can be determined from these values. Note that these optimized values are different than those found for the same structures subjected to harmonic excitation. The optimal parameters determined for all other locations considered for each uncoupled frequency ratio investigated can be

found in Appendix K to Appendix O.

4.5 Study of Structure with Equal Modal Damping Ratio Values Equipped with TLD(s)

This section investigates the response of torsionally coupled structures equipped with TLD(s). For comparative purposes, the same configurations and absorber locations specified for TMD configurations are used. The TLD utilized in this study consists of rigid rectangular tank(s) each equipped with two damping screens (see Figure 2.3). The two damping screens are located at $x_1 = 0.4L$ and $x_2 = 0.6L$, each having a solidity value of S_i and selected such that the system response can be minimized. The quiescent fluid depth, h, to tank length, L, ratio is selected to be 0.125. In order to match and compare with the results for structures equipped with TMDs, mass ratio values of 0.01 and 0.02 are used. The mass ratio value is defined in this section as

$$\mu = \frac{\sum m_{eq_i}}{m_s} \tag{4.4}$$

Expressing the total required water mass in the tank as $m_w = \rho bhL$, and substituting into Equation 2.57, the effective mass or mass of the fluid that is participating in the sloshing motion can be expressed as

$$m_{eq} = \frac{8Lm_w}{h\pi^3} \tanh(\frac{\pi h}{L}) \tag{4.5}$$

With h/L selected as 0.125, and the required effective mass known from Equation 4.4, the total required water mass can be obtained. Hence, the dead mass or the non-participating water mass, m_{o_i}, can be obtained through the following relationship

$$m_{o_i} = m_w - m_{eq_i} \tag{4.6}$$

With the dead mass added to the structure, the structure's total mass is modified (see Equation 2.60). Thus, the structure's dynamic properties need to be modified. The modified uncoupled translational frequency can be expressed as

$$\omega_s{}' = \sqrt{\frac{k_s}{m_s + \sum m_{o_i}}} \tag{4.7}$$

The modified tuning ratio values, $\nu_i{}'$, and damping ratio values, $\zeta_i{}'$, are expressed as

$$\nu_i{}' = \frac{\omega_i}{\omega_s{}'} \tag{4.8}$$

and

$$\zeta_i{}' = \frac{c_{eq_i}}{2m_{eq_i}\omega_i} \tag{4.9}$$

respectively. Substituting the modified mass, stiffness and damping matrices shown in Equations 2.60, 2.61 and 2.62 into Equation 2.18, the tuning ratio and damping ratio values can be optimized utilizing the MATLAB(r2007b) optimization toolbox (fmincon). Subsequently, the loss coefficient, C_l, can be obtained by solving Equations 2.57, 2.58 and 2.59. With C_l obtained, the optimal solidity values for screens inside the TLD can be selected either through Equations 2.39 and 2.40 or Figure 2.4. As

perviously stated, the forcing frequency ratio for a structure-TMD system (defined in Equation 3.7) is expressed as

$$\beta = \frac{\omega}{\omega_s} \tag{4.10}$$

However, for a structure-TLD system, due to the modifications in the structural parameters, the forcing frequency ratio is defined as

$$\beta' = \frac{\omega}{\omega_s'} \tag{4.11}$$

It is important to note that the inherent damping ratio in a TLD is amplitude dependent. As such, a change in the value of S_o would modify the mechanical admittance function of the structure-TLD system. This study only considers the response behavior of the structure-TLD system at its targeted design amplitude (i.e. the amplitude at which it has been optimized at). The TLD performance at non-targeting design amplitudes is beyond the scope of this study.

4.5.1 Structure-TLD System Response Behavior

Mechanical admittance function plots of the torsionally coupled structures equipped with a single TLD subjected random excitation are shown in Figure 4.35. Comparing Figure 4.2, corresponding to a single TMD configuration, with Figure 4.35, for a single TLD configuration, it is observed that there is negligible difference in the mechanical admittance functions. This was observed for all uncoupled frequency ratios considered. Furthermore, similar mechanical admittance functions were found between all matching TMD and TLD configurations investigated. It can

be concluded that the frequency response of the torsionally coupled structure is similar when equipped with either an optimized TMD or TLD (at the target design amplitude) having the same mass ratio and absorber location.

Figures 4.36 and 4.37 show the normalized RMS corner response of the torsionally coupled structures equipped with a single TLD for $\mu = 0.01$ and $\mu = 0.02$, respectively. Comparing the normalized RMS values to those found for the torsionally coupled structures equipped with a single TMD having the same mass ratio, negligible difference is found.

The response reduction factors shown in Figure 4.38 for the torsionally coupled structures equipped with single TLD are found to match those shown in Figure 4.5 for the torsionally coupled coupled single TMD systems.

Inspection of Figures 4.39 and 4.40 show minimum and maximum efficiency obtained under random excitation along with the corresponding TLD location. Comparing the maximum and minimum efficiency obtained for the TLD to that of a TMD, it is concluded that both optimized DVAs provide approximately the same level of efficiency.

Figures 4.41 and 4.42 show the maximum efficiency obtained for all the TLD configurations considered in this study. As expected, for all configurations, maximum efficiency is increased as the mass ratio is increased. Similar to that of the torsionally coupled structure-TMD systems, the two different TLDs configuration resulted in the highest efficiency for all the uncoupled frequency ratios considered. A single TLD is as efficient as the two different TLDs for the torsionally stiff structures. However, a single TLD configuration is found to be the least efficient for the strongly torsionally coupled system. Furthermore, the maximum efficiency of the two identical TLDs

configuration is found to exceed that of single TLD configuration only for the strongly torsionally coupled system. Finally, it is found that at least two TLDs are required to reduce the response of the strongly torsionally coupled structure effectively. These findings match those observed for the TMD configurations investigated.

4.5.2 Mechanical Admittance and Optimal TLD Parameters

For the six uncoupled frequency ratios considered, the optimal parameters corresponding to the TLD location resulting in maximum efficiency are given in Tables 4.4 and 4.5. The parameters optimized for each mass ratio are the tuning ratio and the TLD damping ratio. These optimized TLD parameters differs from the optimized TMD parameters. Finally, the optimal parameters, response reduction factor plots, normalized RMS corner response plots, minimum and maximum efficiency plots and the mechanical admittance determined for all other TLD configurations considered for each uncoupled frequency ratio investigated can be found in Appendix P to Appendix U.

4.5.3 Evaluation of TMDs and TLDs Performance

The performance of TMDs and TLDs are compared in Table 4.6. The table compares the minimized lowest response achieved between TMDs and TLDs. A '-' sign is assigned if TLD performs better and a '+' sign is assigned if the TMD provides a better performance.

In general, for the absorber configurations and the uncoupled frequency ratios considered, TLD(s) are more efficient relative to TMD(s) for the torsionally flexible structures. This is attributed to the dead mass added to the structure. The dead

mass due to the non-participating fluid mass helps reduce the torsional motion as the structure's mass moment of inertia is increased. However, for $\omega_\theta/\omega_s = 0.8$, the lowest response achieved for two identical TLDs or a single TLD may not result in a more efficient response as compared to that obtained for the corresponding TMD configuration. This is due to the strong coupling between modes which causes the response of the structure to be sensitive to the increase in mass ratio value. As for strongly torsionally coupled and torsionally stiff structures, TMD(s) results in higher efficiency than TLD(s) for all configurations considered in this study.

4.6 Summary and Conclusions

This chapter reported on numerical simulation results for torsionally coupled systems equipped with DVA(s) under random excitation. The finding for these particular type of structures are summarized here:

- The modal contribution to the total variance plays an important role in determining the tuning strategy.
- Greater efficiency can be achieved by placing the DVA(s) at the edge(s) ($\pm B/2$) of the structure. This is a direct result of the additional DVA(s) mass coupling terms and mass moment of inertia that develops from placing the DVA(s) away from the centre of mass.
- Greatest efficiency was achieved for the two different DVAs configuration as this configuration permits two independent DVAs to be tuned to two different modes. In addition, the mass of each DVA reflects the percentage the mode to which it is tuned to contributes to the total variance.

- For all the DVA configurations except the single DVA configuration, the greatest efficiency was achieved for the strongly torsionally coupled systems.

- The efficiency of a single DVA configuration was found to approach that of the two different DVAs configuration for the torsionally stiff structures considered. This is attributed to the negligible torsional contribution to the total corner response for these structures. However, a single DVA configuration was not efficient in reducing the strongly torsionally coupled system response.

- For the case of four DVAs (Approach I and II), the constraints enforced on the mass ratio reduced the efficiency of this configuration as compared to that of two different DVAs configuration. However, Approach II was found to be more efficient than Approach I for the torsionally flexible structures. This highlights the importance of the freedom in optimizing the DVA parameters for the torsionally flexible structures.

- At least two DVAs were required to suppress the response effectively for the strongly torsionally coupled structure considered as the mass coupling term generated by a single DVA does not aid in reducing the response when two modes are strongly coupled.

- The efficiency of the single DVA configuration was found to exceed that of the two identical DVAs configuration except for the strongly torsionally coupled structure case. This is attributed to the mass coupling term generated by a single DVA aids in reducing the response when the two modes are well separated.

- Targeting the response of the torsional dominant mode was found to amplify the sensitivity to changes in DVA location. This can be concluded from the

response obtained for the two different DVAs configurations.

- The response behavior of the structure-TLD systems at its targeted design amplitude was found to be similar to that of the structure-TMD systems.
- Higher efficiency was obtained in the structure-TMD systems for the strongly torsionally coupled and stiff structures (ω_θ/ω_s = 1.0, 1.2 and 1.3) as compared to the structure-TLD systems. The opposite was found for torsionally flexible structures (ω_θ/ω_s = 0.5 and 0.7).
- All DVA configurations considered were able to attenuate the uncontrolled dynamic response and the efficiency for each configuration was found to increase as the mass ratio was increased.

4.7 Chapter Tables

ω_θ/ω_s	$\sigma_{x_c}(k_s/\sqrt{S_o})$
0.5	11.2419
0.7	12.0774
0.8	10.7306
1.0	10.9082
1.2	8.9172
1.3	8.1881

Table 4.1: Normalized RMS Corner Response of Structures without DVAs subjected to Random Excitation

ω_θ/ω_s	y_1	y_2	y_3	y_4	μ_1	μ_2	μ_3	μ_4	ν_1	ν_2	ν_3	ν_4	ζ_1	ζ_2	ζ_3	ζ_4	$\sigma_{x_c}(\frac{k_s}{\sqrt{S_o}})$
Single TMD																	
0.5	$B/2$				0.01				1.0077				0.0622				8.5022
0.7	$B/2$				0.01				1.0057				0.0673				8.4067
0.8	$B/2$				0.01				0.9041				0.1101				7.6847
1.0	$-B/2$				0.01				0.9238				0.0663				7.2425
1.2	$-B/2$				0.01				0.9706				0.0674				6.0182
1.3	$-B/2$				0.01				0.9739				0.0631				5.6902
Two Identical TMDs																	
0.5	$-B/2$	$B/2$			0.005	0.005			1.0081	1.0081			0.0518	0.0518			8.9314
0.7	$-B/2$	$B/2$			0.005	0.005			1.0114	1.0114			0.0546	0.0546			9.0823
0.8	$-B/2$	$B/2$			0.005	0.005			0.7925	0.7925			0.1189	0.1189			8.0580
1.0	$-B/2$	$B/2$			0.005	0.005			0.9537	0.9537			0.0772	0.0772			6.8842
1.2	$-B/2$	$B/2$			0.005	0.005			0.9723	0.9723			0.0570	0.0570			6.5133
1.3	$-B/2$	$B/2$			0.005	0.005			0.9761	0.9761			0.0528	0.0528			6.0828
Two Different TMDs																	
0.5	$-B/2$	$B/2$			0.0032	0.0068			0.4585	1.0119			0.0470	0.0512			7.7601
0.7	$-B/2$	$B/2$			0.0023	0.0077			0.6527	1.0125			0.0395	0.0575			7.8834
0.8	$-B/2$	$B/2$			0.0033	0.0067			0.7431	1.0091			0.0484	0.0563			6.6911
1.0	$-B/2$	$B/2$			0.0059	0.0041			0.9121	1.0568			0.0617	0.0495			6.0171
1.2	$-B/2$	$B/2$			0.0090	0.0010			0.9675	1.2375			0.0631	0.0258			5.9290
1.3	$-B/2$	$B/2$			0.0096	0.0004			0.9733	1.3320			0.0613	0.0171			5.6668
Four TMDs (Approach-I)																	
0.5	$-B/2$	$-B/2$	$B/2$	$B/2$	0.0025	0.0025	0.0025	0.0025	0.4615	1.0128	0.4615	1.0128	0.0549	0.0362	0.0549	0.0362	8.3121
0.7	$-B/2$	$-B/2$	$B/2$	$B/2$	0.0025	0.0025	0.0025	0.0025	0.6613	1.0198	0.6613	1.0198	0.0577	0.0368	0.0577	0.0368	8.7270
0.8	$-B/2$	$-B/2$	$B/2$	$B/2$	0.0025	0.0025	0.0025	0.0025	0.7550	1.0233	0.7550	1.0233	0.0550	0.0379	0.0550	0.0379	7.3069
1.0	$-B/2$	$-B/2$	$B/2$	$B/2$	0.0025	0.0025	0.0025	0.0025	1.0200	0.9031	1.0200	0.9031	0.0460	0.0458	0.0460	0.0458	6.6298
1.2	$-B/2$	$-B/2$	$B/2$	$B/2$	0.0025	0.0025	0.0025	0.0025	1.0142	0.9389	1.0142	0.9389	0.0395	0.0358	0.0395	0.0358	6.4484
1.3	$-B/2$	$-B/2$	$B/2$	$B/2$	0.0025	0.0025	0.0025	0.0025	0.9426	1.0155	0.9426	1.0155	0.0326	0.0344	0.0326	0.0344	6.0077
Four TMDs (Approach-II)																	
0.5	$-B/2$	$-B/2$	$B/2$	$B/2$	0.0017	0.0033	0.0017	0.0033	0.4614	1.0113	0.4614	1.0113	0.0442	0.0418	0.0442	0.0418	8.9808
0.7	$-B/2$	$-B/2$	$B/2$	$B/2$	0.0037	0.0013	0.0037	0.0013	1.0163	0.6580	1.0163	0.6580	0.0452	0.0383	0.0452	0.0383	9.4075
0.8	$-B/2$	$-B/2$	$B/2$	$B/2$	0.0022	0.0028	0.0022	0.0028	0.7533	1.0215	0.7533	1.0215	0.0504	0.0405	0.0504	0.0405	8.5529
1.0	$-B/2$	$-B/2$	$B/2$	$B/2$	0.0029	0.0021	0.0029	0.0021	1.0157	0.8988	1.0157	0.8988	0.0507	0.0416	0.0507	0.0416	8.2469
1.2	$-B/2$	$-B/2$	$B/2$	$B/2$	0.0030	0.0020	0.0030	0.0020	1.0083	0.9341	1.0083	0.9341	0.0428	0.0316	0.0428	0.0316	6.9602
1.3	$-B/2$	$-B/2$	$B/2$	$B/2$	0.0026	0.0024	0.0026	0.0024	1.0147	0.9419	1.0147	0.9419	0.0348	0.0322	0.0348	0.0322	6.2233

Table 4.2: Optimal TMD Parameters for Torsionally Coupled Systems Equipped with TMD(s) (μ=0.01) subjected to Random Excitation

ω_θ/ω_s	y_1	y_2	y_3	y_4	μ_1	μ_2	μ_3	μ_4	ν_1	ν_2	ν_3	ν_4	ζ_1	ζ_2	ζ_3	ζ_4	$\sigma_{x_c}(\frac{k_x}{\sqrt{S_o}})$
Single TMD																	
0.5	$B/2$				0.02				0.9948				0.0872				7.8776
0.7	$B/2$				0.02				0.9813				0.0962				7.3910
0.8	$B/2$				0.02				0.9068				0.1098				6.2348
1.0	$-B/2$				0.02				0.8880				0.0726				6.5547
1.2	$-B/2$				0.02				0.9619				0.0869				5.2458
1.3	$-B/2$				0.02				0.9651				0.0858				5.0310
Two Identical TMDs																	
0.5	$-B/2$	$B/2$			0.01	0.01			0.9990	0.9990			0.0749	0.0749			8.4057
0.7	$-B/2$	$B/2$			0.01	0.01			0.9955	0.9955			0.0831	0.0831			8.2608
0.8	$-B/2$	$B/2$			0.01	0.01			0.8632	0.8632			0.1554	0.1554			7.0391
1.0	$-B/2$	$B/2$			0.01	0.01			0.9563	0.9563			0.0976	0.0976			5.6897
1.2	$-B/2$	$B/2$			0.01	0.01			0.9682	0.9682			0.0797	0.0797			5.7064
1.3	$-B/2$	$B/2$			0.01	0.01			0.9699	0.9699			0.0748	0.0748			5.4228
Two Different TMDs																	
0.5	$-B/2$	$B/2$			0.0063	0.0137			0.4503	1.0052			0.0648	0.0706			6.8715
0.7	$-B/2$	$B/2$			0.0041	0.0159			0.6393	1.0006			0.0510	0.0783			6.8099
0.8	$-B/2$	$B/2$			0.0051	0.0149			0.7254	0.9886			0.0555	0.0778			5.6542
1.0	$-B/2$	$B/2$			0.0124	0.0076			0.8876	1.0788			0.0817	0.0848			4.9717
1.2	$-B/2$	$B/2$			0.0174	0.0026			0.9578	1.2408			0.0819	0.0484			5.1358
1.3	$-B/2$	$B/2$			0.0189	0.0011			0.9638	1.3341			0.0828	0.0299			5.0029
Four TMDs (Approach-I)																	
0.5	$-B/2$	$-B/2$	$B/2$	$B/2$	0.005	0.005	0.005	0.005	0.4551	1.0097	0.4551	1.0097	0.0779	0.0510	0.0779	0.0510	7.4767
0.7	$-B/2$	$-B/2$	$B/2$	$B/2$	0.005	0.005	0.005	0.005	1.0170	0.6551	1.0170	0.6551	0.0518	0.0838	0.0518	0.0838	7.7322
0.8	$-B/2$	$-B/2$	$B/2$	$B/2$	0.005	0.005	0.005	0.005	1.0185	0.7486	1.0185	0.7486	0.0529	0.0788	0.0529	0.0788	6.3758
1.0	$-B/2$	$-B/2$	$B/2$	$B/2$	0.005	0.005	0.005	0.005	1.0270	0.8884	1.0270	0.8884	0.0627	0.0618	0.0627	0.0618	5.4634
1.2	$-B/2$	$-B/2$	$B/2$	$B/2$	0.005	0.005	0.005	0.005	1.0312	0.9250	1.0312	0.9250	0.0566	0.0498	0.0566	0.0498	5.6218
1.3	$-B/2$	$-B/2$	$B/2$	$B/2$	0.005	0.005	0.005	0.005	1.0262	0.9261	1.0262	0.9261	0.0501	0.0462	0.0501	0.0462	5.3403
Four TMDs (Approach-II)																	
0.5	$-B/2$	$-B/2$	$B/2$	$B/2$	0.0035	0.0064	0.0035	0.0064	0.4549	1.0069	0.4549	1.0069	0.0631	0.0584	0.0631	0.0584	8.3560
0.7	$-B/2$	$-B/2$	$B/2$	$B/2$	0.0026	0.0074	0.0026	0.0074	0.6480	1.0101	0.6480	1.0101	0.0545	0.0632	0.0545	0.0632	8.6738
0.8	$-B/2$	$-B/2$	$B/2$	$B/2$	0.0039	0.0061	0.0039	0.0061	0.7424	1.0131	0.7424	1.0131	0.0667	0.0588	0.0667	0.0588	7.7778
1.0	$-B/2$	$-B/2$	$B/2$	$B/2$	0.0057	0.0043	0.0057	0.0043	1.0210	0.8825	1.0210	0.8825	0.0670	0.0571	0.0670	0.0571	7.2713
1.2	$-B/2$	$-B/2$	$B/2$	$B/2$	0.0058	0.0042	0.0058	0.0042	1.0233	0.9193	1.0233	0.9193	0.0602	0.0449	0.0602	0.0449	6.3750
1.3	$-B/2$	$-B/2$	$B/2$	$B/2$	0.0053	0.0047	0.0053	0.0047	1.0237	0.9242	1.0237	0.9242	0.0516	0.0446	0.0516	0.0446	5.6736

Table 4.3: Optimal TMD Parameters for Torsionally Coupled Systems Equipped with TMD(s) (μ=0.02) subjected to Random Excitation

ω_θ/ω_s	y_1	y_2	y_3	y_4	μ_1	μ_2	μ_3	μ_4	ν_1	ν_2	ν_3	ν_4	ζ_1	ζ_2	ζ_3	ζ_4	$\sigma_{x_c}(\frac{k_x}{\sqrt{S_0}})$
Single TLD																	
0.5	$B/2$				0.01				1.0062				0.0620				8.4971
0.7	$B/2$				0.01				1.0043				0.0671				8.3990
0.8	$B/2$				0.01				0.9080				0.1099				7.6821
1.0	$-B/2$				0.01				0.9209				0.0663				7.2807
1.2	$-B/2$				0.01				0.9693				0.0673				6.0274
1.3	$-B/2$				0.01				0.9725				0.0631				5.6951
Two Identical TLDs																	
0.5	$-B/2$	$B/2$			0.005	0.005			1.0065	1.0065			0.0517	0.0517			8.9241
0.7	$-B/2$	$B/2$			0.005	0.005			1.0099	1.0099			0.0545	0.0545			9.0710
0.8	$-B/2$	$B/2$			0.005	0.005			0.7893	0.7893			0.1189	0.1189			8.0561
1.0	$-B/2$	$B/2$			0.005	0.005			0.9524	0.9524			0.0773	0.0773			6.8873
1.2	$-B/2$	$B/2$			0.005	0.005			0.9709	0.9709			0.0571	0.0571			6.5229
1.3	$-B/2$	$B/2$			0.005	0.005			0.9747	0.9747			0.0528	0.0528			6.0891
Two Different TLDs																	
0.5	$-B/2$	$B/2$			0.0032	0.0068			0.4570	1.0104			0.0469	0.0511			7.7553
0.7	$-B/2$	$B/2$			0.0022	0.0078			0.6505	1.0110			0.0394	0.0573			7.8768
0.8	$-B/2$	$B/2$			0.0033	0.0067			0.7407	1.0077			0.0482	0.0561			6.6850
1.0	$-B/2$	$B/2$			0.0058	0.0042			0.9095	1.0531			0.0610	0.0499			6.0173
1.2	$-B/2$	$B/2$			0.0090	0.0010			0.9661	1.2332			0.0630	0.0262			5.9348
1.3	$-B/2$	$B/2$			0.0096	0.0004			0.9718	1.3273			0.0612	0.0172			5.6707
Four TLDs (Approach-I)																	
0.5	$-B/2$	$-B/2$	$B/2$	$B/2$	0.0025	0.0025	0.0025	0.0025	0.4599	1.0112	0.4599	1.0112	0.0547	0.0361	0.0547	0.0361	8.3049
0.7	$-B/2$	$-B/2$	$B/2$	$B/2$	0.0025	0.0025	0.0025	0.0025	1.0182	0.6590	1.0182	0.6590	0.0367	0.0575	0.0367	0.0575	8.7174
0.8	$-B/2$	$-B/2$	$B/2$	$B/2$	0.0025	0.0025	0.0025	0.0025	1.0217	0.7525	1.0217	0.7525	0.0377	0.0550	0.0377	0.0550	7.2990
1.0	$-B/2$	$-B/2$	$B/2$	$B/2$	0.0025	0.0025	0.0025	0.0025	0.9014	1.0196	0.9014	1.0196	0.0459	0.0466	0.0459	0.0466	6.6352
1.2	$-B/2$	$-B/2$	$B/2$	$B/2$	0.0025	0.0025	0.0025	0.0025	1.0129	0.9377	1.0129	0.9377	0.0397	0.0359	0.0397	0.0359	6.4587
1.3	$-B/2$	$-B/2$	$B/2$	$B/2$	0.0025	0.0025	0.0025	0.0025	1.0139	0.9412	1.0139	0.9412	0.0344	0.0326	0.0344	0.0326	6.0144
Four TLDs (Approach-II)																	
0.5	$-B/2$	$-B/2$	$B/2$	$B/2$	0.0033	0.0017	0.0033	0.0017	1.0098	0.4598	1.0098	0.4598	0.0417	0.0441	0.0417	0.0441	8.2450
0.7	$-B/2$	$-B/2$	$B/2$	$B/2$	0.0037	0.0013	0.0037	0.0013	1.0147	0.6559	1.0147	0.6559	0.0451	0.0381	0.0451	0.0381	8.5779
0.8	$-B/2$	$-B/2$	$B/2$	$B/2$	0.0028	0.0022	0.0028	0.0022	1.0199	0.7509	1.0199	0.7509	0.0404	0.0028	0.0404	0.0028	7.2910
1.0	$-B/2$	$-B/2$	$B/2$	$B/2$	0.0021	0.0029	0.0021	0.0029	0.8962	1.0120	0.8962	1.0120	0.0411	0.0508	0.0411	0.0508	6.6298
1.2	$-B/2$	$-B/2$	$B/2$	$B/2$	0.0020	0.0030	0.0020	0.0030	0.9326	1.0066	0.9326	1.0066	0.0315	0.0431	0.0315	0.0431	6.4570
1.3	$-B/2$	$-B/2$	$B/2$	$B/2$	0.0026	0.0024	0.0026	0.0024	1.0131	0.9405	1.0131	0.9405	0.0349	0.0321	0.0349	0.0321	6.0144

Table 4.4: Optimal TLD Parameters for Torsionally Coupled Systems Equipped with TLD(s) (μ=0.01) subjected to Random Excitation

ω_θ/ω_s	y_1	y_2	y_3	y_4	μ_1	μ_2	μ_3	μ_4	ν_1	ν_2	ν_3	ν_4	ζ_1	ζ_2	ζ_3	ζ_4	$\sigma_{x_c}(\frac{k_s}{\sqrt{S_o}})$
Single TLD																	
0.5	$B/2$				0.02				0.9920				0.0868				7.8720
0.7	$B/2$				0.02				0.9792				0.0956				7.3877
0.8	$B/2$				0.02				0.9050				0.1106				6.2437
1.0	$-B/2$				0.02				0.8835				0.0713				4.5303
1.2	$-B/2$				0.02				0.9593				0.0864				5.2589
1.3	$-B/2$				0.02				0.9624				0.0856				5.0380
Two Identical TLDs																	
0.5	$-B/2$	$B/2$			0.01	0.01			0.9960	0.9960			0.0745	0.0745			8.3943
0.7	$-B/2$	$B/2$			0.01	0.01			0.9929	0.9929			0.0825	0.0825			8.2472
0.8	$-B/2$	$B/2$			0.01	0.01			0.8603	0.8603			0.1569	0.1569			7.0452
1.0	$-B/2$	$B/2$			0.01	0.01			0.9538	0.9538			0.0973	0.0973			5.6915
1.2	$-B/2$	$B/2$			0.01	0.01			0.9656	0.9656			0.0798	0.0798			5.7181
1.3	$-B/2$	$B/2$			0.01	0.01			0.9671	0.9671			0.0748	0.0748			5.4323
Two Different TLDs																	
0.5	$-B/2$	$B/2$			0.0063	0.0137			0.4475	1.0022			0.0645	0.0703			6.8653
0.7	$-B/2$	$B/2$			0.0042	0.0158			0.6354	0.9978			0.0506	0.0779			6.8047
0.8	$-B/2$	$B/2$			0.0051	0.0149			0.7211	0.9863			0.0550	0.0765			5.6531
1.0	$-B/2$	$B/2$			0.0121	0.0079			0.8830	1.0721			0.0808	0.0850			4.9723
1.2	$-B/2$	$B/2$			0.0173	0.0027			0.9550	1.2324			0.0815	0.0491			5.1408
1.3	$-B/2$	$B/2$			0.0188	0.0012			0.9610	1.3246			0.0825	0.0302			5.0079
Four TLDs (Approach-I)																	
0.5	$-B/2$	$-B/2$	$B/2$	$B/2$	0.005	0.005	0.005	0.005	1.0066	0.4521	1.0066	0.4521	0.0508	0.0774	0.0508	0.0774	7.4655
0.7	$-B/2$	$-B/2$	$B/2$	$B/2$	0.005	0.005	0.005	0.005	1.0138	0.6507	1.0138	0.6507	0.0516	0.0834	0.0516	0.0834	7.7202
0.8	$-B/2$	$-B/2$	$B/2$	$B/2$	0.005	0.005	0.005	0.005	1.0154	0.7438	1.0154	0.7438	0.0527	0.0784	0.0527	0.0784	6.3702
1.0	$-B/2$	$-B/2$	$B/2$	$B/2$	0.005	0.005	0.005	0.005	1.0212	0.8845	1.0212	0.8845	0.0618	0.0620	0.0618	0.0620	5.4694
1.2	$-B/2$	$-B/2$	$B/2$	$B/2$	0.005	0.005	0.005	0.005	0.9227	1.0290	0.9227	1.0290	0.0498	0.0570	0.0498	0.0570	5.6333
1.3	$-B/2$	$-B/2$	$B/2$	$B/2$	0.005	0.005	0.005	0.005	0.9236	1.0232	0.9236	1.0232	0.0462	0.0502	0.0462	0.0502	5.3504
Four TLDs (Approach-II)																	
0.5	$-B/2$	$-B/2$	$B/2$	$B/2$	0.0065	0.0035	0.0065	0.0035	1.0038	0.4519	1.0038	0.4519	0.0582	0.0627	0.0582	0.0627	7.4072
0.7	$-B/2$	$-B/2$	$B/2$	$B/2$	0.0074	0.0026	0.0074	0.0026	1.0070	0.6439	1.0070	0.6439	0.0630	0.0541	0.0630	0.0541	7.5891
0.8	$-B/2$	$-B/2$	$B/2$	$B/2$	0.0061	0.0039	0.0061	0.0039	1.0100	0.7376	1.0100	0.7376	0.0586	0.0660	0.0586	0.0660	6.3516
1.0	$-B/2$	$-B/2$	$B/2$	$B/2$	0.0042	0.0058	0.0042	0.0058	0.8776	1.0140	0.8776	1.0140	0.0562	0.0672	0.0562	0.0672	5.4661
1.2	$-B/2$	$-B/2$	$B/2$	$B/2$	0.0058	0.0042	0.0058	0.0042	1.0208	0.9170	1.0208	0.9170	0.0605	0.0448	0.0605	0.0448	5.6318
1.3	$-B/2$	$-B/2$	$B/2$	$B/2$	0.0053	0.0047	0.0053	0.0047	1.0204	0.9215	1.0204	0.9215	0.0518	0.0444	0.0518	0.0444	5.3502

Table 4.5: Optimal TLD Parameters for Torsionally Coupled Systems Equipped with TLD(s) (μ=0.02) subjected to Random Excitation

ω_θ/ω_s ratios	0.5	0.7	0.8	1.0	1.2	1.3
Four DVAs (Approach II); $\mu = 0.01$	-	-	-	+	+	+
Four DVAs (Approach II); $\mu = 0.02$	-	-	-	+	+	+
Four DVAs (Approach I); $\mu = 0.01$	-	-	-	+	+	+
Four DVAs (Approach I); $\mu = 0.02$	-	-	-	+	+	+
Two Different DVAs; $\mu = 0.01$	-	-	-	+	+	+
Two Different DVAs; $\mu = 0.02$	-	-	-	+	+	+
Two Identical DVAs; $\mu = 0.01$	-	-	-	+	+	+
Two Identical DVAs; $\mu = 0.02$	-	-	+	+	+	+
Single DVA; $\mu = 0.01$	-	-	-	+	+	+
Single DVA; $\mu = 0.02$	-	-	+	+	+	+

Table 4.6: Response Comparison between TMDs and TLDs

4.8 Chapter Figures

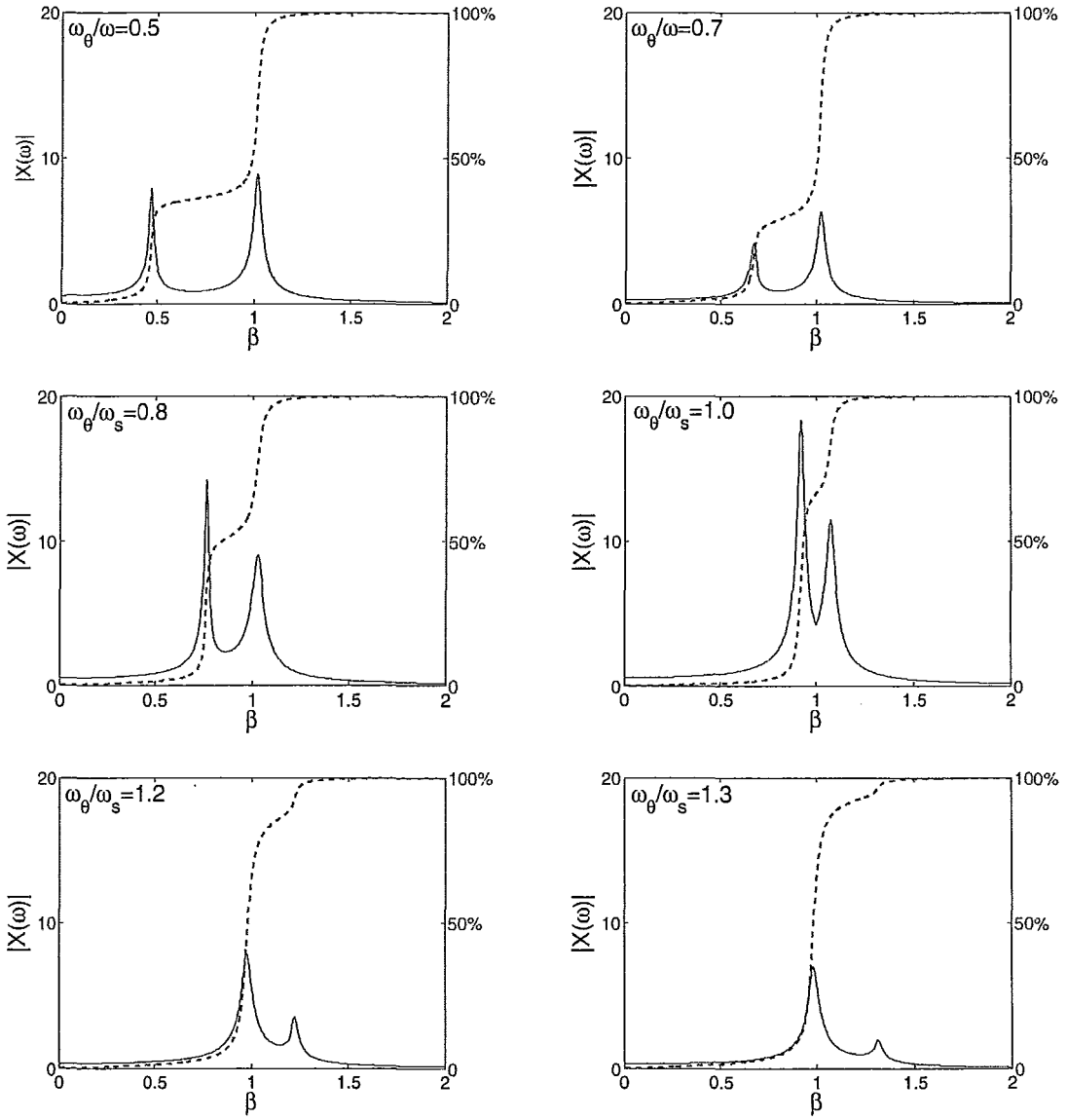

Figure 4.1: Mechanical Admittance Function of Structures without DVA subjected to Random Excitation

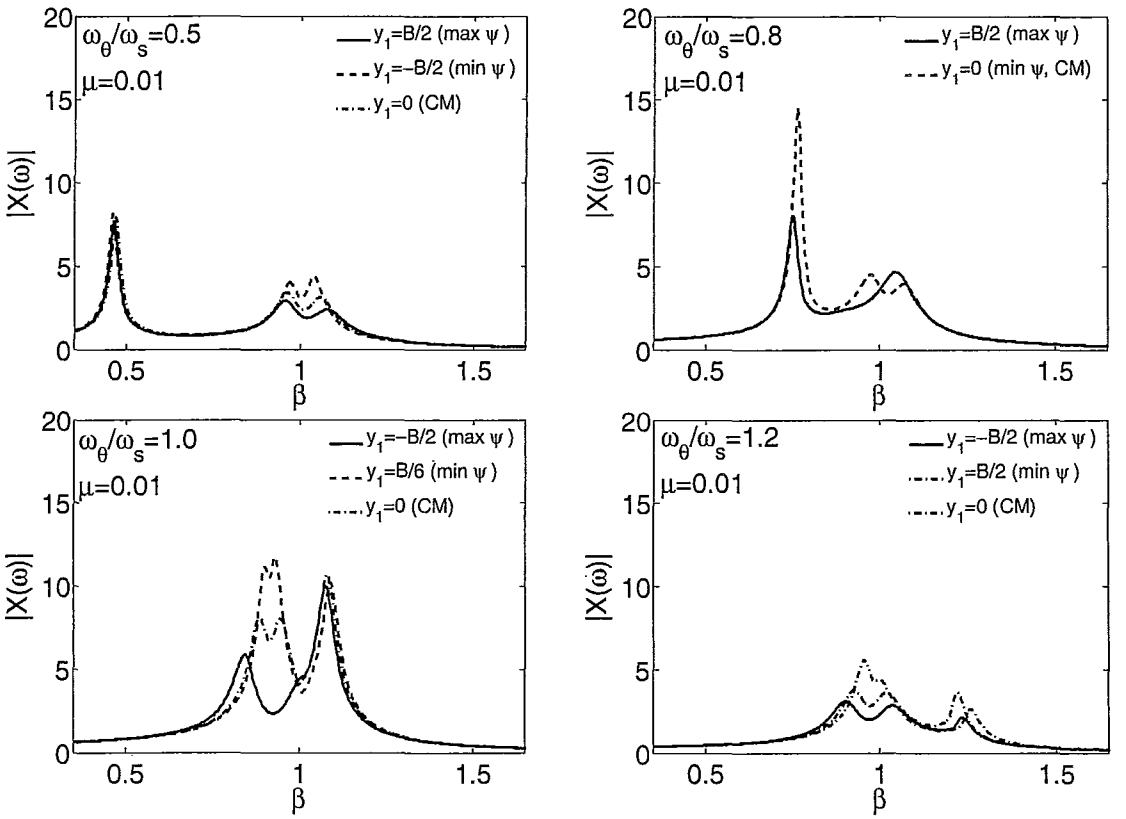

Figure 4.2: Mechanical Admittance Function Plots (Single TMD Configuration) subjected to Random Excitation

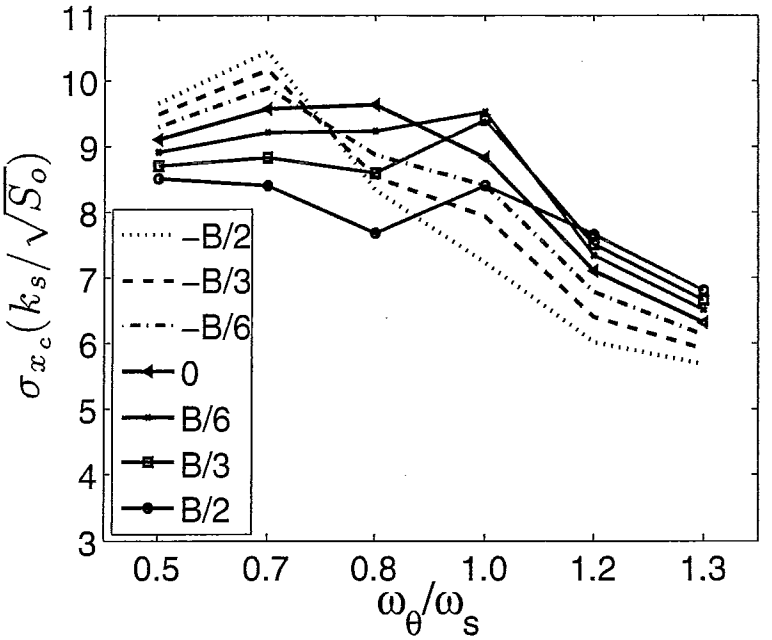

Figure 4.3: Normalized RMS Corner Response of Structures Equipped with Single TMD ($\mu = 0.01$) subjected to Random Excitation

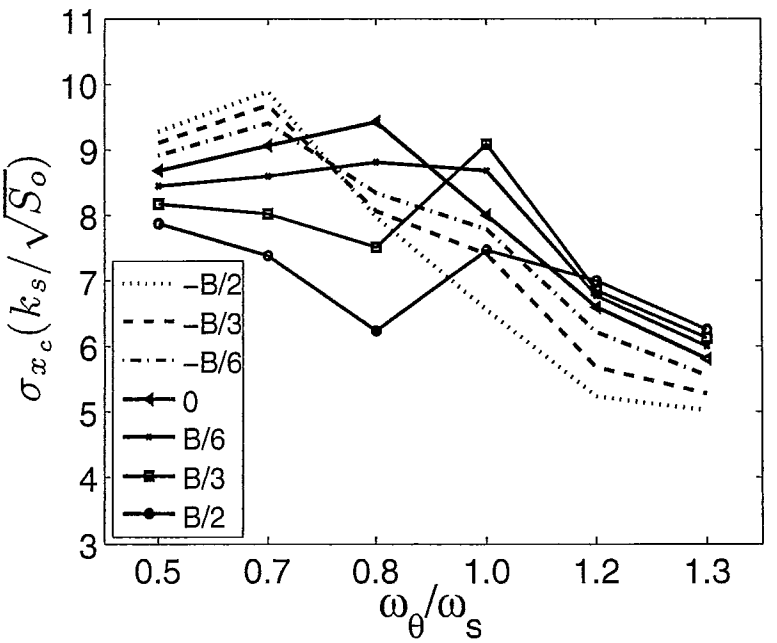

Figure 4.4: Normalized RMS Corner Response of Structures Equipped with Single TMD ($\mu = 0.02$) subjected to Random Excitation

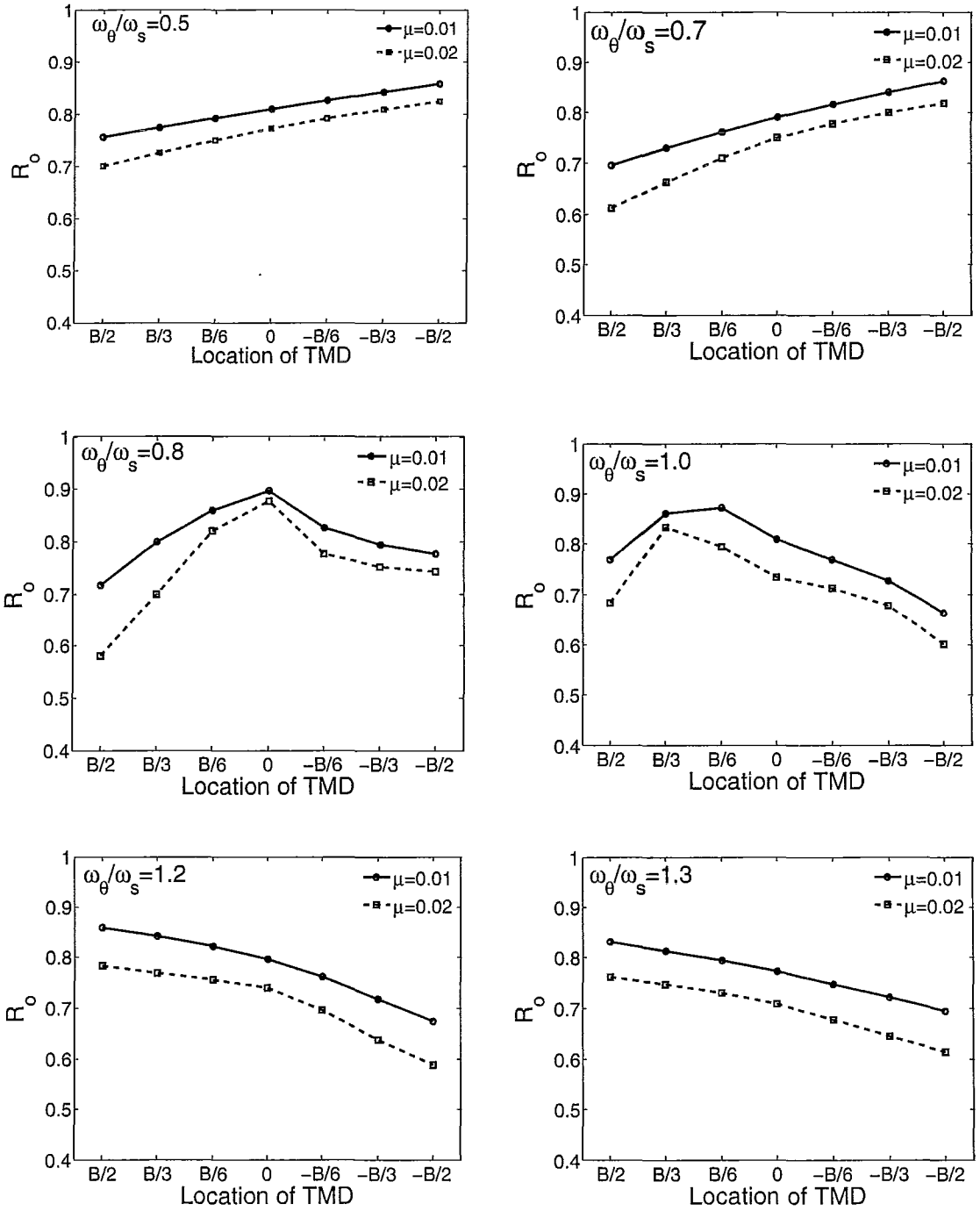

Figure 4.5: Response Reduction Factor for Structures Equipped with Single TMD subjected to Random Excitation

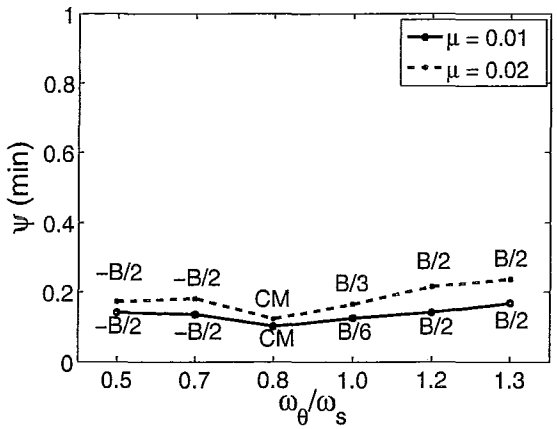

Figure 4.6: Minimum Efficiency Obtained for Single TMD subjected to Random Excitation

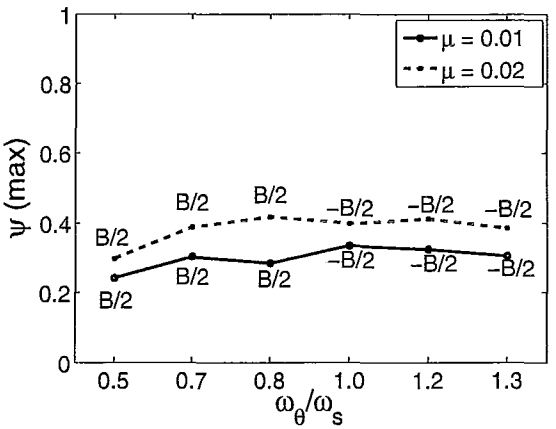

Figure 4.7: Maximum Efficiency Obtained for Single TMD subjected to Random Excitation

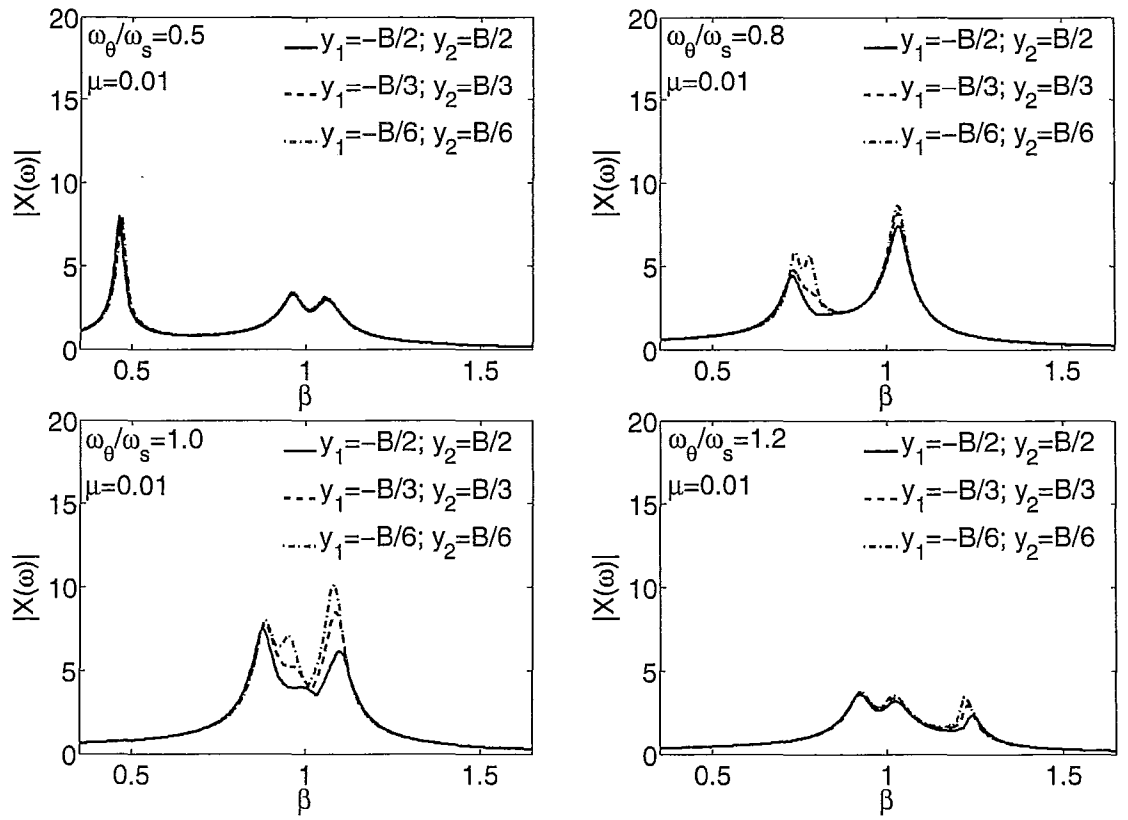

Figure 4.8: Mechanical Admittance Function Plots (Two Identical TMDs Configuration) subjected to Random Excitation

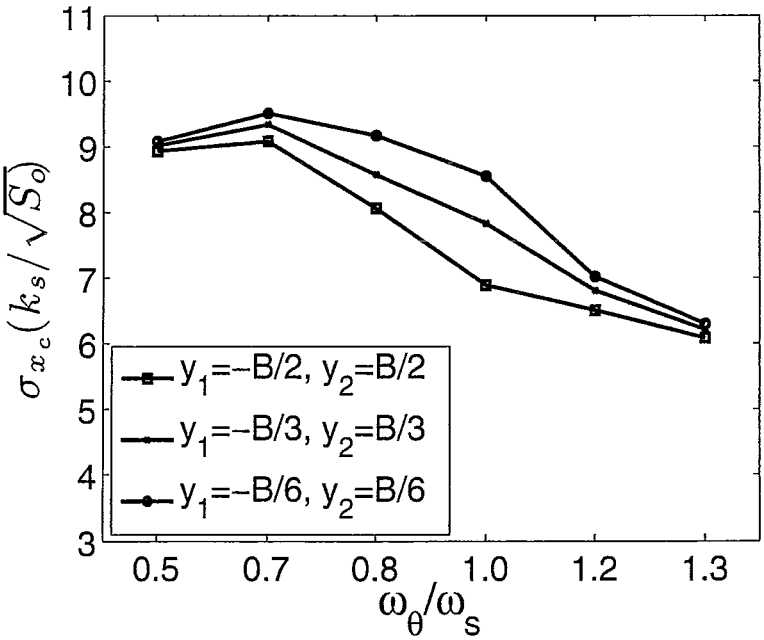

Figure 4.9: Normalized RMS Corner Response of Structures Equipped with Two Identical TMDs ($\mu = 0.01$) subjected to Random Excitation

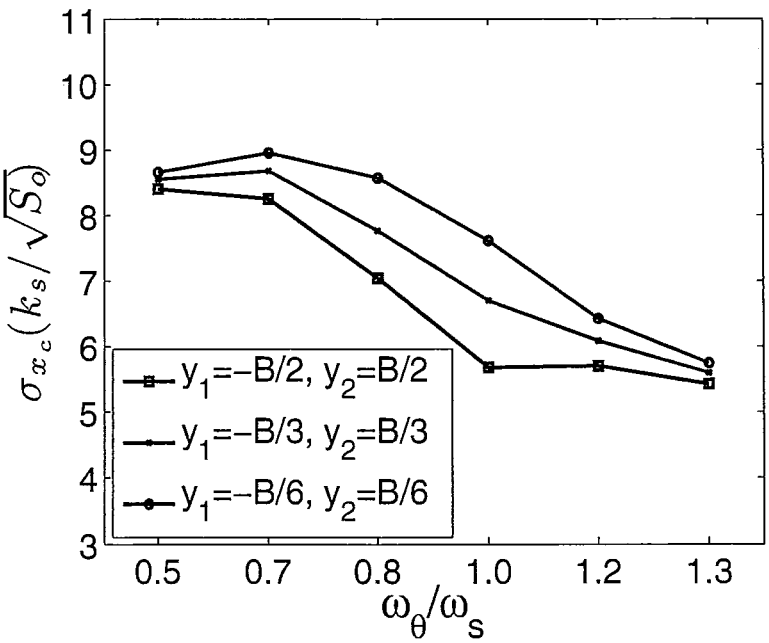

Figure 4.10: Normalized RMS Corner Response of Structures Equipped with Two Identical TMDs ($\mu = 0.02$) subjected to Random Excitation

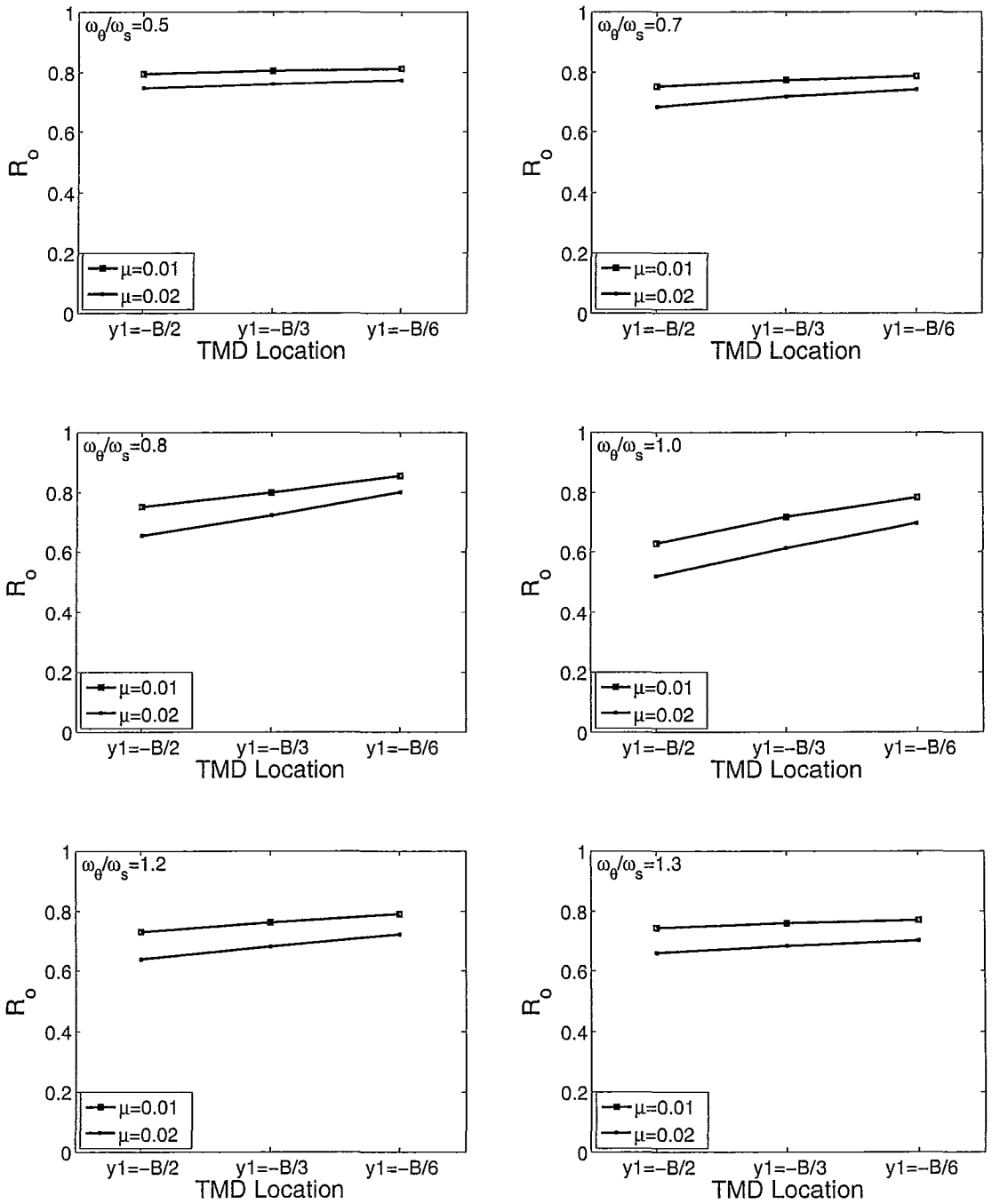

Figure 4.11: Response Reduction Factor for Structures Equipped with Two Identical TMDs subjected to Random Excitation

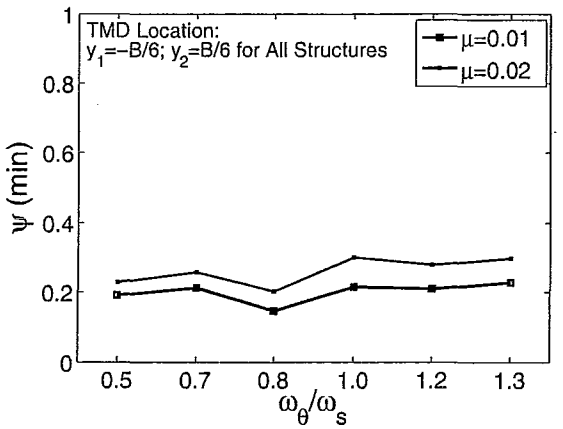

Figure 4.12: Minimum Efficiency Obtained for Two Identical TMDs subjected to Random Excitation

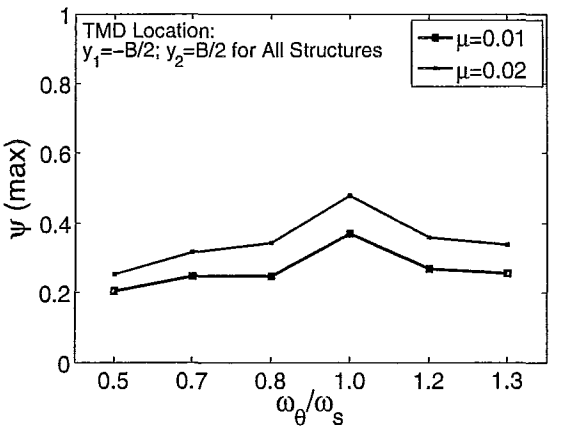

Figure 4.13: Maximum Efficiency Obtained for Two Identical TMDs subjected to Random Excitation

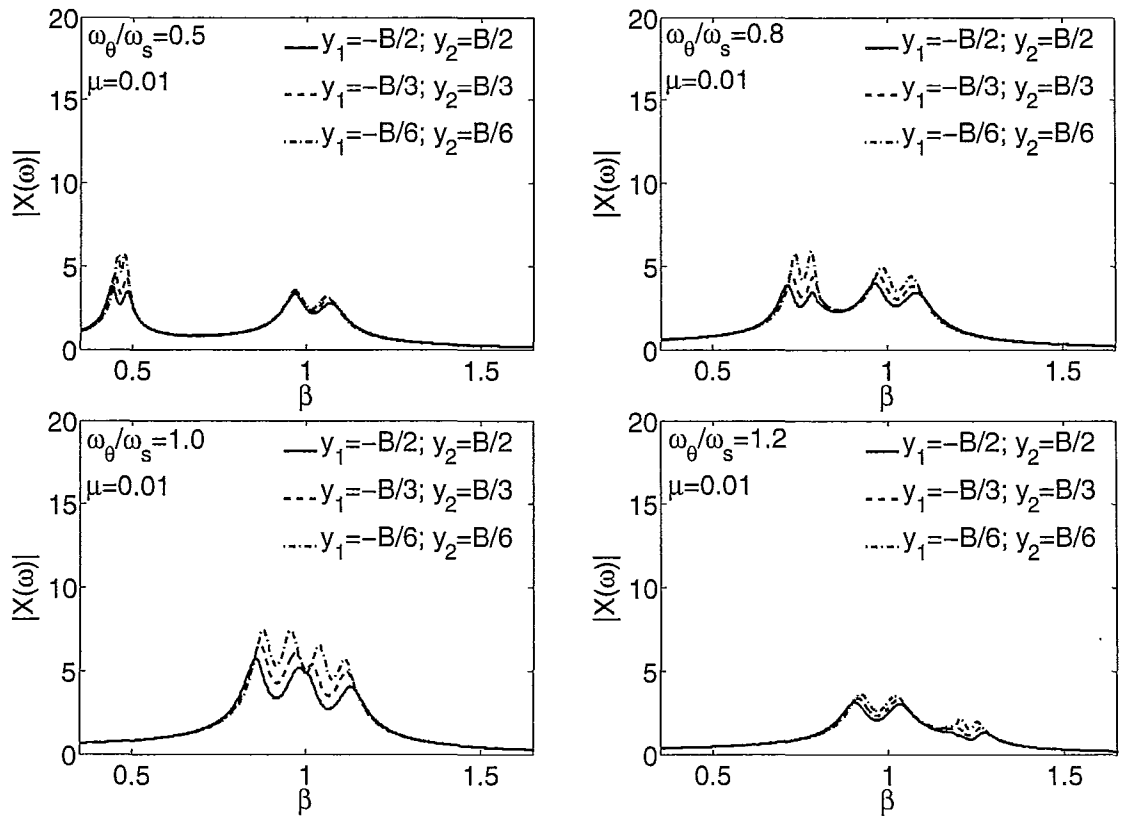

Figure 4.14: Mechanical Admittance Function Plots (Two Different TMDs Configuration) subjected to Random Excitation

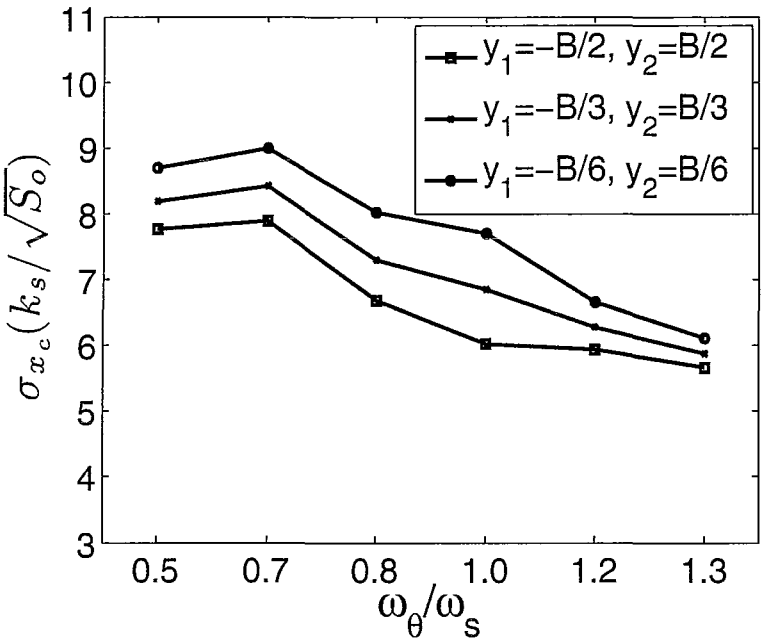

Figure 4.15: Normalized RMS Corner Response of Structures Equipped with Two Different TMDs ($\mu = 0.01$) subjected to Random Excitation

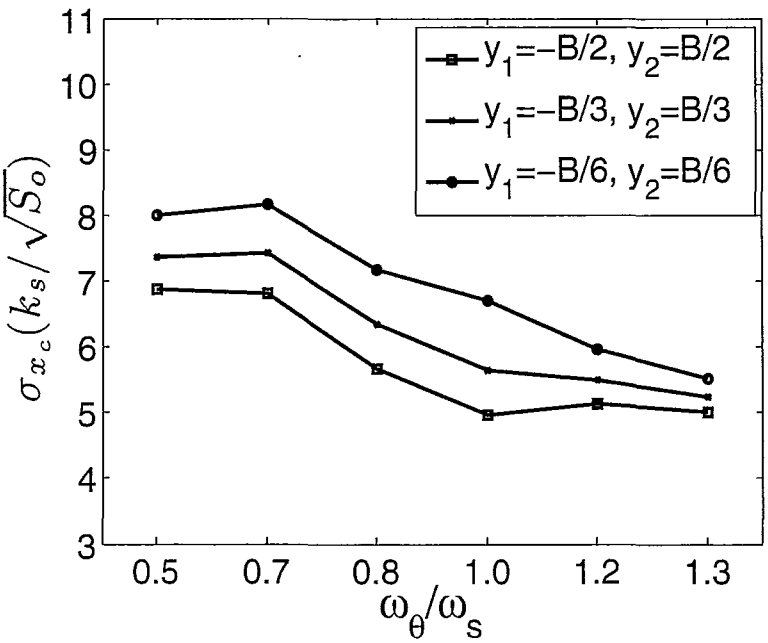

Figure 4.16: Normalized RMS Corner Response of Structures Equipped with Two Different TMDs ($\mu = 0.02$) subjected to Random Excitation

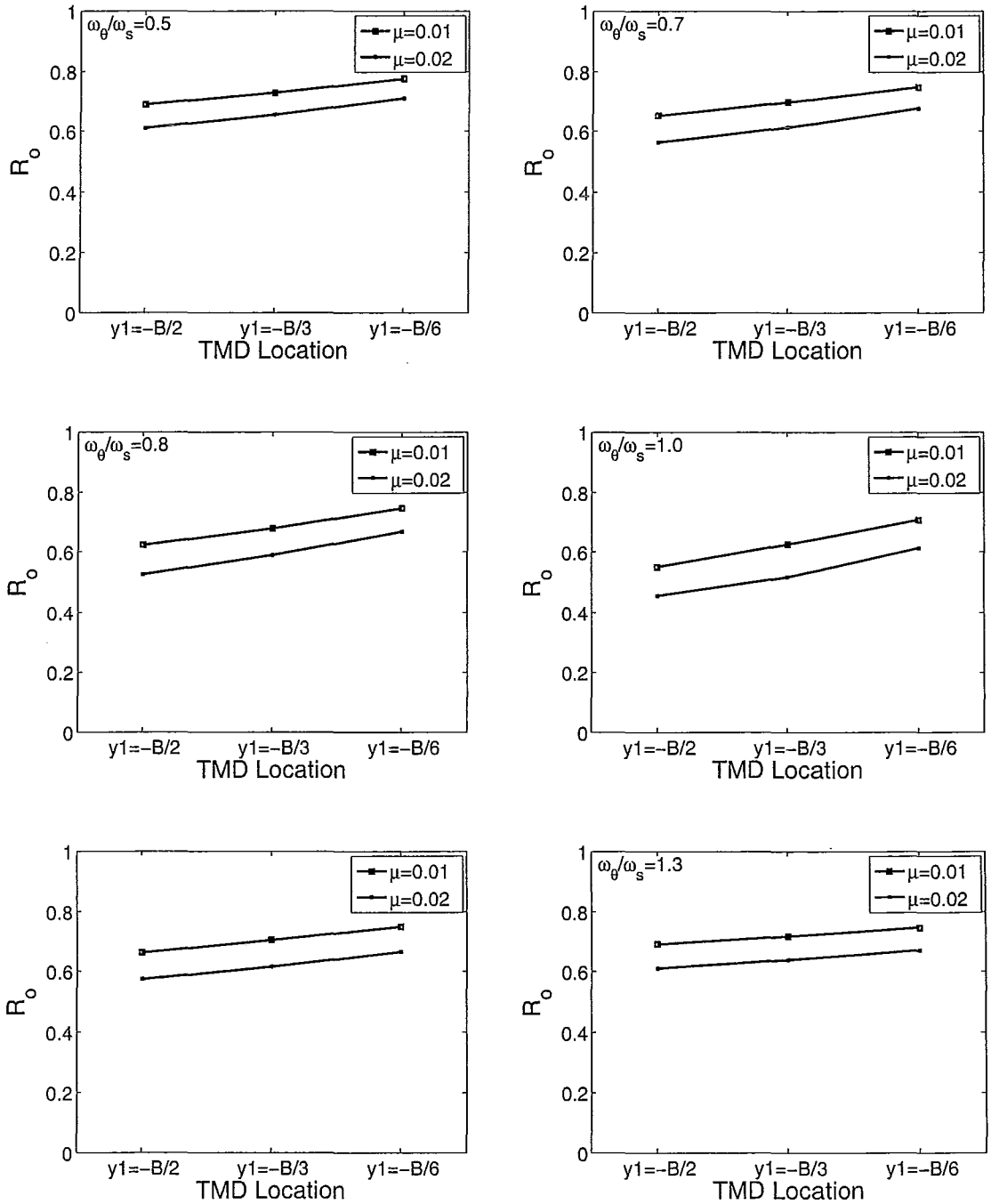

Figure 4.17: Response Reduction Factor for Structures Equipped with Two Different TMDs subjected to Random Excitation

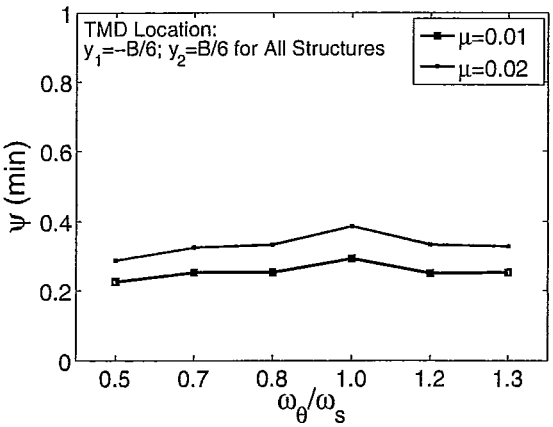

Figure 4.18: Minimum Efficiency Obtained for Two Different TMDs subjected to Random Excitation

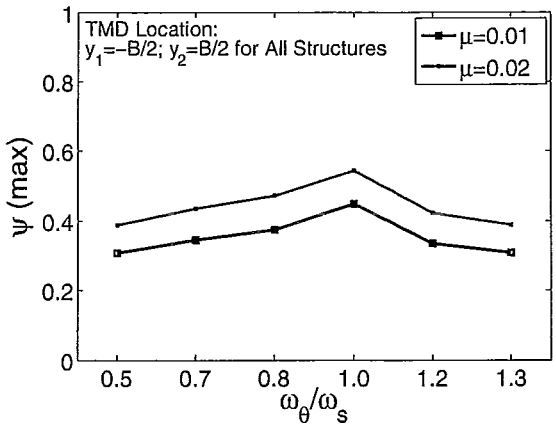

Figure 4.19: Maximum Efficiency Obtained for Two Different TMDs subjected to Random Excitation

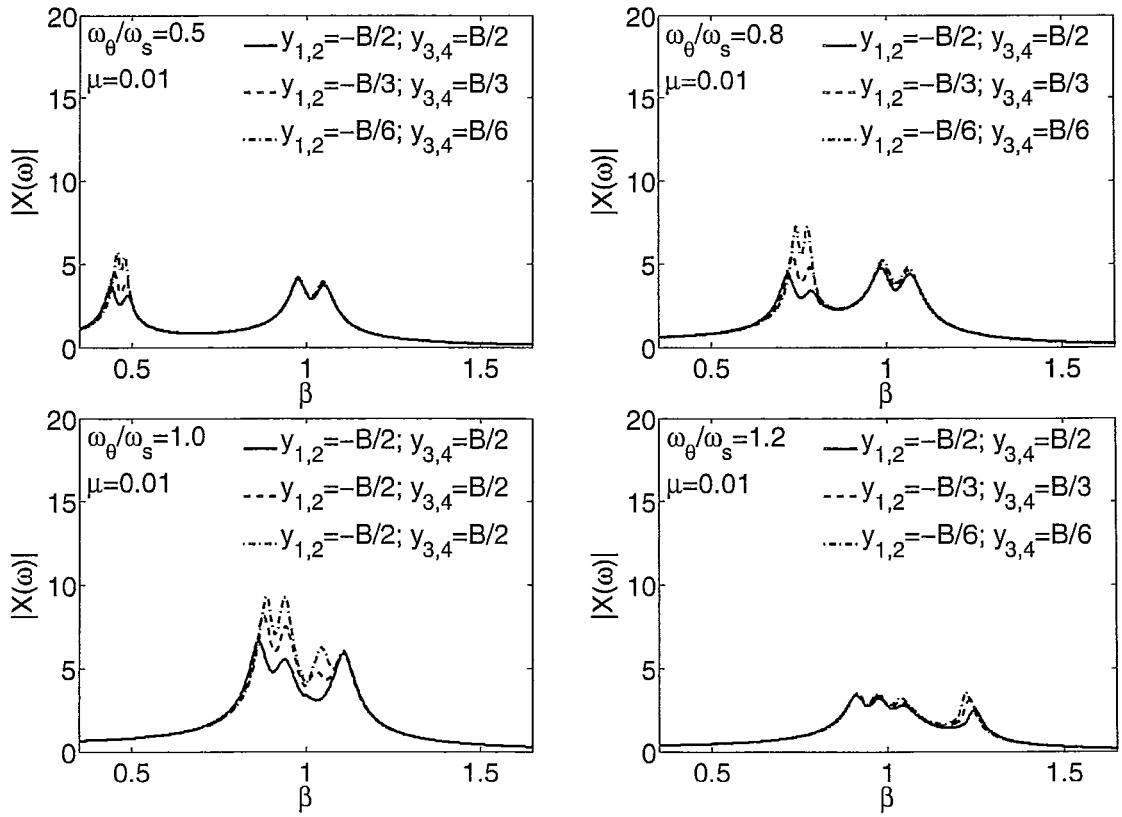

Figure 4.20: Mechanical Admittance Function Plots (Four TMDs Configuration (Approach-I)) subjected to Random Excitation

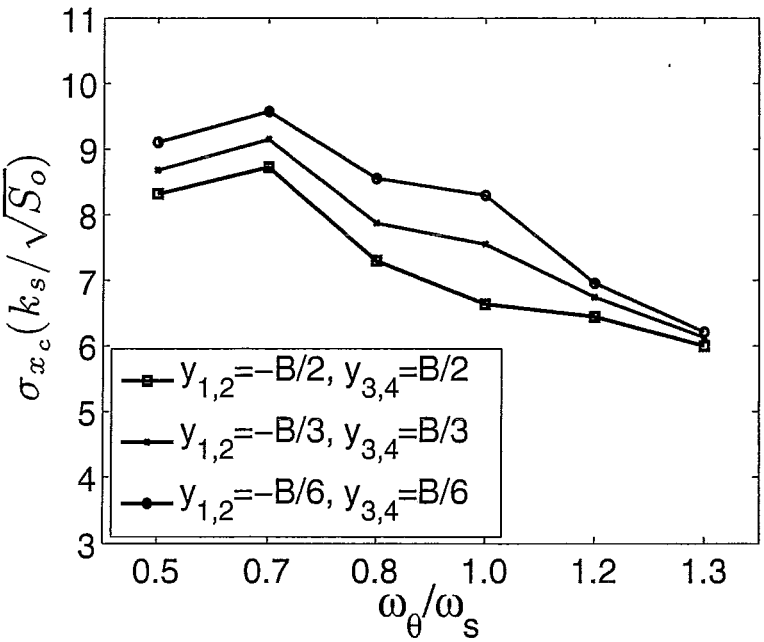

Figure 4.21: Normalized RMS Corner Response of Structures Equipped with Four TMDs ($\mu = 0.01$ Approach-I) subjected to Random Excitation

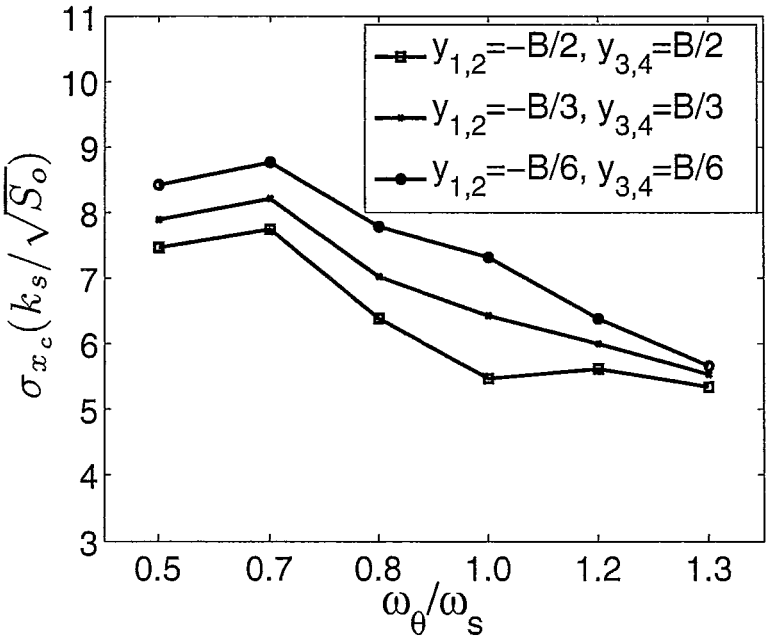

Figure 4.22: Normalized RMS Corner Response of Structures Equipped with Four TMDs ($\mu = 0.02$ Approach-I) subjected to Random Excitation

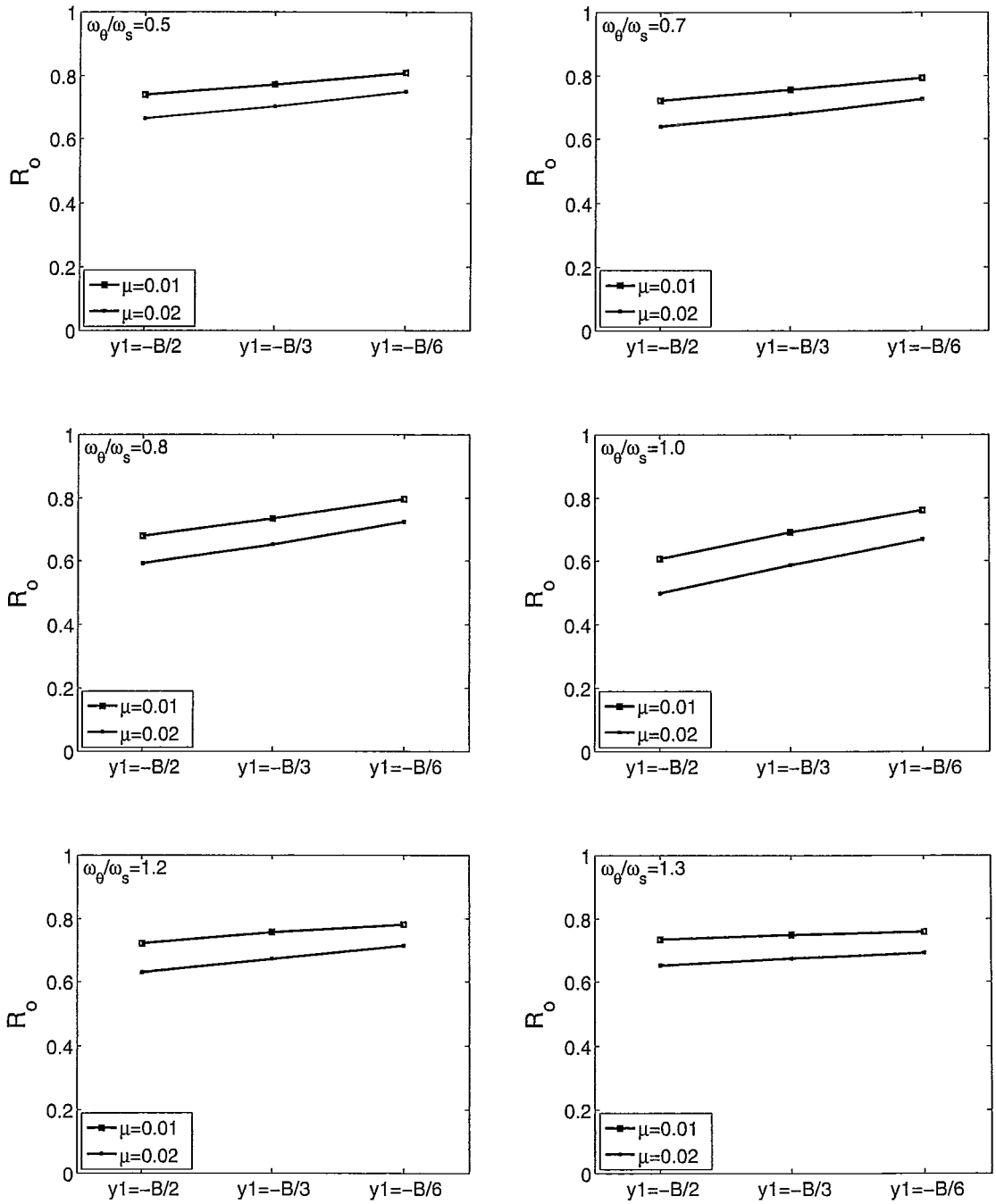

Figure 4.23: Response Reduction Factor for Structures Equipped with Four TMDs (Approach I) subjected to Random Excitation

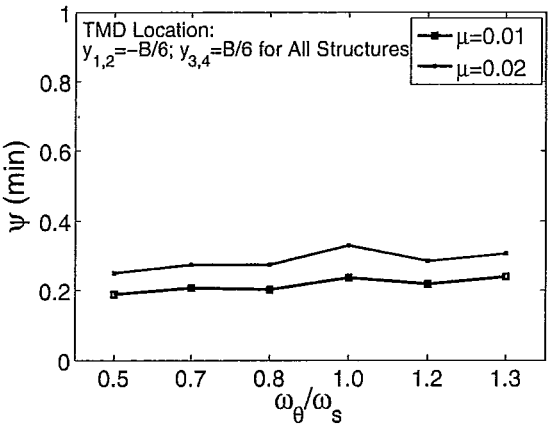

Figure 4.24: Minimum Efficiency Obtained for Four TMDs (Approach I) subjected to Random Excitation

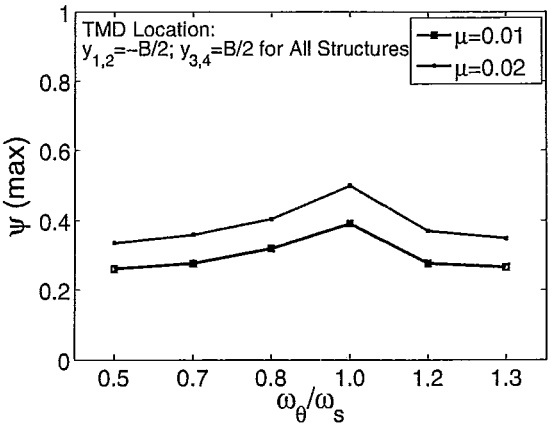

Figure 4.25: Maximum Efficiency Obtained for Four TMDs (Approach I) subjected to Random Excitation

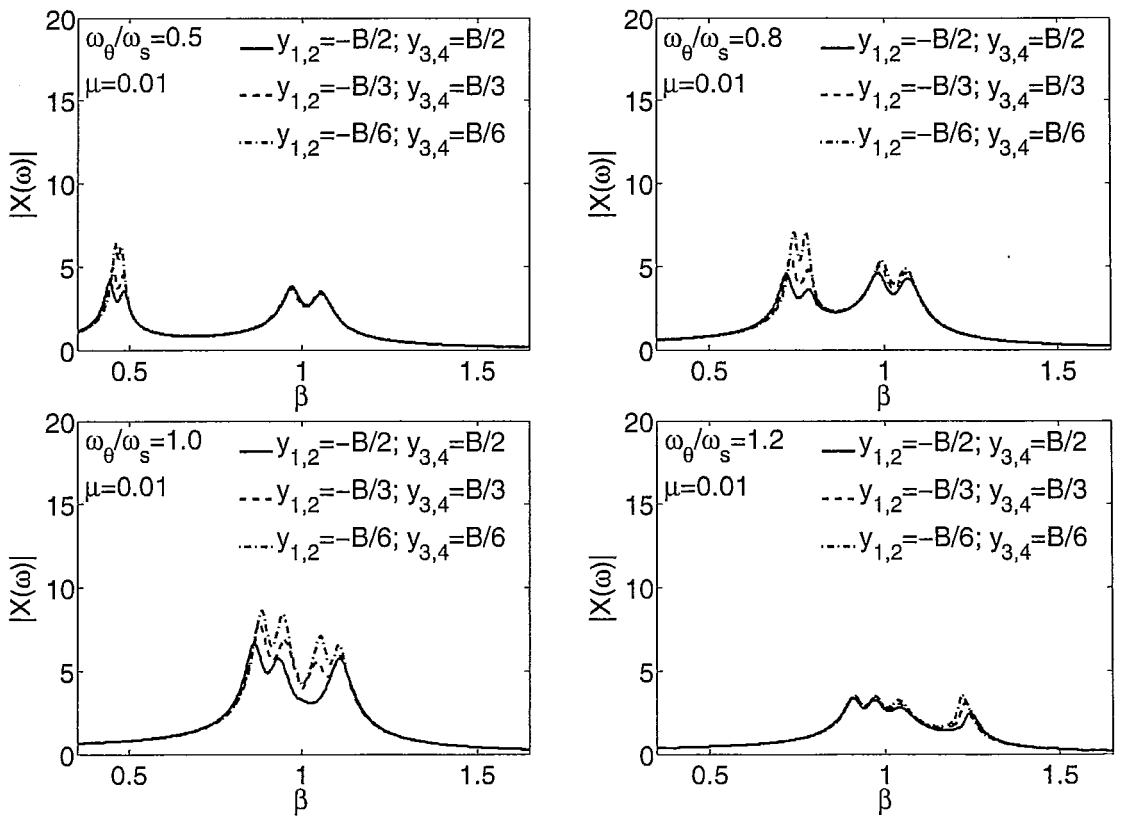

Figure 4.26: Mechanical Admittance Function Plots (Four TMDs Configuration (Approach-II)) subjected to Random Excitation

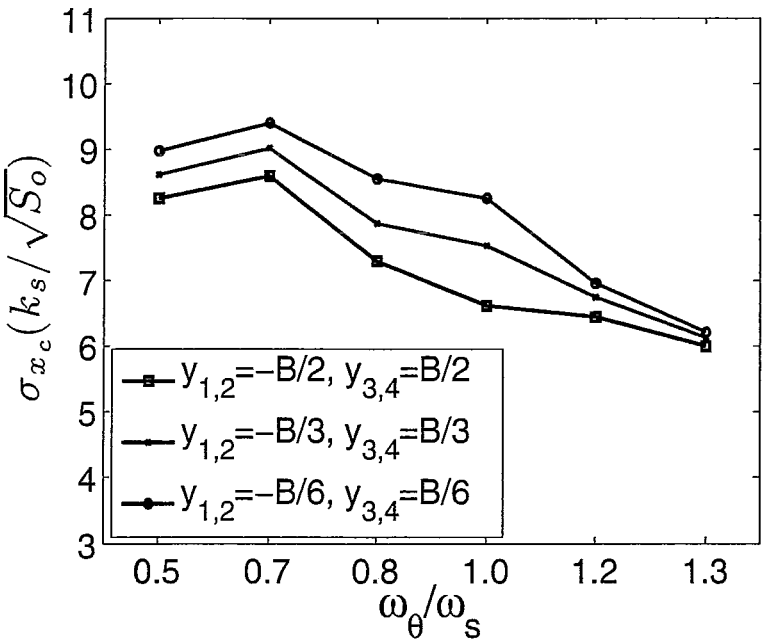

Figure 4.27: Normalized RMS Corner Response of Structures Equipped with Four TMDs ($\mu = 0.01$ Approach-II) subjected to Random Excitation

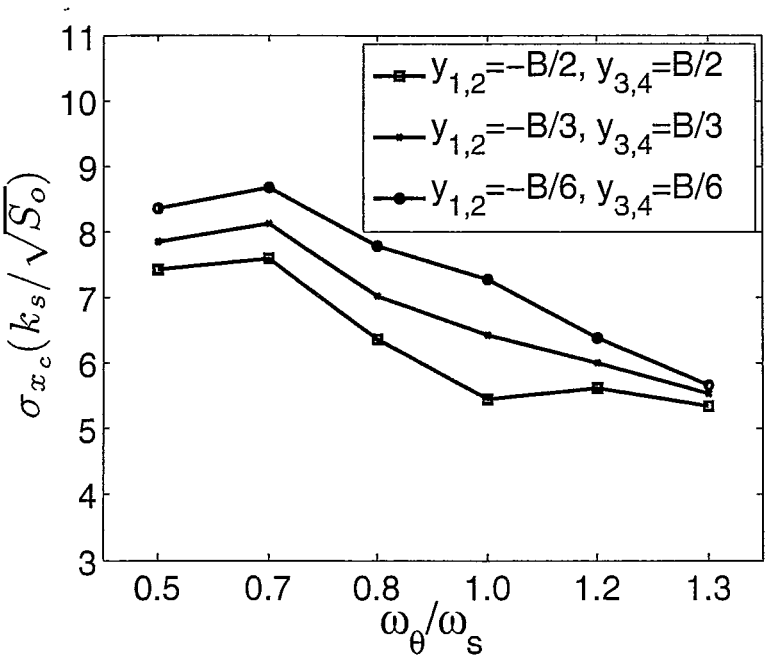

Figure 4.28: Normalized RMS Corner Response of Structures Equipped with Four TMDs ($\mu = 0.02$ Approach-II) subjected to Random Excitation

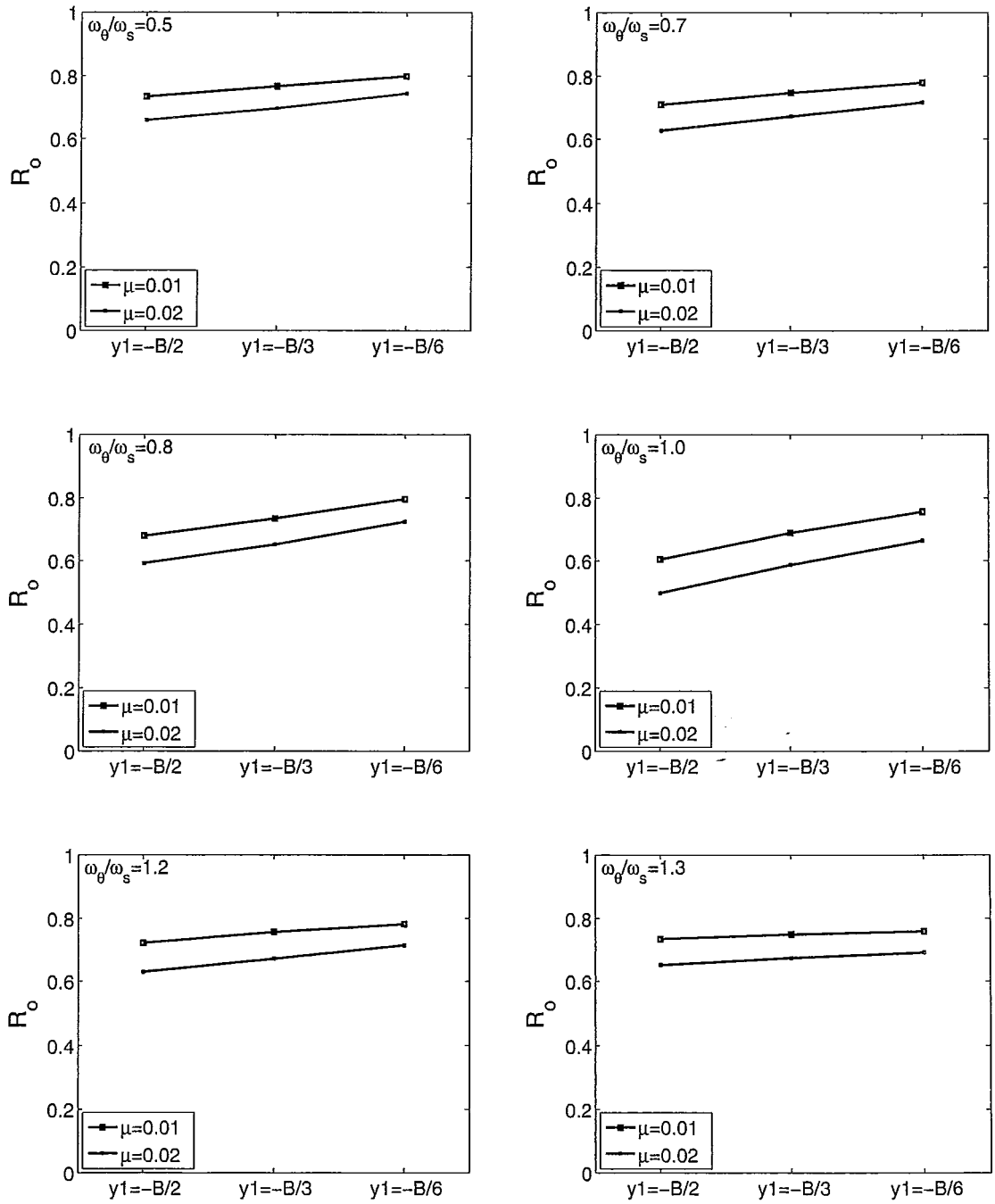

Figure 4.29: Response Reduction Factor for Structures Equipped with Four TMDs (Approach II)

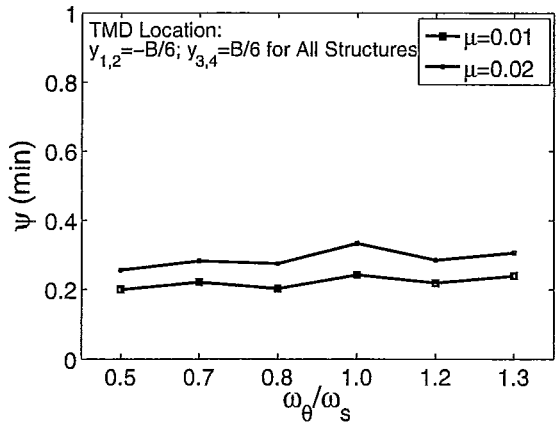

Figure 4.30: Minimum Efficiency Obtained for Four (Approach II) TMDs subjected to Random Excitation

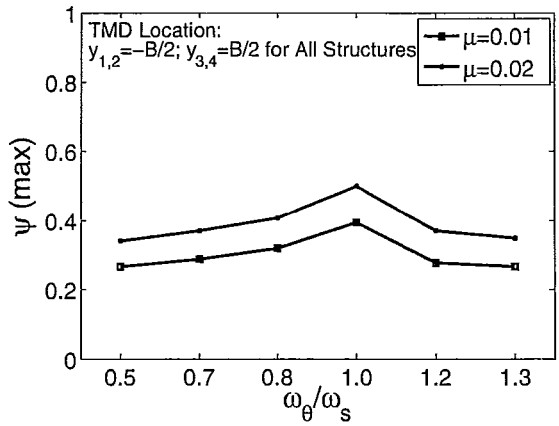

Figure 4.31: Maximum Efficiency Obtained for Four (Approach II) TMDs subjected to Random Excitation

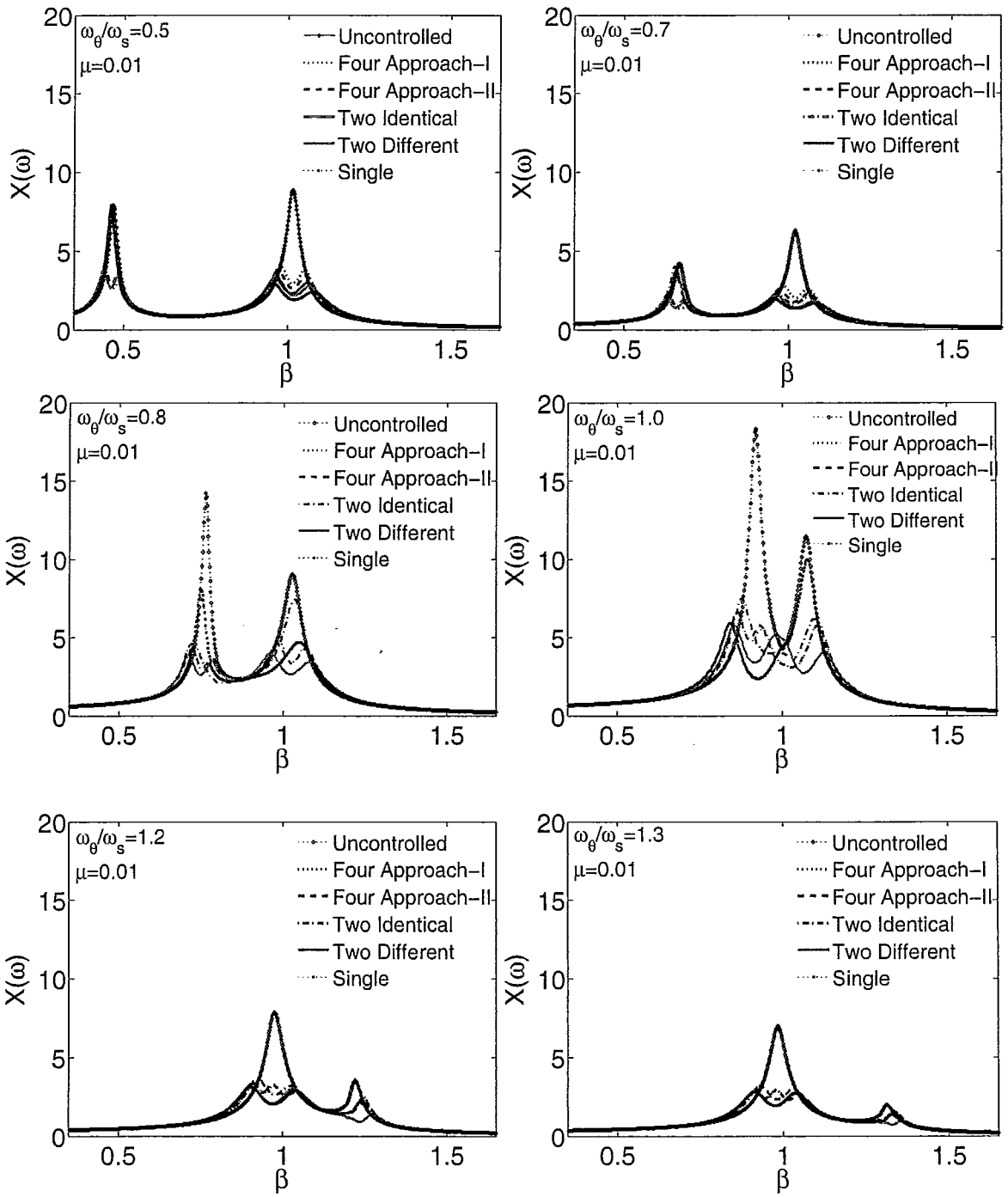

Figure 4.32: Mechanical Admittance Function Plots with Maximum TMD(s) Efficiency Locations subjected to Random Excitation

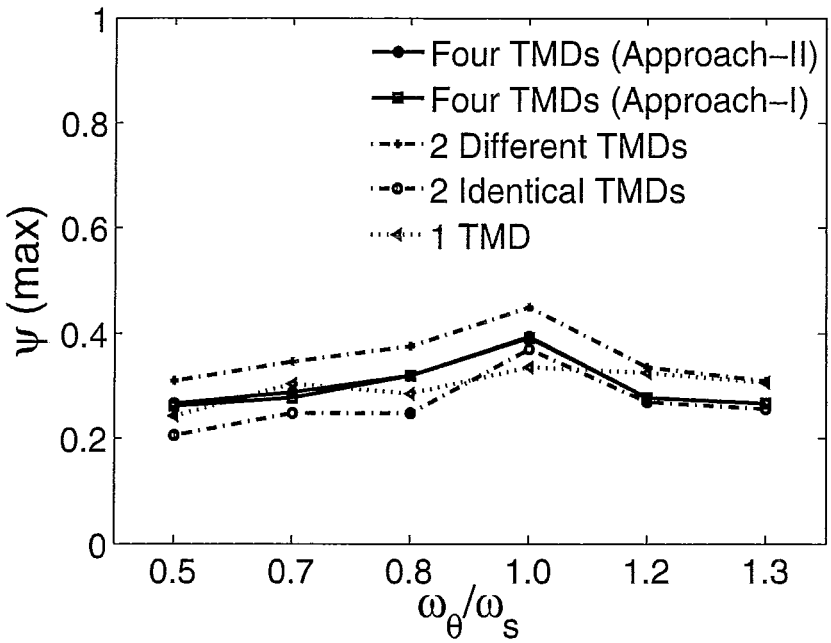

Figure 4.33: Maximum Efficiency Obtained for Different Arrangements of TMDs ($\mu = 0.01$) subjected to Random Excitation

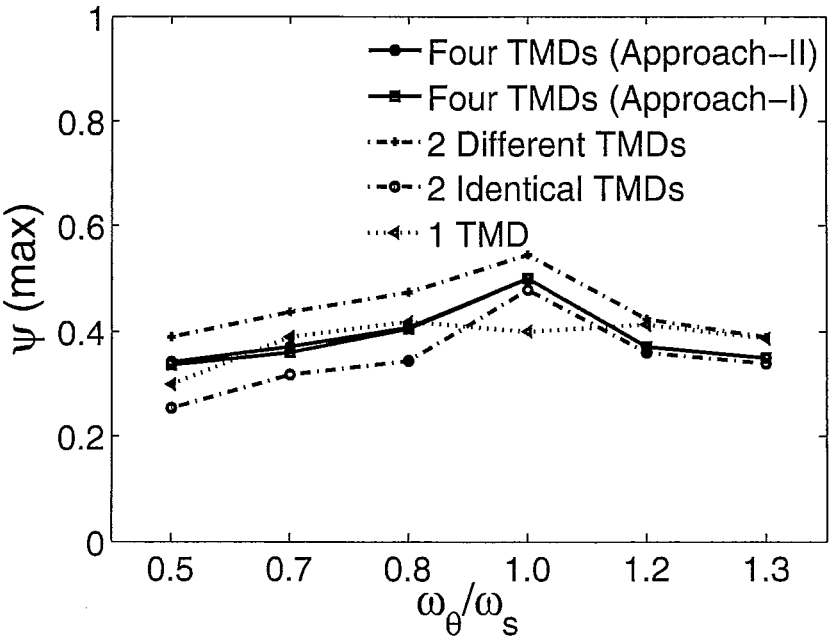

Figure 4.34: Maximum Efficiency Obtained for Different Arrangements of TMDs ($\mu = 0.02$) subjected to Random Excitation

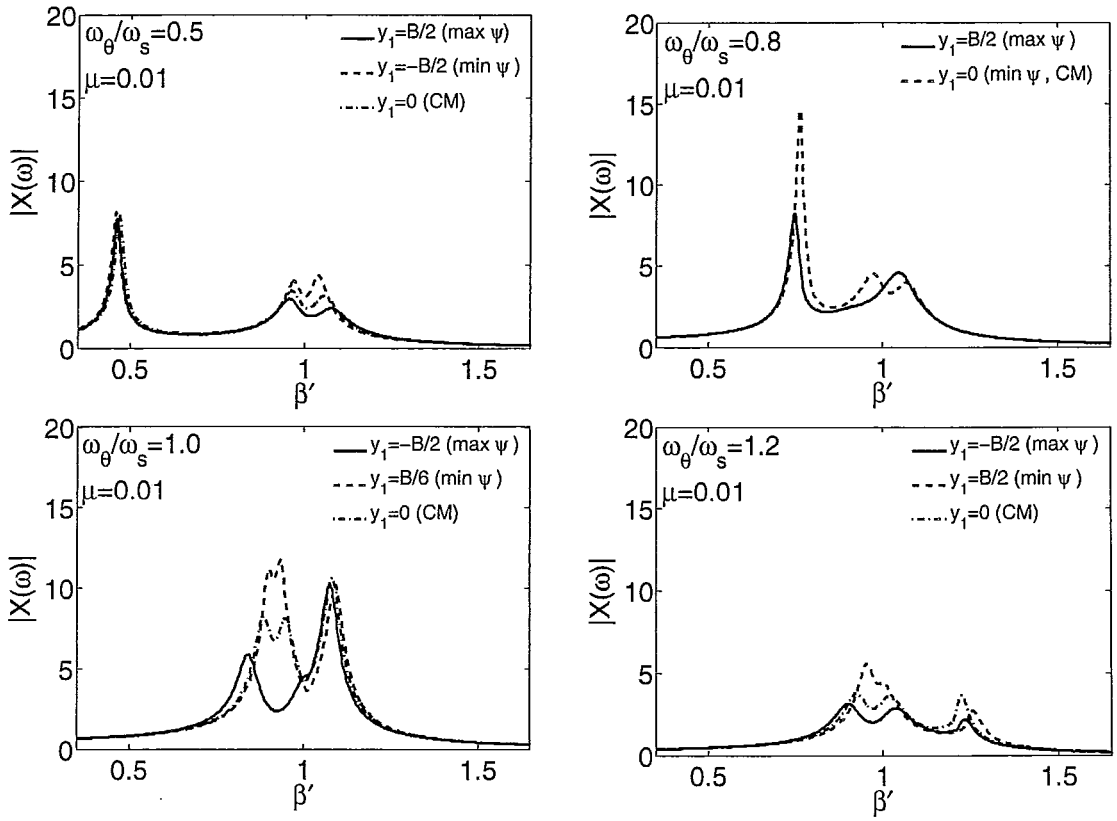

Figure 4.35: Mechanical Admittance Function Plots (Single TLD Configuration) subjected to Random Excitation

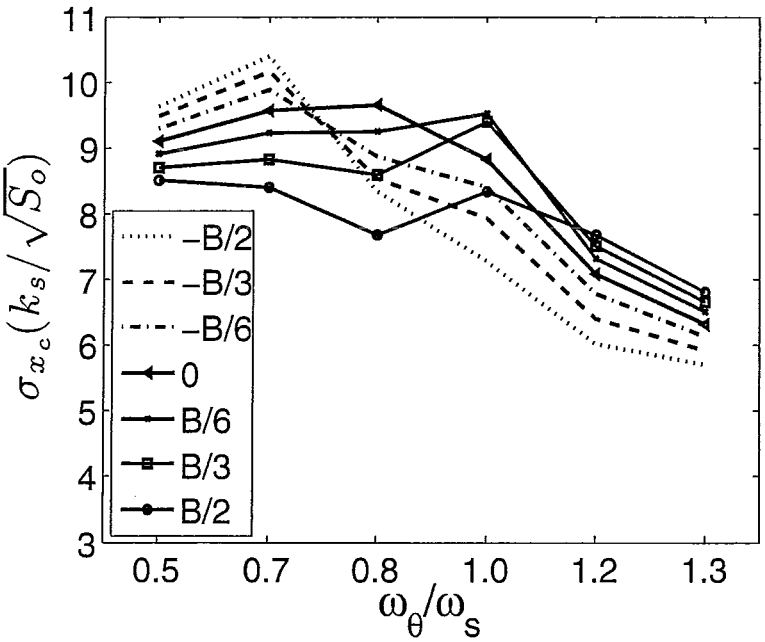

Figure 4.36: Normalized RMS corner Response of Structures Equipped with Single TLD ($\mu = 0.01$) subjected to Random Excitation

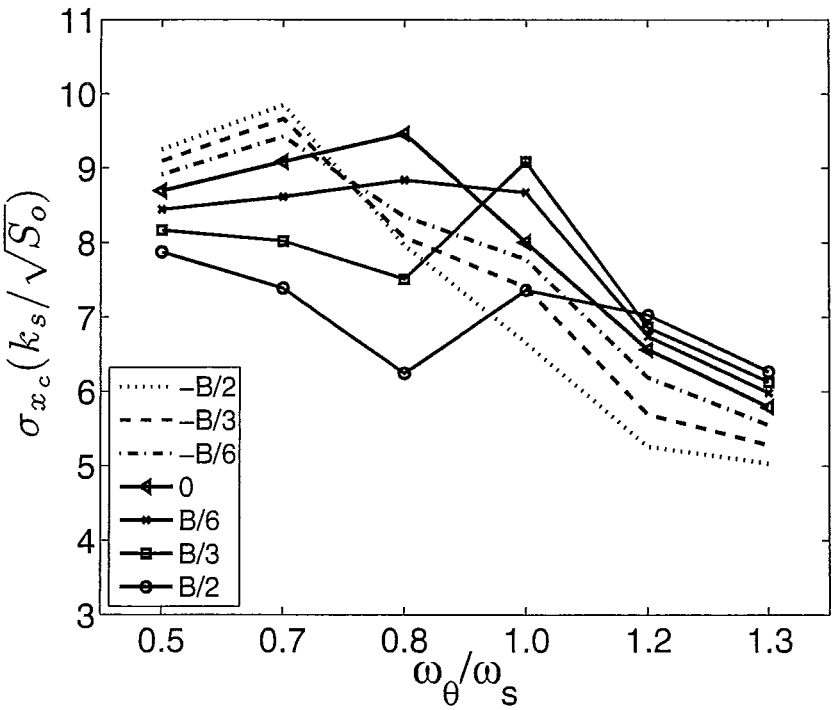

Figure 4.37: Normalized RMS corner Response of Structures Equipped with Single TLD ($\mu = 0.02$) subjected to Random Excitation

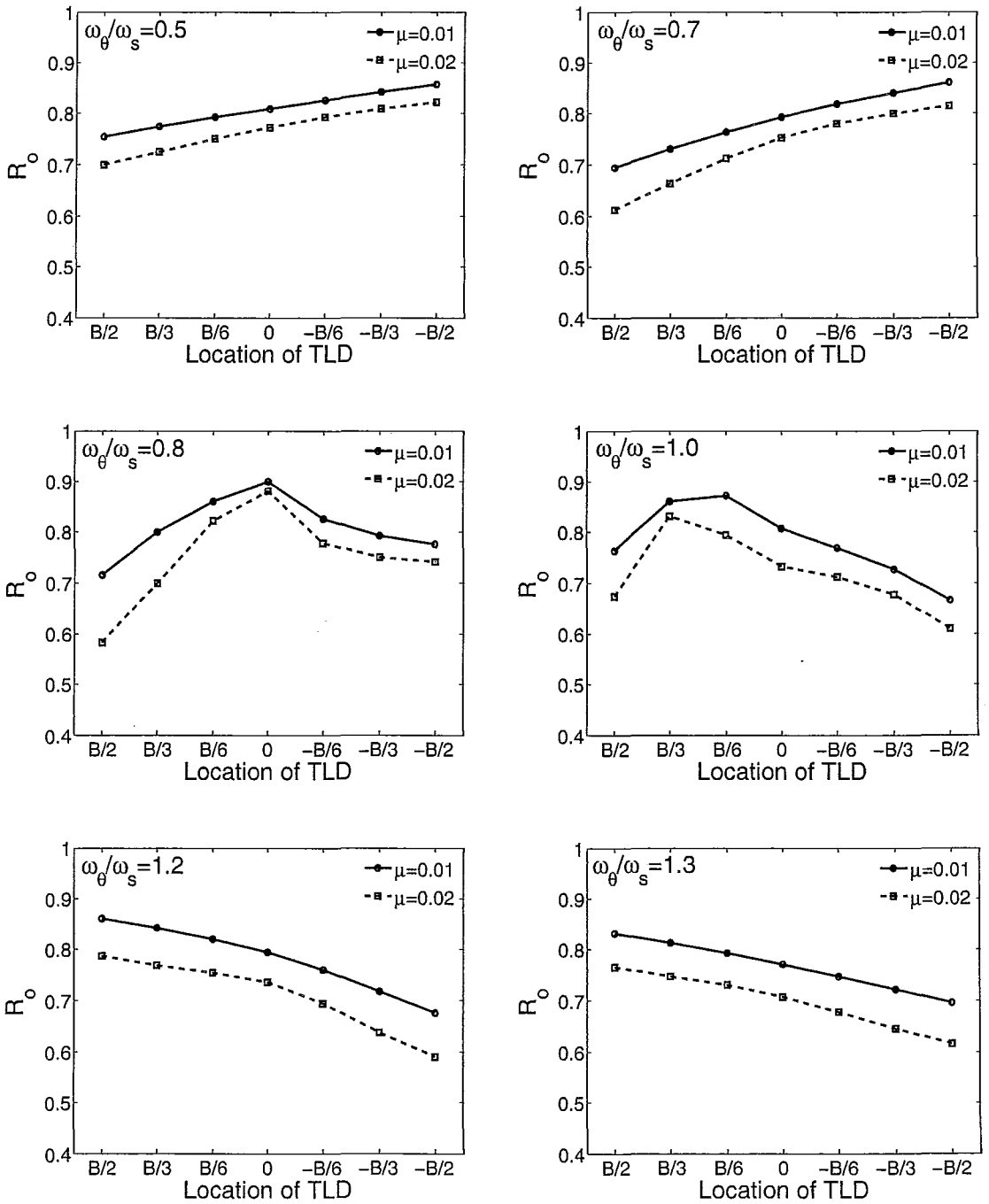

Figure 4.38: Response Reduction Factor for Structures Equipped with Single TLD subjected to Random Excitation

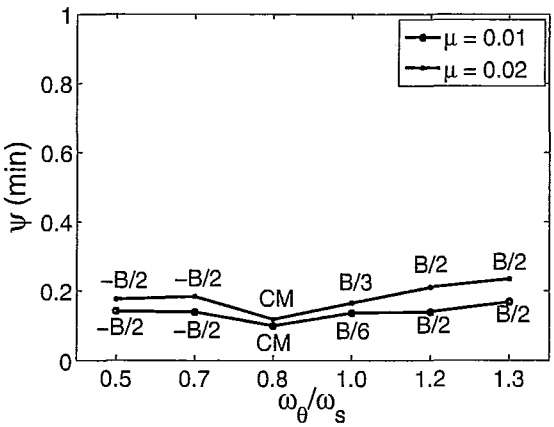

Figure 4.39: Minimum Efficiency Obtained for Single TLD subjected to Random Excitation

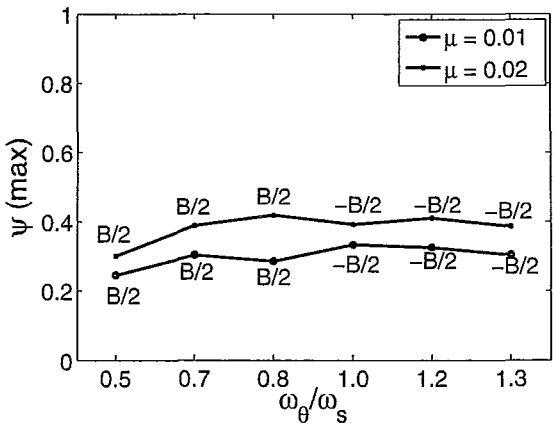

Figure 4.40: Maximum Efficiency Obtained for Single TLD subjected to Random Excitation

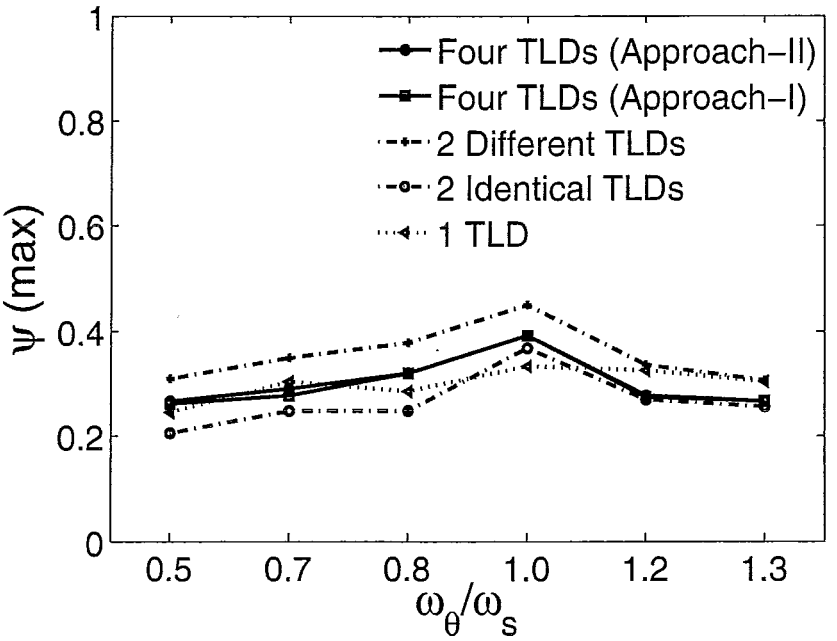

Figure 4.41: Maximum Efficiency Obtained for Different Arrangements of TLDs ($\mu = 0.01$) subjected to Random Excitation

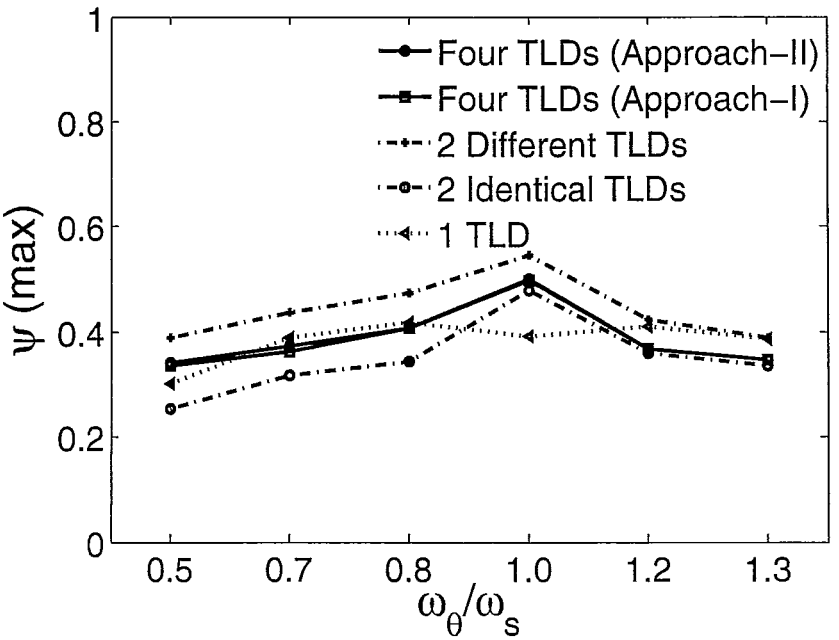

Figure 4.42: Maximum Efficiency Obtained for Different Arrangements of TLDs ($\mu = 0.02$) subjected to Random Excitation

Chapter 5

Torsionally Coupled Systems using Closed-Formed Parameters

5.1 Introduction

The optimal tuning and damping ratio values corresponding to five different TMD configurations were determined in Chapter 3 (Harmonic Excitation) and Chapter 4 (Random Excitation) for torsionally couple structures based on numerical optimization. This chapter investigates the application of closed-form optimal tuning and damping ratio parameters, derived for single-degree-of-freedom (SDOF) systems (Asami *et al.*, 1991, 2002), to torsionally coupled systems. The optimization criteria employed in deriving the optimal parameters for the two excitation types are also discussed. Approximate solutions, which can be applied to damped primary structures are also presented for both harmonic excitation and random excitation. The optimal parameters for a single-degree-of-freedom system described in this chapter are derived for a single-degree-of-freedom structure experiencing translational motion. In

contrast to a SDOF system having pure translational motion, the mode shapes for the torsionally coupled structures investigated are comprised of both translational and torsional motion. As a result, a procedure is introduced that allows the generalized TMD mass ratio for a given TMD configuration to be determined. Expressing the TMD configuration as an equivalent generalized TMD permits application of the optimized SDOF parameters. The response behavior of the optimized generalized structure-TMD system is subsequently compared with that of the torsionally-coupled system. In addition, comparisons are made between the response of a system equipped with TMDs designed using this novel technique to a system equipped with TMDs optimized using the numerical procedures introduced in Chapters 3 and 4.

5.2 Theoretical Background

Two different optimization criteria are considered with regard to the two types of excitation considered in this study. H_∞ optimization technique is employed when a structure is subjected to harmonic excitation, whereas for a structure under random vibration, H_2 optimization technique is applied.

5.2.1 H_∞ Optimization

According to Asami *et al.* (2002), H_∞ was the optimization criterion proposed by Den Hartog and Ormondroyd in 1928. The goal is to minimize the peak response such that two peaks of equal height appear for a two-degree-of-freedom system or a structure-TMD system, in the frequency response function plot. The resulting optimal parameters of a damped vibration absorber attached to an undamped structure

are given as

$$\Omega_{opt} = \frac{1}{1+\mu} \tag{5.1}$$

$$\zeta_{opt} = \sqrt{\frac{3\mu}{8(1+\mu)}} \tag{5.2}$$

where μ is the total mass ratio. As for a damped structure, Asami *et al.* (2002) proposed an approximate solution for the optimal parameters, expressed as follows

$$\begin{aligned}\Omega_{opt} &= \frac{1}{1+\mu} - \zeta_s \frac{1}{1+\mu}\sqrt{\frac{1}{2(1+\mu)}(3+4\mu-\frac{A_oB_o}{2+\mu})} \\ &+\zeta_s{}^2 \frac{C_o - 4(5+2\mu)A_oB_o}{4(1+\mu)^2(2+\mu)(9+4\mu)}\end{aligned} \tag{5.3}$$

$$\begin{aligned}\zeta_{opt} &= \sqrt{\frac{3\mu}{8(1+\mu)}} + \zeta_s \frac{60+63\mu+16\mu^2-2(3+2\mu)A_oB_o}{8(1+\mu)(2+\mu)(9+4\mu)} \\ &+\zeta_s{}^2 \frac{C_1(A+B)\sqrt{2+\mu}+C_2(A_o-B_o)\sqrt{\mu}}{32(1+\mu)(2+\mu)^2(9+4\mu)^3\sqrt{2\mu(1+\mu)}}\end{aligned} \tag{5.4}$$

where ζ_s is the structural damping ratio values and A_o, B_o, C_o, C_1 and C_2 are defined as follow

$$\begin{aligned} A_o &= \sqrt{3(2+\mu) - \sqrt{\mu(2+\mu)}} \\ B_o &= \sqrt{3(2+\mu) + \sqrt{\mu(2+\mu)}} \\ C_o &= 52 + 41\mu + 8\mu^2 \\ C_1 &= -1296 + 2124\mu + 6509\mu^2 + 5024\mu^3 + 1616\mu^4 + 192\mu^5 \\ C_2 &= 48168 + 112887\mu + 105907\mu^2 + 49664\mu^3 + 11632\mu^4 + 1088\mu^5 \end{aligned} \quad (5.5)$$

5.2.2 H_2 Optimization

H_2 Optimization was first proposed by Crandall and Mark (1963). Owing to the fact that random excitation contains infinitely many frequencies, the objective of this optimization technique is to minimize the overall vibration energy of the system. Thus, for white noise excitation, the area under the mechanical admittance function of the system is minimized. The optimal parameters for an undamped structure equipped with a damped absorber were derived by Warburton (1982) using this optimization criterion and are given as follows,

$$\Omega_{opt} = \frac{1}{1+\mu}\sqrt{1+\frac{\mu}{2}} \quad (5.6)$$

$$\zeta_{opt} = \sqrt{\frac{\mu(4+3\mu)}{8(1+\mu)(2+\mu)}} \quad (5.7)$$

As for a damped structure, the approximate optimal parameters are expressed as (Asami *et al.*, 1991)

$$\begin{aligned}\Omega_{opt} &= \frac{1}{1+\mu}\sqrt{1+\frac{\mu}{2}} - \zeta_s(4+\mu)\sqrt{\frac{\mu}{8(1+\mu)^3(2+\mu)(4+3\mu)}} \\ &\quad +{\zeta_s}^2\frac{\mu(192+304\mu+132\mu^2+13\mu^3)}{8(1+\mu)^2(4+3\mu)^2\sqrt{2(2+\mu)^3}} \\ &\quad -{\zeta_s}^3\frac{b_1}{16}\sqrt{\frac{\mu^3}{2(1+\mu)^5(2+\mu)^5(4+3\mu)^7}}\end{aligned} \tag{5.8}$$

$$\begin{aligned}\zeta_{opt} &= \sqrt{\frac{\mu(4+3\mu)}{8(1+\mu)(2+\mu)}} - \zeta_s\frac{\mu^3}{4(1+\mu)(4+3\mu)\sqrt{2(2+\mu)^3}} \\ &\quad +{\zeta_s}^2\frac{-64-80\mu+15\mu^3}{32}\sqrt{\frac{2\mu^5}{(1+\mu)^3(2+\mu)^5(4+3\mu)^5}} \\ &\quad +{\zeta_s}^3\frac{\mu^3 b_2}{32(1+\mu)^2(4+3\mu)^4\sqrt{2(2+\mu)^7}}\end{aligned} \tag{5.9}$$

where b_1 and b_2 are given by

$$\begin{aligned}b_1 &= 4096+13056\mu+15360\mu^2+8080\mu^3+1780\mu^4+101\mu^5 \\ b_2 &= 2048+6912\mu+8064\mu^2+3616\mu^3+288\mu^4-125\mu^5\end{aligned} \tag{5.10}$$

5.3 Generalized TMD Properties

This chapter evaluates the applicability of the available closed-form, tuning ratio and damping ratio values (Equations 5.1 to 5.10), in order to target the response of a particular mode in a torsionally coupled system. This section first outlines the procedures used to apply the closed-form parameters on an undamped torsionally coupled system equipped with two identical TMDs (see Figure 5.1). Subsequently, the outlined procedure is extended to a damped torsionally coupled system. In order to apply the optimal parameters, it is necessary to obtain the generalized properties (see Figure 5.2(a)), which include the generalized properties of the structure, ${m_{s_n}}^*$, ${k_{s_n}}^*$ and ${c_{sn}}^*$. In addition to the generalized mass of the TMDs, ${m_{tmd_n}}^*$, the generalized stiffness of the TMDs, ${k_n}^*$, and the generalized damping of the TMDs, ${c_n}^*$, are also required.

According to Chopra (2000), ${m_{s_n}}^*$ and ${k_{sn}}^*$ can be obtained using the following relationships,

$$[K_s - {\omega_n}^2 M_s]\phi_n = 0 \tag{5.11}$$

$${m_{s_n}}^* = \{\phi_n\}^T [M_s]\{\phi_n\} \tag{5.12}$$

$${k_{s_n}}^* = \{\phi_n\}^T [K_s]\{\phi_n\} \tag{5.13}$$

where ϕ_n is the n^{th} mode shape, M_s is the mass matrix of the structure, K_s is the structure stiffness matrix, and ω_n is the structure's n^{th} natural frequency. Note that

the subscript n corresponds to the mode being considered. The corresponding mode shape and natural frequency for each mode can be obtained by solving the matrix eigenvalue problem in Equation 5.11.

As the mode shape has both translational and torsional components, the resulting mass coupling terms introduced by the TMD must be considered. The generalized mass of the TMD(s) corresponding to the n^{th} structural mode is obtained using the following relationship

$$m_{tmd_n}{}^* = \{\phi_n\}^T [M_{tmd}] \{\phi_n\} \tag{5.14}$$

The TMD mass matrix, M_{tmd}, can be obtained by transferring the mass of the TMDs back to the centre of mass of the structure. The TMD mass matrix can be determined by direct force equilibrium method. Thus, a unit acceleration is imposed on each degree-of-freedom, and the resulting mass influence coefficients can be determined. The derivation of the TMD mass matrix for a 3-dimensional mode shape is represented in Figure 5.3 and expressed as

$$[M_{tmd}] = \begin{bmatrix} m_1 + m_2 & 0 & m_2 e_{y2} - m_1 e_{y1} \\ 0 & m_1 + m_2 & m_2 e_{x2} - m_1 e_{x1} \\ m_2 e_{y2} - m_1 e_{y1} & m_2 e_{x2} - m_1 e_{x1} & m_1({e_{x1}}^2 + {e_{y1}}^2) + m_2({e_{x2}}^2 + {e_{y2}}^2) \end{bmatrix} \tag{5.15}$$

5.3.1 Two Identical TMDs Configuration

This chapter investigates the two identical TMDs configuration. The TMD mass matrix, given by Equation 5.15, corresponding to the two identical TMDs configuration is given by

$$[M_{tmd}] = \begin{bmatrix} m_1 + m_2 & m_2 e_{x2} - m_1 e_{x1} \\ m_2 e_{x2} - m_1 e_{x1} & m_1 {e_{x1}}^2 + m_2 {e_{x2}}^2 \end{bmatrix} \tag{5.16}$$

It is evident from Equation 5.16 that the additional torsional component introduces both coupling terms and a mass moment of inertia term. These additional mass terms depend on TMD location (i.e. e_{x1} and e_{x2}). Once the TMD mass matrix is calculated, the generalized mass ratio for the targeted mode can then be determined by

$${\mu_n}^* = \frac{{m_{tmd_n}}^*}{{m_{s_n}}^*} \tag{5.17}$$

Substituting the generalized mass ratio value back into Equations 5.1 and 5.2 for harmonic excitation and Equations 5.6 and 5.7 for random excitation, the optimal tuning ratio and damping ratio values for the mode being targeted are obtained.

The generalized stiffness, ${k_n}^*$, and the generalized damping, ${c_n}^*$, of the TMDs for the targeted mode can be determined using the relationships (Chopra (2000)),

$${k_n}^* = (\Omega_{opt_n} \omega_n)^2 {m_{tmd_n}}^* \tag{5.18}$$

$${c_n}^* = 2 {m_{tmd_n}}^* \zeta_{opt_n} \omega_{tmd_n} \tag{5.19}$$

where ω_{tmd_n} is the natural frequency of the TMD tuned to the n^{th} mode of the structure. As the generalized stiffness and damping of the TMDs calculated using Equations 5.18 and 5.19 correspond to the targeted mode only, the modal response, which will be discussed in more detail at the end of this section, does not take into the coupling between structural modes.

For a damped torsionally coupled system (see Figure 2.1), the corresponding generalized system is shown in Figure 5.2(b). The structural damping ratio value, ζ_{s_n}, of the targeted mode is required to obtain the closed-form tuning parameters (see Equations 5.3, 5.4, 5.8 and 5.9). The required damping ratio values can be obtained by first calculating the generalized damping of the structure, ${c_{s_n}}^*$. Similar to the generalized stiffness of the structure, the generalized damping can be obtained through

$$ {c_{s_n}}^* = \{\phi_n\}^T [C_s] \{\phi_n\} \tag{5.20} $$

where the damping matrix of the structure is expressed as

$$ [C_s] = \begin{bmatrix} c_{s1} + c_{s2} & c_{s1}y_{s1} - c_{s2}y_{s2} \\ c_{s1}y_{s1} - c_{s2}y_{s2} & c_{s1}{y_{s1}}^2 + c_{s2}{y_{s2}}^2 \end{bmatrix} \tag{5.21} $$

Finally, the required damping ratio values for the mode being targeted can be obtained through

$$ \zeta_{s_n} = \frac{{c_{s_n}}^*}{2\omega_n {m_{s_n}}^*} \tag{5.22} $$

Once the required mass ratio and damping ratio values are obtained, the optimal

stiffness and damping values of the TMD(s) can be calculated for a damped structure.

The modal response of a two-degree-of-freedom system can be obtained by employing equations provided by Asami *et al.* (1991) and can be expressed as follows in terms of the generalized properties of the mode being targeted

$$\frac{x_n}{f_o/k_{s_n}{}^*} = \sqrt{\frac{a_1^2 + a_2^2}{a_3^2 + a_4^2}} \tag{5.23}$$

where constants a_1, a_2, a_3 and a_4 are expressed as

$$\begin{aligned} a_1 &= \Omega_{opt_n}{}^2 - \beta_n{}^2 \\ a_2 &= 2\Omega_{opt_n}\beta_n\zeta_{opt_n} \\ a_3 &= \Omega_{opt_n}{}^2 - (1 + 4\Omega_{opt_n}\zeta_{s_n}\zeta_{opt_n} + (1+\mu)\Omega_{opt_n}{}^2)\beta_n{}^2 + \beta_n{}^4 \\ a_4 &= 2\beta_n((\Omega_{opt_n}{}^2 - \beta_n{}^2)\zeta_{s_n} + \Omega_{opt_n}(1 - (1+\mu)\beta_n{}^2)\zeta_{opt_n}) \end{aligned} \tag{5.24}$$

where β_n is the forcing frequency ratio for the mode being targeted and is expressed as

$$\beta_n = \frac{\omega}{\omega_n} \tag{5.25}$$

Note that x_n represents the modal response of the mode being targeted. The translational and rotational motion of the structure for this mode can be obtained by

$$\{x_s \quad \theta_s\}^T = |\{\phi_n\}|x_n \tag{5.26}$$

The maximum corner response is expressed as

$$x_{c_1,c_2} = x_s \pm \theta_s \frac{B}{2} \tag{5.27}$$

As stated previously, the modal response obtained through Equation 5.26 does not take into account the coupling between modes. To fully capture the interactions between the structure and the TMDs (i.e. the coupling between structural modes), the equations of motion (Equation 2.18) developed in Chapter 2 must be used. However, this requires transferring the generalized stiffness, ${k_n}^*$, and damping, ${c_n}^*$, of the TMD configuration from the centre of mass to the actual TMD locations (i.e. y_1 and y_2 see Figure 2.1) such that the required stiffness, k_1 and k_2, and damping, c_1 and c_2, are obtained (see Figure 2.1). This can be achieved by utilizing Equations 5.28 and 5.29,

$${k_n}^* = \{\phi_n\}^T [K_{tmd}] \{\phi_n\} \tag{5.28}$$

$${c_n}^* = \{\phi_n\}^T [C_{tmd}] \{\phi_n\} \tag{5.29}$$

where K_{tmd} and C_{tmd} are the TMD stiffness and TMD damping matrices, given by Equations 5.30 and 5.31, respectively.

$$[K_{tmd}] = \begin{bmatrix} k_1 + k_2 & k_2 e_{x2} - k_1 e_{x1} \\ k_2 e_{x2} - k_1 e_{x1} & k_1 {e_{x1}}^2 + k_2 {e_{x2}}^2 \end{bmatrix} \tag{5.30}$$

$$[C_{tmd}] = \begin{bmatrix} c_1 + c_2 & c_2 e_{x2} - c_1 e_{x1} \\ c_2 e_{x2} - c_1 e_{x1} & c_1 {e_{x1}}^2 + c_2 {e_{x2}}^2 \end{bmatrix} \tag{5.31}$$

The development of K_{tmd} and C_{tmd} are similar to the approach taken to develop TMD mass matrix in Figure 5.3. Once the stiffness and damping values are obtained, Equation 2.18 can be solved by substituting the mass, stiffness and damping matrices from Equations 2.19, 2.20, and 2.21. Thus, the response of the structure, including the coupling between structural modes is obtained.

5.4 Response Behavior of Generalized Structure-TMD Systems

5.4.1 Undamped System under Harmonic and Random Excitation

This section investigates the response behavior of undamped torsionally coupled systems equipped with two identical TMDs located at the edges ($y_1 = -B/2$; $y_2 = B/2$) of the structure (see Figure 5.1). The corresponding undamped generalized structure is shown in Figure 5.2(a). Structures with uncoupled frequency ratio values of 0.5, 0.7, 0.8, 0.9, 1.0, 1.1, 1.2 and 1.3 are considered. The structures all have the aspect ratio value of 2. The optimal TMD parameters are determined using the available closed-form optimized parameters derived for an undamped single-degree-of-freedom system. The response behavior is investigated for both harmonic and random excitation.

Figures 5.4 and 5.5 show frequency response function plots of undamped torsionally flexible ($\omega_\theta/\omega_s = 0.5$) and torsionally stiff ($\omega_\theta/\omega_s = 1.3$) structures, respectively, for a mass ratio of 0.01. Each frequency response function plot shows the dynamic magnification factor, R, defined in Chapter 3 (Equation 3.4) of the undamped structure (uncontrolled), the modal response of the structure-TMD system obtained using Equations 5.26 and 5.27 which neglects the coupling between structural modes (uncoupled), and the coupled response of the structure TMD system using Equation 2.18 (coupled). For both the torsionally stiff and torsionally flexible systems, the dynamic magnification factor (DMF) corresponding to both mode 1 and mode 2 have two peaks of equal height. This is the anticipated frequency response behavior corresponding to an undamped structure equipped with an optimized TMD for the case of harmonic excitation. Note that the uncoupled plots do not indicate the presence of an additional structural mode. In contrast, the DMF determined using Equation 2.18 (coupled) captures the response of the untargeted mode and coupling between modes.

Inspection of Figure 5.4 shows that for torsionally flexible systems, where the modes are well separated, reduction only occurs in the mode in which the TMD is tuned to. In other words, if the TMDs are tuned to mode 1, there is a negligible response reduction in mode 2. Similarly, if the TMDs are tuned to mode 2, there is a negligible response reduction in mode 1. Note that the natural frequency of mode 1 is reduced slightly due to addition of mass resulting from the addition of TMDs. For the torsionally stiff structure shown in Figure 5.5, it is found that if the TMDs are tuned to mode 1, a reduction in mode 2 also occurs for this particular TMD configuration. This is consistent with findings in Chapter 3. However, if the TMDs are tuned to

mode 2, this has a negligible influence on mode 1.

For the same undamped primary structure, the TMD configuration was optimized for random excitation and the corresponding mechanical admittance function plots are shown in Figures 5.6 and 5.7. Note that the uncoupled mechanical admittance function plots are different than those for the harmonic excitation case. Here the first peak corresponding to the targeted mode is slightly higher than the second peak. This is the expected frequency response behavior of an undamped structure equipped with TMDs optimized for random excitation as the area bounded by the mechanical admittance function is minimized. The same general trends are found for the torsionally flexible and torsionally stiff structures under random excitation as those observed for the harmonic excitation case.

Figures 5.8 and 5.9 show the frequency response function plots and the mechanical admittance function plots of an undamped strongly torsionally coupled structure subjected to harmonic excitation and random excitation, respectively. The shift in the natural frequency due to the addition of the TMDs, in the untargeted mode is more prevalent as a result of the strong coupling between modes. Additionally, for both harmonic and random excitation, the coupled response obtained using Equation 2.18 shows that the targeted mode for strongly torsionally system is influenced by the untargeted mode.

5.4.2 Response of Damped Systems with Equal Damping Ratio Values under Harmonic Excitation

Figure 5.10 shows the frequency response function plots of the torsionally coupled structures with uncoupled frequency ratios of 0.9 and 1.1 for an aspect ratio B/D

= 2. These additional uncoupled frequency ratios are considered along with those previously studied in Chapters 3 and 4 in order to better understand the response behavior of strongly torsionally coupled systems. In addition, this section also investigates the influence of the aspect ratio parameter. Two additional aspect ratio values of $B/D = 1$ and $B/D = 3$ are investigated. The frequency response function plots for $B/D = 1$ are shown in Figure 5.11 while those corresponding to $B/D = 3$ are shown in Figure 5.12. For all torsionally coupled structures considered in this section, a 2% damping ratio is assumed for both modes.

5.4.2.1 Damped Systems (B/D=2) under Harmonic Excitation

This section compares the response obtained utilizing optimal tuning and damping ratio values derived for a damped single-degree-of-freedom system applied to the generalized structure-TMD system outlined in Section 5.3 to that obtained using the optimization technique employed in Chapter 3. It should be noted that for this particular TMD configuration considered, only one mode can be targeted using the generalized structure-TMD approach whereas the entire system is targeted using the numerical technique employed in Chapter 3. A total of eight uncoupled frequency ratios are investigated.

Figures 5.13 to 5.18 show frequency response function plots for each of the uncoupled frequency ratio values. Two plots are shown for each uncoupled frequency ratio value. The plot on the left corresponds to the TMD system tuned to mode 1 whereas the plot on the right corresponds to the TMD system tuned to mode 2. Both plots also contain the response of the uncontrolled structure (no TMD) and the structure-TMD system (system) optimized using the technique employed in Chapter

3.

For the case of the torsionally flexible structures, the generalized structure-TMD approach developed in this chapter is ineffective in reducing the peak response of both modes simultaneously. However, it can be used to effectively reduce the peak response of a single mode. As the natural frequencies of the structural modes approach one another, for example ($\omega_\theta/\omega_s = 0.9$), the generalized structure-TMD approach is found to reduce both the targeted mode and the untargeted mode peak amplitude value. For the strongly torsionally coupled case ($\omega_\theta/\omega_s = 1.0$), when mode 1 is targeted, the reduction in peak amplitude values are found to be similar to those obtained when the entire system is targeted. Note that this is not the case when mode 2 is targeted. For the torsionally stiff structures, using the generalized structure-TMD approach, and targeting mode 1 is found to be as effective as targeting the entire system. This is a result of mode 2, which is torsionally dominated, having a relatively low peak value. As such, even when the TMD configuration is optimized using the numerical technique in Chapter 3, the TMDs are tuned around mode 1. For the torsionally stiff structures, as the uncoupled frequency ratio transitions from 1.2 to 1.3, the reduction in response in the untargeted mode is reduced.

In general, as observed from the frequency response function plots, using the generalized structure-TMD approach and targeting the dominant mode results in a frequency response closer to that using numerical optimization technique as compared to that of targeting the non-dominant mode.

5.4.2.2 Damped Systems (B/D=1 and 3) under Harmonic Excitation

Figures 5.19 to 5.21 show the frequency response function plot for B/D=1 and $\omega_\theta/\omega_s = 0.9$, 1.0 and 1.1. Similar trends to those observed for $B/D = 2$ are found. For the uncoupled frequency ratio value of 0.9, targeting mode 2 using the generalized structure-TMD approach results in modal peak amplitude values similar to those obtained using the numerical procedure to target the entire system. For $\omega_\theta/\omega_s = 1.1$, similar response behavior is found using the numerical optimization procedure which targets the entire system and generalized structure-TMD approach targeting mode 1 as mode 2 has a low peak amplitude value. Frequency response function plots for $B/D = 3$ are shown in Figures 5.22 to 5.24. The frequency response behavior of the strongly torsionally coupled and torsionally stiff structure-TMD systems is similar for all three aspects ratios. For the torsionally flexible structure, the largest discrepancy between the two optimizations technique occur for $B/D = 3$.

5.4.3 Response of Damped Systems with Equal Modal Peak Amplitude Values under Harmonic Excitation

For the case of equal modal peak amplitude values (see Figures 5.25 to 5.27), the numerical optimization targets both modes (i.e. the TMDs are tuned between mode 1 and 2) for $\omega_\theta/\omega_s = 0.8$ and 1.0, whereas the generalized structure-TMD approach is limited in targeting a specific mode. As a result, the effectiveness of the generalized structure-TMD approach is less than that of the system approach. For the case of $\omega_\theta/\omega_s = 1.2$, targeting mode 1 results in similar performance as that obtained from the optimization technique (i.e. both are targeted to mode 1). Therefore, similar response behavior is anticipated.

5.4.4 Optimal Closed-Form TMDs Parameters - Harmonic

The optimal TMDs parameters and the frequency response function plots for the study conducted under harmonic excitations are shown in Appendix W for mass ratio values of 0.01 and 0.02. For reference purposes, the optimal parameters for torsionally coupled systems (B/D=2) with equal modal damping ratio values are shown in Tables 5.1 and 5.2. It is observed that the TMDs parameters obtained using the generalized structure-TMD approach are different than those obtained from the numerical optimization technique described in Chapter 3 (Tables 3.2, 3.3, 3.5 and 3.6).

5.4.5 Response of Damped Systems with Equal Damping Ratio Values under Random Excitation

The three aspect ratios investigated under harmonic excitation described in Section 5.4.2 are investigated here for the case of random excitation. The mechanical admittance functions for $B/D = 1$ with ω_θ/ω_s ratio values of 0.8, 0.9, 1.0 and 1.1 are shown in Figure 5.28 along with the contribution to the total variance as a function of the forcing frequency ratio. The additional two uncoupled frequency ratios, 0.9 and 1.1, considered in this chapter for $B/D = 2$ are shown in Figure 5.29. The mechanical admittance functions corresponding to the largest aspect ratio $B/D = 3$ are shown in Figure 5.30 for five different uncoupled frequency ratio values. The mechanical admittance functions shown in Figures 5.28 to 5.30 are for torsionally coupled structures having equal modal damping values of 2%. It can be observed that for a given uncoupled frequency ratio an increase in aspect ratio results in increased contribution to the total variance from the torsionally dominant mode relative to

the contribution from the translationally dominant mode. In addition, for $B/D = 2$, mechanical admittance function plots corresponding to uncoupled frequency ratio values of 0.8, 1.0 and 1.2 are shown in Figure 5.31 for torsionally coupled structures having equal modal peak amplitude values.

5.4.5.1 Damped Systems (B/D=2) under Random Excitation

The mechanical admittance function plots for six different uncoupled frequency ratios are shown in Figures 5.32 to 5.37. For the torsionally flexible structures ($\omega_\theta/\omega_s = 0.5$ and 0.7), targeting the dominant mode (i.e. the mode contributing the largest amount to the total variance) results in similar response behavior as that obtained when the system is optimized. Mechanical admittance function plots for $\omega_\theta/\omega_s = 0.9$ and 1.0 indicate that the response behavior resulting from targeting the dominant mode is not the same as that obtained when the TMDs optimized using the numerical approach. For numerical optimization case, the TMDs are tuned between modes 1 and 2. However, when the generalized structure-TMD approach is employed, the TMDs are tuned to either mode 1 or 2. Although, for $\omega_\theta/\omega_s = 1.1$, there is also coupling between the modes, the same behavior is not observed as the contribution to the total variance from mode 1 is significantly larger than mode 2. As a result, both the numerical approach and the generalized structure-TMD approach tune the TMD to mode 1. Similarly, for the torsionally stiff systems targeting the dominant mode using the generalized structure-TMD approach results in similar response behavior as that obtained using the numerical optimization approach. This is due to the fact that the translation dominant mode contributes significantly more to the total variance and the frequency between modes 1 and 2 are well separated. This prevents the

TMDs from being tuned between the modes as this is ineffective in suppressing the total response of well separated modes.

5.4.5.2 Damped Systems ($B/D = 1$ and 3) under Random Excitation

The mechanical admittance functions for torsionally coupled systems with $B/D = 1$ are shown in Figures 5.38 to 5.40 and for torsionally coupled systems with $B/D = 3$, the mechanical admittance functions are shown in Figures 5.41 to 5.43. For the uncoupled frequency ratio value of 0.9, a change in B/D ratio results in a substantial change in mode 1's contribution to the total variance (i.e. for $B/D = 1$ approximately 80% is contributed from mode 2; for $B/D = 3$ mode 1 contributes approximately 45% to the total variance). As a result, the coupling effect has a greater influence on the optimal TMD parameters. For $B/D = 1$, targeting mode 2 (the mode with a greater contribution to the total variance) results in similar response behavior compared to that obtained when the numerical optimization approach is employed. However, for $B/D = 3$, as comparable contribution is found between both modes, the TMDs are tuned between modes 1 and 2 when the numerical optimization approach is utilized. As a result, reduced effectiveness results when either mode 1 or 2 are specifically targeted.

5.4.6 Response of Damped Systems with Equal Modal Peak Amplitude Values under Random Excitation

The final structures investigated are torsionally coupled structures with equal modal peak amplitude values with $\omega_\theta/\omega_s = 0.8$, 1.0 and 1.2. The mechanical admittance functions for the three ω_θ/ω_s ratios are shown in Figures 5.44, 5.45 and 5.46,

respectively.

For $\omega_\theta/\omega_s = 0.8$, it can be observed from Figure 5.31 that mode 2 is the greater contributor to the the total variance. Therefore, targeting mode 2 results in similar response behavior as that obtained from optimizing the TMD to reduce overall torsionally coupled system response. Similarly, for $\omega_\theta/\omega_s = 1.2$, mode 1 contributes approximately 75% of the total variance (see Figure 5.31). As a result, targeting mode 1 results in similar response behavior as that obtained when the numerical technique is utilized. For the case of the strongly torsionally coupled system, where approximately both modes contribute equally to the total variance, it can be seen that similar response behavior cannot be achieved by targeting mode 1 or 2 using the generalized structure-TMD approach as that obtained using the numerical optimization technique. This is due to the TMDs being tuned between the modes when the numerical optimization approach is applied whereas for the generalized structure-TMD approach, the tuning is restricted to either mode 1 or 2.

Tables 5.3 to 5.10 provide a qualitative measure indicating which tuning method results in a greater response reduction. In these tables, the performance achieved of the approach utilizing the generalized structure-TMD approach is compared to that of the numerical optimization approach by introducing the performance index ratio, $R_{mode/system}$. This is defined as the ratio of the reduction factor (R_o) obtained from targeting a specific mode to that obtained from targeting the entire system. For $B/D = 2$, equal modal damping ratio of 2% in each mode, for cases where the uncoupled frequency ratio is well separated, i.e. $\omega_\theta/\omega_s = 0.5$, 0.7, 1.2 and 1.3, the generalized structure-TMD approach is found to perform as well as the procedure outlined in Chapter 4 if the correct mode is targeted. This mode can be

easily identified by determining the mode that contributes the largest percentage to the total variance. As the uncoupled frequency ratio approaches 1.0 (i.e. cases of strongly torsionally coupled system), optimizing the entire system results in better overall performance. This is particular evident for the case of the strongly torsionally coupled system (ω_θ/ω_s =1.0) where both modes contribute equally to the total variance. For example, in Table 5.10, a 7% greater reduction is obtained when the TMDs are tuned to the system using the numerical technique.

5.5 Optimal Closed-Form TMDs Parameters - Random

The optimal TMDs parameters and the mechanical admittance function plots obtained from utilizing the generalized structure-TMD approach for systems under random excitations are shown in Appendix X for mass ratio values of 0.01 and 0.02. For reference purposes, the optimal parameters for torsionally coupled systems (B/D=2) with equal modal damping ratio values are shown in Tables 5.11 and 5.12.

5.6 Conclusions and Summary

This chapter presented a technique to target the response of a particular mode using available closed-form parameters under both harmonic and random excitation. A general 3-dimensional TMD mass matrix was developed in order to permit the

application of SDOF-TMD optimization techniques to torsionally coupled structure-TMD systems. The two identical TMDs configuration were studied and comparisons were drawn between the response obtained from targeting a specific mode using the generalized structure-TMD approach to that obtained from the numerical optimization approach which targets the entire system, as outlined in Chapters 3 and 4 for harmonic and random excitation, respectively. The findings in this chapter are summarized as follow:

- As expected, the 'uncoupled' response did not capture the response of the untargeted mode and the coupling between modes for the entire torsionally coupled structure-TMD systems. This is attributed to the inability in capturing the interaction in the two-degree-of-freedom structure TMD system. However, the 'coupled' response has successfully captured this interaction by employing the equations of motion developed for the entire torsionally coupled structure-TMD system. Thus, the generalized structure-TMD approach can be employed in the design of a torsionally coupled structure-TMD system.

- As the uncoupled frequency ratio approaches one, the response of the untargeted mode is found to be influenced by the targeted mode.

- The generalized structure-TMD approach for the two identical TMDs configuration is limited by the fact that only one mode can be targeted at a time. However, as for the numerical optimization approach, where the entire system is optimized using the procedure outlined in Chapters 3 and 4, the two TMDs can be tuned to a frequency that falls between the natural frequencies of the structure. Thus, when strong coupling exists in the structures, the generalized structure-TMD approach is not as effective as the numerical optimization

technique.

- In general, when the uncoupled frequency ratios are well separated, the response of the untargeted mode is not influenced by the targeted mode. This is due to the fact that negligible energy is transfered between the two modes.

- The efficiency of the generalized structure-TMD approach is dictated by the selection of the targeted mode. The designer should select the mode that dominates the overall response. This can be achieved by inspection of the frequency response function or mechanical admittance function for the case of harmonic and random excitation, respectively. For a structure subjected to harmonic excitation, the mode comprised of a higher peak amplitude should be selected. As for a structure subjected to random excitation, the mode which is the greater contributor to the total variance should be selected.

- For the torsionally coupled systems studied under harmonic excitation, the generalized structure-TMD approach is not effective in reducing the overall structural response except for the torsionally stiff structures. However, it can be used to effectively reduce the response of a single mode

- For the torsionally coupled systems studied under random excitation, targeting the correct mode results in a response comparable to that obtained from targeting the entire system. The greatest difference in the reduction in response between optimizing the entire system and targeting the correct mode was found to be less than 8% for the strongly torsionally coupled system.

5.7 Chapter Tables

	Targeted Mode:1			Targeted Mode: 2		
ω_θ/ω_s	ν	ζ	R	ν	ζ	R
0.5	0.4548	0.0966	32.7320	1.0017	0.0653	30.3175
0.7	0.6498	0.0953	31.6904	1.0073	0.0667	22.1831
0.8	0.7444	0.0925	22.9840	1.0119	0.0696	33.0592
1.0	0.9006	0.0820	16.5151	1.0521	0.0825	26.8213
1.2	0.9599	0.0683	11.9284	1.1890	0.0937	24.0673
1.3	0.9687	0.0666	11.2283	1.2780	0.0950	23.8250

Table 5.1: Optimal Parameters for Torsionally Coupled Systems (B/D=2, Equal Modal Damping Ratio) utilizing Closed-Form Solution under Harmonic Excitation (μ=0.01)

	Targeted Mode:1			Targeted Mode: 2		
ω_θ/ω_s	ν	ζ	R	ν	ζ	R
0.5	0.4436	0.1335	30.8384	0.9904	0.0907	30.1591
0.7	0.6342	0.1319	28.0171	0.9953	0.0928	20.6479
0.8	0.7276	0.1286	19.8963	0.9988	0.0964	26.2709
1.0	0.8845	0.1139	11.9203	1.0331	0.1143	18.6552
1.2	0.9478	0.0949	9.4956	1.1617	0.1300	20.1199
1.3	0.9571	0.0922	8.9543	1.2478	0.1319	21.1466

Table 5.2: Optimal Parameters for Torsionally Coupled Systems (B/D=2, Equal Modal Damping Ratio) utilizing Closed-Form Solution under Harmonic Excitation (μ=0.02)

	R_o ($\mu = 0.01$)			R_o ($\mu = 0.02$)		
ω_θ/ω_s	Mode 1	Mode 2	System	Mode 1	Mode 2	System
0.5	0.8888	0.7945	0.7945	0.8527	0.7478	0.7477
0.7	0.8849	0.7521	0.7520	0.8276	0.6850	0.6840
0.8	0.7649	0.7965	0.7509	0.6984	0.7005	0.6560
0.9	0.7738	0.7059	0.6948	0.6656	0.6074	0.5842
1.0	0.6546	0.7198	0.6311	0.5502	0.5932	0.5216
1.1	0.5826	0.7920	0.5814	0.4944	0.6449	0.4919
1.2	0.7315	0.8859	0.7304	0.6417	0.8048	0.6399
1.3	0.7430	0.9363	0.7429	0.6626	0.8798	0.6623

Table 5.3: R_o Comparison between Targeting a Mode or a System (B/D=2) with Equal Modal Damping Ratio under Random Excitation

	$R_{mode/system}$ ($\mu = 0.01$)		$R_{mode/system}$ ($\mu = 0.02$)	
ω_θ/ω_s	Mode 1	Mode 2	Mode 1	Mode 2
0.5	1.1188	1.0001	1.1404	1.0001
0.7	1.1768	1.0002	1.2100	1.0015
0.8	1.0186	1.0607	1.0647	1.0678
0.9	1.1138	1.0160	1.1392	1.0398
1.0	1.0372	1.1405	1.0548	1.1373
1.1	1.0020	1.3622	1.0050	1.3110
1.2	1.0014	1.2128	1.0027	1.2576
1.3	1.0002	1.2604	1.0004	1.3284

Table 5.4: Performance Index Ratio Comparison between Targeting a Mode or a System (B/D=2) with Equal Modal Damping Ratio under Random Excitation

	R_o ($\mu = 0.01$)			R_o ($\mu = 0.02$)		
ω_θ/ω_s	Mode 1	Mode 2	System	Mode 1	Mode 2	System
0.8	0.7471	0.7943	0.7336	0.6799	0.6949	0.6402
0.9	0.7542	0.7156	0.6956	0.6487	0.6116	0.5782
1.0	0.6459	0.7161	0.6209	0.5412	0.5865	0.5110
1.1	0.6035	0.7933	0.6014	0.5115	0.6493	0.5076
1.2	0.7231	0.8803	0.7219	0.6312	0.7954	0.6294

Table 5.5: R_o Comparison between Targeting a Mode or a System (B/D=3) with Equal Modal Damping Ratio under Random Excitation

	$R_{mode/system}$ ($\mu = 0.01$)		$R_{mode/system}$ ($\mu = 0.02$)	
ω_θ/ω_s	Mode 1	Mode 2	Mode 1	Mode 2
0.8	1.0184	1.0827	1.0620	1.0854
0.9	1.0842	1.0288	1.1220	1.0579
1.0	1.0403	1.1534	1.0592	1.1479
1.1	1.0034	1.3190	1.0077	1.2792
1.2	1.0016	1.2195	1.0030	1.2638

Table 5.6: Performance Index Ratio Comparison between Targeting a Mode or a System (B/D=3) with Equal Modal Damping Ratio under Random Excitation

	R_o ($\mu = 0.01$)			R_o ($\mu = 0.02$)		
ω_θ/ω_s	Mode 1	Mode 2	System	Mode 1	Mode 2	System
0.8	0.8295	0.8018	0.7973	0.7657	0.7190	0.7029
0.9	0.8143	0.6779	0.6756	0.7009	0.5921	0.5855
1.0	0.6865	0.7358	0.6679	0.5854	0.6214	0.5649
1.1	0.5226	0.7723	0.5224	0.4447	0.6222	0.4442

Table 5.7: R_o Comparison between Targeting a Mode or a System (B/D=1) with Equal Modal Damping Ratio under Random Excitation

	$R_{mode/system}$ ($\mu = 0.01$)		$R_{mode/system}$ ($\mu = 0.02$)	
ω_θ/ω_s	Mode 1	Mode 2	Mode 1	Mode 2
0.8	1.0405	1.0057	1.0895	1.0230
0.9	1.2052	1.0034	1.1971	1.0114
1.0	1.0279	1.1016	1.0362	1.1000
1.1	1.0004	1.4784	1.0011	1.4006

Table 5.8: Performance Index Ratio Comparison between Targeting a Mode or a System (B/D=1) with Equal Modal Damping Ratio under Random Excitation

	R_o ($\mu = 0.01$)			R_o ($\mu = 0.02$)		
ω_θ/ω_s	Mode 1	Mode 2	System	Mode 1	Mode 2	System
0.8	0.8259	0.7804	0.7774	0.7552	0.6958	0.6824
1.0	0.6788	0.6957	0.6353	0.5631	0.5819	0.5219
1.2	0.7747	0.8451	0.7677	0.6791	0.7791	0.6724

Table 5.9: R_o Comparison between Targeting a Mode or a System (B/D=2) with Equal Modal Peak Amplitude under Random Excitation

ω_θ/ω_s	$R_{mode/system}$ ($\mu = 0.01$) Mode 1	Mode 2	$R_{mode/system}$ ($\mu = 0.02$) Mode 1	Mode 2
0.8	1.0624	<u>1.0039</u>	1.1068	<u>1.0196</u>
1.0	<u>1.0685</u>	1.0950	<u>1.0790</u>	1.1150
1.2	<u>1.0092</u>	1.1009	<u>1.0099</u>	1.1586

Table 5.10: Performance Index Ratio Comparison between Targeting a Mode or a System (B/D=2) with Equal Modal Peak Amplitude under Random Excitation

	Targeted Mode:1			Targeted Mode: 2		
ω_θ/ω_s	ν	ζ	$\sigma_{x_c}(k_s/\sqrt{S_o})$	ν	ζ	$\sigma_{x_c}(k_s/\sqrt{S_o})$
0.5	0.4593	0.0759	9.9919	1.0064	0.0511	8.9320
0.7	0.6559	0.0752	10.6875	1.0121	0.0523	9.0837
0.8	0.7500	0.0741	8.2074	1.0181	0.0538	8.5467
1.0	0.9067	0.0648	7.1402	1.0597	0.0648	7.8515
1.2	0.9657	0.0529	6.5227	1.1986	0.0747	7.8996
1.3	0.9742	0.0513	6.0838	1.2887	0.0758	7.6669

Table 5.11: Optimal Parameters for Torsionally Coupled Systems (B/D=2, Equal Modal Damping Ratio) utilizing Closed-Form Solution under Random Excitation (μ=0.01)

	Targeted Mode:1			Targeted Mode: 2		
ω_θ/ω_s	ν	ζ	$\sigma_{x_c}(k_s/\sqrt{S_o})$	ν	ζ	$\sigma_{x_c}(k_s/\sqrt{S_o})$
0.5	0.4513	0.1065	9.5860	0.9983	0.0720	8.4065
0.7	0.6447	0.1054	9.9954	1.0036	0.0736	8.2730
0.8	0.7377	0.1039	7.4943	1.0088	0.0758	7.5164
1.0	0.8951	0.0910	6.0014	1.0461	0.0910	6.4710
1.2	0.9572	0.0745	5.7219	1.1786	0.1048	7.1764
1.3	0.9662	0.0723	5.4251	1.2666	0.1063	7.2036

Table 5.12: Optimal Parameters for Torsionally Coupled Systems (B/D=2, Equal Modal Damping Ratio) utilizing Closed-Form Solution under Random Excitation (μ=0.02)

5.8 Chapter Figures

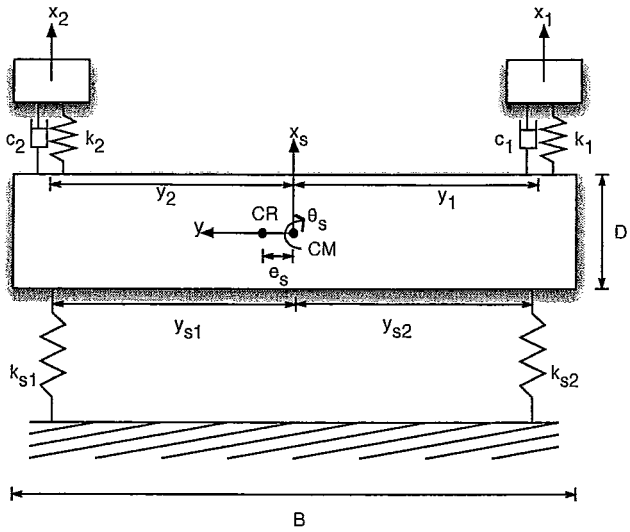

Figure 5.1: Schematic Sketch of Undamped Structure Equipped with Two TMDs

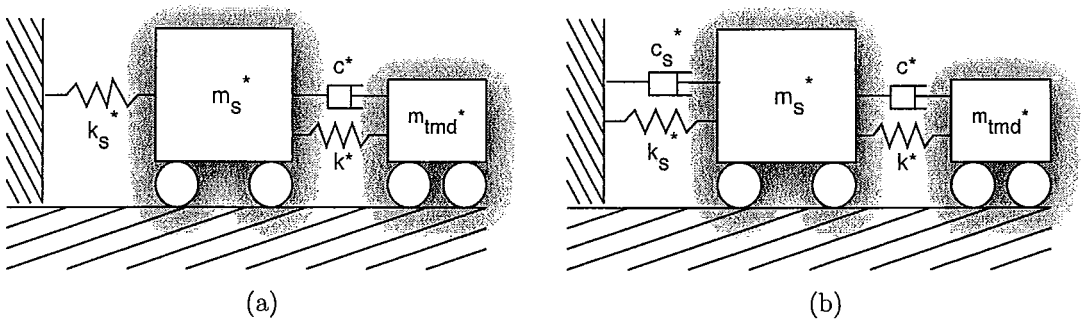

Figure 5.2: Generalized System: (a) Undamped Structure and (b) Damped Structure

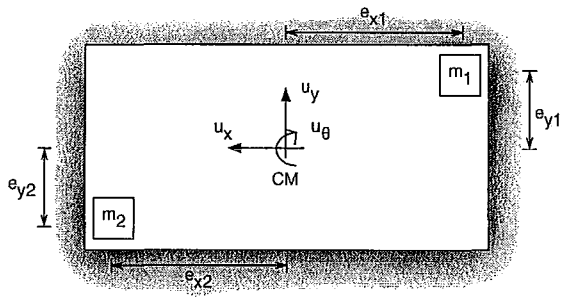

(a)

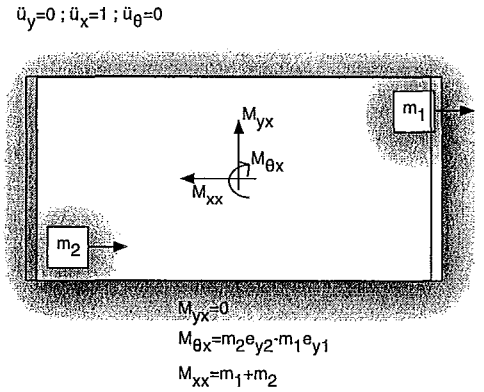

(b)

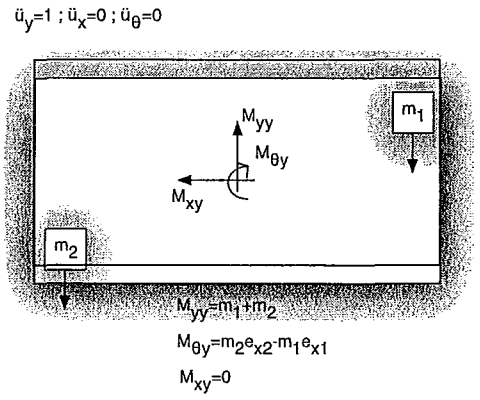

(c)

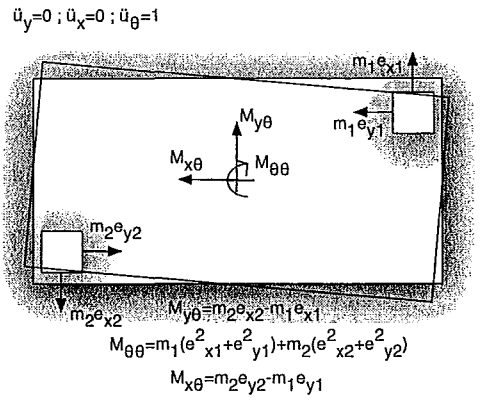

(d)

Figure 5.3: Development of TMD Mass Matrix (a), (b) (c) and (d)

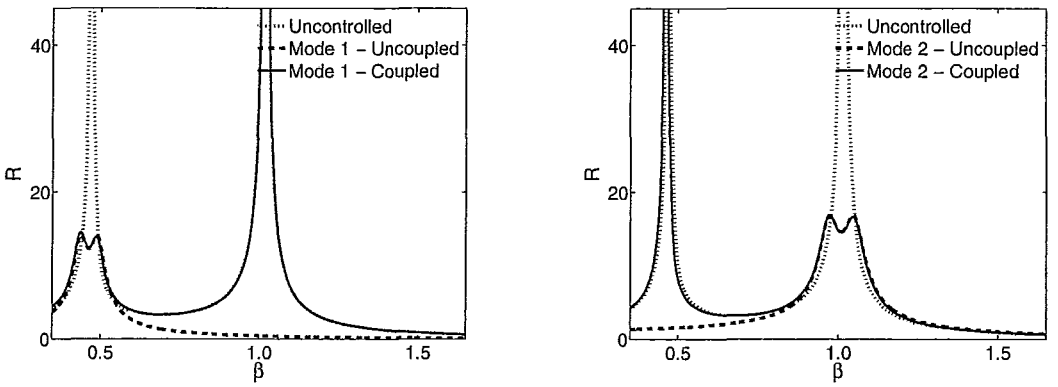

Figure 5.4: Frequency Response Functions of Undamped System subjected to Harmonic Excitation: $\omega_\theta/\omega_s = 0.5$, B/D=2, $\mu = 0.01$

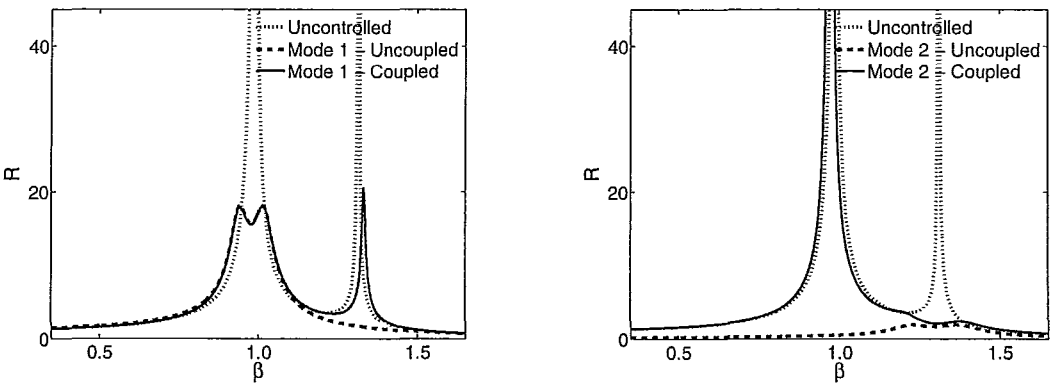

Figure 5.5: Frequency Response Functions of Undamped System subjected to Harmonic Excitation: $\omega_\theta/\omega_s = 1.3$, B/D=2, $\mu = 0.01$

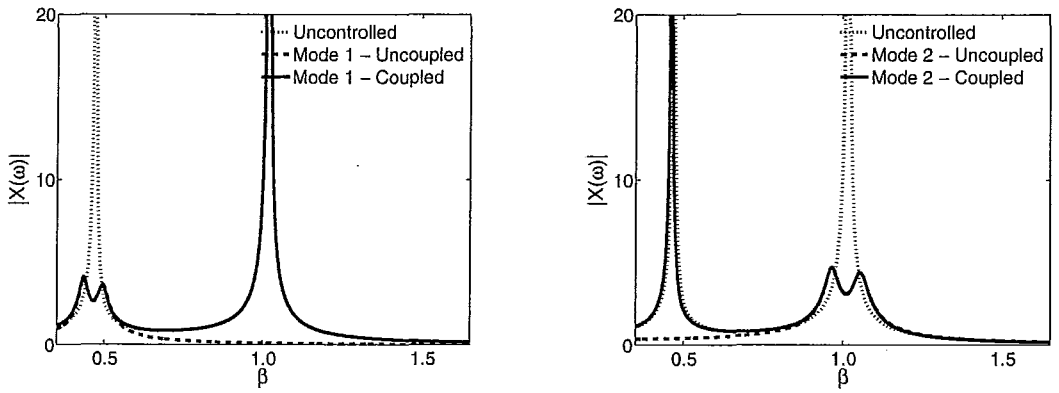

Figure 5.6: Mechanical Admittance Functions of Undamped Structure subjected to Random Excitation: $\omega_\theta/\omega_s = 0.5$, B/D=2, $\mu = 0.01$

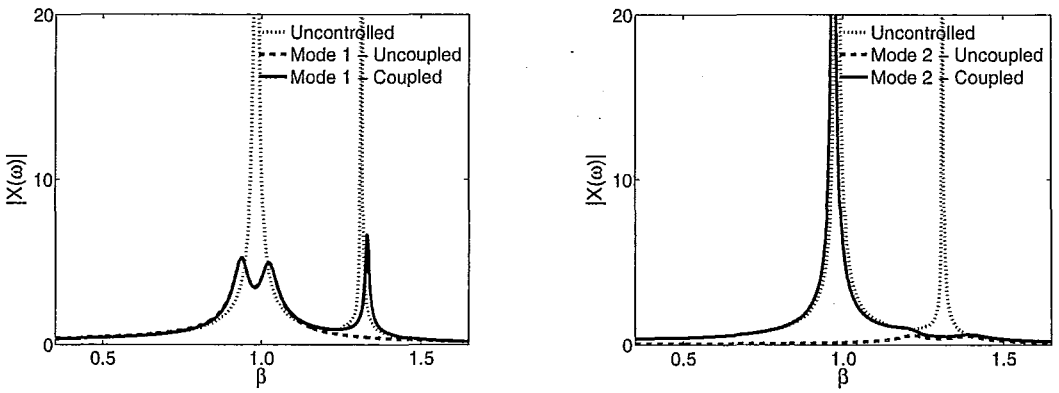

Figure 5.7: Mechanical Admittance Functions of Undamped Structure subjected to Random Excitation: $\omega_\theta/\omega_s = 1.3$, B/D=2, $\mu = 0.01$

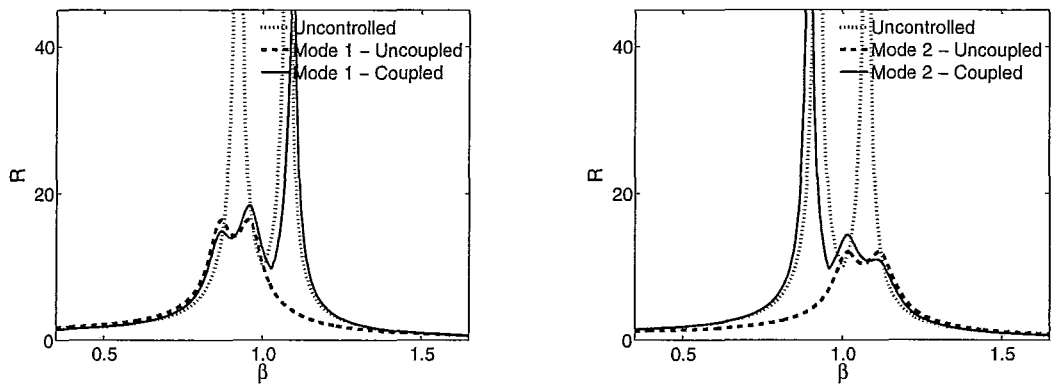

Figure 5.8: Frequency Response Functions of Undamped Structure subjected to Harmonic Excitation : $\omega_\theta/\omega_s = 1.0$, B/D=2, $\mu = 0.01$

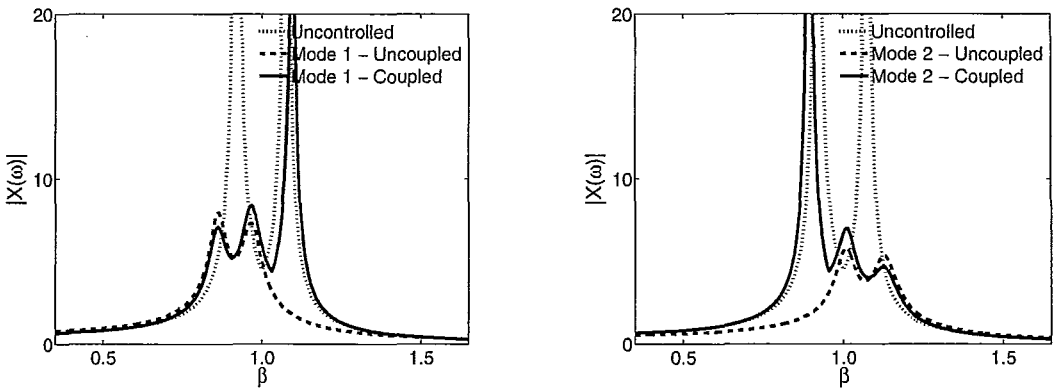

Figure 5.9: Mechanical Admittance Functions of Undamped Structure subjected to Random Excitation : $\omega_\theta/\omega_s = 1.0$, B/D=2, $\mu = 0.01$

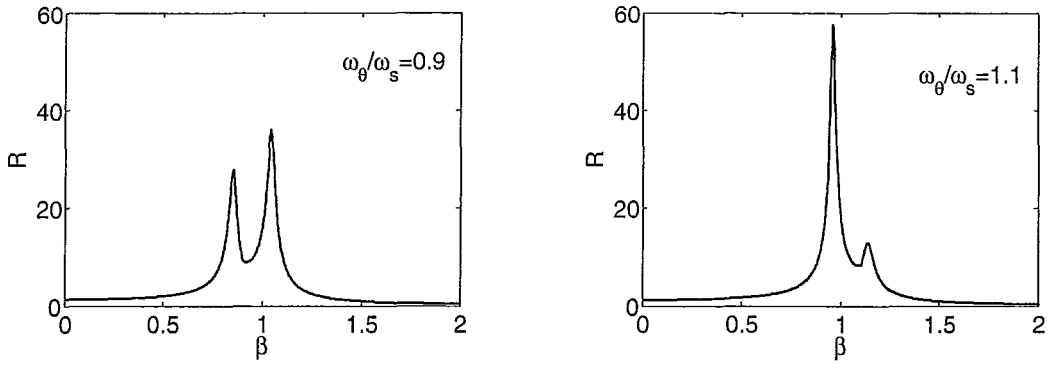

Figure 5.10: Frequency Response Function of Structures ($B/D = 2$) with Equal Damping Ratio Values without DVA subjected to Harmonic Excitation

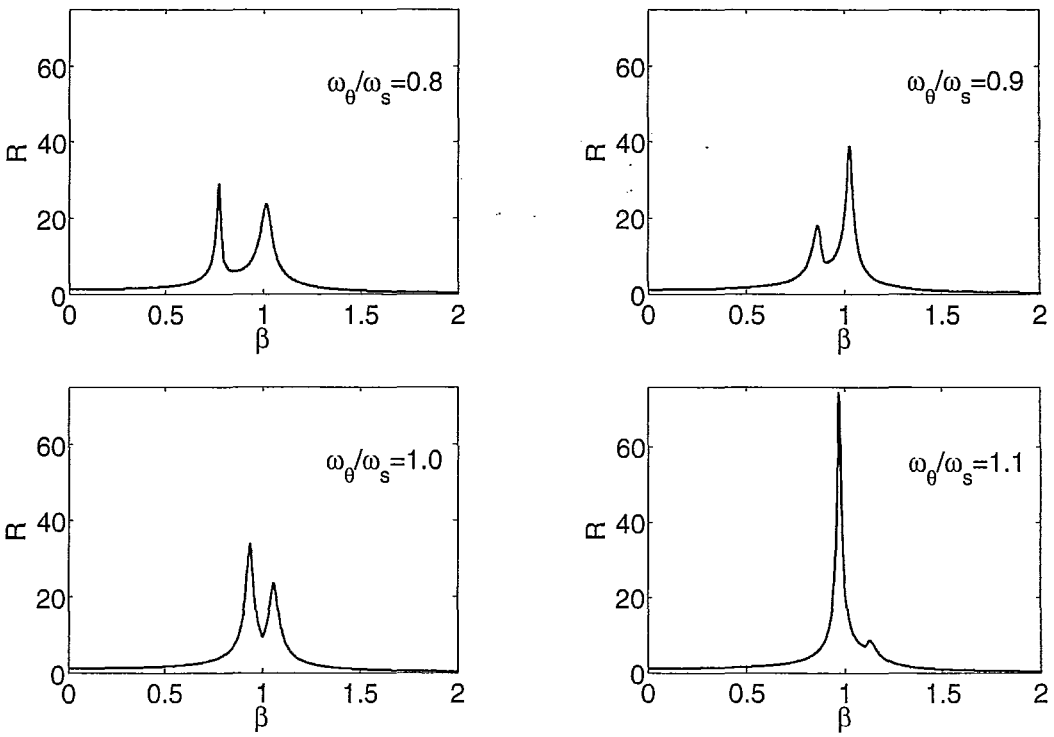

Figure 5.11: Frequency Response Function of Structures ($B/D = 1$) with Equal Damping Ratio Values without DVA subjected to Harmonic Excitation

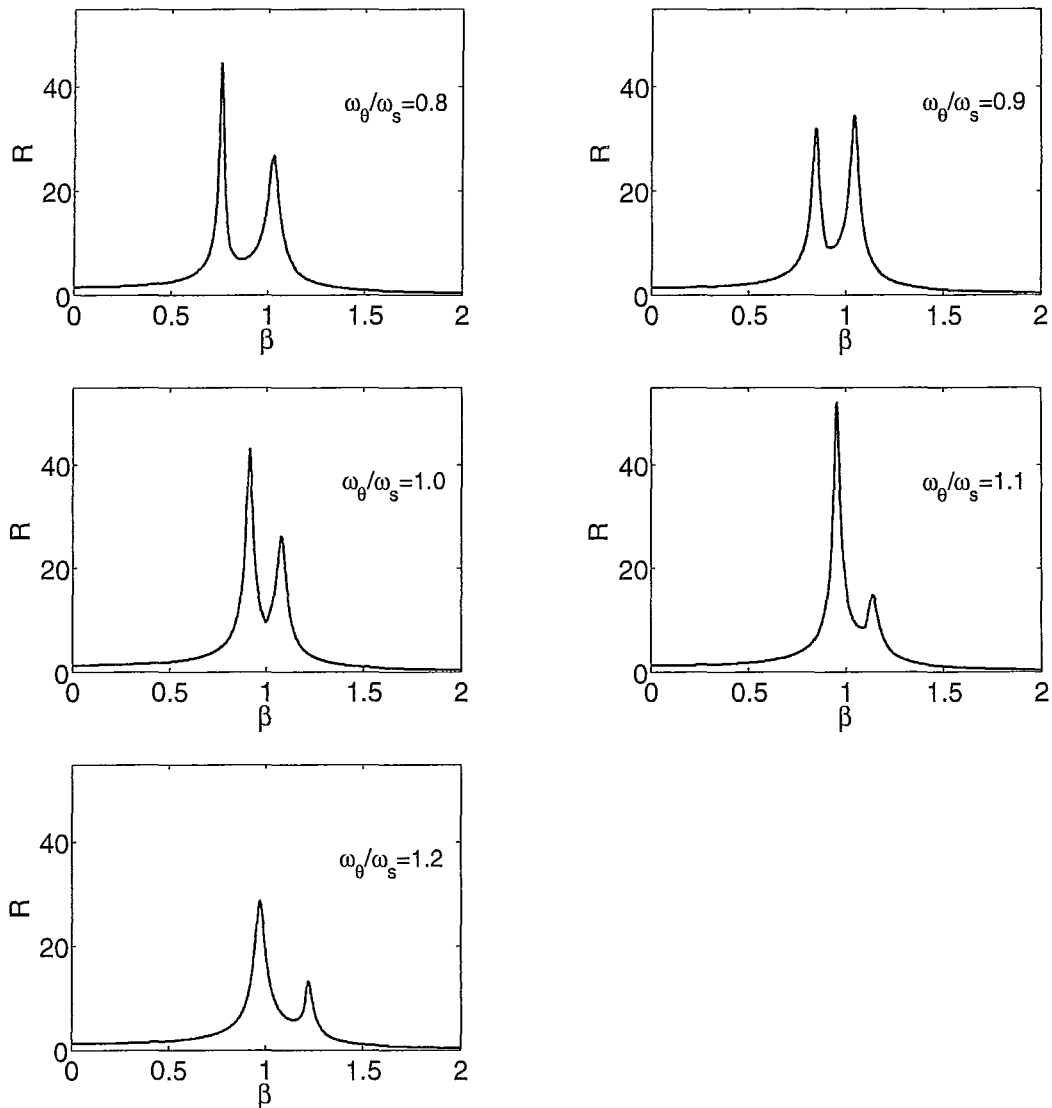

Figure 5.12: Frequency Response Function of Structures ($B/D = 3$) with Equal Damping Ratio Values without DVA subjected to Harmonic Excitation

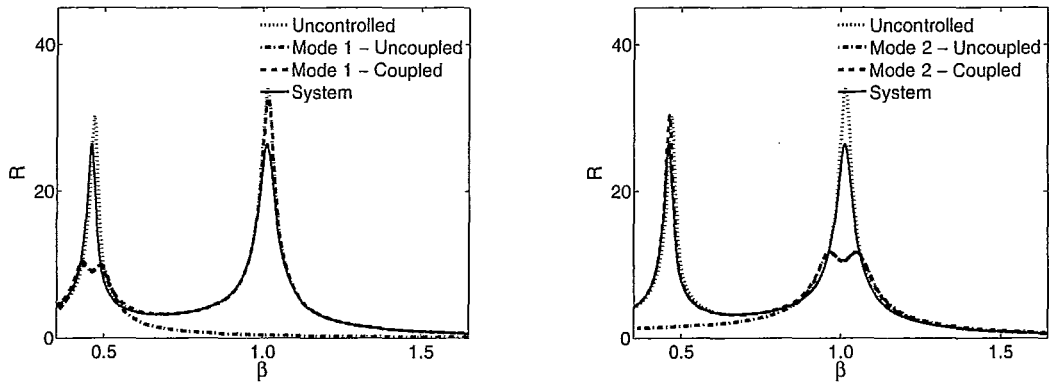

Figure 5.13: Frequency Response Functions Comparison between Targeting a Mode and System (Equal Modal Damping Ratio) subjected to Harmonic Excitation : $\omega_\theta/\omega_s = 0.5$, B/D=2, $\mu = 0.01$

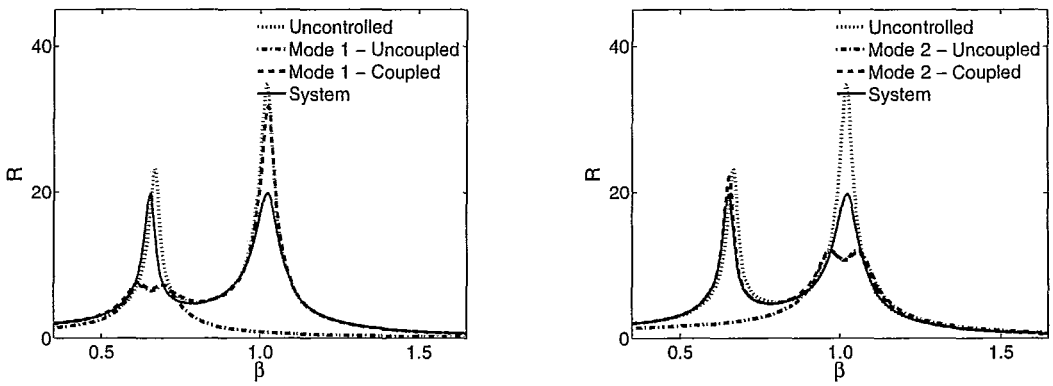

Figure 5.14: Frequency Response Functions Comparison between Targeting a Mode and System (Equal Modal Damping Ratio) subjected to Harmonic Excitation : $\omega_\theta/\omega_s = 0.7$, B/D=2, $\mu = 0.01$

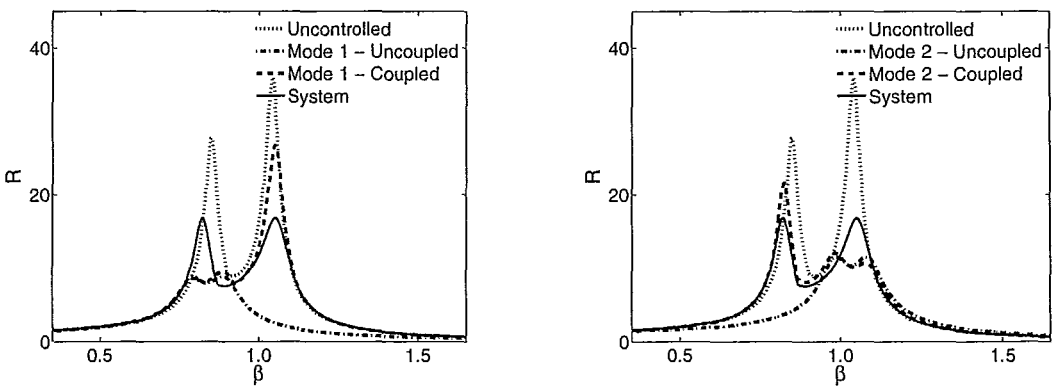

Figure 5.15: Frequency Response Functions Comparison between Targeting a Mode and System (Equal Modal Damping Ratio) subjected to Harmonic Excitation : $\omega_\theta/\omega_s = 0.9$, B/D=2, $\mu = 0.01$

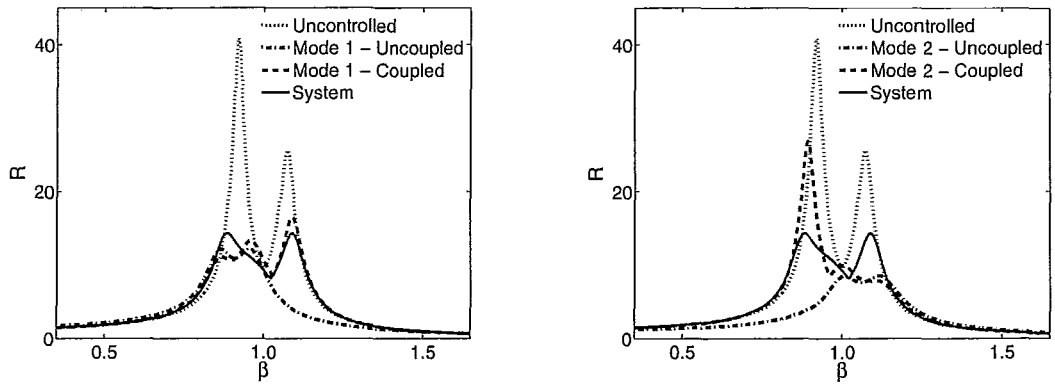

Figure 5.16: Frequency Response Functions Comparison between Targeting a Mode and System (Equal Modal Damping Ratio) subjected to Harmonic Excitation : ω_θ/ω_s = 1.0, B/D=2, $\mu = 0.01$

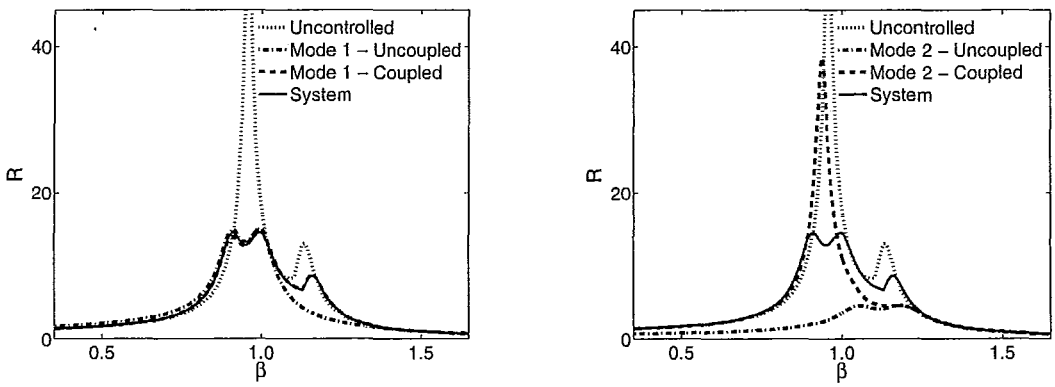

Figure 5.17: Frequency Response Functions Comparison between Targeting a Mode and System (Equal Modal Damping Ratio) subjected to Harmonic Excitation : ω_θ/ω_s = 1.1, B/D=2, $\mu = 0.01$

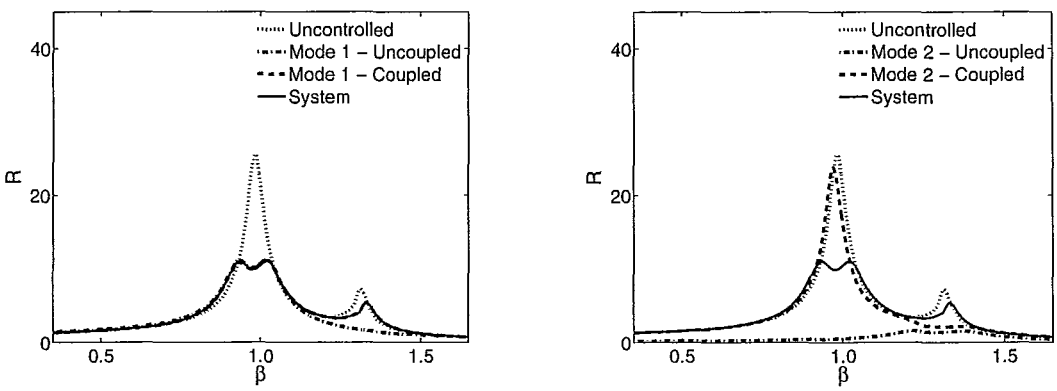

Figure 5.18: Frequency Response Functions Comparison between Targeting a Mode and System (Equal Modal Damping Ratio) subjected to Harmonic Excitation : ω_θ/ω_s = 1.3, B/D=2, $\mu = 0.01$

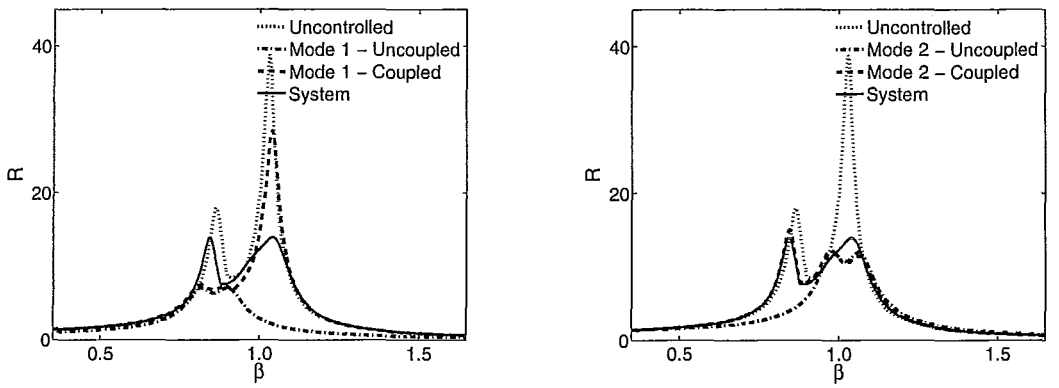

Figure 5.19: Frequency Response Functions Comparison between Targeting a Mode and System (Equal Modal Damping Ratio) subjected to Harmonic Excitation : $\omega_\theta/\omega_s = 0.9$, B/D=1, $\mu = 0.01$

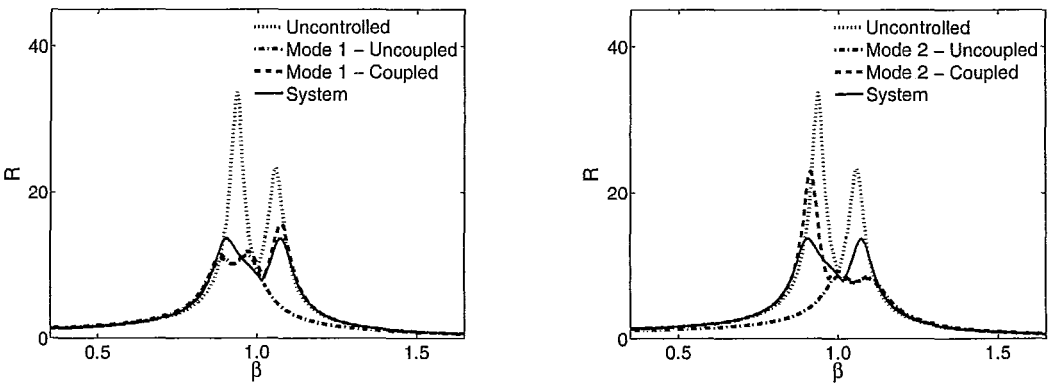

Figure 5.20: Frequency Response Functions Comparison between Targeting a Mode and System (Equal Modal Damping Ratio) subjected to Harmonic Excitation : $\omega_\theta/\omega_s = 1.0$, B/D=1, $\mu = 0.01$

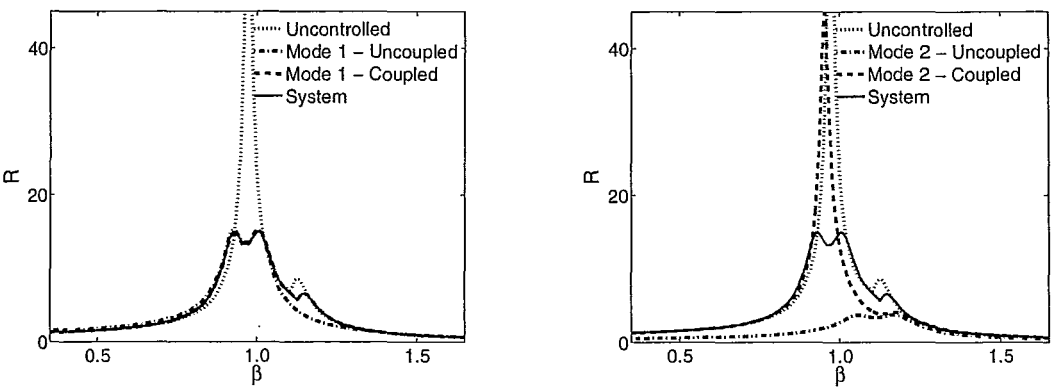

Figure 5.21: Frequency Response Functions Comparison between Targeting a Mode and System (Equal Modal Damping Ratio) subjected to Harmonic Excitation : $\omega_\theta/\omega_s = 1.1$, B/D=1, $\mu = 0.01$

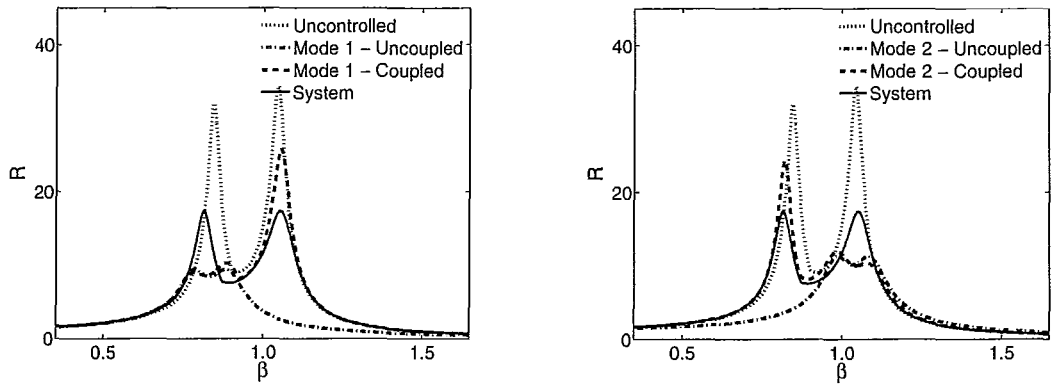

Figure 5.22: Frequency Response Functions Comparison between Targeting a Mode and System (Equal Modal Damping Ratio) subjected to Harmonic Excitation : $\omega_\theta/\omega_s = 0.9$, B/D=3, $\mu = 0.01$

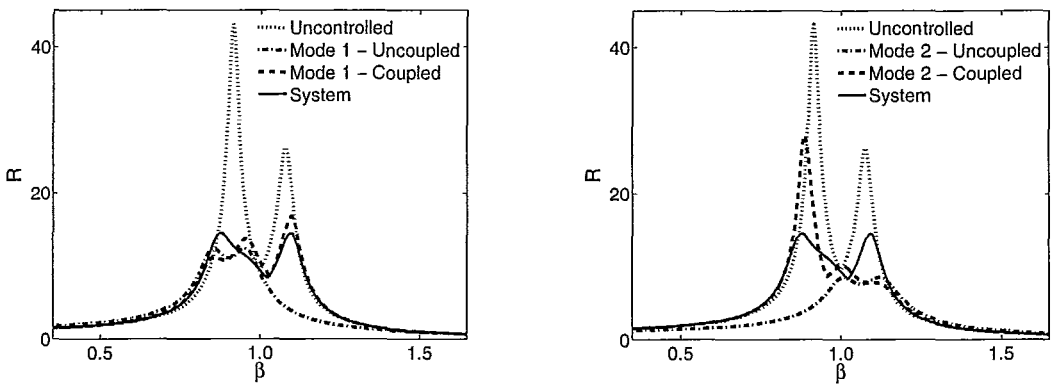

Figure 5.23: Frequency Response Functions Comparison between Targeting a Mode and System (Equal Modal Damping Ratio) subjected to Harmonic Excitation : $\omega_\theta/\omega_s = 1.0$, B/D=3, $\mu = 0.01$

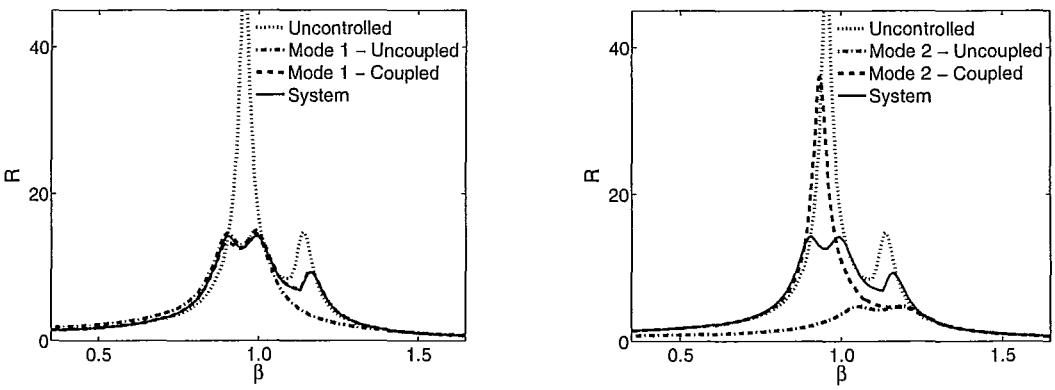

Figure 5.24: Frequency Response Functions Comparison between Targeting a Mode and System (Equal Modal Damping Ratio) subjected to Harmonic Excitation : $\omega_\theta/\omega_s = 1.1$, B/D=3, $\mu = 0.01$

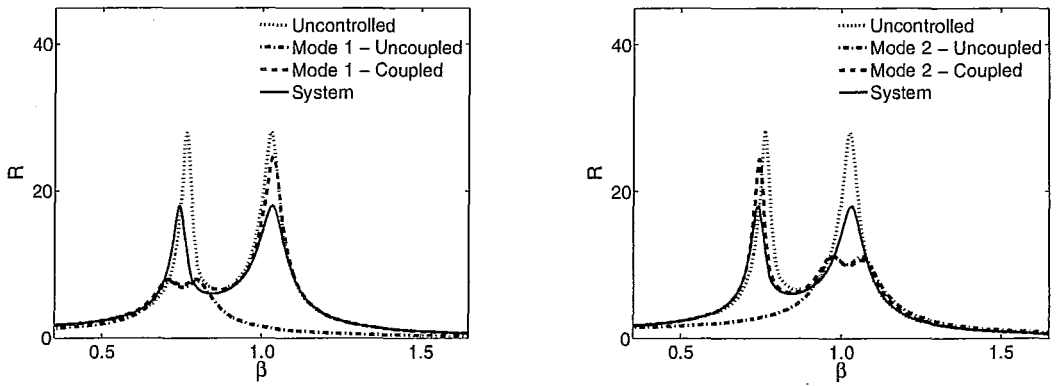

Figure 5.25: Frequency Response Functions Comparison between Targeting a Mode and System (Equal Modal Peak Amplitude) subjected to Harmonic Excitation : $\omega_\theta/\omega_s = 0.8$, B/D=2, $\mu = 0.01$

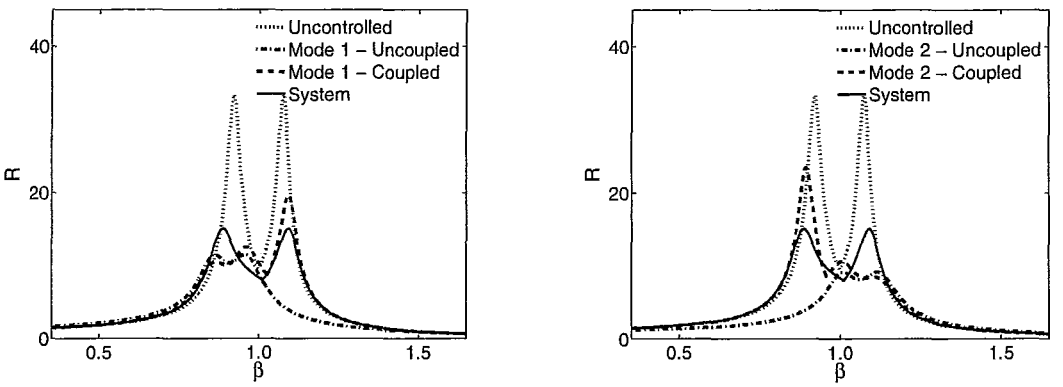

Figure 5.26: Frequency Response Functions Comparison between Targeting a Mode and System (Equal Modal Peak Amplitude) subjected to Harmonic Excitation : $\omega_\theta/\omega_s = 1.0$, B/D=2, $\mu = 0.01$

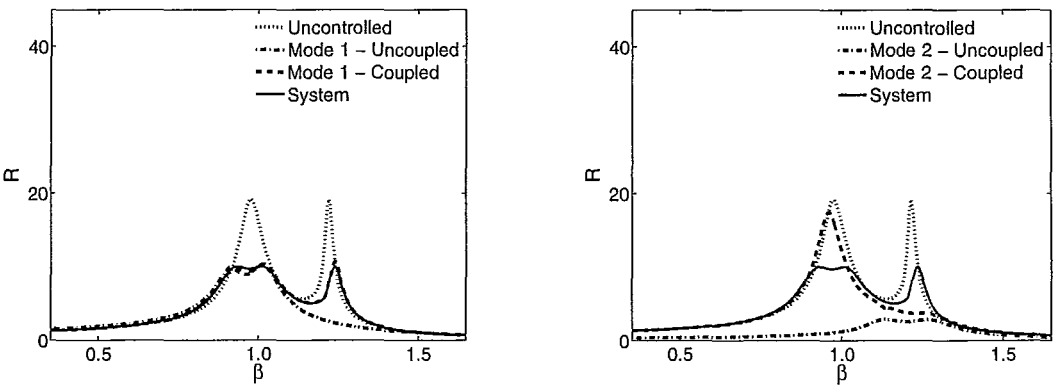

Figure 5.27: Frequency Response Functions Comparison between Targeting a Mode and System (Equal Modal Peak Amplitude) subjected to Harmonic Excitation : $\omega_\theta/\omega_s = 1.2$, B/D=2, $\mu = 0.01$

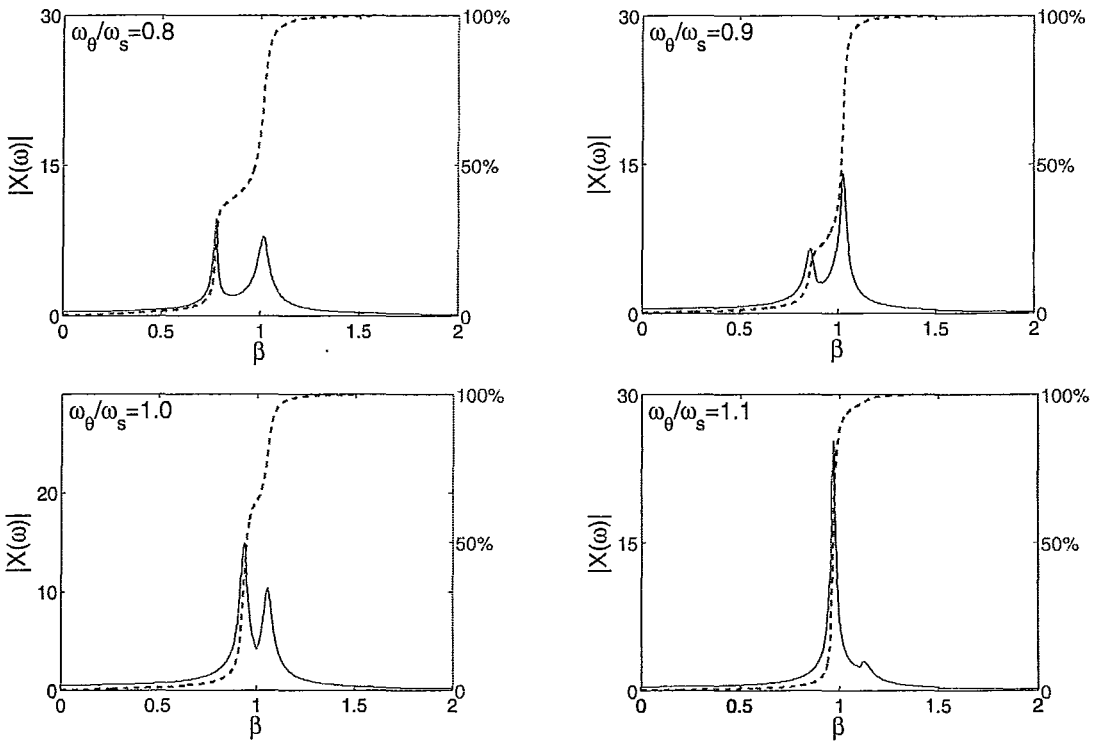

Figure 5.28: Mechanical Admittance Function of Structures ($B/D = 1$) with Equal Damping Ratio Values without DVA subjected to Random Excitation

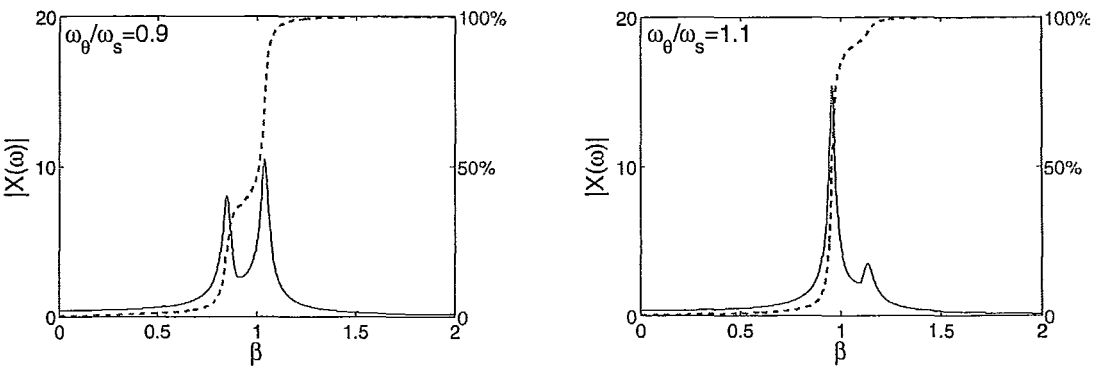

Figure 5.29: Mechanical Admittance Function of Structures ($B/D = 2$) with Equal Damping Ratio Values without DVA subjected to Random Excitation

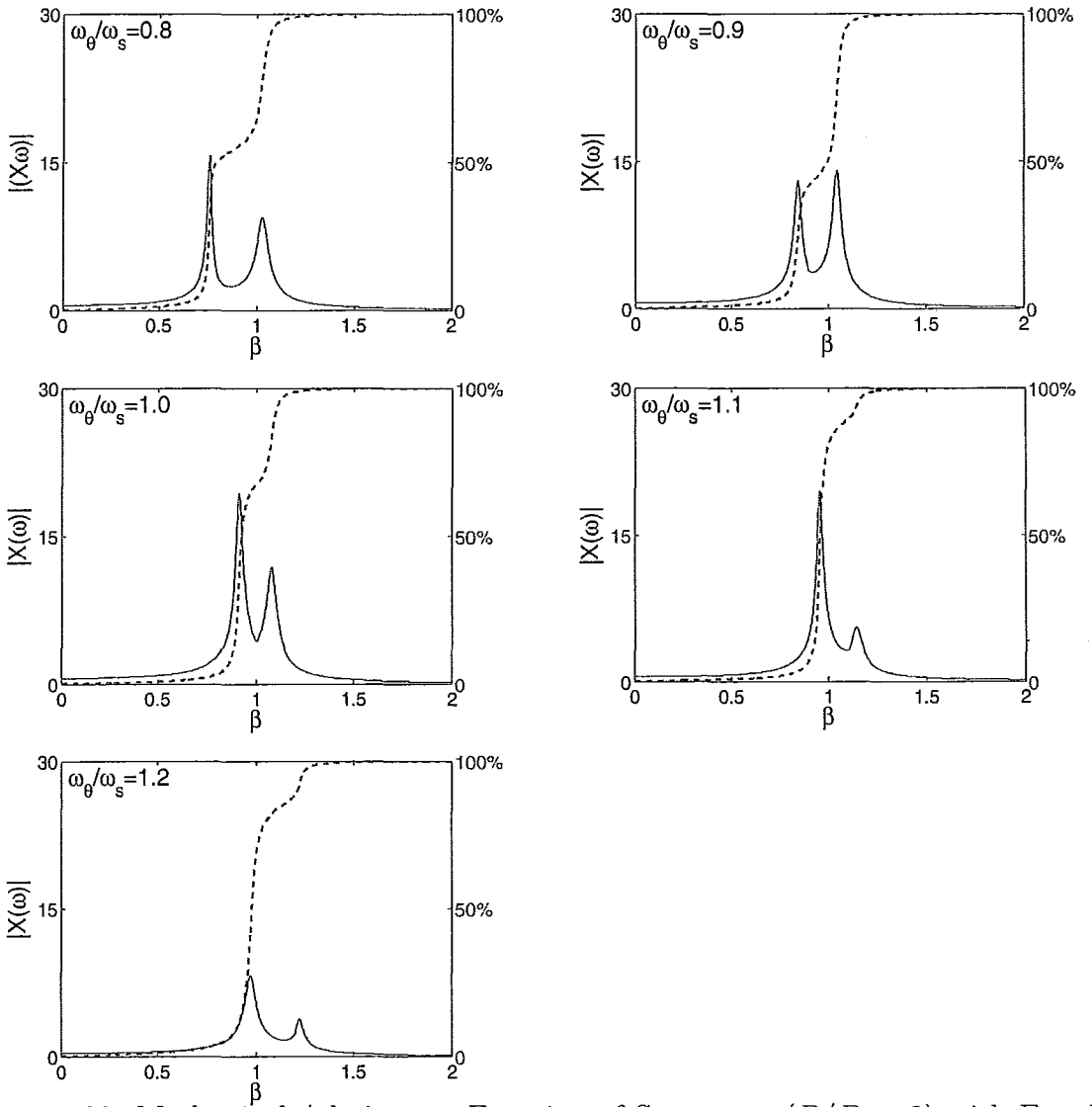

Figure 5.30: Mechanical Admittance Function of Structures ($B/D = 3$) with Equal Damping Ratio Values without DVA subjected to Random Excitation

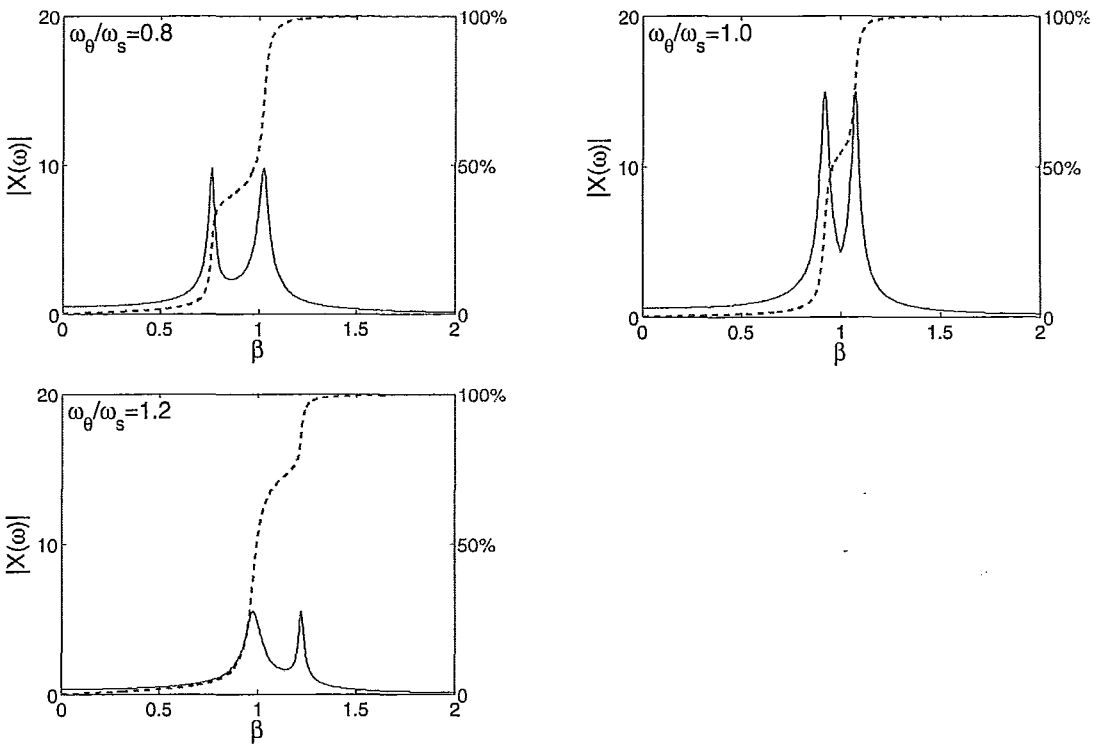

Figure 5.31: Mechanical Admittance Function of Structures ($B/D = 2$) with Equal Modal Peak Values without DVA subjected to Random Excitation

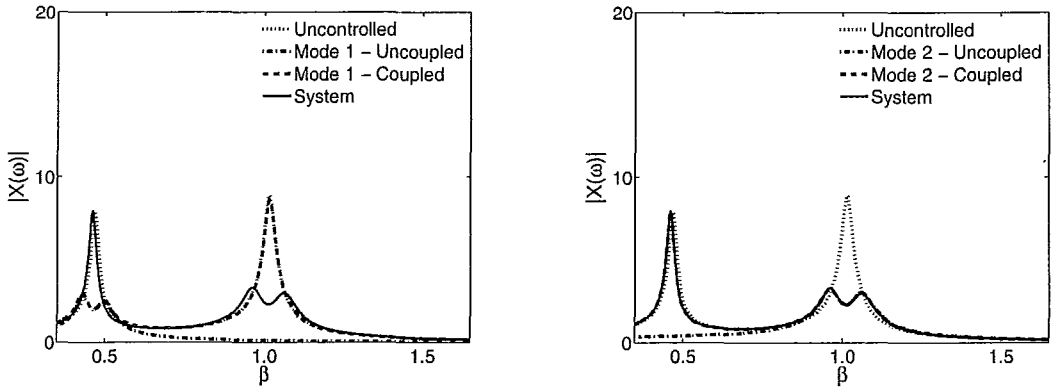

Figure 5.32: Mechanical Admittance Functions Comparison between Targeting a Mode and System (Equal Modal Damping Ratio) subjected to Random Excitation : $\omega_\theta/\omega_s = 0.5$, B/D=2, $\mu = 0.01$

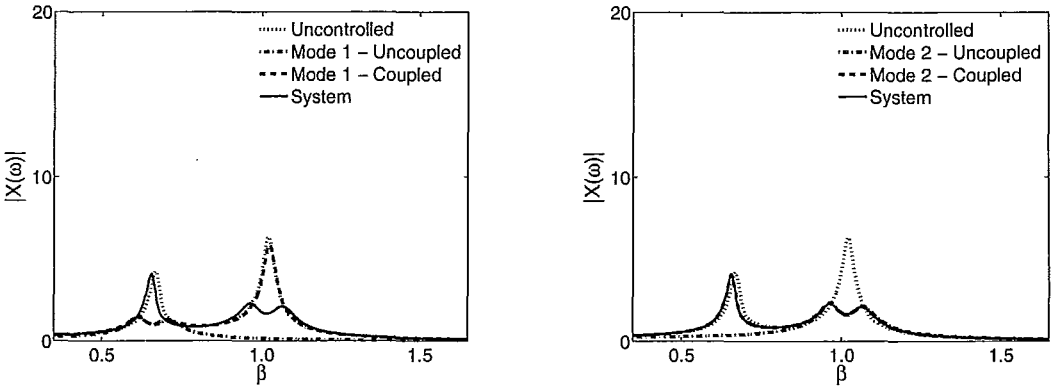

Figure 5.33: Mechanical Admittance Functions Comparison between Targeting a Mode and System (Equal Modal Damping Ratio) subjected to Random Excitation : $\omega_\theta/\omega_s = 0.7$, B/D=2, $\mu = 0.01$

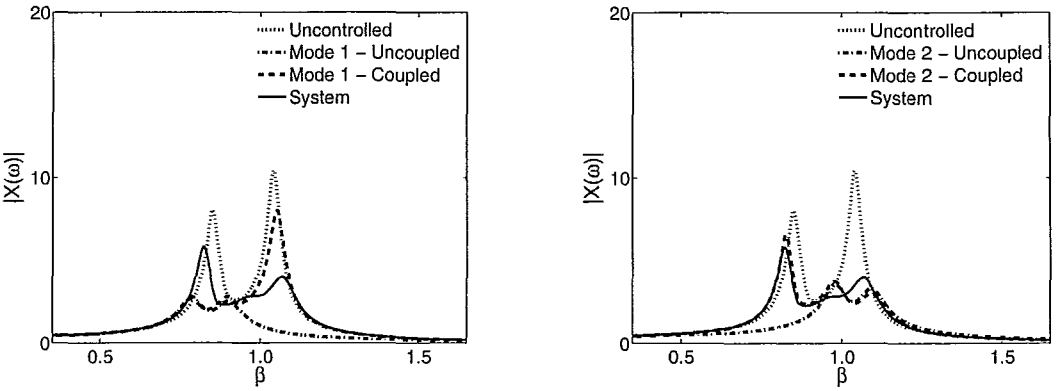

Figure 5.34: Mechanical Admittance Functions Comparison between Targeting a Mode and System (Equal Modal Damping Ratio) subjected to Random Excitation : $\omega_\theta/\omega_s = 0.9$, B/D=2, $\mu = 0.01$

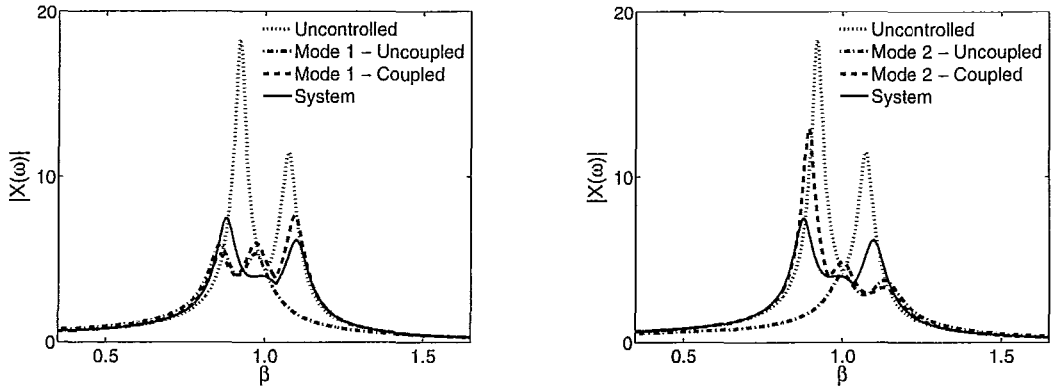

Figure 5.35: Mechanical Admittance Functions Comparison between Targeting a Mode and System (Equal Modal Damping Ratio) subjected to Random Excitation : $\omega_\theta/\omega_s = 1.0$, B/D=2, $\mu = 0.01$

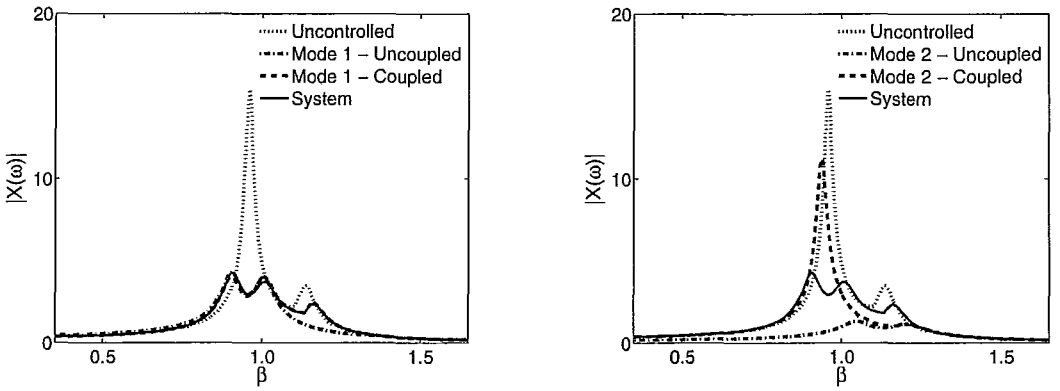

Figure 5.36: Mechanical Admittance Functions Comparison between Targeting a Mode and System (Equal Modal Damping Ratio) subjected to Random Excitation : ω_θ/ω_s =1.1, B/D=2, $\mu = 0.01$

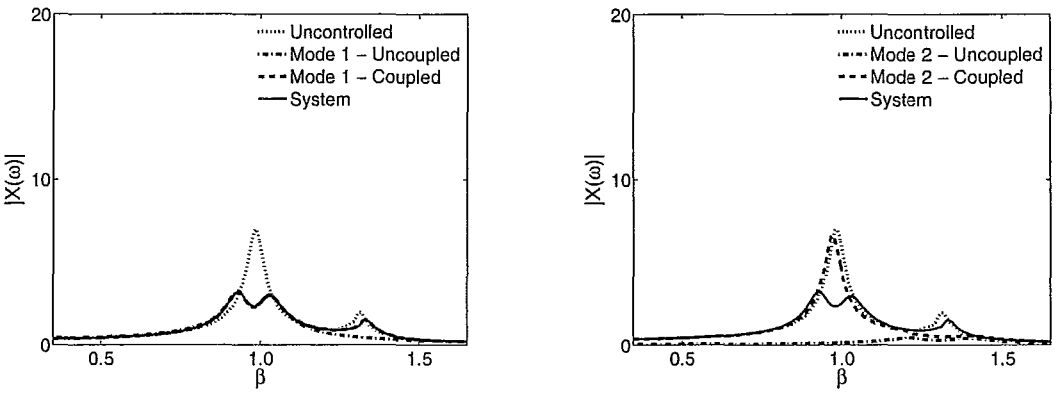

Figure 5.37: Mechanical Admittance Functions Comparison between Targeting a Mode and System (Equal Modal Damping Ratio) subjected to Random Excitation : $\omega_\theta/\omega_s = 1.3$, B/D=2, $\mu = 0.01$

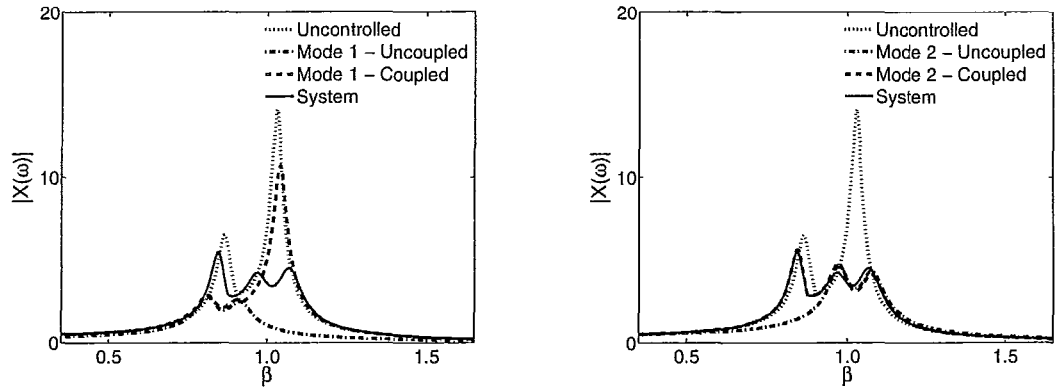

Figure 5.38: Mechanical Admittance Functions Comparison between Targeting a Mode and System (Equal Modal Damping Ratio) subjected to Random Excitation : ω_θ/ω_s =0.9, B/D=1, $\mu = 0.01$

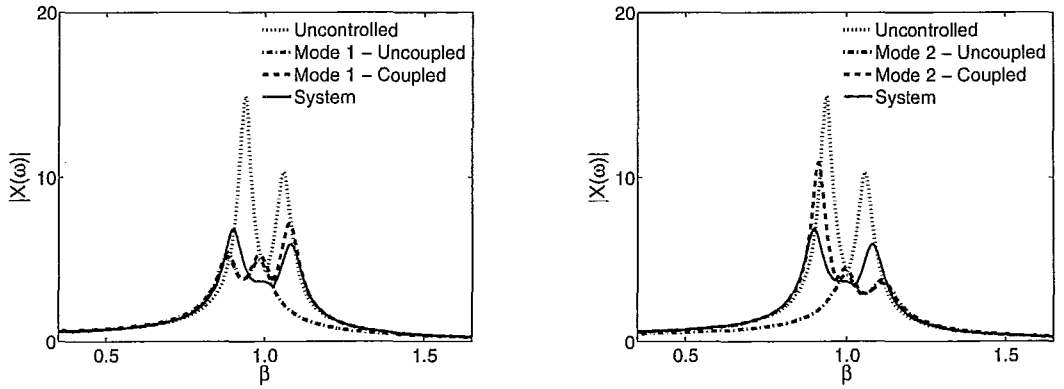

Figure 5.39: Mechanical Admittance Functions Comparison between Targeting a Mode and System (Equal Modal Damping Ratio) subjected to Random Excitation : $\omega_\theta/\omega_s = 1.0$, B/D=1, $\mu = 0.01$

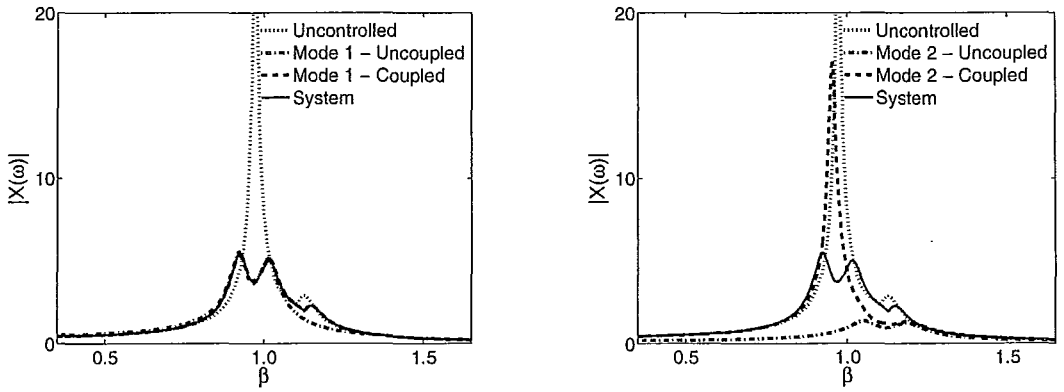

Figure 5.40: Mechanical Admittance Functions Comparison between Targeting a Mode and System (Equal Modal Damping Ratio) subjected to Random Excitation : ω_θ/ω_s =1.1, B/D=1, $\mu = 0.01$

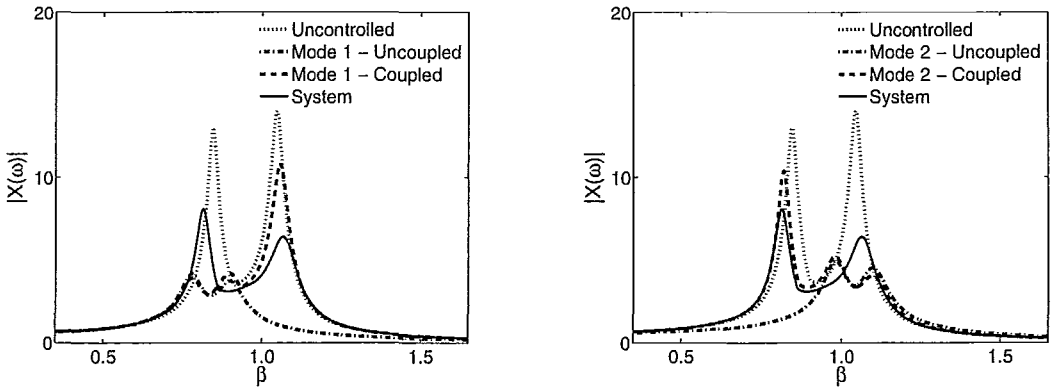

Figure 5.41: Mechanical Admittance Functions Comparison between Targeting a Mode and System (Equal Modal Damping Ratio) subjected to Random Excitation : ω_θ/ω_s =0.9, B/D=3, $\mu = 0.01$

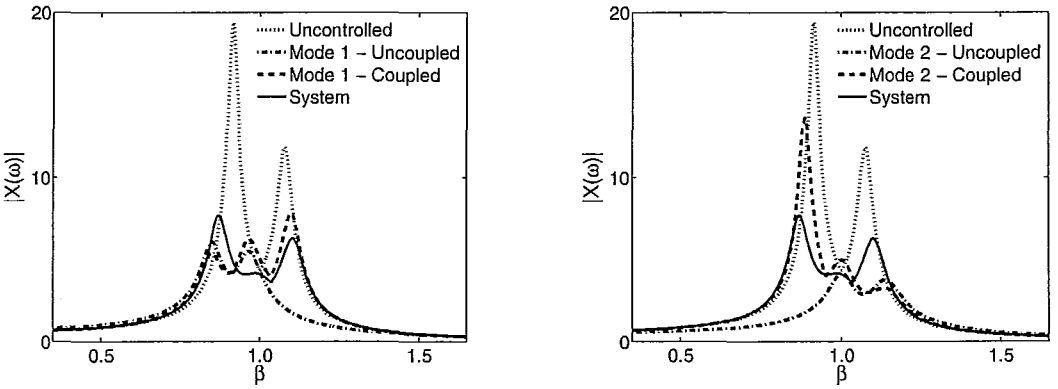

Figure 5.42: Mechanical Admittance Functions Comparison between Targeting a Mode and System (Equal Modal Damping Ratio) subjected to Random Excitation : ω_θ/ω_s = 1.0, B/D=3, $\mu = 0.01$

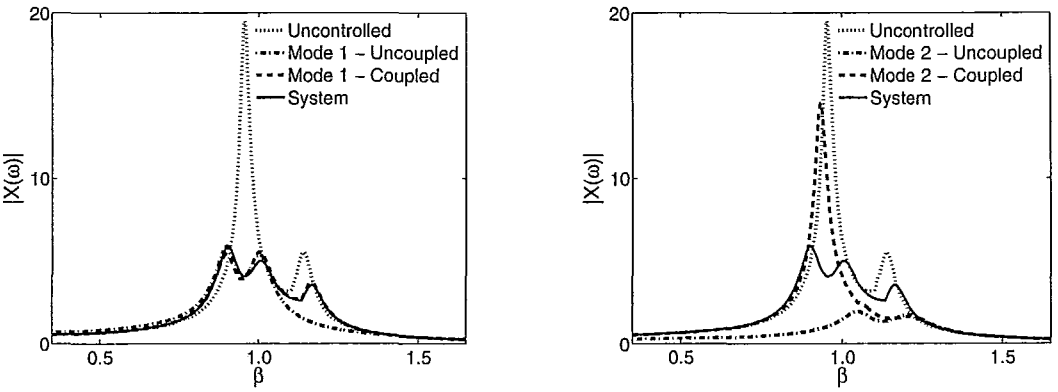

Figure 5.43: Mechanical Admittance Functions Comparison between Targeting a Mode and System (Equal Modal Damping Ratio) subjected to Random Excitation : ω_θ/ω_s =1.1, B/D=3, $\mu = 0.01$

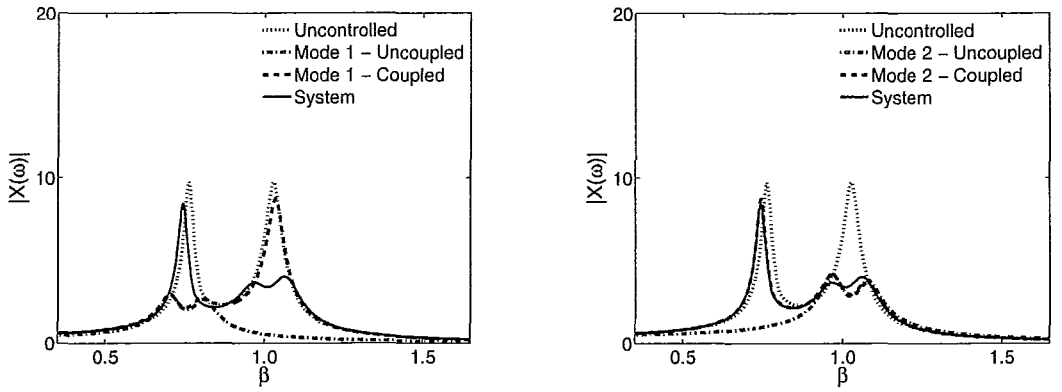

Figure 5.44: Mechanical Admittance Functions Comparison between Targeting a Mode and System (Equal Modal Peak Amplitude) subjected to Random Excitation : $\omega_\theta/\omega_s = 0.8$, B/D=2, $\mu = 0.01$

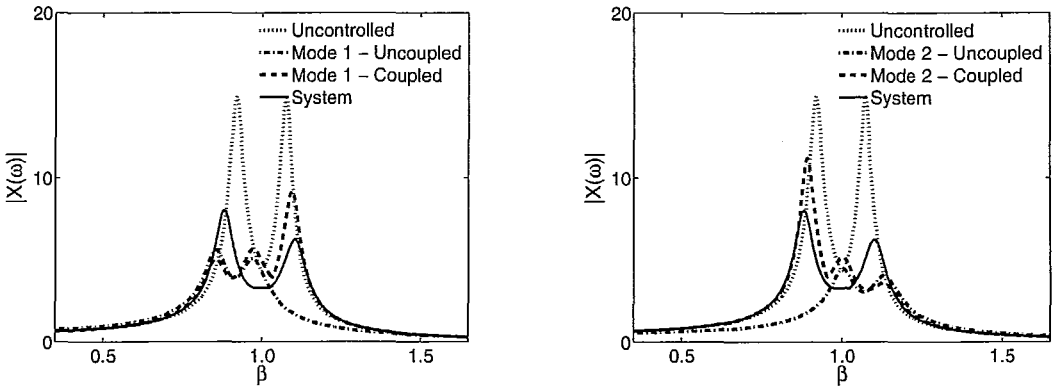

Figure 5.45: Mechanical Admittance Functions Comparison between Targeting a Mode and System (Equal Modal Peak Amplitude) subjected to Random Excitation : $\omega_\theta/\omega_s = 1.0$, B/D=2, $\mu = 0.01$

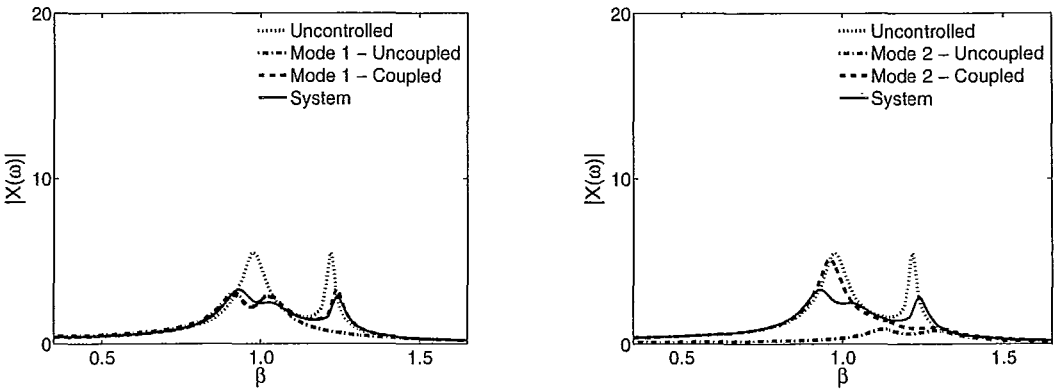

Figure 5.46: Mechanical Admittance Functions Comparison between Targeting a Mode and System (Equal Modal Peak Amplitude) subjected to Random Excitation : $\omega_\theta/\omega_s = 1.2$, B/D=2, $\mu = 0.01$

Chapter 6

Conclusions and Recommendations

6.1 Introduction

This research focused on the response behavior of optimized torsionally coupled structure-DVA systems. Research reported on in Chapters 3 and 4 focused on studying the dynamic response of torsionally coupled structures equipped with different types of dynamic absorbers (TMD(s) and TLD(s)) under harmonic and random excitation using a numerical optimization approach. Chapter 5 focused on the development of a preliminary design tool for torsionally coupled TMD systems.

In Chapters 3 and 4, series of simulations were performed to study the response of different torsionally coupled structure-DVA systems by utilizing MATLAB(r2007b) optimization toolboxes (fminimax and fmincon). The efficiency (ψ) of different dynamic absorbers arrangements were accessed by introducing the response reduction factor (R_o) such that $\psi = 1 - R_o$, where R_o is defined as the ratio of the response of structure equipped with absorber(s) to the response of structure without absorber.

In Chapter 5, closed-form optimal parameters of a two-degree-of-freedom structure -TMD system in the literature were employed in developing a rapid preliminary design tool to target the response of a specific mode in torsionally coupled structure. By introducing the concept of a generalized mass ratio for a structure with 3 dimensional motions such that the TMD mass and mass moment of inertia were taken into account, the closed-form TMD parameters (tuning and damping ratio values) given by (Asami *et al.*, 1991, 2002; Warburton, 1982) were applied to the torsionally coupled TMD system. Detail procedures were given on the design of a torsionally coupled TMD system. The structural response of torsionally coupled system equipped with two identical TMDs subjected to harmonic and random excitation obtained from the method described were verified and evaluated.

6.2 Research Findings

Conclusions obtained for the studies conducted are summarized in this section. The conclusions and findings are valid for the structures selected.

6.2.1 Torsionally Coupled Structures Equipped with TMD(s) subjected to Harmonic Excitation

Numerical simulations were performed on structures with different TMDs arrangements using MATLAB (r2007b) optimization toolbox (fminimax). The study consisted of two parts. Part 1 involved structures with equal damping ratio values (2%) in both modes of vibration whereas Part 2 considered structures with equal modal peak amplitude values such that the response of structures without TMD(s)

are equally dominated by the two modes. For Part 1, structures with uncoupled frequency ratio values of 0.5, 0.7, 0.8, 1.0, 1.2 and 1.3 were considered. As for Part 2, uncoupled frequency ratio values of 0.8, 1.0 and 1.2 were considered. The following conclusions were obtained for the structures considered under harmonic excitations:

- The efficiency of different TMDs configurations were found to be related to the nature of the structures considered, which are torsionally flexible, strongly torsionally coupled and torsionally stiff.

- Locating the TMD(s) at the edge(s) of the structures maximized TMD(s) performance by increasing the mass coupling terms and mass moment of inertia that develops from placing the TMD(s) away from the centre of mass.

- By allowing a unique mass ratio values for each of the TMDs in a two different TMDs configuration, the greatest efficiency was achieved as compared to all other configurations considered.

- For the structures with uncoupled frequency ratio values of 0.8, 1.0 and 1.2, the dynamic response was found to be sensitive to the structural damping. This is in contrast to findings by Warburton and Ayorinde (1980). However, this research focused on optimizing a two-degree-of-freedom primary structure whereas Warburton and Ayorinde (1980) focused on optimizing the response of a single-degree-of-freedom primary structure.

- The efficiency of the single TMD configuration was found to exceed that of the two identical TMDs configuration except for the strongly torsionally coupled structure case. This can be attributed to the mass coupling term generated by

a single DVA that aids in reducing the response when the two modes are well separated.

- At least two TMDs are required to reduce the dynamic response of the strongly torsionally coupled systems effectively as the mass coupling term generated by a single TMD does not aid in reducing the response when two modes are strongly coupled.

- At least two tuning ratios are required to suppress the dynamic response of the torsionally flexible structures effectively as the mass moment of inertia generated by the TMDs tuned to the torsionally dominant mode do not aid in suppressing the response of the higher frequency translational mode.

- A single TMD was found to be inefficient in reducing the response of the strongly torsionally coupled system. Therefore, TMD configuration is an important parameter which should be considered in the design of TMDs for strongly torsionally coupled structure. However, the efficiency of a single TMD configuration was found to approach that of the two different TMDs configuration for the torsionally stiff structures.

- The additional mass constraint placed on the four TMD configurations (Approach I and II) limited the efficiency in this configuration for the torsionally coupled structures as compared to that of the two different TMDs configuration. The four TMDs configuration (Approach II) was found to be more efficient in reducing the response of the torsionally flexible structures compared to that of Approach I. This indicates the importance of minimizing the constraints placed on selecting TMDs parameters.

- For TMD configurations where only one tuning ratio can be employed (a single TMD and two identical TMDs configurations), tuning the TMD(s) around the translation dominant mode can reduce the response of the torsionally dominant mode in the torsionally stiff structures as a result of the inertia forces generated by the TMD(s).

- All TMD configurations considered were able to attenuate the uncontrolled dynamic response and the efficiency for each configuration was found to increase as the mass ratio was increased.

- The generalized mass ratio value plot can be used to evaluate the response behavior and the TMD location resulting in maximum and minimum efficiency.

6.2.2 Torsionally Coupled Structures Equipped with DVA(s) subjected to Random Excitation

The response of torsionally coupled systems with different DVAs (TMD/TLD) arrangements under random excitation was studied. Optimization toolbox (fmincon) from MATLAB (r2007b) was utilized to minimized the mean square corner displacement. Numerical simulations were performed on structures with 2% damping ratio in both modes of vibration. The response obtained for the structure-TLD systems, at its designed target amplitude, was compared to that of the structure-TMD systems. Structures with uncoupled frequency ratio value of 0.5, 0.7, 0.8, 1.0, 1.2 and 1.3 are selected. The following conclusions were obtained for the structures considered under random excitation:

- The modal contribution to the total variance plays an important role in determining the tuning strategy.

- Greater efficiency can be achieved by placing the DVA(s) at the edge(s) ($\pm B/2$) of the structure. This is a direct result of the additional DVA(s) mass coupling terms and mass moment of inertia that develops from placing the DVA(s) away from the centre of mass.

- Greatest efficiency was achieved for the two different DVAs configuration as this configuration permits two independent DVAs to be tuned to two different modes. In addition, the mass of each DVA reflects the percentage the mode to which it is tuned to contributes to the total variance.

- For all the DVA configurations, except the single DVA configuration, greatest efficiency was achieved for the strongly torsionally coupled systems.

- The efficiency of a single DVA configuration was found to approach that of the two different DVAs configuration for the torsionally stiff structures considered. This is a result of the negligible torsional contribution to the total corner response for these structures. However, a single DVA configuration was not effective in reducing the strongly torsionally coupled system response.

- For the case of four DVAs (Approach I and II), the constraints enforced on the mass ratio reduced the efficiency of this configuration as compared to that of two different DVAs configuration. However, Approach II was found to be more efficient than Approach I for the torsionally flexible structures. This highlights the importance of the freedom in optimizing the DVA parameters for the torsionally flexible structures.

- At least two DVAs were required to suppress the response of the strongly torsionally coupled structure considered effectively as the mass coupling term generated by a single DVA does not aid in reducing the response when two modes are strongly coupled.

- The efficiency of the single DVA configuration was found to exceed that of the two identical DVAs configuration except for the strongly torsionally coupled structure case. This can be attributed to the mass coupling term generated by a single DVA that aids in reducing the response when two modes are well separated.

- Targeting the response of the torsional dominant mode was found to amplify the sensitivity to changes in DVA location. This can be concluded from the response obtained for the two different DVAs configurations.

- The response behavior of the structure-TLD systems at its targeted design amplitude was found to be similar to that of the structure-TMD systems.

- Higher efficiency was obtained in the structure-TMD systems for the strongly torsionally coupled and stiff structures ($\omega_\theta/\omega_s = 1.0$, 1.2 and 1.3) as compared to the structure-TLD systems. The opposite was found for torsionally flexible structures ($\omega_\theta/\omega_s = 0.5$ and 0.7).

- All DVA configurations considered were able to attenuate the uncontrolled dynamic response and the efficiency for each configuration was found to increase as the mass ratio was increased.

6.2.3 Torsionally Coupled Systems using Closed-Form Parameters

By utilizing the concept of generalized properties of a structure-TMD system, a design method for a torsionally coupled TMD system under both random and harmonic excitations using the closed-form parameter was developed. The method was verified by comparing the response obtained from the closed-form solutions and those obtained by solving the equations of motion of the structure-TMD systems. The torsionally coupled systems were optimized using the method developed to target the response of a specific mode and the numerical approach utilizing MATLAB (r2007b) optimization toolboxes. The results obtained from the two different optimization approaches were compared and evaluated.

- As expected, the 'uncoupled' response did not capture the response of the untargeted mode and the coupling between modes for the entire structure-TMD system. However, the 'coupled' response successfully captured these interactions by employing the equations of motion developed for the entire structure-TMD system. Thus, the generalized structure-TMD approach can be employed in the design of a structure-TMD system.

- As the uncoupled frequency ratio approaches one, the response of the untargeted mode is found to be influenced by the targeted mode.

- The generalized structure-TMD approach for the two identical TMDs configuration is limited by the fact that only one mode can be targeted at a time. However, in the numerical optimization approach, where the entire system is optimized using the procedure outlined in Chapters 3 and 4, the two identical

TMDs can be tuned to a frequency that falls between the natural frequencies of the structure. Thus, when strong coupling exists in the structure, the generalized structure-TMD approach is not as effective as numerical optimization technique.

- The efficiency of the generalized structure-TMD approach is dictated by the selection of the targeted mode. The designer should select the mode that dominates the overall response. This can be accomplished through inspection of the frequency response function or mechanical admittance function for the case of harmonic and random excitation, respectively. For a structure subjected to harmonic excitation, the mode comprised of a higher peak amplitude should be selected. As for a structure subjected to random excitation, the mode which is the greater contributor to the total variance should be selected.

- For the torsionally coupled systems studied under harmonic excitation, the generalized structure-TMD approach is not as effective in reducing the overall structural response, except for the case of torsionally stiff structures. However, it can be used to effectively reduce the response of one mode exclusively.

- For the torsionally coupled systems studied under random excitation, targeting the correct mode results in a response comparable to that obtained from optimizing the entire system. The greatest difference in the reduction in response between optimizing the entire system using the numerical technique and targeting the correct mode using the generalized structure-TMD approach was found to be less than 8% for the strongly torsionally coupled system.

6.3 Future Recommendations

The study conducted focused on a 2-dimensional torsionally coupled structures equipped with multiple TMD(s) or TLD(s) subjected to either harmonic or random excitation. The objective of this study was to investigate and evaluate the performance of different DVA configurations. The following recommendations are suggested for future studies:

- An experimental program should be conducted on the numerical studies performed to verify the results obtained.
- The studies carried focused on a 2-dimensional torsionally coupled systems. An investigation on a 3-dimensional torsionally coupled systems should be considered.
- For torsionally coupled structures equipped with TLD(s), the study focused on evaluating the response behavior of the structure-TLD system at its designed target amplitude. Further studies should be conducted on the performance of torsionally coupled structure-TLD system at non-targeted response amplitudes.
- The rapid design tool proposed in Chapter 5 was verified by two dimensional torsionally coupled structures equipped with two identical TMDs. This preliminary design tool can be extended to two and three dimensional structures with different DVA arrangements.

Bibliography

Asami, T., Wakasono, T., Kameoka, K., and Hasegawa, M. (1991). Optimal Design of Dynamic Absorbers for a System Subjected to Random Excitation. *JSME Internatioal Journal*, **34**(2), 218–226.

Asami, T., Nishihara, O., and Baz, A. M. (2002). Analytical Solutions to H_∞ and H_2 Optimization of Dynamic Vibration Absorbers Attached to Damped Linear System. *Journal of Vibration and Acoustics*, **124**(2), 284–295.

Baines, W. D. and Peterson, E. G. (1951). An Investigation of Flow Through Screens. *Transactions of the ASME*, **73**, 467–468.

Bauer, H. F. (1984). Oscillations of Immiscible Liquids in a Rectangluar Container: A New Damper for Excited Structures. *Journal of Sound and Vibration*, **93**(1), 117–133.

Beards, C. (1995). *Engineering Vibration Analysis with Application to Control Systems*. Elsevier, Burlington.

Brock, J. E. (1946). A Note on Damped Vibration Absorber. *Journal of Applied Mechanics*, **13**(4), A–284.

Carrier, G. F. and Miles, J. W. (1960). On the Annular Damper for a Freely Precessing Gyroscope. *Journal of Applied Mechanics*, **27**, 237–240.

Cassolato, M. R. (2007). *The Performance of a Tuned Liquid Damper Equipped with Inclined and Oscillatiing Damping Screens.* Master's thesis, McMaster University, Hamilton, Canada.

Caughey, T. K. (1963). Equivalent Linearization Techniques. *Journal of Acoustical Society of America*, **35**, 1706–1711.

Chopra, A. K. (2000). *Dynamics of Structures: Theory and Application to Earthquake Engineering.* Prentice Hall, New Jersey, 2nd edition.

Crandall, S. H. and Mark, W. D. (1963). *Random Vibration in Mechanical Systems.* Academic Press, New York.

Den Hartog, J. P. (1956). *Mechanical Vibrations.* McGraw-Hill, New York, 4th edition.

Fediw, A. A., Isyumov, N., and Vickery, B. J. (1995). Performance of Tuned Sloshing Water Damper. *Journal of Wind Engineering and Industrial Aerodynamics*, **57**(2-3), 237–247.

Fujino, Y., Pacheco, B. M., Chaiseri, P., and Sun, L. M. (1988). Parametric Studies of Tuned Liquid Damper (TLD) using Circular Containers by Free-Oscillation Experiments. *Structural Engineering / Earthquake Engineeing*, **5**(2), 381–391.

Fujino, Y., Sun, L., Pacheco, B. M., and Chaiseri, P. (1992). Tuned Liquid Damper (TLD) for Suppressing Horizontal Motion of Structures. *Journal of Engineering Mechanics*, **118**(10), 2017–2030.

Hahnkamm, E. (1932). Die Dämpfung von Fundamentschwingungen bei veränderlicher Erregergrequenz. *Ing. Arch.*, **4**, 192–201.

Halcrow Yolles (2007). Retrieved November 21, 2008 from <www.halcrow.com/halcrowyolles/projects/featured_projects/1_king_west.htm>.

Hamelin, J. (2007). *The Effect of Screen Geometry on the Performance of a Tuned Liquid Damper.* Master's thesis, McMaster University, Hamilton, Canada.

Holland, J. (1975). *Adaption in Natural and Artifical Systems.* University of Michigan Press, Ann Arbor, MI.

Jacquot, R. G. and Foster, J. E. (1977). Optimal Cantilever Dynamic Vibration Absorbers. *Journal of Engineering for Industry*, **99**(1), 138–141.

Jangid, R. S. and Datta, T. K. (1997). Performance of Multiple Tuned Mass Dampers for Torsionally Coupled System. *Earthquake Engineering and Structural Dynamics*, **26**(3), 307–317.

Kaneko, S. and Ishikawa, M. (1999). Modelling of Tuned Liquid Damper with Submerged Nets. *Journal of Pressure Vessel Technology*, **121**(3), 334–343.

Kaneko, S. and Yoshida, O. (1999). Modeling of Deepwater-Type Rectangular Tuned Liquid Damper with Submerged Nets. *Journal of Pressure Vessel Technology*, **121**(4), 413–422.

Kareem, A. (1983). Mitigation of Wind Induced Motion of Tall Buildings. *Journal of Wind Engineering and Industrial Aerodynamics*, **11**(1-3), 273–284.

Kareem, A. (1990). Reduction of Wind Induced Motion Utilizing a Tuned Sloshing Damper. *Journal of Wind Engineering and Industrial Aerodynamics*, **36**(2), 725–737.

Kareem, A. and Sun, W. J. (1987). Stochastic Response of Structure with Fluid-Containing Appendages. *Journal of Sound and Vibration*, **119**(3), 389–408.

Kareem, A., Kijewski, T., and Tamura, Y. (1999). Mitigation of Motions of Tall Buildings with Specific Examples of Recent Applications. *Wind and Structures, An International Journal*, **2**(3), 201–251.

Lamb, H. (1932). *Hydrodynamics.* Cambridge University Press, London (England).

Lin, C.-C., Ueng, J.-M., and Huang, T.-C. (1999). Seismic Response Reduction of Irregular Buildings using Passive Tuned Mass Dampers. *Engineering Structures*, **22**(5), 513–524.

McNamara, R. J. (1977). Tuned Mass Dampers for Buildings. *Journal of the Structural Division*, **103**(9), 1785–1798.

Morison, J. R., O'Brien, M. P., Johnson, J. W., and Schaaf, S. A. (1950). The Force Exerted by Surface Waves on Piles. *Petroleum Transactions AIME*, **189**, 149–154.

New York Architecture Images (n.d.). Retrieved November 21, 2008 from <www.nyc-architecture.com/UES/UES001.htm>.

OCCDC (2005). Case Study 1 King West Retrieved November 21, 2008 from <occdc.org/pdf/1%20King%20West.pdf>.

Ozer, M. B. and Royston, T. J. (2005). Extending Den Hartog's Vibration Absorber Technique to Multi-Degree-of-Freedom Systems. *Journal of Vibration and Acoustics*, **127**, 341–350.

Pansare, A. and Jangid, R. (2003). Tuned Mass Dampers for Torsionally Coupled Systems. *Wind and Structures, An International Journal*, **6**(1), 23–40.

Petit, F., Loccufier, M., and Aeyels, D. (2009). On the Attachement Location of Dynamic Vibration Absorbers. *Journal of Vibration and Acoustics*, **131**(034501).

Petti, L. and De Iuliis, M. (2009). Robust Design of a Single Tuned Mass Damper for Controlling Torsional Response of Asymmetric-Plan Systems. *Journal of Earthquake Engineering*, **13**, 108–128.

Shimizu, T. and Hayama, S. (1987). Nonlinear Responses of Sloshing Based on the Shallow Water Wave Theory. *JSME Internatioal Journal*, **30**(263), 806–813.

Singh, M. P., Singh, S., and Moreschi, L. M. (2002). Tuned Mass Dampers for Response Control of Torsional Buildings. *Earthquake Engineering and Structural Dynamics*, **31**(4), 749–769.

Soong, T. and Dargush, G. (1997). *Passive Energy Dissipation Systems in Structural Engineering*. Wiley, New York.

Sun, L. M., Fujino, Y., Pacheco, B. M., and Isobe, M. (1989). Nonlinear Waves and Dynamic Pressures in Rectangular Tuned Liquid Damper (TLD). Simulation and Experimental Verification. *Structural Engineering / Earthquake Engineeing*, **6**(2), 251–262.

Sun, L. M., Fujino, Y., Pacheco, B. M., and Chaiseri, P. (1992). Modelling of Tuned Liquid Damper (TLD). *Journal of Wind Engineering and Industrial Aerodynamics*, **43**(3), 1883–1894.

Sun, L. M., Fujino, Y., Chaiseri, P., and Pacheco, B. M. (1995). The Properties of Tuned Liquid Dampers using a TMD Analogy. *Earthquake Engineering and Structural Dynamics*, **24**(7), 967–976.

Taipei Financial Center Corp. (2005). Retrieved November 21, 2008 from http://<www.taipei-101.com>.

Tait, M. J. (2008). Modelling and Preliminary Design of a Structure-TLD System. *Engineering Structures*, **30**(10), 2644–2655.

Tait, M. J., Damatty, A. A. E., and Isyumov, N. (2004). Testing of Tuned Liquid Damper with Screens and Development of Equivalent TMD Model. *Wind and Structures, An International Journal*, **7**(4), 215–234.

Tait, M. J., Damatty, A. E., Isyumov, N., and Siddique, M. (2005). Numerical Flow Models to Simulate Tuned Liquid Dampers (TLD) with Slat Screens. *Journal of Fluids and Structures*, **20**(8), 1007–1023.

Tait, M. J., Isyumov, N., and Damatty, A. A. E. (2007). Effectiveness of a 2D TLD and Its Numerical Modeling. *Journal of Structural Engineering*, **133**(2), 251–263.

Tamura, Y. (1998). Application of Damping Devices to Suppress Wind-Induced Responses of Buildings. *Journal of Wind Engineering and Industrial Aerodynamics*, **74-76**, 49–72.

Tamura, Y., Fujii, K., Ohtsuki, T., Wakahara, T., and Kohsaka, R. (1995). Effectiveness of Tuned Liquid Dampers Under Wind Excitation. *Engineering Structures*, **17**(9), 609–621.

Uniform Building Code (1997). International Conference of Building Officals, Whitter, CA.

Vandiver, J. K. and Mitome, S. (1979). Effect of Liquid Storage Tanks on the Dynamic Response of Offshore Platforms. *Journal of Petroleum Technology*, **31**(10), 1231–1240.

Warburton, G. B. (1982). Optimal Absorber Parameters for Various Combinations of Response and Excitation Parameters. *Earthquake Engineering and Structural Dynamics*, **10**(3), 381–401.

Warburton, G. B. and Ayorinde, E. . (1980). Optimum Absorber Parameters for Simple Systems. *Earthquake Engineering and Structural Dynamics*, **8**(3), 197–217.

Warnitchai, P. and Pinkaew, T. (1998). Modelling of Liquid Sloshing in Rectangular Tanks with Flow-Damping Devices. *Engineering Structures*, **20**(7), 593–600.

Weld, F. and Modi, V. J. (1989). Vibration Damping through Liquid sloshing, part I. A nonlinear Analysis. *Journal of Vibration, Acoustics, Stress, and Reliability in Design*, **18**(5), 149–156.

Wu, B., Ou, J.-P., and Soong, T. (1997). Optimal Placement of Energy Dissipation Devices for Three-Dimensional Structures. *Engineering Structures*, **19**(2), 113–125.

Yu, J.-K., Wakahara, T., and Reed, D. A. (1999). A Non-Linear Numerical Model

of the Tuned Liquid Damper. *Earthquake Engineering and Structural Dynamics*, **28**(6), 671–686.

Zhang, J., Zeng, K., and Jian, J. (2009). An Optimal Design of Bi-Directional TMD for Three Dimenional Structure. *Computational Structural Engineering*, pages 935–941.

Appendix

Appendices A to X, which include the optimized structural response, optimal DVA parameters, frequency response functions and mechanical admittance functions, are contained in the CD attached.